GENERAL NOTES

DSIR Journals

The following journals are published quarterly by the New Zealand Department of Scientific and Industrial Research:
N.Z. Journal of Agricultural Research
N.Z. Journal of Botany
N.Z. Journal of Crop and Horticultural Science
N.Z. Journal of Geology and Geophysics
N.Z. Journal of Marine and Freshwater Research
N.Z. Journal of Zoology.

A full list of DSIR publications may be obtained free of charge from the Publications Officer, DSIR Publishing, P.O. Box 9741, Wellington, New Zealand.

Subscriptions

Subscriptions will be accepted only on advance payment and only for a full calendar year. The prices of each of the above journals are:

Personal subscription rates—
New Zealand NZ$96.25
Australia NZ$99.50
Outside New Zealand and Australia US$83.50

Institutional subscription rates—
New Zealand NZ$181.50
Australia NZ$177.00
Outside New Zealand and Australia US$151.00

All prices include packing and postage, and GST within New Zealand

Single copies are available, prices on request.

Subscriptions should be forwarded to the Publications Officer, DSIR Publishing, P.O. Box 9741, Wellington, New Zealand. Cheques should be made payable to the Department of Scientific and Industrial Research.

Copyright

All DSIR journals subscribe to the Fair Copying Declaration issued by the Royal Society (London), which allows libraries and other organisations to supply bona fide inquirers with a single copy of any paper not otherwise available to them, subject to normal copyright and acknowledgment conditions.

Permission to photocopy for internal or personal use or the internal or personal use of specific clients is granted by the Department of Scientific and Industrial Research for libraries and other users registered with the *Copyright Clearance Centre* (CCC), provided that the stated fee per copy is paid directly to the CCC, 21 Congress Street, Salem, MA 01970, USA. Special requests should be addressed to DSIR Publishing.

The code on the first page of an article indicates the above consent and includes the fee per copy to be paid to the CCC.

Incorporation of copyrighted material into papers or textbooks to be published requires permission from the copyright holder, DSIR. Permission should be sought from the Manager, DSIR Publishing.

Reproduction, in full or in part, of authors' abstracts, with acknowledgment, is authorised.

INFORMATION FOR AUTHORS

New Zealand Journal of Geology and Geophysics publishes original research papers in all aspects of the earth sciences in general, including geology, geophysics, soil science, and the atmospheric sciences, relevant to New Zealand, its associated territories, and Antarctica. Review articles, preliminary notes, Letters to the Editor, book reviews, and thesis summaries are also published.

Papers published or under consideration elsewhere will not be accepted; but publication elsewhere of an abstract or extended summary does not preclude publication in full in this journal. In this context, restricted circulation of reports or theses does not constitute publication.

Submission of manuscripts

This journal is produced on IBM and Apple Macintosh computers and is offset printed from laser printer copy. Authors should preferably supply formatted text stored on disks, to the following specifications:

3.5" Apple Macintosh disks (Microsoft Word or MacWrite); 5.24" IBM compatible disks (most current MS-DOS word processing packages such as Microsoft Word, Wordstar, and Word Perfect V4).

Papers can also be supplied through electronic mail. The text should be broken up into files of no more than 50 blocks each (approximately 8 single-spaced pages make 50 blocks). Text and table files must be separate.

Our VAX mail address is:
Overseas—CB%NZ.GOVT.DSIR.SRWYMTJ
New Zealand—PSI%4600000060::SRWYMTJ
DSIR—WNV::SRWYMTJ

Disks or electronic mail should not be sent until the paper has been accepted or revised. When supplying soft copy please specify the word processing package used, and include a printout of all files.

A full list of instructions for preparing manuscripts is printed in the first issue of each volume and may be obtained separately on request. Intending authors are advised to check the style of presentation and conventions used in any recent issue of the journal.

New Zealand Journal of

Geology and Geophysics

Volume 32 / Number 2 / 1989

DSIR
Wellington

New Zealand Journal of Geology and Geophysics
Vol. 1, No. 1 (February 1958)

Volume 32, Number 1 published 12 April 1989

This journal is abstracted in: Aquatic Sciences and Fisheries Abstracts; Bibliography and Index of Geology; Biological Abstracts; Bulletin Signaletique; Chemical Abstracts; Current Contents; Geo Archive; INIS Atomindex; IRL Life Sciences Collection; Mineralogical Abstracts; New Zealand Science Abstracts; Oceanic Abstracts; Pollution Abstracts; Science Citation Index.

ISSN 0028–8306

Published by DSIR Publishing,
P.O. Box 9741, Wellington, New Zealand

Typeset by Marian Jefferies, DSIR Publishing, Wellington
PRINTED BY WRIGHT AND CARMAN LTD, UPPER HUTT, NEW ZEALAND

New Zealand Journal of Geology and Geophysics, 1989, Vol. 32: 191–196
0028–8306/89/3202–0191 $2.50/0

New paleomagnetic results from Blind River: Revised magnetostratigraphy and tectonic rotation of the Marlborough region, South Island, New Zealand

G. M. TURNER
A. P. ROBERTS
Institute of Geophysics
Research School of Earth Sciences
Victoria University of Wellington
P. O. Box 600
Wellington, New Zealand

C. LAJ
C. KISSEL
A. MAZAUD
S. GUITTON
Centre des Faibles Radioactivites Domaine du C.N.R.S.
Avenue de la Terrasse
91190, Gif-sur-Yvette
France

D. A. CHRISTOFFEL
Institute of Geophysics
Victoria University of Wellington

Abstract Part of the Upper Miocene–Lower Pliocene mudstone section at Blind River, northern Marlborough, which was the subject of a paleomagnetic study by Kennett and Watkins in 1974, has been resampled and the data reinterpreted. The new results do not concur entirely with those of Kennett and Watkins. In particular, we do not find the uppermost normal event of their record. This implies a more uniform deposition rate and a later date of 5.6 m.y. for the first occurrence of *Globorotalia conomiozea* in the section. The new data also show a declination anomaly of 36 ± 4° to the east. This is thought to be due to clockwise rotation within the active tectonic belt of New Zealand, between the Pacific and Australian plates. This declination anomaly is slightly larger than those reported from sites in the northern part of the tectonic belt, suggesting that the deformation is more complex than a simple block rotation.

Keywords paleomagnetism; magnetostratigraphy; Miocene; Pliocene; polarity transitions; virtual geomagnetic pole; tectonic rotation

Received 17 August 1987; accepted 2 November 1988

INTRODUCTION

The Blind River and Stace Stream sections occur at latitude 41°44'S and longitude 174°03'E in the Marlborough region of the South Island of New Zealand. They consist of some 1200 m of massive blue-grey mudstones of Late Miocene to Early Pliocene age, with minor siltstone and sandstone horizons unconformably overlying a basement of Triassic–Jurassic greywacke and argillite. The sections have been the subject of previous magnetostratigraphic, biostratigraphic, and stable isotope investigations.

The locations of the sites used by Kennett & Watkins (1974) in their magnetostratigraphic study are shown in Fig. 1. Their results, given as the latitude of the virtual geomagnetic pole (VGP), and the revised magnetostratigraphic interpretation of their work by Loutit & Kennett (1979), are shown in Fig. 2. These two papers will be referred to below as K&W and L&K, respectively.

K&W originally interpreted the two normal episodes in the upper part of their record as the split Gilbert 'C' event. The reassignment of these normal episodes to Chron 5, c. 1 m.y. older, by L&K, is based on the detection of a decrease of about 0.5 per mil in the $^{13}C/^{12}C$ ratio in benthic foraminifera in the long reversed section immediately below the normal episodes. Such a $\delta^{13}C$ shift had previously been found in deep-sea cores from the Pacific and Indian Oceans, at depths corresponding to the upper part of Chron 6 (Keigwin 1979; Keigwin & Shackleton 1980). The two lower normal episodes of K&W were now interpreted as falling in Chrons 6 and 7. This revision also removed an apparent discrepancy of 1 m.y. between major cooling episodes in the South Pacific and elsewhere and established the synchroneity of the Kapitean Stage in New Zealand and the Messinian of the Mediterranean region. At each of their sites, K&W presented paleomagnetic data from the level of thermal demagnetisation which yielded the lowest directional scatter between the two or three specimens measured. Thus, at many sites, the natural remanent magnetisations have been used whereas, at others, the directions after demagnetisation at 100 or 200°C were taken. They then applied a three-site running average to the virtual geomagnetic pole positions to obtain the data shown in Fig. 2. We believe that this method of data selection may have caused serious errors in the interpretation of the results, as discussed below.

FIELDWORK AND SAMPLING DETAILS

Our initial intention was to sample in detail the Chron 5 polarity transitions which have been studied extensively at Mediterranean sites almost antipodal to New Zealand (Valet & Laj 1981, 1983) and hence to gain insight into the geometry of the transitional geomagnetic field.

In November 1984, we sampled a section in Stace Stream corresponding to K&W sites 6–11 and which spans their R–N transition. In February 1986, we returned to sample the

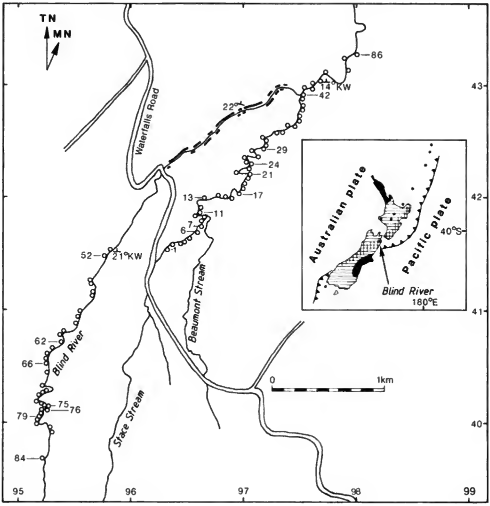

Fig. 1 The Blind River–Stace Stream area, showing the sampling sites of Kennett & Watkins (numbered open circles) and of this study (solid bars). Grid marks are from NZMS 260 sheets P29 and Q29. Inset shows the location of the Blind River section in relation to the major tectonic structures around New Zealand (after Walcott 1984). Solid black, stable land area; horizontal lines, areas undergoing slow deformation; cross-hatching, areas of rapid deformation; dots, active volcanoes. Kennett & Watkins's dip and strike measurements are labelled KW.

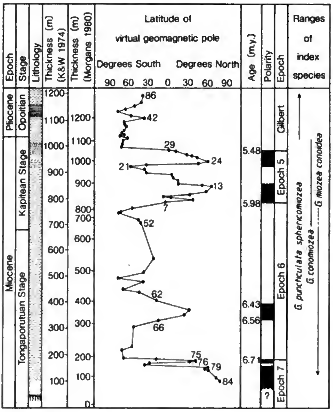

← **Fig. 2** *(Opposite)* Results of Kennett & Watkins (1974), with magnetostratigraphic interpretation of Loutit & Kennett (1979). Sites mentioned in the text are numbered. Two scales of stratigraphic thickness are shown: that used by Kennett & Watkins, and that of Morgans (1980). Also shown are the occurrences of some key planktonic foraminiferal species. Throughout the text the magnetostratigraphic term "Epoch" has been replaced by "Chron" in line with modern practice. Sediment lithologic symbols: dots, sandstone; fine dashes, silstone; coarser dashes, mudstone.

uppermost N–R transition recorded by K&W between their sites 26 and 30. The exposure of this part of the sequence is considerably better in Blind River than in Stace Stream. Precise correlation of horizons between Stace Stream and Blind River is difficult as the lithology is uniformly massive and there are only a few minor bands of sandstone on which the bedding orientation can be measured. K&W recorded dips of 21° and 14°, with strikes east-west for two such horizons, in the southern Blind River part of the section and just north of the Blind River–Stace Stream confluence, respectively (Fig. 1). We found it difficult to verify the strikes of these measurements to an accuracy better than ±20° because of the unevenness of the surfaces. We did, however, record a dip of 22° with a strike of 107° on a pair of sandstone beds in the middle of the northern Blind River section (Fig. 1). This agrees with the value used by Morgans (1980) in his biostratigraphic work and with the strike of the Miocene/

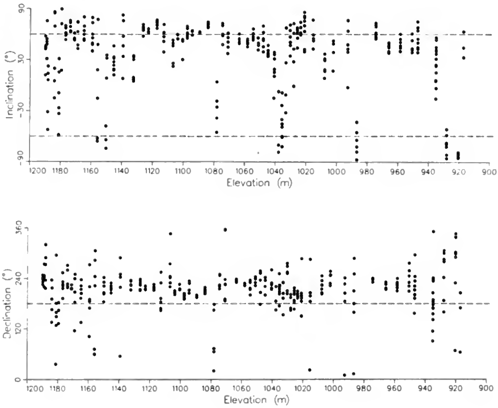

Fig. 3 Declination and inclination of NRM results from 1986 Blind River sites. Dashed lines indicate the axial dipole values of declination and inclination for reversed and normal polarity. Elevations correspond to those of Morgans (1980).

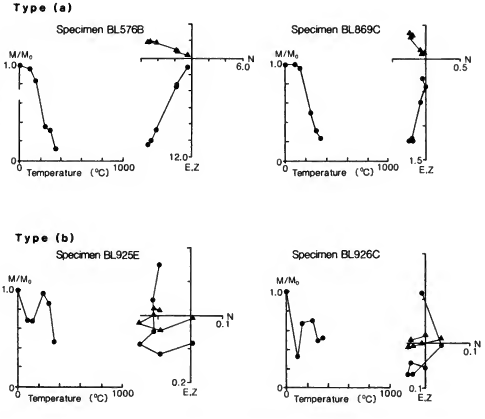

Fig. 4 Thermal demagnetisation plots for typical specimens of type (a) and type (b) (see text). For each specimen the left hand plot shows normalised intensity against temperature, the right hand plot shows the variation of vertical (Z) with northerly (N) components as dots and easterly (E) with northerly (N) components as triangles during demagnetisation. Units are 10 A/m.

Pliocene boundary shown cutting the sections by K&W. If we assume a dip of 22° and strike of 107°, our section (Fig. 1) covers a stratigraphic thickness of 270 m and corresponds to K&W sites 17–42. In the upper part, which K&W found to be reversed, we sampled at stratigraphic intervals of c. 5 m and in the part corresponding to their upper N–R transition, at intervals of < 0.5 m.

A total of 940 cores were collected from 308 sites and were cut into over 3800 specimens. These were divided into two sets for analysis in France and New Zealand. The French

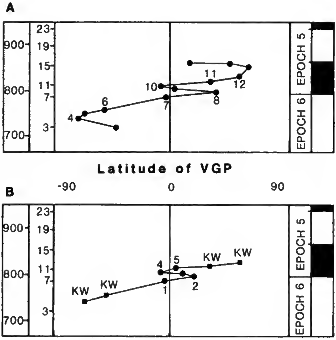

Fig. 5 Comparison of Kennett & Watkins' results with results from this paper for the latitude of the VGP during the R–N transition at 840 m elevation.

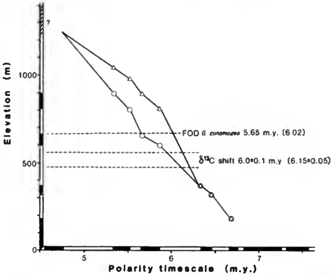

Fig. 6 Deposition curves for the Blind River section inferred from the magnetostratigraphic interpretations of Loutit & Kennett (open triangles), and of this paper (open circles). Dates for the FOD of *Globorotalia conomiozea* and the $\delta^{13}C$ shift obtained from the new interpretation are shown, with those from the interpretation of L&K in parentheses.

and New Zealand measurements, both using cryogenic magnetometers and standard methods of thermal and alternating field demagnetisation, gave essentially the same results and so will be discussed together.

1986 RESULTS

Magnetograms of the declination and inclination of the natural remanent magnetisation (NRM) of the Blind River section are shown in Fig. 3. NRM intensities ranged from 5×10^{-5} to 5×10^{-2} A/m. Throughout the section sampled, the NRMs are predominantly reversed but there are six groups of sites with normal inclinations, some of which have normal declinations. At the NRM stage, the French results were more scattered than those from New Zealand. This is not surprising, as the New Zealand specimens were shielded from external magnetic fields at all times from sampling to measurement. The French specimens underwent considerable periods unshielded before NRM measurement. None of the normal NRM directions, however, appear to be of primary origin. After careful stepwise demagnetisation, the entire section displays reversed polarity.

Examples of the behaviour of typical specimens on demagnetisation are shown in Fig. 4. Both thermal and alternating field demagnetisations were attempted but thermal demagnetisation proved to be more efficient and reliable in separating secondary and primary components of magnetisation. Many specimens displayed spurious behaviour at peak alternating fields above 30 mT while, below this level, sufficient isolation of the primary remanence was not achieved. Of the specimens subjected to thermal demagnetisation, c. 50% showed evidence of mineralogical changes accompanied by growth of an anomalous magnetisation between 350°C and 385°C. However, efficient removal of secondary components was usually achieved by 250°C. In general, three patterns of behaviour emerged on stepwise demagnetisation:

(a) Stable reversed magnetisation, with only a small secondary component, readily removed at low demagnetisation temperatures (e.g., specimens BL576B and BL869C from elevations of 1025 and 975 m, respectively).

(b) Reversed primary magnetisation overprinted with a strong normal component, so that the resultant NRM is normal (e.g., specimens BL925E and BL926C, both from elevation 930 m). The mean vector removed from these specimens between 20°C and 250°C is D = 8°E, I = –66°, α–95 = 11°, N = 5, indistinguishable from the present-day field (D = 22°E, I = –67°), or an axial dipole field (D = 0°, I = –60.7°).

(c) Random, unsystematic behaviour on demagnetisation. It is often difficult to define an endpoint direction for such specimens but, when possible, it is reversed. Such specimens showed a high degree of magnetic viscosity on even a laboratory timescale of days or hours. Many of these specimens came from sites with normal NRMs at elevations between 1030 and 1040 m which correspond to the uppermost normal event of K&W.

The mean direction of primary magnetisation from specimens of types (a) and (b) is D = 216.3°, I = 58.9°, α–95 = 2.4°, N = 63, compared with a reversed axial geocentric dipole field direction of D = 180°, I = 60.7°. Thus, although the inclinations are indistinguishable, we record a clockwise rotation of 36.3 ± 3.7° in declination from the axial dipole value.

DISCUSSION

Revised magnetostratigraphy of the Blind River section

The complete absence of the uppermost normal episode of K&W from our 1986 Blind River results was a major surprise. Despite the uncertainty in the strike of the bedding and hence in the correlation between Stace Stream and Blind River, we

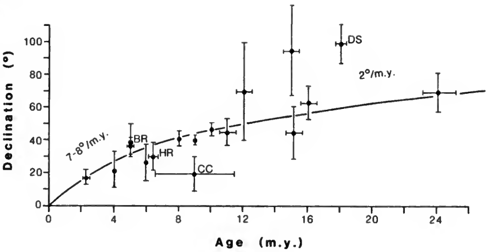

Fig. 7 The clockwise rotation of the Wairoa region of the North Island of New Zealand, from Wright & Walcott (1986), with declination anomalies for the southern part of the tectonic belt superimposed. BR, Blind River; HR, Hinakura Road; CC, Cape Campbell; DS, Deadmans Stream.

are certain that the uppermost site interpreted by K&W as normal (i.e. their site 29), must lie in the lower half of our Blind River section. We were therefore led to a closer inspection of the original K&W dataset. At only three of the seven sites (23–29) in the uppermost normal section, were demagnetised data used in the construction of the VGP curve, and these three sites yield intermediate VGPs. It is possible that, at the four other sites, a strong normal overprint of recent origin caused better coherence of the NRM directions and that the primary direction was reversed but was not isolated (as with our type (c) specimens). From our results we must conclude that this "event" is an artefact of incomplete cleaning of the remanent magnetisation and the method of data selection used by K&W.

Our investigations of the reversals recorded by K&W in the lower part of the section are still continuing. We suggest that a normal event does exist between 840 m and about 900 m. We have recorded a normal direction (D = 72°, I = –71°, α–95 = 4.9°, N = 10 demagnetised at 23 mT) from a site in Stace Stream close to K&W site 13, and we have reproduced the details of the R–N transition at 840 m remarkably closely (Fig. 5). The original data from K&W site 52 (elevation 670 m) are also normal (D = 4.5°, I = –71.2°, N = 2 demagnetised at 199°C). Only after the application of a three-site running mean, in which the data were averaged with data from site 53 some 145 m stratigraphically below, does it appear reversed. We therefore believe that one, or possibly two, normal intervals occur between 930 m, the level to which we sampled in Blind River in 1986, and K&W site 53 at 535 m elevation. An R–N transition must then occur between sites 53 and 52—a stratigraphic interval of 145 m in which there is no outcrop exposed in either Blind River or Stace Stream.

Much of the lower part of the K&W record is based on NRM directions, but as yet we have no new data by which to confirm or revise it. The evidence we now have suggests that if the two normal intervals of Chron 5 do occur in the upper part of the section, then both must be lower than reported by K&W. The uppermost reversed portion of the record is thickened to at least 350 m, and the reversed interval in the middle of the record is shortened to something between 155 and 295 m, assuming the lowermost 400 m of the K&W record to be correct.

The best constraints we can now place on the magnetostratigraphy of the section are summarised on the vertical axis of Fig. 6. The positions of the transitions as reported by K&W, transferred onto the elevation scale of Morgans (1980), are retained below 500 m. Above 500 m the two normal intervals of Chron 5 have been placed so as to be consistent with all observations described above. Plotting the elevations of the transitions against the polarity timescale of Lowrie & Alvarez (1981), gives an inferred sedimentation curve (open circles). Similarly, the open triangles show the sedimentation curve inferred from the reinterpretation by L&K of the original data of K&W.

The main result of our revision is to reduce the variations in sedimentation rate between 400 and 800 m, giving a more linear fit, with an average deposition rate of 0.53 m/thousand years. The first occurrence datum (FOD) of *Globorotalia conomiozea* at 660 m (K&W) is now interpreted as occurring near the base of the reversed part of Chron 5 at a date of 5.65 m.y. as opposed to the top of Chron 6 at 6.1 m.y. (L&K). This is considerably closer to the age of 5.6 m.y. at which the FOD of *G. conomiozea* has recently been reported both in the South Pacific at DSDP site 588 (Hodell & Kennett 1986) and in the Mediterranean (Langereis et al. 1984). Whether the Pacific and Mediterranean taxa are actually related is uncertain (Scott 1980), however, through successive revisions of the magnetostratigraphy and chronology of key sections, the dates of their FODs are steadily converging.

The ages of the first and last occurrences of other species found in the Blind River section are not significantly affected by our revision. Neither can anything precise be said about the date of the $\delta^{13}C$ "shift", as its position cannot be determined accurately in the section (L&K 1979). It remains in the upper part of Chron 6, consistent with reports from other Pacific and Indian Ocean cores (Keigwin & Shackleton 1980).

Tectonic rotations

We record a clockwise declination anomaly of 36 ± 4° in the mean direction of primary remanence at Blind River (1986 results). Blind River is situated in the axial tectonic belt of New Zealand (Fig. 1, inset), between the Australian and Pacific plates, which is thought to have undergone considerable clockwise rotation during the Neogene (Walcott 1984). Wright & Walcott (1986) have studied paleomagnetic declination anomalies in sediments from the Wairoa area, in the northern part of the tectonic belt. They have deduced a mean rate of rotation of about 5°/m.y., accelerating from 2 °/m.y. between 20 and 10 m.y. to 7–8° /m.y. from 5 m.y. to the present. They

associate this acceleration with a change in the Euler rotation pole between the two plates.

It is not clear whether the southern part of the tectonic belt has rotated at the same rate as the north, but our data provide a means of testing the hypothesis for the most recent part. On Fig. 7, the Blind River anomaly, $\Delta D = 36 \pm 4°$, if assigned an age of 5 m.y., lies just above the best fitting line of Wright & Walcott (1986) for the northern region. Our anomaly is somewhat greater than two previously reported results from older Tongaporutuan sediments, at Hinakura Road, Wairarapa, southern North Island ($\Delta D = 30 \pm 8°$) and Cape Campbell, northern South Island ($\Delta D = 20 \pm 11°$) (Walcott et al. 1981). The only other published data from the southern portion of the tectonic belt are from sediments of Altonian age (18 m.y.) at Deadmans Stream (Mumme & Walcott 1985), which record an anomaly $\Delta D = 99 \pm 12°$, also significantly above the curve for the northern region. We therefore consider it likely that the deformation which has been giving rise to tectonic rotation during the Neogene is more complex in the southern portion of the tectonic belt than in the northern portion.

ACKNOWLEDGMENTS

Financial support for this study was provided by le Centre National de la Recherche Scientifique, France, and by the Internal Research Committee of Victoria University of Wellington. We are grateful to R. I. Walcott who gave us a copy of Kennett & Watkins' original data which was kindly supplied to him by J. P. Kennett. Sincere thanks are due also to the Orchard, Waddy, and Kerr families of Blind River and Seddon for their hospitality and generosity during both fieldwork seasons.

REFERENCES

Hodell, D. A.; Kennett, J. P. 1986: Late Miocene–Early Pliocene stratigraphy and paleoceanography of the South Atlantic and Southwest Pacific Oceans: a synthesis. *Paleoceanography 1*: 285–311.

Keigwin, L. D. Jun. 1979: Late Cenozoic stable isotope stratigraphy and paleoceanography of DSDP sites from the East equatorial and Central North Pacific Ocean. *Earth and planetary science letters 45*: 361–382.

Keigwin, L. D. Jun; Shackleton, N. J. 1980: Uppermost Miocene carbon isotope stratigraphy of a piston core in the equatorial Pacific. *Nature 284*: 613–614.

Kennett, J. P.; Watkins, N. D. 1974: Late Miocene–Early Pliocene paleomagnetic stratigraphy, paleoclimatology and biostratigraphy in New Zealand. *Geological Society of America bulletin 85*: 1385–1398.

Langereis, C. G.; Zachariasse, W. J.; Zijderveld, J. D. A. 1984: Late Miocene magnetobiostratigraphy of Crete. *Marine micropaleontology 8*: 261–281.

Loutit, T. S.; Kennett, J. P. 1979: Application of carbon isotope stratigraphy to Late Miocene shallow marine sediments, New Zealand. *Science 204*: 1196–1199.

Lowrie, W.; Alvarez, W. 1981: One hundred million years of geomagnetic polarity history. *Geology 9*: 392–397.

Morgans, H. E. G. 1980: Stratigraphy of the Neogene sequence at Blind River, Marlborough. *New Zealand Geological Survey report pal 36*. 18 p.

Mumme, T. C.; Walcott, R. I. 1985: Paleomagnetic studies at Geophysics Division, 1980–1983. Wellington, New Zealand. Department of Scientific and Industrial Research. *Geophysics Division report 204*. 62 p.

Scott, G. H. 1980: *Globorotalia inflata* and *G. crassaformis* from Blind River, New Zealand: recognition, relationship and use in the uppermost Miocene and Lower Pliocene biostratigraphy. *New Zealand journal of geology and geophysics 23*: 665–677.

Valet, J. P.; Laj, C. 1981: Palaeomagnetic record of two successive Miocene geomagnetic reversals in Western Crete. *Earth and planetary science letters 54*: 53–63.

——— 1983: Invariant and changing transitional field configurations in a sequence of geomagnetic reversals. *Nature 311*: 552–555.

Walcott, R. I. 1984: Reconstructions of the New Zealand region for the Neogene. *Palaeogeography, palaeoclimatology, palaeoecology 46*: 217–231.

Walcott, R. I.; Christoffel, D. A.; Mumme, T. C. 1981: Bending within the axial tectonic belt of New Zealand in the last 9 m.y. from paleomagnetic data. *Earth and planetary science letters 52*: 427–434.

Wright, I. C.; Walcott, R. I. 1986: Large tectonic rotation of part of New Zealand in the last 5 m.y. *Earth and planetary science letters 80*: 348–352.

New Zealand Journal of Geology and Geophysics, 1989, Vol. 32: 197–203
0028–8306/89/3202–0197 $2.50/0

Magnetic susceptibilities of Westland–Nelson plutonic rocks: Discrimination of Paleozoic and Mesozoic granitoid suites

A. J. TULLOCH
New Zealand Geological Survey
Department of Scientific and Industrial Research
P. O. Box 30 368
Lower Hutt, New Zealand

Abstract A portable magnetic susceptibility meter allows rapid in situ estimation of the magnetite content of granitoid rocks, and hence provides a guide to their I- or S-type character.

Except for some muscovite-bearing granites above about 71% SiO_2 and some orthogneisses of the Charleston Metamorphic Group, the susceptibility measurements clearly discriminate between Westland–Nelson granitoids of known Mesozoic (magnetite-bearing, I-type) and Paleozoic (magnetite-free, S-type) age. Although some Mesozoic granites lack magnetite, no magnetite-bearing Paleozoic granites have been recognised.

Precise susceptibility measurements of a suite of S-type biotite granites show that their very weak susceptibilities are proportional to modal biotite content. Ilmenite and pyrrhotite in these S-type granites have no measureable affect on susceptibility measurements. Deformation locally reduces susceptibility on an outcrop scale, whereas contact metamorphism/hydrothermal alteration may increase or decrease susceptibility.

Aeromagnetic anomalies in the Westland–Nelson region of New Zealand are associated more generally with magnetite-bearing I-type granitic rocks than with lamprophyre dikes (and hypothetical magnetic source bodies), and it is considered that several anomalies are due to the granitic rocks, one variety of which is apparently associated with lamprophyre swarms.

Keywords magnetic susceptibility; Westland; Nelson; granitoid rocks; aeromagnetic anomalies; lamprophyre dikes; magnetite; pyrrhotite; biotite

Received 14 October 1987; accepted 6 December 1988

INTRODUCTION

Magnetic susceptibility is defined as the magnetisation per unit magnetic field applied. By far the most significant paramagnetic (i.e. magnetisable) mineral in rocks is magnetite (including Ti-magnetite and maghemite). The paramagnetic minerals hematite, ilmenite, and pyrrhotite have susceptibilities three orders of magnitude less than that of magnetite, and biotite is a further order smaller (Collinson 1983). Unless otherwise specified, the mineral assumed to dominate the susceptibilities reported here is magnetite.

Magnetic susceptibility has been used, especially in Japan, to discriminate between ilmenite-bearing and magnetite-bearing granitoid rocks (Ishihara 1977) which are broadly similar to the S-type and I-type granite groups, respectively, of Chappell & White (1974) (Whalen & Chappell 1988). The measurement of susceptibility provides for the instant, semiquantitative measurement of magnetite content of rock.

The magnetic susceptibility meter used in this study was a model JH-8 (Geoinstruments, Finland). It is battery powered, about the size of a paperback book, and weighs 0.5 kg. It is very suitable for routine field use. The units of volume susceptibility measured, and quoted herein, are dimensionless SI units $\times 10^{-5}$. Reading errors are ± 1 at 0–100, ± 10 at 100–1000, and ± 100 at 1000–10 000 scale.

Magnetic susceptibility is also recorded for most of the rock samples held in the Geophysics Division rock catalogue (Whiteford & Lumb 1975). Measurements on the same samples by New Zealand Geological Survey and Geophysics Division instruments indicate both sets of data to be generally comparable (P. J. Oliver pers comm).

Remanent magnetisation has not been measured in this study, nor is it recorded in the compilation of rock properties by Whiteford & Lumb (1975). However, some remanent magnetisation data on relevant lithologies are presented in Hunt & Nathan (1976).

SEMIQUANTITATIVE MEASUREMENT OF SUSCEPTIBILITY

Assuming a homogeneous distribution of magnetite in a rock, the measured degree of susceptibility largely depends on two factors in relatively unweathered rocks—the nature of the magnetite itself, and the physical form of the rock in question.

Magnetite susceptibility can be affected by two parameters—chemical composition and grain size of magnetite. The former effect is likely to be relatively small provided that the ulvospinel component is not dominant (which is likely in these slowly cooled plutonic rocks where Ti exsolves into ilmenite). (Some analytical data for Westland–Nelson rocks is given later and is not considered further). A simple experiment was performed to determine the effect of magnetite grain size. A sample of magnetite powder (P8125) was sieved to three size fractions, which were then mixed into 36 g of silicon carbide grinding powder

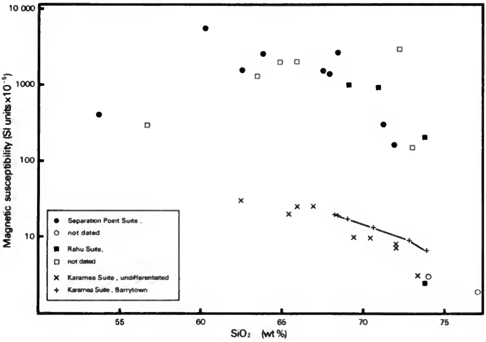

Fig. 1 Magnetic susceptibilities of Westland–Nelson granitoid rocks from Table 1 plotted against SiO_2 (where available). Barrytown samples are connected by a line.

to produce small "rocks", each containing 0.5 wt% magnetite. Results (averages of 30 readings on each sample, in different orientations and 3 remixings) on <90 μm, 90–500 μm, and > 500 μm were 73, 67, and 59, respectively, suggesting that susceptibility measurements of rocks should not be used to quantitatively determine magnetite content unless the grain sizes are broadly comparable. This result is the opposite of that reported by Shandley & Bacon (1966) who recorded a marked decrease of susceptibility for grain sizes less than c. 40 μm. However, they achieved their range of grain sizes by crushing, which may have had a detrimental effect on the results due to transient high temperatures and oxidation.

Sample form is a much more critical factor when recording measurements in the field, than the nature of the magnetite, although easier to allow for. Two features affect readings: rock surface geometry (roughness), and the size/volume of sample. Normal rough surfaces of granite hand specimens or outcrops, which keep parts of the meter head 5–10 mm away, give readings up to 20% lower than flat-sawn faces, which allow the sensor a smooth contact. In addition, simple tests have shown that the minimum volume required to give a true reading is represented by a sample at least 5 cm thick, with a (sawn) face no less than 10 × 10 cm. For example, 3 specimens of sample 83/112 gave the following readings: 15 × 10 × 5 cm = 4500; 15 × 5 × 3 = 3500; 8 × 3 × 3 = 3100, 8 × 3 × 1 = 2500. For best results, therefore, samples should be ≥ 15 × 10 × 5 cm and prepared with a sawn face. However, providing outcrop surfaces are of comparable roughness, and several readings are taken over an outcrop, field measurements are quite adequate for most purposes.

In practice, 5 or 10 readings were taken over an outcrop to check for homogeneity. If readings were similar, the highest value was recorded. Likewise for hand specimens, for which the meter was moved around the sample to achieve the highest reading. In either case, providing anomalously high values are not observed (suggesting grossly heterogeneous distribution of magnetite), the variation is considered to be due to imperfect surface geometry, and the highest reading reflects the closest approach to the actual value.

The geometry effect (especially short-wavelength surface roughness) could have been reduced somewhat by raising the detector a fixed amount above the surface by means of a spacing bracket (J. Cassidy pers. comm.) but this was not done in this reconnaissance study.

Bearing in mind the size and geometry considerations outlined above, the values reported in Table 1 are considered to be within +5 to −10% of the actual value.

PLUTONIC ROCKS OF WESTLAND–NELSON

Distinction of I-type (Mesozoic) and S-type (Paleozoic) granitoids

Magnetic susceptibility measurements on a representative selection of granitoid and associated rocks from Westland and Nelson (Tulloch 1983, 1988) are presented in Table 1. Samples were selected to represent the compositional range exhibited by the dominant granitic rock types. Samples which have been chemically analysed are also plotted in Fig. 1.

These data show that the I-type Mesozoic granitoid rocks (Rahu and Separation Point Suites), generally yield significantly higher susceptibilities than the Paleozoic granitoids (S-type Karamea Suite, Tulloch 1983). The most important exception is at high SiO_2 values, where the trends appear to converge. Mineralogically the overlap region is usually characterised by granites where primary muscovite and garnet appear. In at least two of the three Mesozoic samples which plot in the Karamea Suite field, garnet crystallisation may have removed all available Fe, precluding formation despite high oxygen fugacity. Where muscovite is absent, or a rock is dominated by biotite and/or hornblende, magnetic susceptibility can be used to distinguish the Mesozoic (I-type, generally magnetite-bearing) from Paleozoic (S-type, magnetite-free) suites. Both groups of rocks exhibit a decrease in susceptibility proportional to decreasing Fe content.

Two units (Steele Granodiorite of the Paparoa Range, P. White pers. comm.; and, at least part of, Tarn Summit

Table 1 Magnetic susceptibilities of representative Westland–Nelson granitoid and associated rocks.

Unit/lithology(1)	Mafic minerals (2)	Sample no./ grid ref. (3)	Magnetic susceptibility (4)
Separation Point Suite			
Onahau Pluton*	m,b	P45418	2
Mt Olympus Pluton*	m,b	P45421	3
Knuckle Hill Pluton*	m,b	P46441	10
Separation Point Batholith granite	m,g	P901	0
Separation Point Batholith granite	b	P46102	160
Separation Point Batholith granite	b	P35816	160
Separation Point Batholith granite	b	P35825	500
Separation Point Batholith granite	b	P35830	300
Separation Point Batholith granodiorite	b	P35839	1200
Separation Point Batholith granodiorite	b	P45888	1400
Separation Point Batholith granodiorite	h,b	P35838	1500
Separation Point Batholith granodiorite	h,b	P35969	1000
Separation Point Batholith granodiorite	h,b	P35972	2500
Macey Granite	h,b	OU45320	1500
Pensini Granodiorite	b	P38309	2600
Pearse Granodiorite	h,b	P46113	400
McIntosh Monzodiorite	h,b	P38080	5500
Rahu Suite			
Bald Hill granite	m,b	OU45269	1
Te Kinga granite*	m,b	P45487	6
Arahura granite*	m,b	P45664	150
Mt Ross granite	m,b	OU45237	200
Pa Point granite*	b	P45269	3000
Ripsaw Granodiorite	b	OU45201	900
Berlins Porphyry	b	L29/148275	1000
Jays Creek granodiorite*	b	P45213	1400
Turiwhate quarry granodiorite*	h,b	P45154	1300
Hohonu Ra granodiorite*	h,b	P45924	2500
Hohonu Ra granodiorite*	h	P45929	2000
Kaniere quartz monzonite	h,b	P46002	2000
Canavans monzodiorite*	p,h,b	P45964	300
Karamea Suite			
Tarn Summit granite	m,b	OU45151	3
O'Sullivans Granite	m,b	P41937	8
Maybelle Bay granite	b	K30/743028	8
Barrytown Granite	b	See Fig. 2	3-19
Tarn Summit granite	b	AT2016	14
Oparara granite	b	P45397	10
McWha granite	b	P45396	10
Foulwind Granite	b	K29/825387	20
Whale Creek granodiorite	b	L29/433357	25
Mt Mantell granodiorite	b	GY219	30
Tarn Summit tonalite	b	OU45087	26
Miscellaneous			
Glenroy granulite	p,h,b	GY302	200-900
Glenroy granulite	p,h,b	GY1B	210
Rotoroa gabbronorite	p,h,b	P45391	5000
Rotoroa diorite	h,b	RT/1	70
Tobin Diorite	h,b	L31/328791	55
Thirsty Creek norite	p,h,b	P45229	4500
diorite, E Hohonu River float	p,h,b	P45443	5000
Camptonite, Victoria Ra	p,h,b	AT1517	6000
Camptonite, Te Kinga	p,h,b	P45280	4000
Trachyandesite, Hohonu Ra	p,h,b	P45574	2000
Basalt, L. Poerua	p,h	P45491	1500
Greenland Group greywacke	m	J31/685771	18
Greenland Group argillite	m	J31/685771	20

(1) Units not directly dated, and included in suite by petographic/chemical correlation, are denoted *.
(2) Mafic minerals, p pyroxene, h hornblende, b biotite, m muscovite, g garnet.
(3) Where no sample number is given, the reading was taken at grid referenced outcrop. P, NZGS P Collection; OU, Otago University Geology Department Collection; other samples are AJT sample numbers.
(4) SI units $\times 10^{-5}$, see text for discussion of errors.

Facies B granodiorite of the Victoria Range, Tulloch 1979) whose trace element chemistries, especially moderately high Sr, might suggest correlation with the Rahu Suite, have relatively low Fe^{3+}/Fe^{2+} and carry no magnetite. There is clear evidence here of a further distinct granitoid suite or suites. The Tarn Summit Facies B granodiorite is cut by a leucogranite dike which has a model minimum age of 273 Ma (Tulloch & Whitla unpubl. data) suggesting it is unlikely to be Mesozoic. Other magnetite-free Cretaceous plutonic rocks with Rahu/ Separation Point chemical characteristics, including

moderately high Fe^{3+}/Fe^{2+}, occur within the Charleston Metamorphic Group (Kimbrough & Tulloch in press). Such rocks are characterised by ductile deformational fabrics.

Biotite-poor, high SiO_2 granites with susceptibility values in excess of c. 20–30 probably contain trace amounts of magnetite, and are likely to be I-types. Mafic rocks (≤ 55% SiO_2) give variable, nondiscriminatory results. Low readings for the Pearse Granodiorite (in which ilmenite dominates over magnetite) of the Separation Point Suite probably reflect the lower oxidation state of these less evolved magmas. Conversely, gabbroic rocks from the Devonian Riwaka Complex (see Fig. 3) give high (5000 +) readings.

The magnetic susceptibilities recorded for these rocks are presumed to dominantly reflect the modal magnetite contents, and, in general, the grain-size variation between granites is not likely to significantly affect this conclusion. Few data on magnetite modal contents or compositions are available, but Nathan (1974) and Tulloch (1979) report 0.5% (av.) and 0.6% magnetite, for the Berlins Porphyry and Ripsaw Pluton, respectively. Measured susceptibilities for these rocks (Table 1) were 1000 and 900, respectively. TiO_2 contents of these magnetites are 0.3–4.0% and < 0.1%, respectively; a single magnetite analysis (Tulloch unpubl.) from the Separation Point Batholith (P45888, Table 1) yields < 0.1% TiO_2.

Results for two other major groups of rocks are also presented in Table 1. Various basaltic and lamprophyric dike rocks give high (1500–6000) readings but are volumetrically insignificant, whereas the widespread Greenland Group metasedimentary rocks give low (18–20) readings.

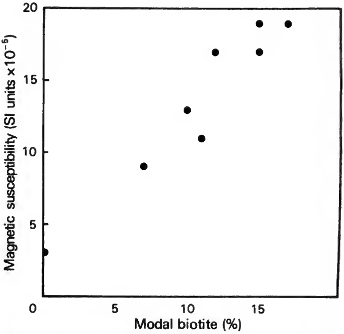

Fig. 2 Magnetic susceptibility of biotite granites from the Barrytown Pluton (Tulloch & Brathwaite 1986; Laird 1988) showing correlation with modal biotite content. New Zealand Geological Survey Petrology Collection sample nos P45600, 45605, 45608–45613, 46012. Reading errors on the susceptibility meter are considered to be ± 1. Biotite modes were obtained from point counts of 50 × 35 mm thin sections. Grain size is mostly in the range 0.5–2.5 mm, and a minimum of 1200 points per thin section were counted.

The "biotite effect", and pyrrhotite, in S-type granites

There is a slight tendency for more mafic (biotite-rich) S-type granitoids to give higher susceptibility readings, despite the apparent absence of magnetite (Fig. 1).

Susceptibility measurements were made of a suite of granites from the Barrytown Pluton, (Laird 1988) for which modal analyses were available (Tulloch unpubl.). The results are plotted in Fig. 2, where susceptibilities are approximately proportional to biotite content. Pyrrhotite was identified in a polished mount of one of the samples which gave a relatively high reading (P45611*). However, as its abundance was estimated to be < 0.01% of the rock, even at the maximum of the susceptibility range for pyrrhotite recorded by Collinson (1983), its effect on the bulk-rock susceptibility will be negligible compared to that of the more abundant biotite. Ilmenite abundance is estimated to be < c. 5% of the modal biotite, and, as its susceptibility is only slightly greater than that of biotite (Collinson 1983), its effect is considered to be subordinate to that of biotite. No magnetite was observed in optical examination of a polished section of P45611, and the susceptibility values obtained are consistent with those reported for biotite in Collinson (1983). Furthermore the relatively reduced state of the biotite renders magnetite unlikely as a co-existing phase (Fe^{2+}/Fe^{3+} = 0.88 in P45611).

When crushing granitic rocks in the field and testing for magnetite with a hand magnet, the possible occurrence of pyrrhotite should not be overlooked.

*P numbers refer to the New Zealand Geological Survey (NZGS) Petrology Collection.

Susceptibility variations on the outcrop scale

Much of the susceptibility variation recorded at outcrops is probably due to variations in surface geometry. However, some outcrops studied in more detail did reveal variations on the 1–3 m scale which clearly indicated heterogeneous magnetite distribution. For example, roadside outcrops of the Separation Point Batholith in the upper Buller valley yielded values mostly in the range 200–600 (pegmatites = 20–30). The measurements were recorded on lithologically apparently homogeneous granite over an 800 m section along the main road, from M29/719443–726439 (NZMS 260 grid ref.). One rather weathered outcrop in this section (P46472) consistently yielded much lower values of 20–30. Similar weathering in many other outcrops did not greatly affect susceptibility, and investigation of a hand specimen revealed that the opaque mineral assemblage was dominated by ilmenite, with minor magnetite largely restricted to exsolution lamellae. Although the susceptibility is much lower than usual for a biotite-bearing Separation Point Suite granite, it is probably still higher than a Karamea Suite rock of similar low (2–3%) biotite content.

On a large outcrop at the base of Mitchells waterfall in the Hohonu Range of North Westland (K32/788390) the variation was mostly in the range 1600–2000, but distinctive (20–50 cm) patches rich in pinkish K-feldspar, and mafic xenoliths, were both in the range 3000–4000. A similar effect was observed at Totaranui (N25/105433) in the Separation Point Batholith, where 30 cm diameter K-feldspar-rich clots have susceptibilities of c. 2000, compared with 1200–1500 in the surrounding granite. I consider that these clots represent aggregates of early-formed crystals including magnetite. Such intrapluton variations have not been systematically

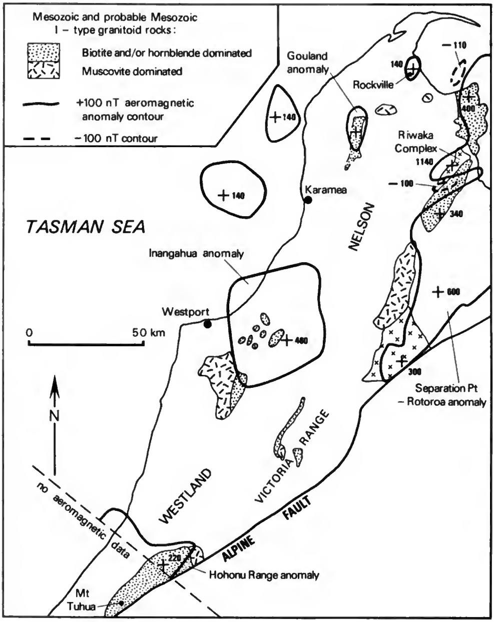

Fig. 3 Geological map of North Westland–Nelson showing relationship of Mesozoic I-type granites to aeromagnetic anomalies (> 100 nT) from Reilly (1970). Maxima of anomalies located are at + or – with value in nT. On-land data were collected at 3 km, offshore data at 460 m, above sea level. Mesozoic orthogneisses of the Charleston Metamorphic Group are not shown.

studied in this project, but susceptibility studies have been used in detailed studies of complex plutons which contain magnetite (e.g., Gastil et al. 1986).

Mylonitic and cataclastically deformed magnetite-bearing rocks were observed to have susceptibilities up to 75% lower than their adjacent protoliths. For example, mylonitic rocks (i.e., rocks plastically deformed, at temperatures exceeding 300–350°C) in Thirsty Creek (K32/915378), near Rotomonau, yield readings of 700–1000. The rocks considered to be their undeformed equivalents (Hohonu Range and Jays Creek granodiorites; Table 1) give readings of 1400–2500. Cataclastic deformation bands, 0.5–1 m wide, and rich in epidote, cutting Hohonu Range granodiorite in Mitchells waterfall yield readings as low as 400 compared to the adjacent granodiorite readings in the range 1600–2000.

Hydrothermal alteration in which new magnetite is formed, or existing magnetite is altered to other Fe-oxides/hydroxides, may increase or decrease susceptibilities. In the aureoles of lamprophyric dikes at Mitchells waterfall and nearby Camp Point, susceptibilities drop from c. 2000 in the unaltered granodiorite to c. 400 adjacent to the dikes. The effect extends c. 40–50 cm out from the dikes, over which distance the rocks are moderately fenitised, so measurements to characterise the bulk volume of granites should not be made in the vicinity of dikes.

Conversely alteration of the aegirine-riebeckite granite dike at Sams Creek (Takaka) locally increases susceptibilities from 10–20 to c. 3000 where hydrothermal magnetite has replaced mafic minerals, in an early stage of hydrothermal alteration.

AEROMAGNETIC ANOMALIES OF NORTH WESTLAND–NELSON

Review of observed anomalies

Aeromagnetic maps (Reilly 1970—1:250 000, 9 km line spacings) of the Nelson–North Westland foreland define four main anomalies > 100 nT (Fig. 3). The relationship between these anomalies and the rocks that underlie them is discussed below. The following discussion is based on induced magnetisation (i.e., susceptibility) data only. However, the

few data on remanent magnetisation that are available suggest that induced magnetisation (*Ji*) is approximately equal to, or greater than, remanent magnetisation (*Jr*) for the rocks in question. Thus Hunt & Nathan (1976) reported that for Berlins Porphyry, McIntosh Monzodiorite, and Buller lamprophyre dikes, *Ji* (A/m) = 0.479, 5.54, and 2.86, respectively, while *Jr* (A/m) = 0.181, 8.21, and 2.46, respectively.

Separation Point–Lake Rotoroa

This extensive anomaly is largely related to the Rotoroa Igneous Complex and its presumed extension under the Moutere gravels (Hunt 1978) and the Riwaka Complex. However, much of the western edge of the anomaly is underlain by, and apparently related to, magnetite-bearing biotite and hornblende-biotite I-type granites of the Separation Point Batholith. Low values over the central part of the Separation Point Batholith due east of Karamea are probably due to a dipolar effect from the intense Riwaka Complex magnetic anomaly to the north. Although the southern segment of the Separation Point Batholith lies outside the anomaly, much of this segment comprises muscovite-bearing granites, in which magnetite is low or absent (e.g. Table 1 samples P901, P46102) because of the paucity of Fe in these relatively highly evolved rocks.

Mt Gouland

A small anomaly, with a maximum of 240 nT, is situated on the northeastern margin of the Karamea Batholith. Although not mapped in detail, most granitoid samples (c. 20) available in the NZGS Petrology Collection from within the anomaly, have I-type characteristics and susceptibilities in the range 250–4000 (av. 1300). These values are much higher than the surrounding Karamea Suite granites and Lower Paleozoic sedimentary rocks, and the I-type granites are considered to be the source of the aeromagnetic anomaly. Parallelism of the anomaly with the trend of the Separation Point Batholith (and the Separation Point Suite Mo-granite belt) strengthens the association, although the anomaly is based only on three flight lines of data. The only mafic dike rocks in the collection were a dolerite and a basalt, with susceptibilities of 1500 and 600.

Inangahua

This magnetic anomaly has been attributed to a hypothetical source body for camptonitic lamprophyres by Hunt & Nathan (1976) but they also considered the McIntosh Monzodiorite (Separation Point Suite) to be a possible source. However, recent structural studies (Tulloch & Kimbrough in press) suggest that much of the area immediately north of the lower Buller Gorge is allocthonous (i.e., it has been detached from its originally contiguous middle/upper crust and is now tectonically juxtaposed on uplifted lower/middle crust). This strongly suggests that the Berlins Porphyry and McIntosh Monzodiorite are "rootless", and are unlikely to be directly related to the rocks responsible for the Inangahua magnetic anomaly.

Hohonu Range

This anomaly, for which only partial aeromagnetic map coverage is available, is also associated with camptonitic lamprophyre dikes, and an origin similar to that for Inangahua has been proposed by Hunt & Nathan (1976). However, other magnetic rocks do occur in the region (cf. Hunt & Nathan) in the form of relatively highly magnetic I-type granites of the Rahu Suite, which dominate the Hohonu Range, as well as the ranges south to, and including, Mt Tuhua (e.g., samples P45924, P45154, P46002, Table 1). The average susceptibility of the lamprophyric rocks is marginally greater than that for the granitoids, but they only account for < 5% of the exposed rocks (Hamil 1972).

Less intense anomalies also occur near Rockville in Golden Bay and off the coast near Karamea. The former is obscured by upper Cenozoic sediments but could possibly be related to an extension of the Central Sedimentary Belt (Cooper 1979). A 45 nT anomaly over the Victoria Range is probably related to the I-type Ripsaw, Mt Ross, and Macey plutons (Table 1) (Tulloch 1979), but lamprophyre dikes also occur, although less frequently than in the Inangahua and Hohonu areas. The magnitude of the Victoria Range anomaly may have been decreased by the "dipolar effect" of the strong Inangahua anomaly to the NNW.

DISCUSSION

Although Hunt and Nathan conclude that the Inangahua and Hohonu magnetic anomalies are related to hypothetical lamprophyre source magma chambers, I suggest that the correlation of at least some of the positive anomalies with I-type granitoids is significant. As remanent magnetisation has not been measured, the susceptibility values cannot be used directly in interpretation of the aeromagnetic anomalies. However, remanent magnetisation is likely to be of similar magnitude to the measured induced component (see above), and the orientation of the dipolar effect south of the Inangahua and Gouland anomalies suggests that the remanent component is indeed approximately in the same direction as the induced component (i.e. normal). Furthermore, magnetostratigraphic data (Haq et al. 1987) indicate that > 75% of the period of Early Cretaceous plutonism was magnetically normal, and the paleomagnetic data of Grindley & Oliver (1979) indicate that < 50° of rotation has occurred since the Late Cretaceous. Thus, the susceptibility values should be approximately proportional to the intensity of the anomalies.

The association of lamprophyres with such anomalies may in fact be secondary in nature, that is, the lamprophyre swarms appear to be closely associated with the Rahu Suite I-type granites, as the three main lamprophyre swarms (Inangahua, Hohonu and Victoria) are also centres of Rahu Suite plutonism. Conversely, most mafic dikes intruding the Greenland Group are basalts. The Gouland anomaly and the Separation Point Batholith apparently completely lack lamprophyres, and only scarce basaltic dikes are reported. Worldwide, there is recognised a general association of lamprophyres with slightly older granitoid rocks (Carmichael et al. 1974). This relationship may only be circumstantial, with the lamprophyres following fractures produced earlier by the granites, and possibly deriving some secondary "volatile additives" (Rock 1977) from a long-lived, deep, hydrothermal circulation system set up by the passage of the hot granites to the upper crust. However, the apparent association of some lamprophyres with a particular type of granite (equivalent to the "I-Caledonian" of Pitcher (1982) i.e., Caledonian granites in the U.K., Rahu Suite in N.Z.) may suggest a more direct relationship, as recently proposed (Macdonald et al. 1986) for Caledonian magmatism in the U.K.

Although there is some evidence (Cooper 1986) for the existence of a lamprophyre source body under the Haast swarm, a significant local increase in metamorphism, which would be expected in the exposed rocks only 2 km above a body of any significant size, is not evident in the metamorphic map of Cooper (1974). Furthermore, if such a body as shallow as 2 km at Haast only gives rise to 40 nT anomalies, then a similar body 10 km deep (Hunt & Nathan) at Inangahua is unlikely to contribute a significant component of the observed 400 nT anomaly.

In summary, I conclude that where lamprophyres occur as the sole magnetic rocks, as at Haast, the anomalies are weak; where magnetite-bearing granites occur on their own (Separation Point, Gouland) moderate anomalies are produced. The largest anomalies (Inangahua and Hohonu Ranges) are associated with the proximity of both lamprophyres and magnetite-bearing granites, although it is unlikely that the Berlins Porphyry and McIntosh Monzodiorite contribute significantly to the Inangahua anomaly.

CONCLUSIONS

1. The presence of magnetite in rocks can be readily ascertained in the field (or laboratory) with a light-weight portable magnetic susceptibility meter.
2. Most Mesozoic granites in Westland–Nelson contain magnetite; conversely no magnetite-bearing granites of Paleozoic age are known.
3. Weak susceptibilities measured in S-type granites of the Karamea Suite are proportional to biotite and considered to be due to biotite. Pyrrhotite is common in such granites but occurs in amounts too small to be measured by the equipment used in this study.
4. Some aeromagnetic anomalies in Westland–Nelson may be due, at least in part, to associated magnetite-bearing I-type granites.

ACKNOWLEDGMENTS

This work was stimulated by that of John Cobbing (British Geological Survey) and Gordon Gastil (San Diego State University). For help in the field, discussion, and advice I am grateful to Gordon Gastil, Brent Fry, Trevor Hunt, Bob Brathwaite, and, in particular, Peter Oliver. The manuscript was critically read and greatly improved by Alan Cooper (Otago University), John Cassidy (Auckland University), and Trevor Hatherton (Geophysics Division, DSIR). I am also grateful to Alison Lee for processing my scrawl into words, and Geoff Gregory for editorial comments.

REFERENCES

Carmichael, I. S. E.; Turner, F. S.; Verhoogen, J. 1974: Igneous petrology. New York, McGraw-Hill. 739 p.

Chappell, B. W.; White, A. J. R. 1974: Two contrasting granite types. *Pacific geology 8*: 173–174.

Collinson, D. W. 1983: Methods in rock magnetism and paleomagnetism. London, Chapman and Hall. 503 p.

Cooper, A. F. 1974: Multiphase deformation and its relationship to metamorphic recrystallisation at Haast River, South Westland, New Zealand. *New Zealand journal of geology and geophysics 17*: 855–880.

————1986: A carbonatitic lamprophyre dike swarm from the Southern Alps, Otago and Westland. *Royal Society of New Zealand bulletin 23*: 313–336.

Cooper, R.A. 1979: Lower Paleozoic rocks of New Zealand. *Journal of the Royal Society of New Zealand 9*: 29–84.

Gastil, G.; Diamond, J.; Knaack, C. 1986: The magnetite-ilmenite line in peninsular California. *Geological Society of America abstracts with programs 18*: 109.

Grindley, G. W.; Oliver, P. J. O. 1979: Paleomagnetism of Upper Cretaceous dikes, Buller Gorge, North Westland, in relationship to the bending of the New Zealand Orocline. *Royal Society of New Zealand bulletin 18*: 131–147.

Hamil, L. J. 1972: Geology of the western Hohonu Range, north Westland. Unpublished B.Sc. (Hons) thesis, lodged in the Library, University of Otago, Dunedin.

Haq, B. U.; Hardenbol, J.; Vail, P. R. 1987: Chronology of fluctuating sea-levels since the Triassic. *Science 235*: 1156–1167.

Hunt, T. 1978: Stokes magnetic anomaly system. *New Zealand journal of geology and geophysics 21*: 595–606.

Hunt, T.; Nathan, S. 1976: The Inangahua magnetic anomaly, New Zealand. *New Zealand journal of geology and geophysics 19*: 395–406.

Ishihara, S. 1977: The magnetite-series and ilmenite-series granitic rocks. *Mining geology 27*: 293–305.

Kimbrough, D. L.; Tulloch, A. J. in press: Early Cretaceous age of orthogneiss from the Charleston Metamorphic Group, New Zealand. *Earth and planetary science letters.*

Laird, M.G. 1988: Sheet S37—Punakaiki. Geological map of New Zealand 1:63 360. Wellington, New Zealand. Department of Scientific and Industrial Research.

Macdonald, R.; Rock, N. M. S.; Rundle, C. C.; Russell, O. J. 1986: Relationships between late-Caledonian lamprophyric, syenitic and granitic magmas in a differentiated dyke, southern Scotland. *Mineralogical magazine 50*: 547–557.

Nathan, S. 1974: Petrology of the Berlins Porphyry: a study of the crystallisation of granitic magma. *Journal of the Royal Society of New Zealand 4*: 463–483.

Pitcher, W. S. 1982: Granite type and tectonic environment. *In*: Hsu, J. K. *ed.* Mountain building processes. London, Academic Press.

Reilly, W. I. 1970: Sheets 15—Buller, 18—Hurunui and 13—Golden Bay. Magnetic map of New Zealand 1:250 000. Total force anomalies. Wellington, New Zealand. Department of Scientific and Industrial Research.

Rock, N. M. 1977: The nature and origin of lamprophyres: some definitions, distinctions and derivations. *Earth science reviews 13*: 123–169.

Shandley, P. D.; Bacon, L. O. 1966: Analysis for magnetite utilizing magnetic susceptibility. *Geophysics 31*: 398–409.

Tulloch, A. J. 1979: Plutonic and metamorphic rocks of the Victoria Range segment of the Karamea Batholith, southwest Nelson, New Zealand. Unpublished Ph.D. thesis, lodged in the Library, University of Otago, Dunedin.

————1983: Granitoid rocks of New Zealand: a brief review. *Geological Society of America memoir 159*: 5–20.

————1988: Batholiths, plutons and suites: nomenclature for granitoid rocks of New Zealand. *New Zealand journal of geology and geophysics 31*: 505–509.

Tulloch, A. J.; Brathwaite, R. L. 1986: Granitoid rocks and associated mineralisation of Westland–Nelson, New Zealand. *New Zealand Geological Survey record 13*: 65–92.

Tulloch, A. J.; Kimbrough, D. L. in press: The Paparoa Metamorphic Core Complex, South Island New Zealand: Cretaceous extension associated with the fragmentation of the Pacific margin of Gondwana. *Tectonics.*

Whalen, J. B.; Chappell, B. W. 1988: Opaque mineralogy and mafic mineral chemistry of I- and S-type granites of the Lachlan fold belt, southeast Australia. *American mineralogist 73*: 281–296.

Whiteford, C. M.; Lumb, J. T. 1975: A catalogue of physical properties of rocks. Vol. 3: listing by rock type. *Geophysics Division report 107*. Wellington, New Zealand. Department of Scientific and Industrial Research.

New Zealand Journal of Geology and Geophysics, 1989, Vol. 32: 205–216
0028–8306/89/3202–0205 $2.50/0

Aranuian radiocarbon dates from moraines in the Mount Cook region, New Zealand

C. J. BURROWS
Plant Science Department
University of Canterbury
Private Bag
Christchurch, New Zealand

Abstract 18 new radiocarbon dates were obtained for organic materials, associated mainly with soils buried by till, from sites in the lateral moraines of Mount Cook glaciers, particularly the Tasman. The 23 New Zealand (i.e., Institute of Nuclear Sciences, DSIR, Lower Hutt) dates now available from the Tasman Glacier, taken at face value, indicate that there were glacier expansion periods there about 3450–3000, 2280, 1800–1620, 1200–900, 860, 680, 340, and < 250 radiocarbon years ago. Taking into account the statistical counting error, the ages of some of the date sets overlap. Excluding a few problematical age determinations, and those on whole soil samples, the full range of dates now available from moraines of Mount Cook glaciers (including those from the New Zealand laboratory and a laboratory in Hannover, West Germany), taken at face value, shows that glacier expansion episodes have occurred: c. 8000 years ago, probably in the 6th millennium B.P., c. 3690–3000, c. 2550–2280, c. 2110–1620, c. 1255–900, c. 860, c. 680, c. 550, c. 340, and < 250 radiocarbon years ago.

The dates and the associated geomorphic evidence indicate that the glacier shrinkage which ensued from about A.D. 1900 to at least A.D. 1984 has been the most profound for at least the last 3500 years.

Keywords C–14; dates; Mount Cook; glaciers; moraines; Tasman Glacier; chronology; glacier expansion; glacier shrinkage; erosion; collapse; paleomoraine surfaces; paleosols

INTRODUCTION

Plant remains and soils are buried and preserved in glacial moraines, particularly through plastering of ice-marginal debris over pre-existing surfaces, as glacier levels rise during expansion periods (Burrows 1973). Nine radiocarbon dates from the Mount Cook region were earlier reported from samples taken from sites exposed by glacier shrinkage and subsequent erosion in the lateral moraines of the Tasman and Mueller Glaciers and from a moraine in Black Birch Creek (Burrows 1973, 1980). This paper reports 18 additional dates from the Tasman, Ball, Mueller, and Hooker Glaciers; 5 were briefly described by Burrows & Gellatly (1982) and another 4 by Gellatly (1982). The work resulted from visits to the region in November–December 1980 and November 1981. The dates reported here and in Burrows (1973, 1980) were all obtained at the Institute of Nuclear Sciences laboratory, Lower Hutt, New Zealand.

Other dates from samples collected from moraines of the Mount Cook glaciers have recently been published (Gellatly et al. 1985; Röthlisberger 1987). The dated samples were collected by F. Röthlisberger and A. Gellatly early in 1980 and processed at the Niedersachsisches Landesamt für Bodenforschung, Hannover, West Germany. Some of them were obtained from the same general localities as the samples which are listed here, but for only a few is it possible to be sure that exactly the same horizons were sampled. Comparisons are made later, in the discussion.

The dates are presented in Table 1 according to the half-life for radiocarbon of 5568 years (old $T^1/_2$), the half-life of 5730 years (new $T^1/_2$), and the latter, also corrected for secular variation in the formation of radiocarbon. In the text, only the uncorrected dates, according to the 5568 year half life, are referred to (i.e., "radiocarbon years").

BALL GLACIER: BALL BLUFF SITE

The Ball Glacier is a west bank tributary of the Tasman Glacier, 10 km upvalley of the Tasman's terminus (Fig. 1). The Ball Glacier surface, in A.D. 1883, near the confluence of the two glaciers, was above the level of a high moraine crest (about 1070 m above sea level), (Green 1883) and it remained high there until about 1930. By 1981 it had shrunk some 90–100 m below this level and there had been considerable lateral erosion of the ice-marginal deposits (in places back to bedrock). About 100 m up the southern side of the valley of the Ball Glacier from the old Ball Hut site, the glacier shrinkage revealed soil layers and remains of vegetation which had been buried as the glacier volume increased after a previous period of shrinkage (Fig. 2). In 1981 the glacier surface was 40–50 m below the lowest observed organic deposit. The soil and plant remains form a discontinuous mantle over steep (25 –45°) bedrock, firm bouldery till, and possible kame or colluvial deposits, which formed the ancient sidewall of the glacier valley. In this locality there is no well-defined lateral moraine.

All of the dates obtained (NZ 5501, 3220 ± 60 years B.P.; NZ 5502, 3220 ± 80 years B.P.; NZ 5503, 3130 ± 80 years B.P.; and NZ 5508, 2990 ± 100 years B.P.) may record the same episode of rise of the glacier surface during a single expansion period (Fig. 3). Although they form a chronological sequence from bottom to top, the ranges of the dates (± 2 standard deviations) overlap. It is likely that glacier expansion

Received 28 July 1986, resubmitted 28 October 1987, accepted 25 July 1988

began to bury soil and vegetation about 3200 radiocarbon years ago and that the ice surface rose progressively higher to reach a level near or above the highest position reached in A.D.1880–1890. There is no indication from this site of any fluctuations of the Ball Glacier during the period 3200 radiocarbon years ago to A.D. 1880, although this is likely, from other evidence to be considered later.

Prior to 3200 radiocarbon years ago the north-facing valley-wall slope at Ball Bluff was densely clad in vegetation containing *Podocarpus nivalis* (and probably other shrubs and herbs including *Chionochloa* spp., which usually accompany it on such sites), under which a mature steepland soil had formed. Stems of *P. nivalis*, up to 2 m long and 100 mm in diameter, were observed. The exposed paleosol, where it is still intact, consists of a thin, dark-grey, organic, silty A horizon over a yellowish-brown, sandy, silty B horizon, up to 30 cm thick (Table 2). In many places only a truncated B horizon remains. The maturity of the subsoil indicates a long period of undisturbed soil formation (cf. data in Gellatly 1982). The A and B soil horizons at this site (Table 2), and others to be described later, are predominantly silty and sandy, often with few or no coarser clasts.

TASMAN GLACIER: OLD BALL HUT SITE

As the ice support has been lost during glacier shrinkage, the lateral moraines of the Tasman Glacier near the Ball Hut site, at and just south of the Ball Glacier confluence, have begun to collapse. Extensive fissuring and minor fault-scarp formation is evident. The slump features occur at intervals uphill, forming a complex series of large subhorizontal cracks on the valley wall colluvial cones, and even on the bedrock of the dividing ridge between the Ball and Tasman Glaciers c. 500 m above the glacier surface. On the proximal side of the right-lateral moraine of the Tasman Glacier, deep and very steep (30–60°) gullies, with intervening sharp ridges, have been eroded in the firm till (Fig. 4). Paleosols and vegetation remains are exposed along the collapse scarps and eroded proximal moraine surfaces.

In the absence of precise levelling, and because of the variable amounts of vertical collapse, it is often difficult to relate the levels of organic deposits and soils to previous positions of lateral moraine crests or any fixed points. Thus, although during the fieldwork careful estimates were made of positions of dated deposits, in relation to the uppermost

Table 1 Radiocarbon dates from the Mount Cook region.

Laboratory no.	Dates (years B.P.) Old $T^1/_2$	New $T^1/_2$	New $T^1/_2$ corrected	Material	Stratigraphic position	Significance
Tasman Glacier: Ball Bluff site (grid ref. H36/832278, altitude 1050–1085 m)						
NZ 5501	3220 ± 60	3320 ± 60	3520 ± 90	Branches from soil surface	38 m below crest of A.D. 1880 ice limit, 40 m above present glacier.	Series of dates for a glacial expansion which progress-sively buried a soil and vegetation; they postdate a period of soil and vegetation development.
NZ 5502	3220 ± 80	3310 ± 80	3520 ± 90	Branches from soil surface	18 m below crest of A.D. 1880 ice limit.	
NZ 5503	3130 ± 80	3220 ± 80	3410 ± 80	Branches from soil surface	15 m below crest of A.D. 1880 ice limit.	
NZ 5508	2990 ± 100	3080 ± 110	3260 ± 160	Soil, peaty organic matter and twigs	12 m below crest of A.D. 1880 ice limit.	
Tasman Glacier: Old Ball Hut site (grid ref. H36/832278 – 835285, altitude 1015 –1065 m)						
NZ 5335	2280 ± 50	2350 ± 50	2410 ± 80	Branches from soil surface	Proximal side of a fossil moraine, 50 m below moraine crest.	Dates a period of glacial expansion; postdates a period of soil and vege-tation development.
NZ 5507	1195 ± 105	1230 ± 110	1175 ± 11	Branches from soil surface	On a fossil moraine crest 3 – 5 m below moraine crest.	Dates a period of glacial expansion; postdates a period of soil and vegetation development; assumed to be the same surface as for NZ 5505.
NZ 5505	1035 ± 60	1065 ± 65	1015 ± 65	Branches from soil surface	Proximal side of fossil moraine, 12–20 m below moraine crest (which is much eroded).	Dates a period of glacial expansion: postdates a period of soil and vegetation development
NZ 5506	< 250	< 250	–	Branches from soil surface	Beneath deposit of flow till 2.5m below its surface.	Dates a period of glacial expansion.
NZ 5504	< 250	<250	–	Twigs and organic soil	Former moraine surface 2 m below moraine crest.	Dates a period of glacial expansion.

(Continued on facing page)

moraine crest (A.D. 1880), there may be some elevational discrepancies between the estimated positions of particular horizons and those recorded in earlier studies (Burrows 1980).

Figure 5 shows the two main localities near the old Ball Hut site (northernmost) and the present Ball Shelter (southernmost). Most of the exhumed paleosurfaces which can be observed in this locality represent former proximal sides of lateral moraines; a few are crests, or distal sides of the lateral moraines. One locality near Ball Shelter (X in Fig. 5) is a place where an outflow of debris from the glacier surface occurred through a depression in the moraine, burying a soil and vegetation (Fig. 6). The dates so far obtained from these sites (including those given in Burrows 1980) fall into five sets (about 2280, 1800, 1110, 680, and <250 years B.P.). The dates within each set overlap (± 2 s.d.).

The surfaces that were dated had existed long enough for vegetation to grow on them (often on both their proximal and distal faces) and for soils to develop (Fig. 6, 7, 8, 9). The main plant species, identified from wood, leaf and other plant remains, are *Podocarpus nivalis* and *Phyllocladus alpinus*. A few mosses and herbaceous angiosperm species have also been identified. On the paleosurfaces dated 2280 ± 50 years B.P. (NZ 5335) and 684 ± 48 years B.P. (NZ 711), *P. nivalis* was very abundant on the proximal side of the moraine. At one locality near Ball Shelter, in November 1981, remains of a *P. alpinus* shrubbery, in situ, dated 1035 ± 60 years B.P. (NZ 5505), was in view on the exhumed proximal side of the fossil lateral moraine (Fig. 9).

Each individual paleomoraine surface, with plant remains and soils on proximal and distal faces, indicates that, after a period of moraine construction during a glacier expansion period, the glacier then shrank downward below the crest. The lengths of glacier contraction periods are difficult to determine, although the development of yellow-brown soil B horizons (Table 2) as well as shrubby vegetation cover on moraine surfaces, suggest an elapse of at least hundreds of years between some of the expansion periods. Subsequently the moraines were overwhelmed as the ice level rose again and till or other ice-marginal debris was deposited, encasing and preserving the plant remains and soil. As the moraines presently erode or collapse, the outlines of the former moraine surfaces are often revealed by the soils, or sometimes by lines of yellowish, weathered cobbles and boulders. Complete profiles of some fossilised moraine crests are evident (Fig. 7). They were preserved by rises of the glacier level high enough

Table 1 *(Continued)*

Laboratory no.	Dates (years B.P.) Old $T^1/_2$	New $T^1/_2$	New $T^1/_2$ corrected	Material	Stratigraphic position	Significance
Tasman Glacier: Novara site (grid ref. H36/867459 – 460, altitude 1005 –1050 m)						
NZ 5334	3450 ± 80	3550 ± 80	3810 ± 110	Branches from soil surface	70 m below crest of moraine, 40 m above present glacier.	Dates a glacial expansion; postdates a period of soil and vegetation development.
NZ 5333	3360 ± 110	3460 ± 120	3690 ± 140	Soil-like apparently water-laid deposit	43 m below moraine crest.	Enigmatic; may date soil material which has been redeposited after moraine disturbance.
NZ 5500	1660 ± 65	1710 ± 65	1645 ± 70	Twigs from above soil	21.5 m below moraine crest.	Dates a glacial expansion; postdates a period of soil and vegetation development; assumed to be the same surface as for NZ 5332.
NZ 5332	1620 ± 65	1670 ± 65	1600 ± 65	Branches from soil surface	26 m below moraine crest.	Dates a glacial expansion; postdates a period of soil and vegetation development.
NZ 5254	933 ± 58	961 ± 60	–	Soil	14.0 m below moraine crest.	Dates a soil which was buried by a glacial expansion; assumed to be the same surface as for NZ 5331.
NZ 5331	864 ± 58	889 ± 60	841 ± 63	Branches from soil surface	17 m below moraine crest.	Dates a glacial expansion; postdates a period of soil and vegetation development.
NZ 5330	343 ± 56	353 ± 58	425 ± 58	Branches from soil surface	10.5 m below moraine crest.	Dates a glacial expansion; postdates a period of soil and vegetation development.
Mueller Glacier: Left-lateral moraine (grid ref. H36/753191, altitude 920 m)						
NZ 5329	1130 ± 45	1160 ± 45	–	Soil	14 m below moraine crest, 90 m above present glacier.	Dates a glacial expansion; postdates a period of soil and vegetation development (cf. NZ 4507, Burrows1980).
Hooker Glacier: Hooker Hut site (grid ref. H36/775398, altitude 1080 m)						
NZ 5253	684 ± 57	705 ± 59	–	Sedge leaves from above soil	On 3 m+ sand; beneath 13 cm sandy soil buried by >3 m of coarse colluvium; in trough on distal side of moraine, 60 m above present glacier.	Minimal age for lateral moraine and dates burial of soil by snow avalanche-deposited debris.

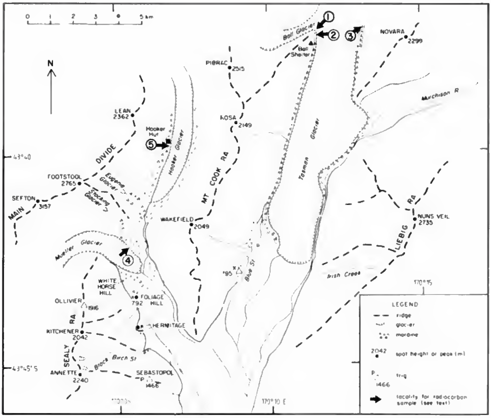

Fig. 1 Localities of radiocarbon sample sites mentioned in the text.

Fig. 2 Exhumed soil with wood (arrows), Ball Bluff site, here dated 3220 ± 60 years B.P. (NZ 5501).

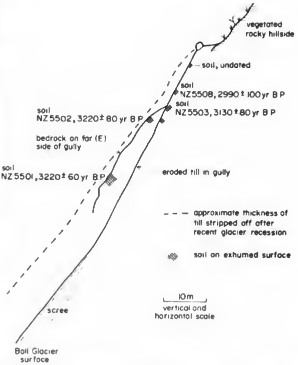

Fig. 3 Diagram of Ball Bluff site with exposures of exhumed soil with wood.

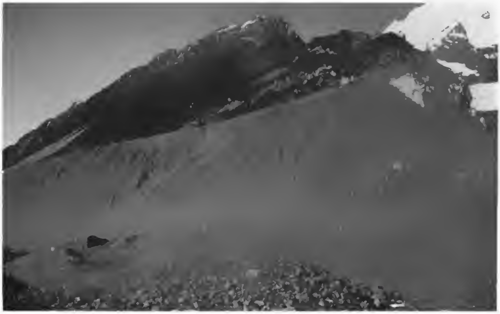

Fig. 4 View of proximal side of Tasman Glacier west lateral moraine, near the Old Ball Hut site, from the surface of the Tasman Glacier. Ball Bluff is on the right. Note slump cracks on slopes above the moraine.

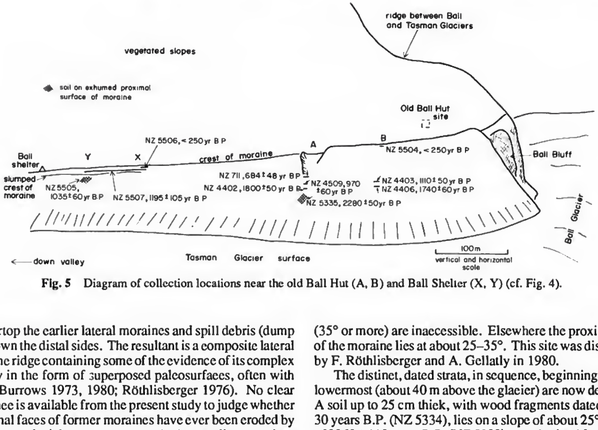

Fig. 5 Diagram of collection locations near the old Ball Hut (A, B) and Ball Shelter (X, Y) (cf. Fig. 4).

to overtop the earlier lateral moraines and spill debris (dump till) down the distal sides. The resultant is a composite lateral moraine ridge containing some of the evidence of its complex history in the form of superposed paleosurfaces, often with soils (Burrows 1973, 1980; Röthlisberger 1976). No clear evidence is available from the present study to judge whether proximal faces of former moraines have ever been eroded by fluvial or glacial processes, or whether earlier moraines underwent any collapse, prior to the processes which are occurring now. Evidence of possible disturbance of paleosurfaces is outlined in the discussion.

TASMAN GLACIER: NOVARA SITE

On the eastern side of the Tasman Glacier, beneath the slopes of Mt Novara, erosion and a collapsed section of lateral moraine have exposed soil and plant remains extending about 300 m along the moraine (Fig. 10, 11, 12). At the northern end of the exposure, soil profiles on very steep bedrock and till (35° or more) are inaccessible. Elsewhere the proximal face of the moraine lies at about 25–35°. This site was discovered by F. Röthlisberger and A. Gellatly in 1980.

The distinct, dated strata, in sequence, beginning with the lowermost (about 40 m above the glacier) are now described. A soil up to 25 cm thick, with wood fragments dated 3450 ± 30 years B.P. (NZ 5334), lies on a slope of about 25°. A date of 3360 ± 110 years B.P. (NZ 5333) was obtained from a thin, horizontal, yellow-brown, soil-like layer 27 m higher. This horizon seems unrelated to the lower soil. Unlike the buried paleosols in the moraines, it appears to have been deposited by water.

Next in sequence are soil exposures, about 33 m and 38 m, respectively, above the lowermost soil, but about 250 m further south. Two dates from wood, 1620 ± 65 (NZ 5332) and 1660 ± 65 years B.P. (NZ 5500), are interpreted as being for separate exposures of one soil. Two dates 864 ± 58 (NZ 5331), for wood, and 933 ± 58 years B.P. (NZ 5254), for soil, were obtained from soil exposures 4 m and 7 m higher,

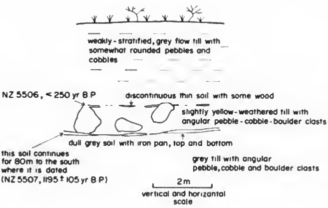

Fig. 6 Diagram of exposure at X, Fig. 5, showing a lower soil (dated 1195 ± 105 years B.P., NZ 5507 at position 80 m to the south) and an upper soil, with wood, dated < 250 years B.P. (NZ 5506). The latter had been buried by flow till extruded through a depression in the former moraine.

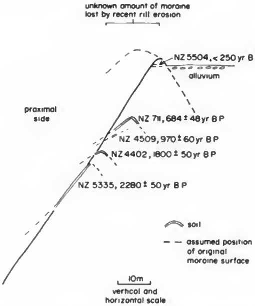

Fig. 8 Composite diagram of buried soils and former moraine surfaces at A, Fig. 5.

Fig. 7 Exposure in gully at A, Fig. 5, showing former lateral moraine crest outlined by soil with wood (arrows), dated 684 ± 48 years B.P. (NZ 711).

Fig. 9 Exhumed soil with wood, representing a former *Phyllocladus alpinus* shrubbery (arrows), on the proximal side of a former lateral moraine at Y, Fig. 5. Dated 1035 ± 60 years B.P. (NZ 5505). Some modern plants are evident, fallen with blocks of soil from the eroded moraine crest above.

Table 2 Soil profiles from exhumed paleosurfaces in lateral moraines in the Tasman Valley (see Fig. 1 for sites).

Ball Bluff site

1. On 30° slope, 38 m below crest of moraine; near locality for sample NZ 5501.
   Till,
   A 10–15 cm greyish-brown (10YR 5/2) organic sandy silt, with branches and roots of shrubs,
   B 10–30 cm bright yellowish-brown (10YR 5/8–6/6) sandy silt with some angular pebbles near the base, on pale brown-weathered (10YR 6/3) bedrock.

Old Ball Hut site

2. Profile exposed 2 m below crest of moraine; locality for sample NZ 5504.
   Till,
   A–C 8–15 cm slightly organic sand,
   till.
3. Profile exposed 4 m below crest of moraine; locality for sample NZ 5507.
   Bluish-grey till,
   A 5–10 cm dark brown (10YR 3/3) organic sandy silt,
   BG 5–8 cm pale grey (10YR 5/1–5/2) stony sandy silt with small pieces of wood (?roots),
   2 mm iron pan,
   dull grey till.
4. On 25–30° slope 14 m below crest of moraine; near locality for sample NZ 5505.
   Till,
   A 10 cm dark brown (10YR 3/3) organic sandy silt,
   B 20 cm brown to dark yellowish brown (10YR 4/3–4/4), or dark greyish brown (10YR 4/2) sandy silt with thin (2 mm) iron pan top and bottom,
   till.

Novara site

5. Profile exposed 17 m below crest of moraine; locality for sample NZ 5331.
   Till,
   A–C 5–20 cm greyish-brown (10YR 5/2) organic silty sand with small branches and roots,
   thin (3 mm) iron pan,
   till.
6. Profile exposed 26 m below crest of moraine; locality for sample NZ 5332.
   Till,
   B 10–40 cm brown to yellowish brown (10YR 5/3–5/4) sandy silt with some stems or roots of shrubs,
   till.
   [N.B. this is a truncated profile, lacking an A horizon].
7. Profile exposed 70 m below crest of moraine; near locality for sample NZ 5334.
   Till,
   A–C 10 cm dark greyish brown to brown (10YR 4/2–4/3) sandy silt, mottled light brownish grey (10YR 6/2), with some brown organic patches and thin (2 mm) iron pan top and bottom.

respectively, than the higher of the previous two dated horizons. These, also, are judged to be from separate exposures of one soil. The older, soil, date is judged to be less precise than that for wood. Finally, some 3.5 m higher than the uppermost of the last two dated horizons, and 10.5 m below the present moraine crest, a date of 343 ± 45 years B.P. (NZ 5330) was obtained for wood, on a soil. The fossil wood from the Novara site includes *Podocarpus nivalis* and *Phyllocladus alpinus*.

The reconstructed, composite sequence of buried paleomoraine surfaces at the Novara site is shown in Fig. 12. Taken at face value (and excluding NZ 5333), the dates fall into four sets (about 3450, 1650, 860 and 340 years B.P.). However, when the Novara dates are compared with the Ball Bluff – Ball Hut dates (Table 3), some of the sets overlap, within the range of the youngest and oldest date, ± 2 s.d. (1405–850, 980–748, and 780–588 years B.P.). This demonstrates the difficulty of using radiocarbon dates to pinpoint events and for correlation, when the original dates are chronologically close and have a standard deviation of 50 years or more. Judged by the stratigraphic evidence, it is probable that there were at least two distinct glacier expansion events between 1405 and 588 radiocarbon years ago.

MUELLER GLACIER

A date of 1130 ± 50 years B.P. (NZ 5329) was obtained from a thin soil lying 1 m above a more prominent soil in the left-lateral moraine of the Mueller Glacier. The latter soil is assumed to be that which gave the date 1010 ± 50 years B.P. (NZ 4507) (Burrows 1980). The dates are within the same age range and appear to indicate the same episode of glacier expansion.

HOOKER GLACIER

Some 120 m south of the Hooker Hut site on the western side of the Hooker Glacier, leaves of sedges which lay over a buried soil were dated 685 ± 57 years B.P. (NZ 5253) (Fig. 13). The soil had formed on a sand and silt layer filling a trough on the distal side of a lateral moraine crest some 60 m above the present glacier surface. The leaves and soil had been buried by a large, still active, colluvial cone which, each winter and spring, has rock debris deposited on its surface by snow avalanches. The date provides a minimal age for formation of the moraine (which A. F. Gellatly (pers. comm.) assumes to be much older, on rock weathering rind evidence). It also indicates the time of burial of the soil by snow avalanche activity which may have been more vigorous than now.

DISCUSSION

Other published dates and interpretation problems

Gellatly et. al. (1985) published 23 radiocarbon dates from moraines in the central Southern Alps, including 4 from the Ball Hut site, and 9 from the Novara site. All samples were collected early in 1980, either by F. Röthlisberger, or by Röthlisberger and A. Gellatly, and processed in the Hannover, West Germany, radiocarbon laboratory. Gellatly (1982) listed 9 more radiocarbon dates for samples also collected from lateral moraines of Mount Cook glaciers by F. Röthlisberger, or by Röthlisberger and herself (2 from Dixon, 1 from Wheeler, and 2 from Baker Glaciers, all tributaries of the Murchison Glacier; 2 from Mueller and 2 from Hooker Glaciers). These latter dates and others from Westland were published by Röthlisberger (1987).

The array of dates for the Ball Hut and Novara sites will mainly be considered here, although, by means of a composite figure (Fig. 14), comparisons are made between dates for these and other samples from the Mount Cook region. Comparisons are also made between samples where material from the same horizon was dated by both the New Zealand and Hannover laboratories (Table 4).

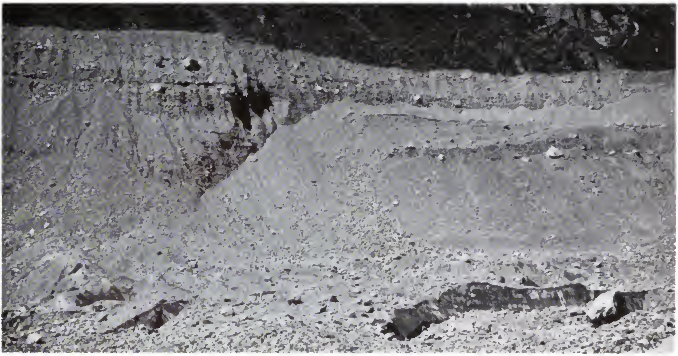

Fig. 10 View of proximal side of Tasman Glacier east lateral moraine, Novara site, from the surface of the Tasman Glacier.

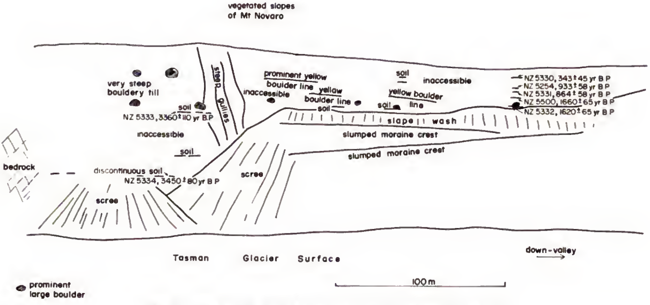

Fig. 11 Diagram of collection positions at the Novara site (cf. Fig. 10).

There are difficulties in comparing radiocarbon dates from samples processed by different laboratories. One source of between-laboratory variation is experimental error arising from standards, instrumental and operator differences. Both New Zealand and Hannover laboratories use A.D. 1950 as reference year, a $\delta^{13}C$ value of –25%, a standard of N.B.S. oxalic acid, and the results are calculated using a half-life of 5568 years for radiocarbon. Geyh et. al. (1985) mentioned six cross-check datings to test calibration accuracy between the Hannover and New Zealand laboratories. A mean difference of 90 ± 45 years was found for 5 samples, but one set of dates differed by 1000 years. The latter result was presumed by Geyh et. al. to arise from the dating of different samples. Otherwise, discrepancies between results may occur simply because the materials dated contain different amounts of radiocarbon.

For Röthlisberger and Gellatly's collections, the German laboratory did its determinations for the Mount Cook samples on either (1) humic acid from whole soil samples; (2) total organic substance from whole soil samples; or, rarely (3) wood, assumed to be contaminated by humic acid. The dated samples in the present study were almost all wood. Table 4 compares pairs of samples from each laboratory which can be assumed, with confidence, to come from the same horizons.

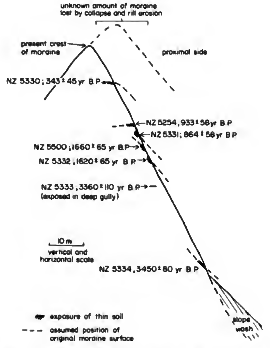

Fig. 12 Composite diagram of buried soils and former moraine surfaces at the southern end of the Novara site exposure. The maximum heights of moraines for NZ 5334 and NZ 5500–5332 are not known.

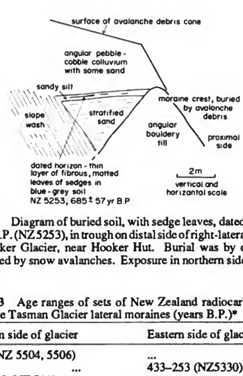

Fig. 13 Diagram of buried soil, with sedge leaves, dated 685 ± 57 years B.P. (NZ 5253), in trough on distal side of right-lateral moraine of Hooker Glacier, near Hooker Hut. Burial was by colluvium deposited by snow avalanches. Exposure in northern side of gully.

Table 3 Age ranges of sets of New Zealand radiocarbon dates from the Tasman Glacier lateral moraines (years B.P.)*

Western side of glacier		Eastern side of glacier
<250 (NZ 5504, 5506)		...
...		433–253 (NZ5330)
780–588 (NZ 711)	?	...
...		980–748 (NZ 5331)
1405–850 (NZ 4509, 4403, 4404, 4405, 5505, 5507)		...
1900–1620 (NZ 4406, 4402)?		1790–1490 (NZ 5332, 5500)
2380–2180 (NZ 5335)		...
3340–2970 (NZ 5501, 5502, 5503, 5508)		3610–3290 (NZ 5334)

*Ranges of ages given ±2 standard deviations for the oldest and youngest radiocarbon date in each set. Dates on soils omitted.
... refers to the absence of a correlative deposit.

Geyh et. al. (1985) listed the organic components for buried soils associated with moraines as being: wood and other fragments of plant material such as fine roots; humus; and "micro-residuals" (often mainly very resistant lichen fragments). Other biologically resistant organic substances accumulate in soils during humification (Paul & McLaren 1975; Matthews 1981). Thus the buried paleosols contain carbon of mixed age, which may extend over an age range of hundreds, or thousands, of years.

Radiocarbon dates on humic acids (extracted with NaOH) and total organic materials from soils were determined separately by the Hannover laboratory. There may or may not be a close relationship between radiocarbon dates for humic acid and those on total organic content from any sample. From some samples the total organic content gave substantially greater ages (1000 years or more) than did humic acid. This may merely be due to the longer residence time for the more resistant carbon, than for humic acid carbon, in the paleosol, but it may also reflect contamination by young humic acid leached from younger horizons. Wood remains and humic acid from several samples listed by Gellatly et. al. (1985) and Geyh et. al. (1985) gave similar radiocarbon ages. It seems from other results, however, that, at times, humic acids give less precise dates for the times of glacier expansion than does wood (Table 4). A date for the total organic content minus the date for humic acid from the same sample (or better still, minus the date of wood) may give an approximate age for the time that a soil had existed until it was buried by a glacial expansion episode. Matthew's (1980, 1981) results showing age gradient stratification in buried paleosols in Norwegian moraines indicate that there are serious difficulties in interpreting the whole soil radiocarbon dates, however.

Apparently out-of-sequence ages for some horizons at the Novara site (Table 4) may be the result of disturbance of the original stratigraphy. The New Zealand and Hannover dates for the lowermost soil at this site are consistent (NZ 5334, 3450 ± 90 years B.P.; H.v. 12022, 3790 ± 70 years B.P.) but the pairs of dates on horizons 27 m higher are inconsistent (NZ 5333, 3360 ± 110 years B.P.; H.v. 10496, 4605 ± 365 years B.P.; or H.v. 10498, 5690 ± 140 years B.P.). A soil horizon about 30 m higher (not dated in the present study) also

Table 4 Comparisons of radiocarbon dates from the same horizons, obtained by different laboratories. (Dates according to old T½, uncorrected.)

Site	Lab.no.	Material dated	Date (years B.P.)
Novara	NZ 5330	wood	343±45
	H.v. 12024	soil humic acid	525±55
	H.v. 10500	whole soil	765±50
Ball Hut	NZ 5335	wood	2280±50
	H.v. 12021	soil humic acid	2580±65
	H.v. 10494	whole soil	2500±55
Novara	NZ 5334	wood	3450±80
	H.v. 12022	soil humic acid	3790±70
	H.v. 10495	whole soil	4050±80
Sebastopol	NZ 4508	wood	7940±70
	H.v. 10504	wood	8040±80
Novara	NZ 5333	whole soil	3360±110
	H.v. 11257	humic acid	5185±290
	H.v. 10498	whole soil	5690±140
	H.v. 10496	whole soil	4605±365

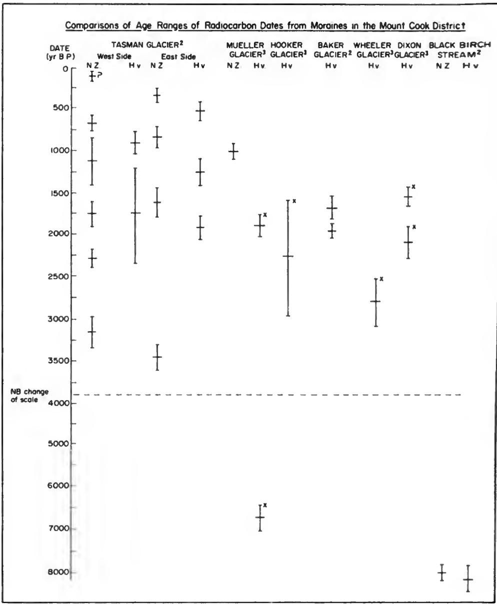

Fig. 14 Composite diagram showing age ranges of radiocarbon dates (±2 standard deviations) from lateral moraines of glaciers at Mount Cook.

1. NZ series: Burrows (1973, 1980, this study, Burrows & Gellatly (1982). H.v. (Hannover) series: Gellatly (1982), Gellatly et. al. (1985), Geyh et. al. (1985), Röthlisberger (1987). Laboratory numbers and other details are given in the text.
2. Only dates on wood (NZ) or humic acid (H.v.) are included.
3. Dates, on whole soils (marked x) included.

gives a relatively old radiocarbon age (H.v. 10499, 4125 ± 130 years B.P.) which (± 2 s.d.) is inconsistent with NZ 5333 and NZ 5334, and barely consistent with H.v. 12022; but it is consistent with H.v. 10496, (which has a large error). Thus, the interpretation of these dates is difficult. In Gellatly et. al. (1985) the numbering in column 6 of their table 1 is confused, but what they appear to mean is that the intermediate three horizons, (at the same level as NZ 5333) (H.v. 10496, H.v. 10497, H.v. 10498) possibly register two glacial expansion periods between about 5200 and 4600 radiocarbon years ago. These authors also suggest that the highest (H.v. 10499) and lowest (H.v. 12022) soil horizons represent two exposures of the same soil. There are no dates for humic acid or wood from the highest soil; the dates for whole soil (4050 ± 80 years B.P. for the lowest, H.v. 10495, and 4125 ± 130 years B.P. for the highest, H.v. 10499) are consistent with each other. Careful examination of the lowest soil, when the sample NZ 5334 was being collected, showed that the paleosurface slopes uphill at about 25° (i.e., it appears to be on a proximal paleomoraine surface). There is no field evidence to show that the surface is continuous upslope within the moraine to the position of H.v. 10499 (Gellatly's 1982 interpretation). The intermediate dated horizons, representing one or more older paleosurfaces, must be distal to such a surface (not proximal, as shown by Gellatly (1982, p. 158), and inferred by Gellatly et. al. (1985). It is likely that these problematical dated horizons are not associated with in situ paleomoraine surfaces. The NZ 5333 horizon is unusual in being a horizontal layer, indicating fluvial deposition. Gellatly et. al. (1985) and F. Röthlisberger's field notes (pers. comm.) also show that H.v. 10497 and H.v. 10496 are "sedimented B horizons". It may be that erosional disturbance, or collapse of an old moraine crest at this locality, before the formation of the soil at NZ 5334, caused redeposition of fine material containing carbon which had originated either from a soil on an old moraine, or even from a soil on the nonglacial surfaces distal to the Tasman left lateral moraine. If so, the dates for H.v. 11457, H.v. 10497 and H.v. 10496 cannot be related to glacial episodes with confidence. In view of the agreement of the ages for the lowest dated soils at Ball Bluff and Novara sites (this study) (NZ 5501, 3220 ± 60 years B.P. and NZ 5334, 3450 ± 80 years B.P., respectively) it is assumed here that these soils occur on the oldest unequivocally in situ surfaces so far discovered among the Tasman Glacier lateral moraines.

The correlations and glacial succession during the Aranuian

The moraines of the Tasman Glacier have yielded the most comprehensive array of radiocarbon dates from any New Zealand locality for buried soils indicating episodes of glacier expansion and contraction in the last 3500 radiocarbon years (cf. Burrows & Gellatly 1982, fig. 15). The interpretation of some of the dates as indicating distinct episodes of glacier oscillation is not without its problems, as outlined above. Geyh et. al. (1985) used doubled standard deviations for comparisons of sets of radiocarbon dates, according to the recommendation of the International Study Group (1982) (and cf. Geyh 1980). More elaborate statistical treatment for comparing radiocarbon dates for correlations is not warranted for the present array of dates, given the heterogeneity of dated material and the limited number of dates from any one site. Unless dates are well separated (usually at least 100 years apart and often much more, according to the specific standard deviations), they cannot be used to indicate distinct glacial episodes.

Considering only the samples on wood (this study), and those on humic acid in soils or wood (Gellatly et. al. 1985; Geyh et. al. 1985), and excluding the dates for H.v. 10496, H.v. 10497, H.v. 10498, and H.v. 11457 from the Novara site, most of the dates from the Tasman Glacier, from Hannover and New Zealand laboratories, are broadly comparable. However, the Hannover dates further complicate interpretation of the period from about 2710 to 590 years B.P. Taking all the available dates into account, there is overlap among the dates (± 2 s.d.) throughout this period. The evidence from superposed soils from Novara and Ball Hut sites shows that there were at least four and probably five distinct glacial expansion periods during this time. This emphasises the importance of using short-lived materials (like small branches or leaves) for dating if particular episodes (such as glacier expansion periods) are to be identified. Humic acid could be longer lived and composite in age over periods of hundreds of years. Only the dates on wood are accepted here as indicating ages close to the time when the soils, vegetation and moraines were overwhelmed by glacier expansion.

From the stratigraphic and vegetational evidence alone, the period before 3610–2970 radiocarbon years was a time of major recession of the Tasman Glacier. The times before 2380–2180 radiocarbon years and 1405–850 radiocarbon years were also periods when the Tasman Glacier levels were low (compared with the A.D.188 to A.D.1930 limits). The dates on whole soils and humic acid do not contradict these conclusions.

The Hannover radiocarbon dates for Mueller, Hooker, Dixon, and Wheeler Glaciers are not strictly comparable with the dates described above from the Tasman Glacier, as they were all determined on whole soils. However, one dated whole soil sample from the Mueller Glacier from a position 35 m beneath the present, truncated, left-lateral moraine crest (H.v. 10511, 6750 ± 135 years B.P.) (Röthlisberger 1987) seems to show that an expansion of the glacier buried a surface some time earlier than any of the dates from the Tasman Valley. The actual date of burial may have been as much as a thousand years after 6750 years B.P.

Taking all of the radiocarbon dates on wood or humic acid at face value, glacial expansion events have occurred in the Mount Cook region c. 8000, c. 3690–3000, c. 2550–2280, c. 2110-1620, c. 1255–900, c. 860, c. 680, c. 550, c. 340 and <250 radiocarbon years ago (Tables 1, 3). There was also an expansion period some time after 6750 years B.P. (probably in the 6th millennium B.P.). Gellatly (1982, 1985) has recognised five main periods of glacier activity in the Mount Cook region, based on the range of modal weathering rind thicknesses on surface boulders, mainly from the terminal or latero-terminal moraine complexes. They are: 8000, 5000–4000, 3500–2200, 1800–840, <500–100 years B.P. Thus there is good agreement between the radiocarbon and rock-weathering rind chronologies for the region.

Burrows (1980, 1982) claimed that the glacier contraction which has been occurring from about A.D.1900 to the present day in the Mount Cook region (and accelerating since about A.D.1950) is the greatest and/or the most prolonged of any in the last 2000 years. It is now evident that this recent period of contraction of the Tasman Glacier is the most profound of any in the last 3500 years. Moraines which are now collapsing and/or eroding rapidly contain soil and organic material showing that the Tasman Glacier began to expand at least 3500 radiocarbon years ago, after a relatively long period of recession. This expansion period built lateral moraines (apparently the original framework of the composite lateral moraine complex of today) which had periodic accretions of till during subsequent glacier expansions up to the late 19th century A.D. These moraines remained intact until recently because they continued to be supported by glacier ice. Thus, the ice levels probably never fell lower than about 70–80 m below the highest moraine crests in the last 3500 years. Both Hooker and Mueller Glaciers are very much shrunken at present and some of their lateral moraines have undergone collapse. Their moraines show, however, that their behaviour has been somewhat different from that of the Tasman, in recent millennia (cf. Burrows 1973, 1980; Gellatly 1982). There is insufficient evidence, in the form of radiocarbon dates, to reconstruct their history in as much detail.

ACKNOWLEDGMENTS

I gratefully acknowledge much help from the Mount Cook National Park authorities and permission to collect samples. I am very grateful for hospitality from friends at Mount Cook, particularly Martin and Jane Heine. I thank Anne Gellatly and Hans Konlechner for their company and assistance during collecting trips. Ian Owens, Peter Birkeland, Anne Gellatly, and an unknown reviewer criticised versions of the script. The work of personnel at the N.Z. Geological Survey, DSIR, Lower Hutt (particularly Eileen Tiller) and at the Institute of Nuclear Sciences laboratory, Lower Hutt (particularly R. C. McGill) is acknowledged with thanks. The studies were done with the assistance of grants from the N.Z. University Grants Committee, the University of Canterbury Grants Committee, and the Department of Plant Science, University of Canterbury.

REFERENCES

Burrows, C. J. 1973: Studies on some glacial moraines in New Zealand—2. Ages of moraines of the Mueller, Hooker and Tasman Glaciers. *New Zealand journal of geology and geophysics 16*: 831–855.

———1980: Radiocarbon dates for post-Otiran glacial activity in the Mount Cook region, New Zealand. *New Zealand journal of geology and geophysics 23*: 239–248.

———1982: On New Zealand climate within the last 1000 years. *New Zealand journal of archaeology 4*: 157–167.

Burrows, C. J.; Gellatly, A. F. 1982: Holocene glacier activity in New Zealand. *Striae 18*: 41–47.

Gellatly, A. F. 1982: Holocene glacial activity in Mt Cook National Park, New Zealand. Unpublished Ph.D. thesis, lodged in the library, University of Canterbury, Christchurch.

————1985: Glacial fluctuations in the Central Southern Alps, New Zealand: documentation and implications for environmental change during the last 1000 years. *Zeitschrift für Gletscherkunde und Glazialgeologie 21*: 259–264.

Gellatly, A. F.; Röthlisberger, F.; Geyh, M. A. 1985: Holocene glacier variations in New Zealand (South Island). *Zeitschrift für Gletscherkunde und Glazialgeologie 21*: 265–273.

Geyh, M. A. 1980: Holocene sea-level history: case study of the statistical evaluation of ^{14}C dates. *Radiocarbon 22*: 695–704.

Geyh, M. A.; Röthlisberger, F.; Gellatly, A. 1985: Reliability tests and interpretation of ^{14}C dates from palaeosoils in glacier environments. *Zeitschrift für Gletscherkunde und Glazialgeologie 21*: 275–281.

Green, W. S. 1883: The high alps of New Zealand. London, MacMillan.

International Study Group 1982: An inter-laboratory comparison of radiocarbon measurements in tree rings. *Nature 298*: 619–623.

Matthews, J. A. 1980: Some problems and implications of ^{14}C dates from a podzol buried beneath an end moraine at Haugabreen, southern Norway. *Geografiska Annaler 62A*: 185–208.

————1981: Natural ^{14}C age/depth gradient in a buried soil. *Die Naturwissenschaften 68*: 472–474.

Paul, E. A.; McLaren, A. D. *ed.* 1975: Soil biochemistry IV. New York, Dekker.

Röthlisberger, F. 1976. Gletscher-und Klimaschwankungen im Raum Zermatt, Ferpècle und Arolla. *Die Alpen 52*: 59–152.

————1987: 10 000 Jahre Gletschergeschichte der Erde. Aarau, Verlag Sauerländer.

Röthlisberger, F.; Haas, P.; Holzhauser, H.; Keller, W.; Bircher, W.; Renner, F. 1980: Holocene climatic fluctuations—radiocarbon dating of fossil soils (fAh) and woods from moraines and glaciers in the Alps. *Geographica Helvetica 35*: 21–52.

New Zealand Journal of Geology and Geophysics, 1989, Vol. 32: 217–223 217
0028–8306/89/3202–0217 $2.50/0

An early Holocene glacial advance in the Macaulay River valley, central Southern Alps, New Zealand

M. J. McSAVENEY
New Zealand Geological Survey
University of Canterbury
Private Bag
Christchurch, New Zealand

IAN E. WHITEHOUSE
Division of Land and Soil Sciences
Department of Scientific and Industrial Research, Ilam
P.O. Box 29 199
Christchurch, New Zealand

Abstract A 10 km long valley glacier terminating between Lower Tindill and Tom Streams, in the Macaulay River valley, central Southern Alps, New Zealand, at 8690 ± 120 years B.P. (NZ 6473A), is inferred from radiocarbon-dated deposits of till that were formerly thought to be of nonglacial origin. The glacial advance is one of three dated early Aranuian (post-14 000 years B.P.) advances in South Island. A group of undated moraines to the east of the Main Divide of the Southern Alps, collectively known as the Birch Hill moraines, may include moraines of similar age to the Macaulay River deposits, but represent a substantial interval of time. Available radiocarbon dates suggest that previous correlation of Birch Hill moraines with the c. 12 000 year old Waiho Loop moraine at Franz Josef Glacier is unlikely. Early Holocene glacial deposits of similar age to the Macaulay deposits are found in arctic Canada, western United States, and in the European Alps, so the triggering minor climatic change may have been global in extent. If the event formed moraines elsewhere, they remain undated, and may lie beneath present-day ice or have been destroyed by subsequent neoglacial advances.

Keywords radiocarbon dating; early Holocene; Aranuian; New Zealand; Southern Alps; moraines

INTRODUCTION

Direct radiocarbon dates of glacial events are rare in New Zealand, and unequivocal early Holocene glacial advances are rare globally and not hitherto shown conclusively for New Zealand (Grove 1979). Here we re-examine and reinterpret an early Holocene deposit formerly accepted to be of nonglacial origin, and add a directly dated advance at about 8500 years B.P. to the New Zealand glacial chronology. The local, regional, and global significances of the minor advance are also examined.

Received 18 October 1985, resubmitted 5 April 1988, accepted 15 June 1988

In our use of the terms "date" and "age", we reject the suggested jargon of Colman *et al.* (1987) and follow common English usage—"date" refers to when something occurred; and "age" refers to how old something is. Thus, a glacial advance is an event which may be "dated", it does not have an "age", and can not be "aged". A deposit left by this event has an "age", which relates directly to the "date" of the event which formed it. It is "aged" like wine by the passage of time. The process of determining its "age" involves estimating the "date" of its origin, and is correctly called "dating" notwithstanding that this term has other common usages.

The radiocarbon date NZ 548A of 8460 ± 120 years B.P. (Grant-Taylor & Rafter 1971, p. 384), from a sample collected by A. C. Beck in 1963, is described as from "peat on fan debris and overlain by moraine" at a site in the upper Macaulay River valley, central Southern Alps, New Zealand (Fig. 1). Burrows (1972), from an examination of the site in 1967, doubted that it records a glacial event, and suggested that the overlying bouldery deposit is from a landslide. Beck (1972) accepted Burrow's suggestion without reservation. Since 1972, the date has not been considered in syntheses of the New Zealand glacial chronology. There has been no work on other glacial evidence in the valley.

Not long before our first visit in 1980, a large section of a terrace riser beside Macaulay River, from which Beck's sample was taken, was laid bare by stream-bank erosion. The detail of the section viewed by us supports Beck's original interpretation. We infer a greatly expanded state of glaciers in the Macaulay River valley, which led to the destruction of a shrub forest dated by NZ 548A and a new, but not significantly different, confirming radiocarbon date (NZ 6473A) of 8690 ± 120 years B.P. At this time, the Macaulay River valley supported a glacier some 10 km long. About 14 500 years ago, the glacier linked with an expanded Godley Glacier to feed ice to the southern end of Lake Tekapo, c. 60 km from the head of Macaulay River. Only small cirque glaciers persist on the surrounding peaks today.

PHYSIOGRAPHY OF THE UPPER MACAULAY RIVER VALLEY

Macaulay River drains a 300 km² alpine valley between the north–south-trending Sibbald and Two Thumb Ranges and is a tributary of Godley River which drains to Lake Tekapo. The valley heads c. 8 km east of the Main Divide of the Southern Alps. The area of the basin above the dated deposits is c. 50 km². Surrounding peaks rise to 2800 m at Mt Sibbald, with much of the drainage divide rising 150–300 m above the permanent snowline, at about 2100 m, to support small cirque glaciers around the rim of the valley head. Although there no longer is a valley glacier present, large snow avalanches still sweep much of the upper valley floor to 1160 m each winter and early spring.

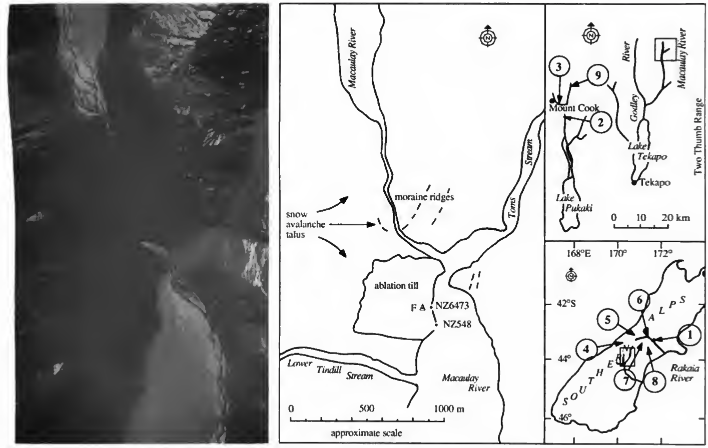

Fig. 1 Location of radiocarbon-dated till in Macaulay River valley, central Southern Alps, New Zealand. Aerial photograph 580/2A (1974) reproduced by permission of Department of Survey and Land Information. NZ 6473 is at lat. 43°34'40"S, long. 170°36'30"E. Circled numbers refer to: (1) Acheron River; (2) Birch Hill; (3) Black Birch Stream; (4) Canavan Knob; (5) Cropp River; (6) Griffiths Stream; (7) Meins Knob; (8) Prospect Hill; and (9) Tasman Glacier.

LOCATION OF THE MACAULAY RIVER SITE

The published grid reference and site description indicate that Beck's radiocarbon sample was taken from the west bank of Macaulay River, downstream of its junction with Toms Stream, and c. 700 m upriver of Lower Tindill Stream (Fig. 1). The likely site is very easily located in the field, and the only uncertainty is whether changes since 1963 have removed the true site and exposed a new site which superficially resembles the old. The sample was from a section exposed in the riparian terrace riser below an extensive hummocky surface with a relief of up to 10 m, from which boulders protrude up to 3 m. The deposits underlying this surface now have yielded another independent radiocarbon sample (NZ 6473), whose age (8690 ± 120 years B.P.) supports the accuracy of NZ 548 at 8460 ± 120 years B.P.

THE CONTROVERSY OVER THE ORIGIN OF THE MACAULAY DEPOSITS

Burrows (1972) believed the dated deposit to be landslide material unrelated to any glacial activity. We disagree with this interpretation and, as indicated below, believe the deposits to be ablation and basal till, or possibly flow till. About 600 m upstream from the sample sites, and c. 50 m higher, are the large remnants of several nested loops of terminal moraine, buried on the western edge by a currently active, but well vegetated, snow avalanche talus (Fig. 1). We agree completely with Burrows's (1972) interpretation of all of these features. The moraine shapes are distinctive, and where exposed in the river bank, their materials are mixtures of very large boulders, gravel, sand and silt, and small pockets of well-stratified silt and sand, typical of the till associated with moraines adjacent to existing glaciers in the central Southern Alps. The snow avalanche talus is strongly furrowed and positioned below a steep basin which can funnel avalanching snow to the apex of the cone.

THE SECTION AND OUR INFERRED ORIGINS OF THE DEPOSITS

The material underlying the extensive hummocky surface, which slopes down valley from the moraine loops and avalanche talus, is exposed in a 200 m long section along the west bank of Macaulay River. The section shows sandy silt mantled, poorly sorted, rounded gravels, overlain by two very poorly sorted, angular, bouldery diamictons which are capped with a silty yellow-brown soil (Fig. 2).

The basal deposit at the southern end of the section is poorly bedded, coarse, rounded gravel. At least two channels are cut into it in the central part of the section. This gravel is thought to be a fragment of an old alluvial fan from Lower Tindill Stream.

The basal gravel at the northern end of the section is less coarse, more rounded, and better bedded than that at the southern end, and it dips slightly southward, towards the gravel of the old alluvial fan (Fig. 2). It coarsens greatly

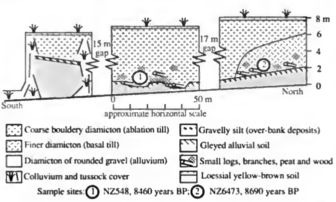

Fig. 2 Section exposed on western side of Macaulay River upstream of Lower Tindill Stream. Site marked for NZ 548 closely corresponds to original site description made in 1963, but may not be the true site because an unknown amount of streambank erosion has subsequently cleaned the face of the section.

northward, over a few tens of metres, up-dip along the section, indicating very close proximity to its source. We infer it to be a deposit of Macaulay River very near (perhaps only tens of metres) to a glacier terminus which is not exposed. The contact between the old fan of Lower Tindill Stream and this river gravel is obscured by talus at the base of the terrace riser.

Grey silt, c. 200 mm thick and containing root fragments, overlies the basal river gravel at the northern end of the section. Southward, the basal fan gravels are capped by gleyed silt and sand in the channels and grey gravelly silt between the channels. These silt and sand layers are probably part of a buried soil (or paleosol) developed in overbank deposits from flooding of Lower Tindill Stream or possibly Macaulay River. They appear to be typical of the fine deposits found at the distal extremities of many low gradient alluvial fans in the region today. No plant remains were found in these layers at the southern end of the section, but, in the infilled channel sections, abundant small logs and branches are present, locally forming a mat of peaty plant remains. It is most likely that Beck's peat sample came from within the southernmost of these channels (Fig. 2).

A variety of deposits cap the paleosol. Most are associated with, and gradational to, a coarse diamicton with sharply angular boulders that blankets the whole section. This diamicton is c. 1–3 m thick, except over the channels, where it is up to 6 m thick. At the southern end of the section, it rests directly on the paleosol with a gradational contact over c. 0.5 m. Within and at the base of the diamicton over the channels, there are pods of contorted silt and clay containing peat, abraded logs, small branches, and many wood fragments.

At the northern end of the section, the diamicton is separated from the underlying paleosol by c. 4 m of a much finer and more weakly bedded diamicton containing a much higher proportion of rounded pebbles than the overlying material. At its base, this bedded deposit contains many pieces of small logs and twigs, much fragmented and abraded, which were sampled (NZ 6473) for radiocarbon dating. The proportion of wood decreases upward, and no wood is apparent in its upper 1 m, nor in the unbedded diamicton above it. The weakly bedded deposit is not laterally continuous along the section. At its southern end, it ceases abruptly after 30 m of continuous exposure, as shown in Fig. 2. Its northern end is obscured. A very different deposit containing many large (200–400 mm diam.), rounded boulders occurs c. 5 m further northwards. We believe that the weakly bedded diamicton is basal till, from a glacier which advanced over a scrub-covered river terrace. That this basal till is not continuous over the entire section is regarded as a quirk of nature: we could find no reason for its abrupt termination.

The ubiquitous overlying coarse diamicton contains some clues to its origin. It lacks abundant fine material, and it is clast supported. It gives the appearance of having been washed clean of silt and sand prior to deposition. Adjacent boulders within it are of slightly different lithologies, structures, and textures, and no boulders could be found where the internal structures of one could be traced laterally into adjacent boulders. Few of the boulders were fractured, but bruising of edges and corners was common. We have seen all of the features of this deposit in debris associated with modern glaciers in the region, and we infer the material to be ablation till. These features contrast strongly with those of rock-avalanche deposits of similar lithologies (Shreve 1968; McSaveney 1978; Whitehouse 1983) which we have examined widely throughout the Southern Alps.

The whole section is capped with a thin, silty yellow-brown soil, inferred to be loess, which discontinuously blankets the entire hummocky area. Deep soil erosion on the hummocky surface above the outcrop has exposed the uppermost deposits beneath the soil in a number of hummocks. Over the northern half of the surface, at least as far south as Trig F (Fig. 1), the exposed deposits contain sparse rounded cobbles and boulders, including some with well-preserved striae. Such materials are absent from the diamicton that blankets the exposed section but occur in the deposit inferred to be basal till. We surmise that the basal till extends more widely and locally protrudes through the supposed ablation till as hummocks. We offer no explanation as to why the "basal till" should have such an irregular upper surface, nor why the "ablation till" should be so oddly distributed between the hummocks.

We were unable to eliminate a less likely possibility that the deposits could have originated from just two very large debris flows occuring within a few centuries of each other. If this were so, however, the materials can have originated only from upvalley in the terminal moraine loops where they are breached, or on a steep glacier surface sloping upvalley from the innermost of them. If the latter were the case, the deposits would fit the definition of flow till (Hartshorn 1958). Whether the materials originated at the moraines, or on the glacier surface associated with them, we believe that such large flows would have required the glacier to have been abutting the moraines, in order to provide the hydrostatic conditions to initiate flow.

The deposits are not what we would expect to see formed in a catastrophic draining of a moraine-dammed lake, and there is no evidence of the former existence of such a lake. A steep and active snow-avalanche talus buries the moraine loops to the north, but if the deposits in the exposed section were formed from snow avalanching, we would expect to see more evidence of stratification in the section, caused by many avalanches each depositing a small amount of detritus. There is evidence of but two events in the coarser diamictons, and if these were snow avalanches, they contained so much debris that they would have been better classified as debris avalanches or rock avalanches. The deposits, however, are not those of such avalanches. The evidence supports Beck's simpler, original inference that the dated material underlies a till sheet associated with the former presence of glacial ice.

THE SIGNIFICANCE OF THE EARLY HOLOCENE GLACIAL DEPOSITS

Local

The radiocarbon-dated materials (NZ 548A, 8460 ± 120 years B.P.; NZ 6473A, 8690 ± 120 years B.P.), from within till-like deposits at the Macaulay River sites, precisely date the events which formed the deposits from which the samples were taken, at least to within the few decades that it took for the dated twigs to grow. There is no statistically significant difference between the two dates, and we infer them to date the same episode of forest destruction. The deposits lie downvalley from a series of substantial terminal moraine loops. They overlie, and therefore postdate, a soil formed on glacial outwash gravel deposited very near to a glacier terminus. The soil suggests a substantial period of stability, of perhaps one or two thousand years for the sites, before they were overwhelmed. The uppermost, sheet-like deposit of coarse bouldery diamicton slopes upvalley to a wide breach in the terminal moraines. We infer that the uppermost deposit postdates the moraines, even though it lies downvalley of them. We do not suppose a substantial age difference, however, as we found no evidence for one when investigating the deposits while calibrating a surface rock weathering-rind growth curve (Whitehouse et al. 1986).

The deposits and the radiocarbon dates provide evidence of a 10 km long glacier in the Macaulay River valley, at c. 8500 years B.P., where no valley glacier exists today. From the evidence of the very substantial moraines and the soil development on the glacial outwash beneath the destroyed shrub forest, we infer that this extensive glacier persisted at about this length for some considerable time—perhaps several thousands of years—with repeated minor fluctuations. Nearby modern analogues at the termini of Hooker, Mueller, and Tasman Glaciers, at Mt Cook, have deposits which span the last 4000 years all within a few hundred metres of extant ice (Gellatly 1984). This persistence may have been aided by frequent snow avalanches onto the former glacier trunk, and the extensive distribution of high cirques around the valley perimeter, which probably fed ice avalanches onto the valley glacier, long after the cirque glaciers had become disconnected from it.

Regional

The deposits of the expanded glacier in the Macaulay River valley are correlated by McGregor (1967) with the Birch Hill moraines, 18 km downvalley from the present Tasman Glacier terminus, which also have been correlated with the Waiho Loop moraine at Franz Josef Glacier, Westland (Suggate 1961; Burrows 1980), now dated by many radiocarbon dates from a site at Canavan Knob as occuring at least within the range 11 450 ± 200 (NZ 4234, Wardle 1978) to 12 510 ± 120 years B.P. (Beta 12607, Mercer 1988) (Table 1). The only radiocarbon date from the Birch Hill moraines is QL 59 (5590 ± 30 years B.P., Porter 1975) from basal peat overlying the moraine, which does not assist in resolving correlations in the age range of 8000–12 500 years B.P. The radiocarbon date (NZ 1651) of 11 950 ± 200 years B.P. (Read 1976), from within extensive contorted lake sediments at the southern end of Lake Pukaki, is described by Burrows (1980) as enigmatic, but it is consistent with active glacier ice occupying the lake at that time. This would suggest that correlation of the Birch Hill moraines with the Waiho Loop moraine is highly unlikely. McGregor's correlation of Birch Hill with the dated Macaulay deposits is supported by soil and weathering-rind studies. Burrows (1980) noted that the innermost Birch Hill moraines have similar soils to that developed on a deposit 13 km upvalley at Black Birch Stream, Mt Cook, dated at 7940 ± 70 years B.P. (NZ 4508, Burrows 1980), and he implicitly accepted that the Macaulay deposits formed within some part of the span of time represented by the Birch Hill moraines, for

Table 1 Radiocarbon dates from early Aranuian glacial deposits in South Island, New Zealand (all dates are calculated using the old half-life). All samples were boiled in distilled water, but GX 9981, GX 10053, and Beta 12607 had further treatment of boiling in NaOH. Canavan Knob dates are means of three dates weighted according to reciprocal variance (with error limits given as weighted standard error of the mean).

Lab. no.	Locality	Type of deposit	Date (years B.P.)	Reference
GX 9981 GX 10053 Beta 12100	Canavan Knob, Westland	Wood under till	12 414 ± 106	Pooled from Mercer (1988)
NZ 1651	Lake Pukaki, Canterbury	Wood in contorted sand	11 950 ± 200	Read (1976)
NZ 4234 NZ 6923 NZ 6973	Canavan Knob (Same site as other three dates above)	Wood under till	11 550 ± 115	Pooled from Mercer (1988)
NZ 1290	Acheron River, Canterbury	Plant fragments in silt from proglacial lake	11 650 ± 200	Burrows (1979)
NZ 6576	Cropp River, Westland	Wood at base of till	10 250 ± 150	Basher (1986)
NZ 6473	Macaulay River, Canterbury	Wood in till	8690 ± 120	This paper
NZ 548	Macaulay River, Canterbury	Peat beneath till	8460 ± 120	Grant-Taylor & Rafter (1971) Burrows (1972)
NZ 1287	Meins Knob, Rakaia River	Wood in till	4540 ± 105	Burrows & Russell (1975)

which he allocated some 3500 years. In addition, Birkland (1982) noted that weathering-rind thicknesses on Birch Hill moraines suggest an age of about 9000 years (± 20%), but noted that the precision of the method does not preclude an 11 500 year age. Other major valley systems in the eastern Southern Alps have as yet undated remnants of moraines in intermediate positions between the moraines of the Late Glacial maximum, and moraines of the Neoglacial advances. Collectively these intermediate moraines have become known informally as the "Birch Hill" moraines, with the "type" site at Birch Hill. As at Birch Hill and Macaulay River, most of these moraines are multiphased, with significant weathering differences between their early and late phases (Burrows 1975; Burrows & Russell 1975; Burrows et al. 1976; Chinn 1981; Birkland 1982). We believe that one of the younger of these phases has been dated at Macaulay River. As yet, there is no locality where more than one may be dated.

Wood at the base of till within what is inferred to be a poorly preserved terminal moraine at Cropp River, Westland, 4 km from a small cirque glacier at the valley head and many kilometres inside the limits of the Late Glacial maximum extent of ice from the Hokitika drainage basin, recently has been dated at 10 250 ± 150 years BP (NZ 6576, Basher 1986; Basher & McSaveney in press). This provides evidence of an episode of glacier resurgence intermediate in age between the dated deposits at Macaulay River and at Waiho Loop. This could correlate with earlier phases of moraine building for the "Birch Hill" moraines, as this would be consistent with the likely range of ages represented by the deposits, but we await dates from east of the Divide to establish this as more than speculation.

Burrows (1980) reported a further occurrence of dated wood in "till" (NZ 4508; 7940 ± 70 years B.P.) (from Black Birch Stream, mentioned above); however, more recent review work calls into question the glacial origin of this deposit (J. H. Mercer pers. comm. 1986; Gellatly et al. 1988). We too have examined the site. Although the deposit contains many striated and faceted boulders of undoubted glacial origin, we believe that it is too closely associated with the deposit of a rock avalanche from the slopes above which overrode and eroded glacial and glaciofluvial deposits and a shrub forest independently dated by us (NZ 7230, 7240 ± 90 years B.P. and NZ 7231, 7660 ± 95 years B.P.), for this date to be used with confidence in a New Zealand glacial chronology. Although the differences in ages are marginally statistically different, there is greater difference in apparent age between NZ 7230 and NZ 7231, which are stratigraphically identifiable as dating the same unit, than there is between NZ 7231 and NZ 4508, which we could not identify positively as dating different units.

To the north, in the major drainage basin of Rakaia River, Burrows (1979) reported dated organic material (NZ 1290, 11 650 ± 200 years B.P.) from lake silts in a former proglacial lake in the Acheron River valley that is believed to have been associated with Rakaia ice (Soons 1983). A bog-bottom date of 11 900 ± 200 years B.P. (NZ 1652, Burrows & Russell 1975) from Prospect Hill, 43 km further upstream in the Rakaia River valley, indicates that Rakaia ice had receded from that site by this time. The two are not incompatible if the lake were long, and the Prospect Hill site near to, but above, the glacier surface. In the headwaters of Wilberforce River, a major northern tributary of Rakaia River, a rock avalanche fell on an ice-free alpine valley bottom (Griffiths Stream) near to the Main Divide at 10 250 ± 150 years B.P. (NZ 5010, Whitehouse & Griffiths 1983); and at Meins Knob, within a kilometre of the early 20th century terminus of Lyell Glacier, ice had gone from a site 240 m vertically above this large valley glacier at the head of Rakaia River by 9480 ± 130 years B.P. (NZ 4484, Burrows 1979).

Although there is a range of intermediate age dates from bog-bottom deposits lying on glacial deposits in the Southern Alps, the next oldest glacial deposit directly dated by wood in till is 4540 ± 105 years B.P. (NZ 1287, Burrows & Russell 1975) at Meins Knob within a kilometre of the early 20th century valley glacier terminus, and at about the same altitude. This is not to say that there is a paucity of terminal moraines in South Island intermediate in age between the last Late Glacial maximum and the Neoglacial—it is the radiocarbon dating that is rare.

Global

Despite Grove's (1979) global synthesis, there is current international controversy about the climate of the early Holocene. Osborn & Davis (1987) remarked on the few data on early Holocene glacier fluctuations, and the apparent absence of a consistent global pattern for the Holocene prior to the Neoglacial. They noted nothing earlier than 6000–5000 years age in North America, except perhaps about 8500–8000 years age presently being debated in the literature. Beget (1983), on the other hand, cited an advance in the North Cascades (White Chuck Drift) and numerous dates from Baffin Island and around the Laurentide Ice Sheet from this time. In their summary of the early Holocene history of this ice sheet, Dyke & Prest (1987) remarked that end moraines formed by Keewatin ice c. 8600–8400 years age signify a response of the ice sheet to climatic forcing. Röthlisberger (1976) and Schneebeli (1976) reported a directly dated advance in the Swiss Alps at 8400 ± 120 years B.P. (Ly-749), confirming the indirectly dated Venediger advances of Patzelt (1974), and Heuberger (1974). Mahaney's (1987) reinterpretation of moraines at Mt Kenya leaves no early or mid-Holocene moraines in Africa. In southern South America, in similar latitudes to South Island, Mercer (1988) found a total absence of end moraines known to date from the interval 14 000–5000 years age, although there are a number of dates of basal peats that are permissible (10 000 ± 140 years B.P., I-2209, Mercer (1968); 10 105 ± 325 years B.P., GX 8683; and 10 375 ± 380 years B.P., GX 8684, Mercer (1984). In Peru, at 14°S., the 50 km² Quelccaya Ice Cap was within 2 km of its present margins by 12 230 ± 180 years B.P. (DIC 687), and, after a small readvance about 11 000 years ago (overridden peats dated at 11 185 ± 185, GX 4325; 11 070 ± 125, DIC 685; and 10 910 ± 160 years B.P., I-8209), had shrunk behind its present margins by 9980 ± 255 years B.P. (DIC 685), and still was smaller than today at 2670 ± 95 (DIC 680) and 1395 ± 190 (GX 4930) years B.P. (Mercer 1985).

Whatever the fluctuations of glaciers were beyond New Zealand during the early Holocene, many appear to have taken place largely inside the limits of present-day and Neoglacial ice. Many of the Neoglacial advances elsewhere, including those of recent centuries, appear to have been proportionately much greater than those in South Island, New Zealand, to the extent that their deposits and the still-present ice may mask much of the glacial record of the earlier postglacial interval. This does not preclude a conclusion that there was a minor global fluctuation of climate favorable to glacier growth about 8500 years ago.

CONCLUSION

Directly dated advances of glaciers at Franz Josef Glacier about 12 000 years B.P., in the Cropp River valley about 10 250 years B.P., and in the Macaulay River valley about 8500 years B.P., represent a sequence of significant, but probably quite minor, glacial advances in South Island, New Zealand, punctuating an otherwise extremely rapid deglaciation between the last full-glacial readvance about 14 500–14 000 years ago and the onset of neoglaciation about 5000–4500 years ago. There are not many correlative advances beyond New Zealand, but evidence of others possibly is obscured beneath present-day ice.

ACKNOWLEDGMENTS

We thank C. J. Burrows, T. J. Chinn, J. M. Soons, and the late J. H. Mercer for their discussions and comments.

REFERENCES

Basher, L. R. 1986: Pedogenesis and erosion history in a high-rainfall, mountainous drainage basin—Cropp River, New Zealand. Unpublished Ph.D. dissertation, lodged in the Library, Lincoln College, University of Canterbury, Christchurch, New Zealand.

Basher, L. R.; McSaveney, M. J. in press: An early Aranuian glacial advance at Cropp River, central Westland, New Zealand. *Journal of the Royal Society of New Zealand.*

Beck, A. C. 1972: Post-Otiran moraines in Canterbury, Further comment. Letter to the editor. *New Zealand journal of geology and geophysics 15*: 299.

Beget, J. E. 1983: Radiocarbon-dated evidence of world-wide early Holocene climate change. *Geology 11*: 389–393.

Birkland, P. W. 1982: Subdivision of Holocene glacial deposits, Ben Ohau Range, New Zealand using relative-dating methods. *Geological Society of America bulletin 93*: 433–449.

Burrows, C. J. 1972: Post-Otiran moraines in Canterbury. Comment. Letter to the editor. *New Zealand journal of geology and geophysics 15*: 296–299.

———1975: Late Pleistocene and Holocene moraines of the Cameron Valley, Arrowsmith Range, Canterbury, New Zealand. *Arctic and alpine research 7*: 125–140.

———1979: A chronology for cool-climate episodes in the Southern Hemisphere 12,000–1000 years B. P. *Palæogeography, palæoclimatology and palæoecology 27*: 287–347.

———1980: Radiocarbon dates for post-Otiran glacial activity in the Mount Cook region, New Zealand. *New Zealand journal of geology and geophysics 23*: 239–248.

Burrows, C. J.; Russell, J. B. 1975: Moraines of the upper Rakaia Valley. *Journal of the Royal Society of New Zealand 5*: 463–477.

Burrows, C. J.; Chinn, T. J.; Kelly, M. 1976: A note on implications of new radiocarbon dates for glacial activity in New Zealand near the Pleistocene–Holocene boundary. *Boreas 5*: 57–60.

Chinn, T. J. H. 1981: Use of rock weathering rind thickness for Holocene absolute age-dating in New Zealand. *Arctic and alpine research 13*: 33–45.

Colman, S. M.; Pierce, K. L.; Birkeland, P. W. 1987: Suggested terminology for Quaternary dating methods. *Quaternary research 28*: 314–319.

Dyke, A. S.; Prest, V. K. 1987: Late Wisconsinan and Holocene history of the Laurentide Ice Sheet. *Géographie physique et Quaternaire 41 (2)*: 237–263.

Gellatly, A. F. 1984: The use of rock weathering-rind thickness to redate moraines in Mount Cook National Park, New Zealand. *Arctic and alpine research 16*: 225–232.

Gellatly, A. F.; Chinn, T. J. H.; Röthlisberger, F. 1988: Holocene glacier variations in New Zealand : a review. *Quaternary science reviews 7*: 227–242.

Grant-Taylor, T. L.; Rafter, T. A. 1971: New Zealand radiocarbon age measurements—6. *New Zealand journal of geology and geophysics 14*: 364–402.

Grove, J. M. 1979: The glacial history of the Holocene. *Progress in physical geography 3 (1)*: 1–54.

Hartshorn, J. H. 1958: Flow till in south-eastern Massachusetts. *Bulletin of the Geological Society of America 69*: 477–482.

Heuberger, H. 1974: Alpine Quaternary glaciation. Pp. 318–338 *in:* Ives, J. D.; Barry, R. G. *ed.* Arctic and alpine environments. London, Methuen.

McGregor, V. R. 1967: Holocene moraines and rock glaciers in the central Ben Ohau Range, South Canterbury, New Zealand. *Journal of glaciology 6*: 737–748.

McSaveney, M. J. 1978: Sherman Glacier Rock Avalanche, Alaska, U.S.A. Chapter 6 *in:* Voight, B. *ed.* Rockslides and avalanches. 1, Natural phenomena. *Developments in geotechnical engineering 14A*: 197–258.

Mahaney, W. C. 1987: Reinterpretation of moraines at c. 4000 m in the Mt Kenya Afroalpine area. *Palæogeography, palæoclimatology, palæoecology 60*: 47–57.

Mercer, J. H. 1968: Variations of some Patagonian glaciers since the late-glacial. *American journal of science 266*: 91–109.

———1984: Simultaneous climatic change in both hemispheres and similar bipolar interglacial warming: evidence and implications. *Geophysical monograph 29* (Maurice Ewing volume 5): 307–313.

———1985: Changes in the ice cover of temperate and tropical South America during the last 25,000 years. *In*: Garleff, von K.; Stingl, H. *ed.* Südamerika: Geomorphologie und Päläoökologie des jüngeren Quartärs. *Zentralblatt für Geologie und Paläontologie, Teil 1, Jahrgang 1984, Heft 11/12*: 1661–1665.

———1988: The age of the Waiho Loop terminal moraine, Franz Josef Glacier, Westland. *New Zealand journal of geology and geophysics 31*: 95–99.

Osborn, G.; Davis, P. T. 1987: Holocene glacier fluctuations. *Episodes 10 (1)*: 26–28.

Patzelt, G. 1974: Holocene variations of glaciers in the Alps. *In*: Les méthodes quantitatives d'étude des variations du climat au cours du Pleistocene. *Colloques Internationaux du Centre National de la Recherche Scientifique 219*: 51–59.

Porter, S. C. 1975: Equilibrium-line altitudes of late Quaternary glaciers in the Southern Alps, New Zealand. *Quaternary research 5*: 27–67.

Read, S. A. L. 1976: Upper Waitaki Power Development Scheme: Pukaki Lake Control, Engineering geological completion report. *New Zealand geological survey engineering report* EG 268. 43 p.

Röthlisberger, F. 1976: Gletscher- und Klimaschwankungen im Raum Zermatt, Ferpeck und Arrolla. *Die Alpen 52*: 59–132.

Schneebelei, W. 1976: Untersuchungen von Gletscherschwankungen in Val de Bagnes. *Die Alpen 52*: 5–58.

Shreve, R. L. 1968: The Blackhawk Landslide. *Geological Society of America special paper 108*: 47 p.

Soons, J. M. 1983: The changing face of the evidence: an examination of proxy data for climate change during the Late Pleistocene in New Zealand. Pp. 151–158 *in:* Vogel, J. C. *ed.* Late Cainozoic paleoclimates of the Southern Hemisphere. Rotterdam, A A. Balkema.

Suggate, R. P. 1961: The upper boundary of the Hawera Series. *Transactions of the Royal Society of New Zealand geology 1*: 11–16.

Wardle, P. 1978: Further radiocarbon dates from Westland National Park and the Omoeroa River mouth, New Zealand. *New Zealand journal of botany 16*: 147–152.

Whitehouse, I. E. 1983: Distribution of large rock-avalanche deposits in the central Southern Alps, New Zealand. *New Zealand journal of geology and geophysics 26*: 271–279.

Whitehouse, I. E.; Griffiths, G. A. 1983: Frequency and hazard of large rock avalanches in the central Southern Alps, New Zealand. *Geology 11*: 331–334.

Whitehouse, I. E.; McSaveney, M. J.; Knuepfer, P. L. K.; Chinn, T. J. 1986: Growth of weathering rinds on Torlesse Sandstone, Southern Alps, New Zealand. Chapter 17, pp. 419–435 *in:* Colman, S. M.; Dethier, D. P. *ed.* Rates of chemical weathering of rocks and minerals. New York, Academic Press.

New Zealand Journal of Geology and Geophysics, 1989, Vol. 32: 225–241
0028–8306/89/3202–0225 $2.50/0

Differentiation of late Pleistocene terrace outwash deposits using geomorphic criteria: Tekapo valley, South Island, New Zealand

JUDITH K. MAIZELS
Department of Geography
University of Aberdeen
Elphinstone Road
Aberdeen AB9 2UF, UK

Abstract This paper reassesses the geological interpretation of outwash deposits of different ages based on new data on terrace elevation and gradient, loess thickness, preserved paleochannel networks, and specific gravity of clasts of outwash deposits in the Tekapo valley, South Island. The results have shown no significant difference in these measures between the Wolds and Pattersons Terrace deposit, suggesting that they both represent the oldest, highest, steepest, most weathered, and most modified formation in the Tekapo valley. Significant differences have emerged between the Wolds/ Pattersons Terrace Formation and the lower Balmoral Formation, which exhibits a thinner loess cover, higher specific gravity values, and a distinctive dendritic drainage network. The Balmoral Formation is significantly differentiated from the Mt John Formation, which has little loess cover and is traversed by complex braided paleochannel networks. The measures adopted do not discriminate between the Mt John and Tekapo Formations, although loess cover is thinner on the latter. The combined use of these measures of landform, paleochannel pattern, and clast characteristics, has proved a valuable objective means of discriminating between glaciofluvial terrace outwash deposits.

Keywords glaciofluvial sedimentation; outwash; terraces; loess; paleochannels; specific gravity; late Pleistocene; Mackenzie Basin

INTRODUCTION

The development of methods for the differentiation of Pleistocene tills, moraines, outwash, and alluvial fan deposits has proved a vital research area in the elucidation of glacial chronology in New Zealand. However, until recently, many of these studies have been based on relatively subjective or qualitative criteria, such as degrees of landscape dissection and drainage development, freshness of the landscape features, matrix colour and relative degrees of weathering. This study attempts to differentiate a series of outwash terrace deposits in the Tekapo valley, Southern Alps, using a range of objective quantitative criteria applied to both landform and clast characteristics. These criteria include measurements of terrace elevation and gradient, degree of incision, drainage network development, thickness of loess cover, and specific gravity of clasts. A recent study by G. McGregor (1981) has proposed specific quantitative measures for the differentiation of Pleistocene tills in the Tekapo valley, based particularly on specific gravity and percentage absorption of clasts in moraines related to different glaciations. This study attempts to complement and extend McGregor's approach by using quantitative measures relevant to glaciofluvial outwash landforms and deposits, to differentiate them according to their relative age, and to use this new information as the basis for mapping the distribution of the different geological formations in the Tekapo valley.

Received 29 July 1987, accepted 23 November 1988

THE TEKAPO VALLEY

The Godley and Macaulay Rivers drain southwards from the Godley Glacier and adjacent icefield and mountain slopes of the Southern Alps, into the long ribbon-shaped Lake Tekapo (Fig. 1). Lake Tekapo lies in a scoured bedrock depression c. 130 m deep, impounded behind large terminal moraine complexes. The Tekapo River valley south of Lake Tekapo comprises a series of extensive and distinctive outwash terraces, stretching for over 15 km southwards from well-defined moraine limits. The terraces form a stepped sequence over a height range of almost 100 m, are traversed by complex paleochannel networks (Fig. 2 and 3), and the older surfaces are mantled by thick loess covers, often exceeding 1 m in thickness (e.g., Gair 1967; Webb 1976). The geology of the Tekapo basin is dominated by Tertiary quartz-felspathic greywackes, together with slates and schists. The Tekapo valley forms the northeastern part of the intermontane Mackenzie Basin, a large, faulted tectonic depression, infilled with hundreds of metres of Pleistocene glacial and glaciofluvial sediments (R. Speight 1940). The Southern Alps and adjacent basins have been subject to substantial tectonic uplift associated with the Kaikoura orogeny, and uplift is continuing today.

Former outwash surfaces have been differentially tilted away from the centre of uplift, such that the gradients of the oldest surfaces have been substantially modified from their original depositional gradients.

PLEISTOCENE CHRONOLOGY AND PREVIOUS STUDIES OF TEKAPO OUTWASH TERRACES

The Pleistocene history and glacial chronology of the Mackenzie Basin has attracted much attention in the literature since the early reports by R. Speight (1915, 1921, 1940). J. G. Speight (1961), working in the neighbouring Pukaki River valley, differentiated four landform associations, each representing a successively younger glaciation. The differentiation of each landform association was based on a range of geomorphic criteria including the freshness of the landforms and the amount of topographic detail, the amount

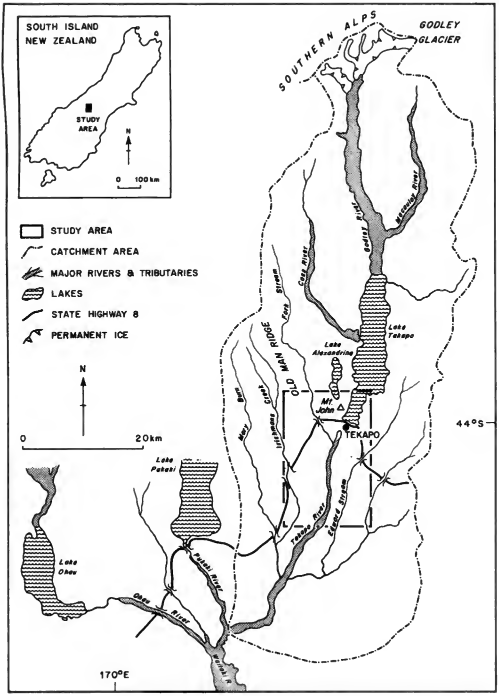

Fig. 1 Location of Tekapo valley, South Island, New Zealand.

of soil and silt cover, and the degree of weathering. Speight identified the Stevenson (oldest), Irishman, Maryburn, and Pukaki (youngest) landform associations (Table 1; Fig. 4A). This classification was confirmed by Gair (1967) for the Mackenzie Basin (Fig. 4B), which he defined as the type area for the equivalent Wolds (oldest), Balmoral, Mt John, and Tekapo (youngest) Formations of the Pleistocene, followed by deposits of the Birch Hill advance and later Holocene glacier fluctuations. Gair (1967) differentiated these deposits according to their morphological field relationships, the degree of erosional modification of moraines, and the degree of weathering of the outwash gravels. The area in the west which Gair identified as the Wolds Formation forms a zone of subdued and well-weathered topography extending southwards from morainic into outwash sediments. A large outlier of gravels which lies to the east and rises above the surrounding terrace surfaces, known as Pattersons Terrace (see Fig. 5), Gair also mapped as the Wolds Formation.

Gair (1967) clearly delimited the Balmoral moraine on the southern side of the Fork Stream, and showed its southward extension into a clearly defined outwash terrace. West of the Tekapo River Gair identified the Mt John terminal moraine merging with small outliers of Mt John outwash, surrounded by the later Tekapo outwash deposits. Farther south, the vast extent of outwash gravel terraces is also interpreted as being of Tekapo age, such that no Mt John outwash deposits occur west of the Tekapo River. East of the river, Tekapo outwash deposits are confined to the present incised channel of the river. Hence Tekapo ice and meltwaters spilled over to the west, over the Mt John moraine and outwash, and cut through the main Mt John moraine to form the present lake outlet. These meltwaters are considered to have left all the Mt John

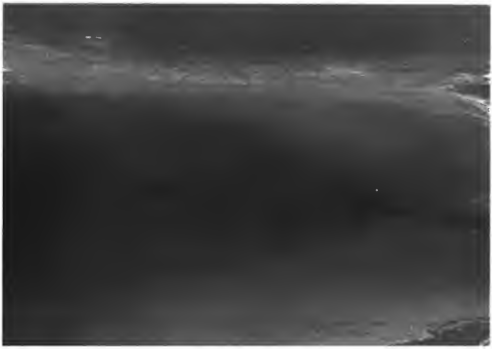

Fig. 2 Aerial view of Balmoral outwash surface illustrating dendritic drainage system superposed on remnants of braided paleochannel system partially masked by loess cover. Tekapo River at top (east) of photo, and Tekapo–Pukaki Canal at right hand edge of photo.

Fig. 3 Aerial view of the Mt John and Tekapo outwash terraces (foreground), with distinctive braided paleochannel systems (looking southwards).

outwash east of the outlet unmodified. Gair's interpretation was modified by Tuck (1975) who recognised several substages of the Balmoral, Mt John, and Tekapo Formations (Table 1; Fig 4C). Tuck's results suggest that virtually all the gravel plains postdating the Wolds represent Tekapo outwash, with the exception of small outliers at the foot of the outermost Mt John moraines. Liedtke's (1980) analysis of the Tekapo deposits generally confirm Gair's (1967) interpretation of the Wolds and Balmoral Formations, and of Pattersons Terrace (Table 1; Fig 4D). Liedtke also suggested that it is difficult to differentiate between Mt John and Tekapo outwash deposits since Tekapo ice and meltwaters reworked the Mt John moraine and outwash deposits. His interpretation therefore suggests that the Mt John and Tekapo outwash sequences are relatively continuous, with the highest areas representing Mt John deposits, and the lower terraces and spillway channels feeding these areas, representing features of the Tekapo stage. Mansergh (pers. comm. 1983) also confirms the interpretations of Gair (1967) and Liedtke (1980), and although Mansergh & Read (pers. comm. 1983) did not separate the Mt John and Tekapo moraine and outwash deposits on their draft map (Fig. 4E), they did identify substages of the Mt John and Tekapo glacier advances.

Mansergh argues, however, that much of the Mt John Formation has been reworked by Tekapo meltwaters, making differentiation difficult (Table 1; Fig 4E). Mansergh & Read (pers. comm.) also regard Pattersons Terrace as representing an early Waimean moraine stage of the Balmoral Formation, rather than a member of the Wolds Formation. This interpretation is based on measures of the specific gravity

(or solid density) values of clasts (ρ_s = 2.670), which were found to be intermediate between those of the main Balmoral (ρ_s=2.682) and the Wolds (ρ_s=2.640) Formations.

Few dates are available for providing an absolute framework for the glacial chronology of the Tekapo valley. J. G. Speight (1961) estimated dates of different surfaces from tectonic movements along the Ostler Fault (Pukaki valley) assuming a constant rate of uplift. Speight's approach estimated ages of c. 105 000, 51 000, and 22 300 years B.P. for the Wolds, Balmoral, and Mt John Formations, respectively. Gair (1967) correlated the four formations in the Mackenzie Basin with those recorded elsewhere in South Island, and considered that they were all Otiran in age (i.e. K1, K2, $K3_1$ and $K3_2$ of Gage & Suggate (1958) and Suggate & Moar (1970; Table 1), although with the possibility that the Wolds Formation might be older than Otiran. Mansergh (pers. comm.) obtained a ^{14}C date for plant matter (*Phyllachne* cf. *colensoi* and *Dracophyllum*) within or beneath the Balmoral lateral moraine of 36 400 ± 3150 years B.P.

Comparison of terrace gradient data for tilted and nontilted surfaces in the Ohau River area suggested ages of c. 16 000 years B.P. for the Mt John surface, and of c. 14 000 years B.P. for the Tekapo surfaces (Mansergh 1973). Wellman (1979) obtained slightly older ages than these by extrapolation of tilted shorelines around Lake Tekapo to the Mt John and Tekapo outwash surfaces. His dates suggested that the Mt John and Tekapo surfaces were formed c. 18 000 and 15 000 years age, respectively (Table 1). Recession of the Tekapo glacier from the moraine bounding the southern end of Lake Tekapo, created the first stages of Lake Tekapo (proto-lake Tekapo). A ^{14}C date of 11 950 ± 200 years B.P. was obtained for a log found in varved lake sediments from a similar setting in nearby Lake Pukaki, representing an early stage of lake formation (Porter 1975). A minimum ^{14}C date for the later Birch Hill readvance of c. 8400 years B.P. was obtained from peat buried beneath a possible moraine (Tuck 1975), although the nature of the dated material has been questioned (Mansergh pers. comm.), and the overlying sediment has also been interpreted as a landslide deposit (Burrows 1972). According to Porter (1975), correlations with dated advances in the Rakaia valley suggest that the Birch Hill advance occurred between 11 900 and 9520 years B.P.

The aim of this paper is to reduce some of the uncertainties associated with the dating classification, and mapping of the outwash deposits in the Tekapo valley, using the series of geomorphic criteria discussed below.

METHODS OF ANALYSIS: DERIVATION OF GEOMORPHIC CRITERIA

Morphological relations

The major morphological units and the morphological relations between successive terrace surfaces were determined by field mapping and mapping from aerial photographs, together with detailed levelling of a traverse from Irishman Creek eastwards

Table 1 Summary of late Pleistocene–early Holocene glacial chronology for the Tekapo area.

Glaciation	Gage & Suggate (1958)(Waimakariri valley/Westland)	Speight (1961, 1963)	McGregor (1963)	Gair (1967)	Suggate & Moar (1970)	Mansergh (1973)	Moar & Suggate (1973)
Neoglacial (Holocene advance)			Sibbalds I. (13 000–9000 years B.P.)	Birch Hill (>5120 ± 140 years B.P.)			
	Poulter Kumara–3	Pukaki = Tekapo	K3 (18 000–13 000 years B.P.)	Tekapo	$K3_2$ (14 500–14 000 years B.P.)	Tekapo (14 000 years B.P.)	Kumara $K3_2$
	Blackwater Kumara–2	Maryburn = Mt John (22 300 ± 350 years B.P.)		Mt John	$K3_1$ (17 000–16 000 years B.P.)	Mt John II I (16 000 years B.P.)	$K3_1$ Younger Kumara $K2_2$
Otiran glaciation	Otarama Kumara–1	Irishman = Balmoral (51 000 years B.P.)		Balmoral	K2 (22 300–18 000 years B.P.)	Balmoral II I (36 400 ± 3150 years B.P.)	
	Woodstock Hohonu	Stevenson = Wolds (105 000 years B.P.)		Wolds			
Interglacial					(?) K1	(?) Wolds	Older Kumara $K2_1$
Waimean glaciation							
Interglacial							
Waimaungan glaciation							
Nature of evidence	Stratigraphy; tectonics.	Weathering; relief; morphological relations; rate of fault movement.	Glacial geomorphology; ice-contact deposits; glacial trimline altitude.	Relative altitude; dissection; weathering; loess cover.	^{14}C dating.	^{14}C dating cf. of gradients; morphological relations.	

to the Tekapo River, crossing outwash surfaces of the four main formations (Fig. 5). The relations between the moraines and the main terrace surfaces, and the changes in elevation and gradient through the terrace sequence, were determined by detailed levelling of a series of longitudinal profiles, based on 700 heights over a total distance exceeding 80 km. The effect of differential uplift and tilting on the original depositional outwash gradients has been determined using three published rates of uplift for parts of the Mackenzie Basin. Wellman (1979) published a shoreline diagram for Lake Tekapo, in which eight shorelines dating from c. 11 500 years B.P., exhibit differential tilting. This diagram allows the calculation of the degree of tilt at different distances southwards in relation to the age of the deposit. It is based on the assumption of constant rate of uplift such that shoreline age is directly proportional to shoreline slope. Extrapolation to the downstream outwash surfaces has allowed the degree of differential tilting of individual outwash surfaces to be estimated, thereby indicating the degree to which the original gradients have been altered. The relationship between distance, tilt, and age of the deposit follows a form similar to that proposed by Adams (1979) for the amount of uplift with increasing distance east of the Alpine Fault, except that since the Wellman curve is much steeper, it generally predicts greater differential tilt rates than Adams's model.

The discrepancies between the estimates reflect Wellman's assumption of a more north–south axis of uplift compared with Adams's model which assumes a more west–east axis. Some differential uplift is also likely to have resulted from isostatic uplift, after melting of the Late Glacial ice.

Mathews (1967) estimated the likely amount of isostatic rebound in the Tasman and Godley valleys from calculations of former glacier long-profiles and associated ice thicknesses at successive stages of the last glaciation, but regarded the amount of differential uplift due to isostasy as negligible.

Loess thickness

Loess thickness has been shown in many studies in southern South Island to increase with relative age of the deposit (e.g., V. McGregor 1963; Raeside 1964; Young 1964, 1967; Bruce 1973a, b; Ives 1973; Tonkin et al. 1974; Webb 1976). The loess is likely to be derived from unvegetated areas that had been recently exposed by deglaciation or exposed on bars and islands within braided reaches of the rivers (Ives 1973; Leamy et al. 1973; Tonkin et al. 1974). Maximum loess accumulation probably occurred during periods of glacial retreat or climatic deterioration (i.e., towards the beginning and end of interglacial periods and during interstadials; e.g., Ives 1973), while more stable periods of soil development are likely to have prevailed during full interglacials (e.g., McKellar 1960; Raeside 1964; Bruce 1973a, b; Tonkin et al. 1974).

The depth of loess cover was determined on the main terrace surfaces in the Tekapo valley by probing at over 100 sites along transect 1 (Fig. 5). These data were supplemented by data from a series of boreholes drilled by the Ministry of Works and Development prior to construction of the

Table 1 *(Continued)*

Porter (1975)	Tuck (1975)	Webb (1976)	Wellman (1979)	Liedtke (1980)	McGregor (1981)	Mansergh & Read (pers. comm)	Maizels (this paper)
Birch Hill >5370 ± 30 to >5590 ± 30; 9520–1190 years B.P.	Birch Hill					Birch Hill c. 8000 years B.P.	
Tekapo +	Tekapo III + II I	Tekapo +	Tekapo (15 000 years B.P.)	Tekapo	Tekapo	Tekapo (14 000–12 000 years B.P.)	Tekapo
				Interstadial			
Mt John (>11 950 ± 200 years B.P.)	Mt John III II I	Mt John (Loess A)	Mt John (18 000 years B.P.)	Mt John	Mt John	Mt John (17 000–16 000 years B.P.)	Mt John
	Balmoral III II I	Balmoral + Wolds Loess A + B)		Balmoral			
Balmoral (>36 400 ± 3150 years B.P.; >34 100 ± 2750 years B.P.)	Wolds			Wolds	Balmoral Wolds	Balmoral II, I, Pattersons Terrace Stadial	Balmoral
Wolds						Wolds	Wolds + Pattersons Terrace
^{14}C dating; relative relief; weathering.	Elevation; loess cover; weathering.	Loess thickness and composition.	Rate of lake shoreline tilting.	Weathering; loess thickness; morphology; height relations.	Weathering; colour; specific gravity.	Specific gravity: fault displacement; morphological relations	Elevation and gradient; loess cover; specific gravity; channel pattern.

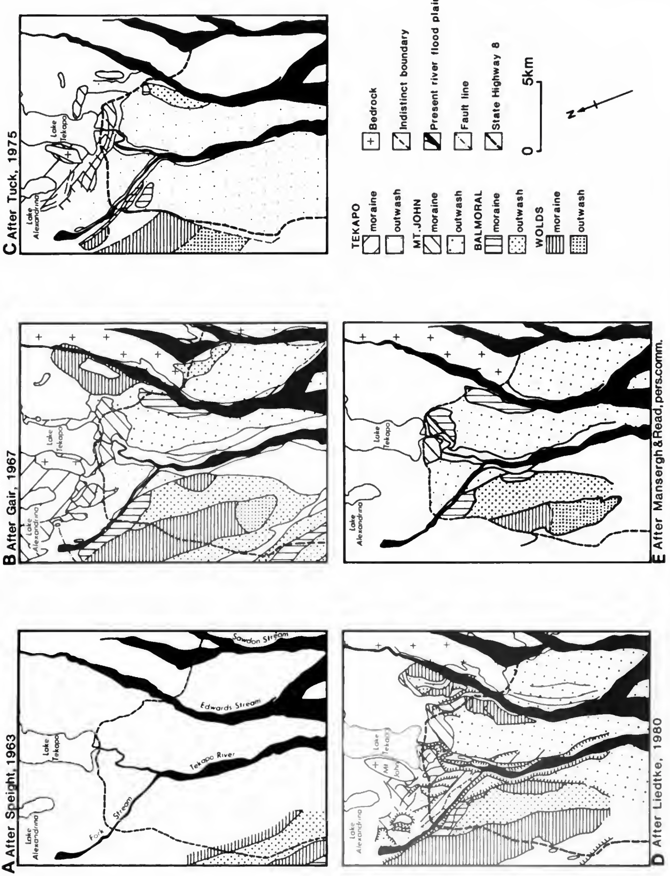

Fig. 4 Previous interpretations of major glacial/glaciofluvial formations in the Tekapo valley, south of Lake Tekapo.

Tekapo–Pukaki Canal, and by data from several pits and dozer cuts.

Differential preservation and development of surface drainage network

The outwash sediments of each formation were probably deposited in complex braided channel systems such as those now characterising many of the glacial meltwater rivers draining the eastern Southern Alps, including the Tekapo, Pukaki, and Tasman Rivers. The extent to which the original braided pattern has been preserved on the terrace surfaces, and the degree of development of subsequent channel systems, is likely to reflect the relative age of the deposit. Once abandoned by meltwaters, the original braided pattern would become obscured by a thickening loess and soil mantle, and later surface drainage derived from direct precipitation and snowmelt runoff would develop an independent or modified drainage network. The paleochannel networks on successive outwash surfaces in the Tekapo valley were mapped from aerial photographs (areas selected shown in Fig. 5), and measures of the drainage networks preserved and developed on these successive terrace surfaces were obtained. These measures identified changes in: (1) channel density, CD, defined as $CD = \Sigma(L/A)$ where L = total channel length and A = sample area of terrace surface; (2) channel frequency, CF, defined as $CF = N/L_T$ where N = no. of channels crossed by a transverse profile across the terrace surface, and L_T is the length of the traverse; (3) mean channel width, W, along the same traverse; and (4) mean surface relief, R, from bar top to channel bed along the traverse. Topologic indices of the degree of braiding were derived from the numbers of links (l), junctions (j), bifurcation nodes (b), and sources (s), in each network over a given sample area (e.g., see Maizels 1979).

Progressive burial of the original braided channel network by loess, and evolution of independent nonbraided systems, would be expected to result in a decrease in CD, CF, and the topologic measures, and an increase in W and R.

Specific gravity of outwash clasts

Several workers have demonstrated that the solid density of particles of a given lithology decreases systematically with prolonged weathering, such that clasts in the oldest sediments exhibit the lowest specific gravity values (e.g., McGregor 1981; Mansergh & Read, pers. comm.). This approach was also applied to the Tekapo valley outwash gravels. Over 70 clast samples of the dominant lithology, a fine-grained greywacke, were selected from freshly exposed surfaces within each formation, for specific gravity determination. Specific gravity was measured as the ratio of the weight of clasts in air to the weight of the same volume of water, and determinations were carried out using standard procedures (cf. Goudie 1981, p. 94; McGregor 1981).

DIFFERENTIATION OF SUCCESSIVE OUTWASH DEPOSITS

Morphological relations

Mapping of moraines and levelling of long profiles (Fig. 6) clearly indicate the upvalley migration by up to 4 km of successive ice limits, from the Wolds to the Mt John/Tekapo glaciations, and the significant decrease in height between the terrace surfaces of each formation. Maximum height differences are found between the Wolds and Balmoral Formations (< 37 m), and between the Balmoral and Mt John Formations (< 39 m), whereas a height difference of up to only c. 9 m exists between the Mt John and Tekapo terraces.

These height differences represent minimum distances of incision, because initial incision would have been succeeded by a period of aggradation. The height differences between terrace surfaces decrease systematically downstream, as the mean gradient of each successive terrace in turn decreases (Fig. 7A), and the longitudinal profiles converge downstream (Fig. 6 and 7B). The mean gradients of the outwash surfaces range from as much as c. 20 m/km on the Wolds outwash to c. 17.5 m/km on the Balmoral, and from 9.3–11.3 m/km on the Mt John terraces to only 7.5 m/km on the lowest Tekapo terrace fragments (Table 2; Fig. 7B). The gradient of the present Tekapo River over the whole study reach averages about 7 m/km. The gradients of the incised flood channels are steeper than those of the adjacent terrace surfaces, particularly in former proximal zones (Table 1; Maizels 1986). The outwash terrace gradients are similar in magnitude to those reported by Mansergh (1973) for the Ohau terraces of 12.5–25 m/km, and by Speight (1963) for the Pukaki terraces of c. 9 m/km.

Comparison of the surveyed gradients and the gradients adjusted for differential tectonic uplift (Table 2) indicates that the older surfaces have been differentially tilted by between c. 9 and 15%, respectively, and the younger surfaces by between c. 4 and 9%, respectively, and with maximum total uplift amounts occurring in proximal zones. By comparison, Mathews (1967) found that the total amount of uplift due to isostatic rebound since the Tekapo advance could have been as much as 33 m, and has added to the uplift caused by tectonism.

Thickness of loess cover

Maximum thickness of loess cover was found on the outlier of Pattersons Terrace (av. c. 1.2 m; Ministry of Works borehole data; Fig. 8), while significantly thinner loess covers were found on both the Wolds and Balmoral surfaces (av. c. 0.9 and 0.8 m, respectively; Fig. 7C, 8 and Table 3). The Mt John and Tekapo surfaces also exhibited significantly less loess cover than the earlier surfaces (c. 0.5 and c. 0.4 m, respectively), but no significant differences were found within the sequence of Mt John and Tekapo terraces (Table 3). The measured thicknesses are somewhat greater than the 2 cm thickness recorded by Tuck (1975) on the Tekapo deposits, and the 0.5 m thickness observed by Liedtke (1980) on the Wolds surface. However, they match more closely Webb's (1976) values of over 0.70–0.95 m on the Wolds and Balmoral surfaces and overlying a paleosol. Some of the discrepancy between values recorded by different workers may reflect the significant variations in loess thickness that can occur on a single outwash surface (e.g., Tonkin et al. 1974). On the Balmoral surface, loess thicknesses were found to be significantly greater over the bar tops of the former braid channels than along the channel courses, including the more deeply entrenched flood channels (see Maizels 1987). Most of the old channels are marked by deflation hollows and linear scours in which the underlying pebble lag is exposed (e.g., Gibbs et al. 1945; Leamy et al. 1973; Webb 1976). By contrast, the variations in loess thickness on the younger Mt John and Tekapo surfaces are such that maximum thicknesses


Lake Alexandrina
MT. JOHN
Lake Tekapo
TR 10
TR 9
Fork Stream
TR 7
MT. JOHN & TEKAPO MORAINE
Edwards Stream
BALMORAL MORAINE
MT. JOHN
WOLDS MORAINE
TR 4
TR 2
SAWDON TERRACE
PATTERSONS TERRACE
TR Ib
TR 5
TR 8
Irishman Creek
TR Ia
TR 5
TR3
Tekapo River
TR 6
Moraine
Outwash
Alluvium
Bedrock
Survey Transect
Survey Transect and Loess Thickness Profile
Area of detailed mapping of Paleochannel Systems
Gravel Sample Sites
Road (S.H. 8)
0
5km

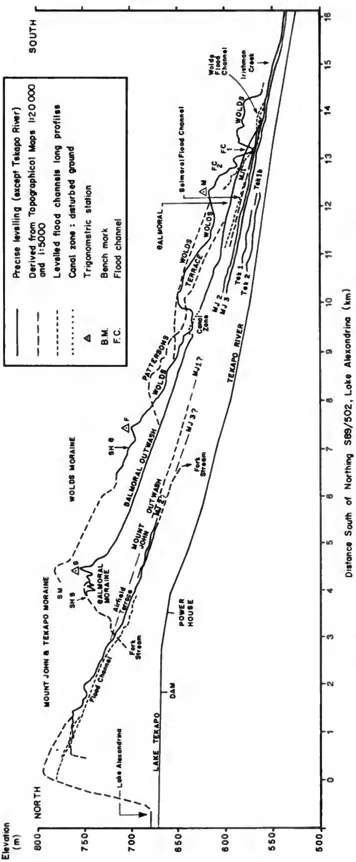

Fig. 6 Longitudinal profiles of the main glacial/glaciofluvial formations in the Tekapo valley.

← Fig. 5 (*opposite*) Morphological map of the Tekapo valley based on interpretation of aerial photographs, and location of survey lines and outwash gravel sampling sites.

are concentrated along the paleochannel courses (see also McKellar 1960). Loess thicknesses in many of these younger channels exceed those of the Balmoral outwash channels (see Fig. 7C and 8).

Nature of the preserved channel pattern

Major contrasts occur in the characteristics of the preserved paleochannel patterns on successive terrace surfaces (Fig. 7D, E and 9). The drainage network on the Wolds surface is fairly indistinct but in some areas appears to comprise a low density, large-scale series of braid bars within widely spaced, broad channels. Elsewhere, a low degree of braiding, with some channel bifurcation, is present between zones of more hummocky terrain exhibiting disjointed drainage courses, depressions, and pools. The networks also include several deep, broad, incised channels (see Fig. 8, 9) dissecting the Wolds surface and cutting through the terrace edge on to the lower Balmoral surface. These deep channels are initiated at transverse, north-facing bluffs, which appear to represent either former ice-contact slopes, or fault scarps (Mansergh pers. comm.). The drainage pattern on Pattersons Terrace is similarly subdued and comprises indistinct braid bars and areas of disrupted drainage, closely resembling that of the Wolds surface. However, the much higher channel density, channel frequency values, and indices of braiding indicate a rather smaller scale, denser, more highly braided network than on the Wolds surface. The Balmoral drainage network is quite distinct from that of either the Wolds or the later outwash surfaces. Here, several integrated dendritic networks have evolved, giving rise to low numbers of bifurcating channels. The main central network rises within the Balmoral moraine complex itself and drains much of the single outwash surface. However, evidence of local areas of former braiding is also present, perhaps reflecting localised preferential erosion of topsoil and loess within the shallower, braided paleochannel courses. The preserved Balmoral channel pattern therefore seems to form a composite network, with a consequent dendritic network superimposed on, and partially revealing (through water and eolian erosion), the underlying original braided network (see also Fitzharris et al. 1982). The lower terraces that have been interpreted as representing Mt John outwash are distinct from both the Wolds and Balmoral surfaces in that they exhibit extensive, complex, highly braided paleochannel networks (Fig. 9). The numerous narrow channels are densely spaced across the outwash surface, and exhibit high numbers of channel junctions and bifurcations. The channel network is readily identified from aerial photographs and on the ground, particularly because vegetation contrasts follow the topographic variations between channels and bars.

The channel courses are frequently lined with fescue grasses and scabweed, while the braid bars, often with gravel deposits exposed, support a scattering of tussock grasses and matagouri (*Discaria toumatou*). These networks are similar

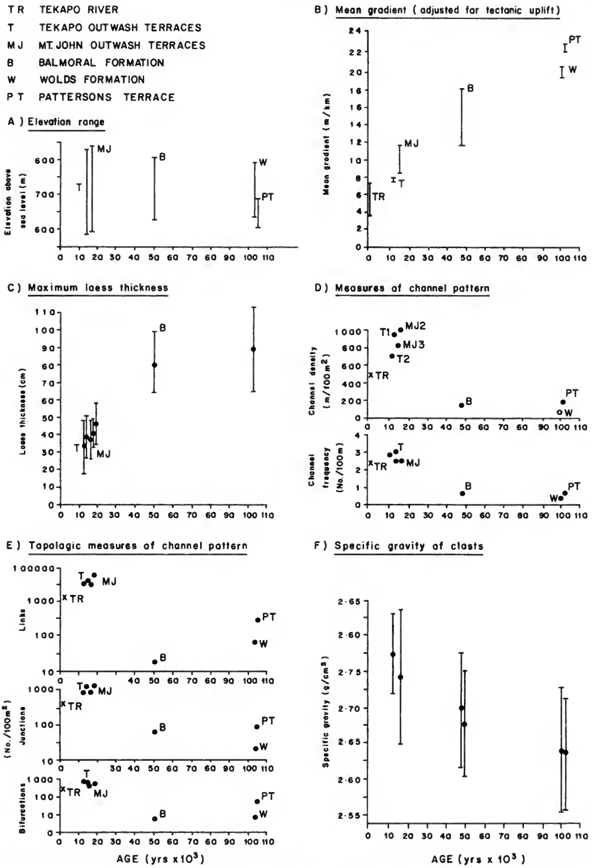

Fig. 7 Measures of geomorphic criteria for successive outwash terrace deposits, Tekapo valley. A Elevation range of each formation. B Mean gradient of each outwash terrace, adjusted for differential tectonic uplift. C Mean and standard deviation of loess thickness for the main outwash terraces. D Paleochannel density and frequency for the main outwash deposits. E Topologic indices of the degree of braiding of paleochannel systems of the main outwash deposits. F Specific gravity of greywacke clasts in the main outwash deposit (see Table 4).

to those described by Powers (1962) on the younger Hurunui terraces, and by McKellar (1960) on the Hawea outwash south of Lake Wanaka. The Tekapo terrace surfaces exhibit highly braided paleochannel patterns, similar to those of the Mt John outwash. Unfortunately, only narrow terrace fragments have been preserved in this area, precluding more extensive sampling of the channel pattern. The present-day channel pattern of the Tekapo River is also braided over much of the study reach. The floodplain includes a number of bars and islands, many of which have become vegetated, leaving a complete hierarchy of channels from active through to almost totally inactive.

Specific gravity (solid density) of outwash clasts

The measurements of specific gravity indicate that those deposits considered to be the oldest also exhibit the lowest specific gravity values (Fig. 7F, and Table 4). The values for the Pattersons Terrace and Wolds deposits and those bounding Irishman Creek, average 2.63, 2.64, and 2.68 g/cm^3 respectively, while those of Balmoral average 2.70, and those of Mt John and Tekapo reach mean values of 2.74 and 2.77 g/cm^3, respectively. The decrease in values with increasing age matches the patterns of change in specific gravity recorded by Mansergh & Read (1983 pers. comm.) and in till by McGregor (1981) (see Table 4A). However, the present data indicate much higher values for the Mt John and Tekapo deposits than McGregor's till data, and a rather lower value for the Pattersons Terrace deposit than that obtained by Mansergh. No significant difference was found between the specific gravity values for the Pattersons Terrace and Wolds deposits, nor between the Mt John and Tekapo deposits (Table 4B). However, the specific gravity values of the Balmoral deposits were found to differ significantly from those of both the Wolds and Mt John deposits.

INTERPRETATION OF RESULTS

Methodological Assumptions

The results of the topographic, gradient, loess thickness, channel network, and specific gravity analyses provide a quantitative and objective basis for the discrimination and classification of the main morphological units in the Tekapo valley. However, the validity of any such classification depends on the validity of the assumptions, and the assessment of likely errors, involved in the interpretation of the quantitative measures obtained. Several assumptions have been made, for example, in the interpretation of the morphological data: (1) Although the longitudinal profiles have been used in the comparison of different deposits, each formation exhibits substantial lateral variation in topography (see Fig. 8); precise height differences and correlations between different surfaces are thus subject to some error. (2) Surfaces of similar elevation are assumed to be of similar age (e.g., Wolds and Pattersons Terrace). However, deposits of similar elevation may have been formed at different times in different parts of the valley, or older (higher) deposits may have been eroded, reworked, or exhumed by later glacial or fluvial activity. (3) The rates of uplift calculated for each outwash surface are based on assumptions of the likely age of the deposit, as proposed by Speight (1961) and Mansergh (1973). The uplift predictions for the older deposits, in particular, are therefore likely to be subject to the greatest error.

The interpretation of decreasing loess thicknesses through the terrace sequence is also based on several assumptions. (1) The basic assumption is that maximum rates of loess accumulation occurred during periods of ice recession, with extensive ice-free and sparsely vegetated areas newly exposed to eolian transport. Hence, great thicknesses of loess cover on a surface are interpreted as representing accumulation during

Table 2 Mean gradient of outwash terrace surfaces and amounts of differential tectonic uplift, Tekapo valley.

Formation		Surveyed mean gradient (m/km)	Amount of differential uplift (m/km) after Adams (1979)	Amount of differential uplift (m/km) after Wellman (1979)	Corrected mean gradient (m/km) after Adams (1979)	Corrected mean gradient (m/km) after Wellman (1979)
Wolds		21.8	1.9	2.9	19.9	18.9
Wolds F.C.*		22.1	1.9	3.1	20.2	19.0
Balmoral		18.8	1.2	2.4	17.6	16.4
Balmoral F.C.		13.0	1.0	1.7	12.0	11.3
Mt John						
Proximal surface†	1	23.4	0.6	1.7	22.8	21.7
Proximal surface†	2	16.3	0.5	1.2	15.8	15.1
Proximal surface†	3	14.3	0.5	1.3	13.8	13.0
Distal surface†	1	11.6	0.3	0.5	11.3	11.1
Distal surface†	2	10.3	0.3	0.4	10.0	9.9
Distal surface†	3	10.3	0.3	0.4	10.0	9.9
Distal surface†	4	8.6	0.3	0.4	8.3	8.2
Tekapo						
Proximal F.C.	1	20.4	0.5	1.6	19.9	18.8
Proximal F.C.	2	21.6	0.5	1.6	21.1	20.0
Proximal F.C.	3	23.3	0.6	1.9	22.7	21.4
Proximal F.C.	4	23.3	0.4	0.5	22.9	22.8
Distal surface	1a	7.8	0.3	0.6	7.5	7.2
Distal surface	1b	7.8	0.3	0.5	7.5	7.3
Distal surface	2	8.0	0.3	0.5	7.7	7.5

*F.C., flood channel.
†Proximal/distal boundary taken as Fork Stream.

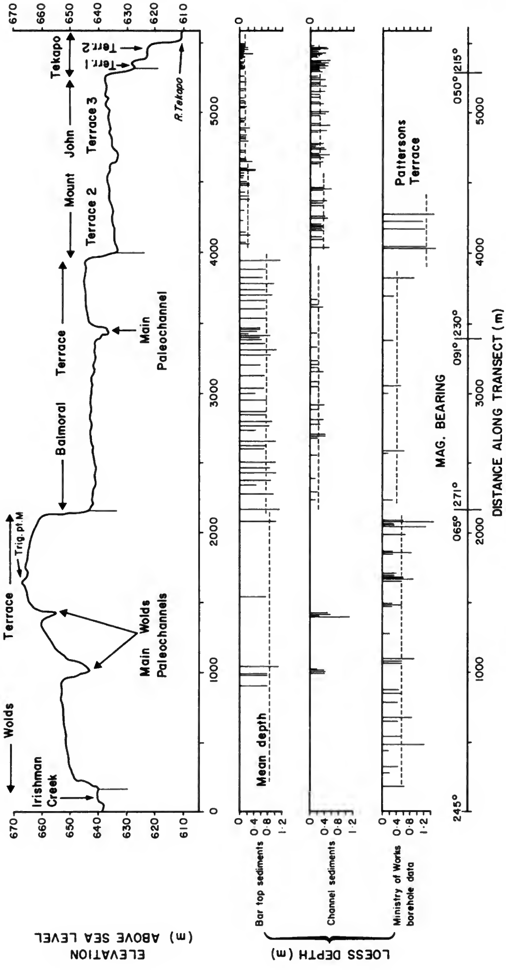

Fig. 8 Transverse profile of loess thickness across the main outwash terrace surfaces.

at least one glacial/interglacial period. However, loess might have accumulated during interglacials when much sediment was available from exposed river sediments (e.g., Ives 1973). The presence of a buried paleosol would provide stronger confirmatory evidence of a prolonged, warm period. (2) The data analysed in this study were obtained from a single transverse profile; no data are available to indicate longitudinal variations between proximal and distal zones. Such a study would help indicate sources of material, assuming a downwind decrease in loess thickness. Thus, this study assumes a constant source and distance of loess transport along a given traverse.

Other assumptions underpin the interpretation of differences in channel pattern characteristics on the terrace surfaces. (1) The basic assumption is that similar drainage patterns developed on each surface prior to its abandonment by meltwaters as the ice margin retreated and/or became increasingly entrenched. This is questionable because, although many proglacial meltwater streams do exhibit complex braided channel systems, the channel pattern that actually develops depends on a wide range of factors. In particular, channel pattern represents a response of the stream to its water and sediment load over a given energy gradient, being carried through a given range of bank materials. Hence, any analysis of channel pattern changes should consider the possible physical and geomorphic controls on these changes. In addition, the approach assumes that no significant downstream changes in channel pattern have occurred, since the sampling transect crosses each terrace surface at a different distance from the former ice margin. A change in pattern may not necessarily represent destruction or obliteration of the "original" pattern, but simply represent the initial development of a different kind of pattern, in response to different hydrologic and geomorphic controls. (2) Two other assumptions made in the generation of quantitative measures of the terrace channel patterns are (a) that the observed terrace fragments

Table 3 Loess thickness on Tekapo valley outwash terraces.

Formation			No. of samples	Thickness (cm) Mean	S.D.	Maximum (cm)
Wolds			2	87.00	22.63	>103
Wolds	FC1u*		3	84.80	18.33	>106
	FC11		3	43.30	3.84	46
	FC2		4	59.13	34.29	>107.5
Balmoral	b*		33	78.73	16.60	112
	c		11	24.75	7.96	39.2
	dh		10	23.60	8.63	39.0
	FC1,2		4	64.80	13.45	83.0
	FC3		4	50.25	4.73	55.5
	FCb		2	17.80	2.55	19.6
Mt John	1b	b	6	31.32	16.36	52.8
		c	5	44.88	11.79	60.4
Mt John	2b		18	22.02	9.85	42.2
	c		16	40.50	7.85	60.0
Mt John	3b		23	17.37	4.79	33.1
	c		28	36.58	10.00	57.2
Tekapo	1b		6	12.67	2.72	16.0
	c		11	38.04	12.20	56.5
Tekapo	2b		14	16.98	7.70	38.0
	c		9	33.32	14.77	57.5
Ministry of Works borehole data						
Wolds			33	55.58	27.25	120.0
Balmoral			8	40.63	26.07	91.0
Pattersons Terrace			11	115.73	26.43	152.0
Irishman Creek			1	60.00		
Mt John 3			3	100.67	16.74	120.0
Mt John 2			1	152.00		

Analysis of variance

(1) Differences within formation.

Formation		Level of significance
Tekapo	1c/2c	ns
	1b/2b	0.050
Mt John	1c/2c	ns
	1c/3c	ns
	1b/2b	ns
	1b/3b	0.050
	2c/3c	0.100
	2b/3b	0.050
Balmoral	c/dh	ns

(2) Differences between formations.

Formation			Level of significance
Wolds/Balmoral	(b)		0.200
/Mt John	(c)		0.005
/Tekapo	(c)		0.005
Balmoral	(b)		
	/Mt John	(c)	0.005
	/Tekapo	(c)	0.005
Mt John	(c)/Tekapo	(c)	ns
	MJ3c/Tek	1c	ns
	MJ3c/Tek	2c	0.200
	MJ3b	1b	0.050

*FC, flood channel; u, upper; l, lower; b, bar top; c, channel bed; dh, deflation hollow.

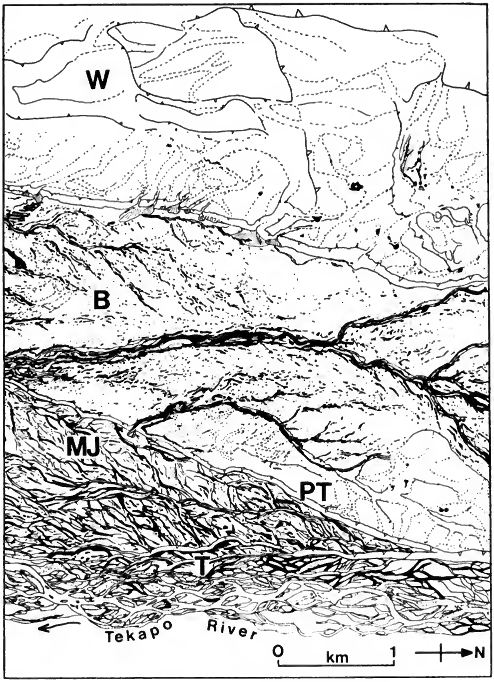

Fig. 9 Paleochannel systems on the main outwash terrace surfaces, west of Tekapo River and south of the Fork Stream. Based on interpretation of 1:20 000 aerial photography. T, Tekapo outwash; MJ, Mt John outwash; B, Balmoral outwash; W, Wolds Formation; PT, Pattersons Terrace (see Fig. 5 for location map).

are representative of the whole former outwash surface, much of which has now been eroded and removed, and (b) that the measurements represent a unified, integrated, contemporaneous channel system, rather than numerous fragments of successive channel systems. Neither of these assumptions can be fully verified in this study. (3) The measures of channel pattern, channel frequency, and degree of braiding on the older deposits are partly based on fragmentary, indistinct evidence of paleochannel courses, and are therefore also subject to some error. (4) The interpretation of clast specific gravity assumes that the initial clast density values were all constant and high, and that weathering of a deposit has affected each clast equally. However, if clasts have been reworked from older deposits, the youngest deposits are likely to include a wide range of "old" clasts. Some clasts from the present bed of the Tekapo River near the Fork Stream confluence, for example, exhibit specific gravity values lower than those recorded for the Mt John deposits (see Table 4).

Origin and chronology of the terrace sequence

The distribution of the main geological formations in the Tekapo valley, based on interpretation of the geomorphic criteria discussed above, is shown in Fig. 10. These data generally confirm the interpretations put forward by Gair (1967), Liedtke (1980), and Mansergh (pers. comm.) (see Fig. 4 and 10). However, several details of these interpretations appear to contradict the present evidence. The present data support the view that Pattersons Terrace is likely to be older (having a thicker loess cover), or at least contemporaneous with, the Wolds Formation. Both deposits are mantled with a thick loess cover. Their high elevations, steep gradients, channel pattern characteristics, and low specific gravity of the

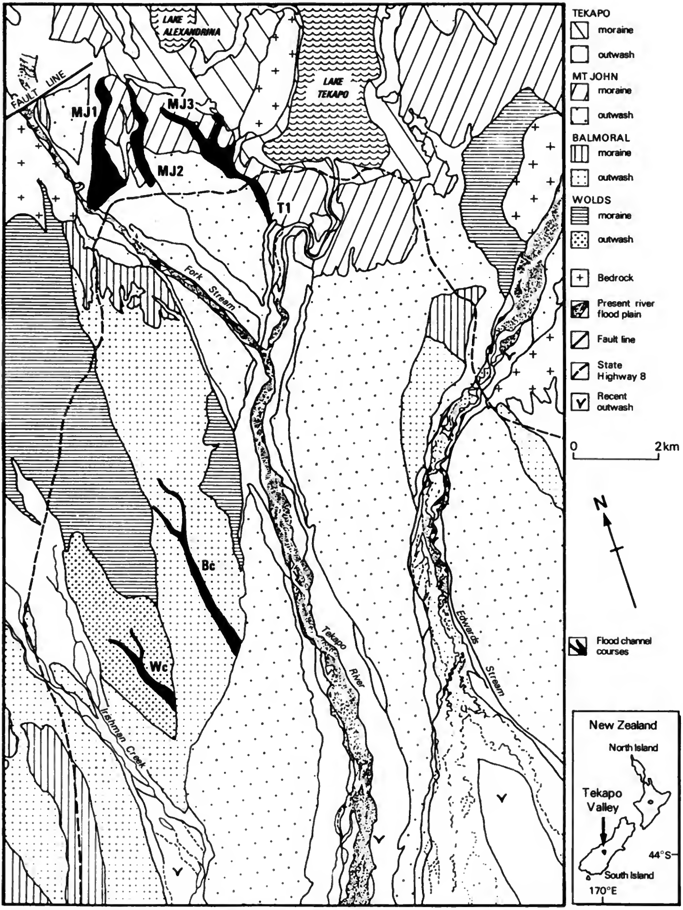

Fig. 10 Proposed interpretation of major glacial/glaciofluvial formations in the Tekapo valley.

Table 4 Specific gravity determinations of outwash clasts, Tekapo valley.

Formation	No. of samples	Specific gravity Mean	S.D.	Comparison with other data McGregor (1981)	Mansergh & Read (pers.comm.)
Tekapo River	15	2.711	0.043		
Tekapo outwash	16	2.773	0.056	2.63 ± 0.027	2.705
Mt John	35	2.741	0.093	2.60 ± 0.070	2.705
Balmoral	27	2.696	0.080	2.58 ± 0.028	2.682
Irishman Creek	10	2.676	0.073		
Wolds	32	2.641	0.087	2.55 ± 0.039	2.640
Pattersons Terrace	20	2.635	0.077		2.670

Analysis of Variance: levels of significance of differences in specific gravity values for different formations.

	Tekapo River	Tekapo	Mt John	Balmoral	Irishman Creek	Wolds	Pattersons Terrace
Tekapo River	–	0.005	0.005	ns	ns	0.005	0.005
Tekapo	0.005	–	ns	0.005	0.005	0.005	0.005
Mt John	0.005	ns	–	0.005	0.005	0.005	0.005
Balmoral	ns	0.005	0.005	–	ns	0.010	0.010
Irishman Creek	ns	0.005	0.005	ns	–	0.020	0.100
Wolds	0.005	0.005	0.005	0.010	0.020	–	ns
Pattersons Terrace	0.005	0.005	0.005	0.010	0.100	ns	–

clasts are not significantly different. Both Pattersons Terrace and the Wolds surface extend from irregular hummocky terrain into steeply graded channelled outwash deposits, exhibiting well-weathered sediments. The Balmoral Formation appears to be younger than the Wolds and Pattersons Terrace deposits. The Balmoral Formation is lower, has a lower gradient, thinner loess cover, and higher clast densities. In addition, the Balmoral surface exhibits a distinct series of dendritic drainage courses. These deposits, in turn, differ significantly in terms of all of the measured geomorphic criteria from those of the younger Mt John deposits. The latter exhibit distinct, highly braided paleochannel systems, mantled with only a thin and often discontinuous loess cover, and are composed of relatively high density clasts. However, the Mt John and Tekapo Formations do not exhibit any significant differences in channel pattern or clast density, although the latter deposits are lower, have lower gradients, and a thinner loess cover. The high relative elevation, steep gradients, and thick loess covers of the Wolds and Pattersons Terrace deposits suggest that these represent the oldest formations in the area, and they are likely to have experienced two interglacials since their formation. This would imply that they may both be older than Waimean, and are hence possibly of Waimaungan age (Table 1). The Balmoral Formation is clearly significantly younger and if, as seems likely, it was formed prior to the last glacial stage, it could date either from the early Otiran , or even from the Waimean glaciation. The relatively fresh appearance of the little-weathered, widely exposed outwash deposits of the Mt John and Tekapo Formations suggest that they date from the last glacial stage or late Otiran glaciation. The two series of deposits cannot be distinguished on the measured geomorphic criteria alone, but it is likely that the main spillway channels through the moraines and the lower terraces in the sequence were formed during and immediately following the Tekapo glacial episode.

The paleochannel systems observed on the terrace surfaces represent the last channels on that surface prior to incision (Maizels 1986), so that they are likely to include a range of aggradational and degradational forms. Progressive glacier entrenchment appears to have acted as a major control on terrace incision (McGregor 1963; Soons 1972; Tuck 1975; Wellman 1979; Liedtke 1980), while high volumes of meltwater discharge associated with rapid ice melt would have provided the mechanism for rapid and substantial downcutting (e.g., Tonkin et al. 1974; Fitzharris et al. 1982). Periods of ice wastage were probably accompanied by the extensive accumulation of loess, derived from freshly deglaciated and still nonvegetated terrain. Incision by meltwaters was followed by periods of lateral planation by streams, reworking sediments on this lower surface, while allowing large thicknesses of loess to accumulate on the higher older surfaces. With continued climatic amelioration, and improved vegetation colonisation associated with interstadial or interglacial conditions, sediment yields diminished, soil development progressed, and fluvial activity stabilised. These activities continued until a further period of glaciation, in which moraine and outwash activity had become confined to an increasingly narrow active zone of the valley floor. While braided glacial meltwater streams spread across the valley floor, snow-fed and summer thaw meltwaters draining the higher, older, loess-mantled surfaces developed into more integrated dendritic channel systems.

ACKNOWLEDGMENTS

I would particularly like to thank Jane Soons,Glenn McGregor, Mark Mabin, and Graham Mansergh for their encouraging and stimulating discussions. Thanks are also expressed to Paul Rodley for tenacious assistance in the field, and to all members of the Department of Geography, University of Canterbury, who generously gave me technical, logistic, and administrative support. Assistance from members of the Ministry of Works at Twizel and in Christchurch is also gratefully acknowledged. The research was funded by the British Federation of University Women and by the Royal Society.

REFERENCES

Adams, J. 1979: Vertical drag on the Alpine Fault. *In*: Walcott, R. I.; Cresswell, M.M. *ed*. The Origin of the Southern Alps. *Bulletin of the Royal Society of New Zealand 18*: 47–54.

Bruce, J. G. 1973a: Loessial deposits in southern South Island, with a definition of Stewarts Claim Formation. *New Zealand journal of geology and geophysics 16*: 533–548.

————1973b: A time-stratigraphic sequence of loess deposits on near-coastal surfaces in the Balclutha district. *New Zealand journal of geology and geophysics 16*: 549–556.

Burrows, C. J. 1972: Post-Otiran moraines in Canterbury. *New Zealand journal of geology and geophysics 15*: 296–299.

Fitzharris, B. B.; Mansergh, G. D.; Soons, J. M. 1982: Basins and lowlands of the South Island. Pp. 343–366 *in*: Soons, J.M.; Selby, M. J. *ed*. Landforms of New Zealand. Longman.

Gage, M.; Suggate, R. P. 1958: Glacial chronology of the New Zealand Pleistocene. *Geological Society of America bulletin 69*: 587–589.

Gair, H.S. 1967: Sheet 20—Mt Cook. Geological map of New Zealand 1:250 000. Wellington, New Zealand. Department of Scientific and Industrial Research.

Gibbs, H. S.; Raeside, J. D.; Dixon, J. K.; Metson, A. J. 1945: Soil erosion in the high country of the South Island. *Department of Scientific and Industrial Research bulletin 92*. 72 p.

Goudie, A. 1981: Geomorphological techniques. Allen & Unwin. 395 p.

Ives, D. 1973: Nature and distribution of loess in Canterbury, New Zealand. *New Zealand journal of geology and geophysics 16*: 587–610.

Leamy, M. L.; Milne, J. D. G.; Pullar, W. A.; Bruce, J. G. 1973: Paleopedology and soil stratigraphy in the New Zealand Quaternary succession. *New Zealand journal of geology and geophysics 16*: 723–744.

Liedtke, H. 1980: Die Pleistozänen Vergletscherungen am Lake Tekapo im Mackenzie-Becken (Canterbury, Neuseeland). Pp. 323–337 *in*: Valentin, H. *ed*. Beiträge zur Geomorphologie und Länderkunde. Berlin, Institute of Geography, Technical University.

Maizels, J. K. 1979: Proglacial aggradation and changes in braided channel patterns during a period of glacier advance : An Alpine example. *Geografiska Annaler 61A*: 87–101.

————1986: Modeling of paleohydrologic change during deglaciation. *Geographie Physique et Quaternaire, Univ. Montreal, XL*: 263–277.

————1987: Large-scale flood deposits associated with the formation of coarse-grained, braided terrace sequences. Pp.135–148 *in*: Ethridge, F. G.; Flores, R. M.; Harvey, M. D. *ed*. Recent developments in fluvial sedimentology. Tulsa, U.S.A. Society of Economic Paleontologists.

Mansergh, G. D. 1973: Quaternary of the Mackenzie Basin. INQUA guide, section I 102.

Mathews, W. H. 1967: Profiles of late Pleistocene glaciers in New Zealand. *New Zealand journal of geology and geophysics 10*: 146–163.

McGregor, G. R. 1981: Weathering characteristics of late Pleistocene tills. *New Zealand journal of geology and geophysics 24*: 107–113.

McGregor, V. R. 1963: The geology of part of Lilybank Station, South Canterbury, New Zealand. Unpublished MSc. thesis, lodged in the Library, University of Auckland. 131 p.

McKellar, I. C. 1960: Pleistocene deposits of the Upper Clutha Valley, Otago, New Zealand. *New Zealand journal of geology and geophysics 3*: 432–460.

Moar, N. T.; Suggate, R. P. 1973: Pollen analysis of Late Otiran and Aranuian sediments at Blue Spur Road (S51), North Westland. *New Zealand journal of geology and geophysics 16*: 333–344.

Porter, S. C. 1975: Equilibrium-line altitudes of Late Quaternary glaciers in the Southern Alps, New Zealand. *Quaternary research 5*: 27–47.

Powers, W. E. 1962: Terraces of the Hurunui River, New Zealand. *New Zealand journal of geology and geophysics 5*: 114–129.

Raeside, J. D. 1964: Loess deposits of the South Island, New Zealand, and soils formed on them. *New Zealand journal of geology and geophysics 7*: 811–838.

Soons, J. M. 1972: Glacial advances in the Rakaia Valley, New Zealand. *New Zealand journal of geology and geophysics 16*: 425–438.

Speight, J. G. 1961: Late Pleistocene geomorphology of an area about Lake Pukaki. Unpublished M.Sc. thesis lodged in the Libary of University of Canterbury.

————1963: Late Pleistocene historical geomorphology of the Lake Pukaki area, New Zealand. *New Zealand journal of geology and geophysics 6*: 160–188.

Speight, R. 1915: The intermontane basins of Canterbury. *Transactions and proceedings of the New Zealand Institute XLVII*: 336–353.

————1921: Notes on a geological excursion to Lake Tekapo. Transactions and proceedings of the New Zealand Institute LIII: 37–46.

————1940: The gravels of the Mackenzie Intermont. *Transactions and proceedings of the New Zealand Institute 70*: 175–187.

Suggate, R. P.; Moar, N. T. 1970: Revision of the chronology of the Late Otira Glacial. *New Zealand journal of geology and geophysics 13*: 742–746.

Tonkin, P. J.; Runge, E. C. A.; Ives, D. W. 1974: A study of late Pleistocene loess deposits, South Canterbury, New Zealand. Part II. Paleosols and their stratigraphic implications. *Quaternary research 4*: 217–231.

Tuck, R. G. 1975: The Late Pleistocene chronology of the Lake Tekapo Valley. Unpublished M.A. thesis, lodged in the Library, University of Auckland. 100 p.

Webb, T. H. 1976: Pedological studies of soils of the Tekapo set in east Lake Pukaki region, south Canterbury, New Zealand. Unpublished M. Agr. Sci. thesis, lodged in the Library, University of Canterbury. 183 p.

Wellman, H. W. 1979: An uplift map for the South Island of New Zealand, and a model for uplift of the Southern Alps. *In*: Walcott, R. I.; Cresswell, M. M. *ed*. The origin of the Southern Alps. *Royal Society of New Zealand bulletin 18*: 13–20.

Young, D. J. 1964: Stratigraphy and petrography of north-east Otago loess. *New Zealand journal of geology and geophysics 7*: 839–863.

————1967: Loess deposits of the west coast of the South Island, New Zealand. *New Zealand journal of geology and geophysics 10*: 647–658.

New Zealand Journal of Geology and Geophysics, 1989, Vol. 32: 243–253
0028–8306/89/3202–0243 $2.50/0

A late Otiran–Holocene paleoenvironment reconstruction based on cave excavations in northwest Nelson, New Zealand

T. H. WORTHY
National Museum of New Zealand
P.O. Box 467
Wellington, New Zealand

D. C. MILDENHALL
New Zealand Geological Survey
Department of Scientific and Industrial Research
P.O. Box 30 368
Lower Hutt, New Zealand

Abstract Excavations of deposits ranging in age from 20 000 years ago, within the Otira glacial maximum, to the commencement of the Holocene 10 000 years ago, from Honeycomb Hill Cave in the Oparara valley, northwest Nelson, New Zealand, have revealed a large fossil avifauna. Faunal and floral analyses indicate that the cave, now in a lowland podocarp/beech forest, was in a subalpine shrub zone with nearby montane forest about 20 000 years ago. From this the existence of substantial forest remnants persisting throughout the Otiran Stage in this region is inferred. The upland moa *Megalapteryx didinus* (Owen) and crested moa *Pachyornis australis* Oliver are inferred to have been primarily inhabitants of montane forest and subalpine shrubland. By contrast, the little bush moa *Anomalopteryx didiformis* (Owen) lived primarily in lowland forests. Other extinct birds inferred to have preferred the open shrubland prevailing in the Oparara during the Otiran are Finsch's duck *Euryanas finschi* Van Beneden, *Aptornis otidiformis* (Owen), and *Harpagornis moorei* Haast. Kakapo *Strigops habroptilus* Gray are only present in younger deposits laid down when forest conditions prevailed, supporting the idea that these were primarily lowland birds.

Keywords cave deposits; paleoenvironment; paleoecology; palynology; fauna; flora; Otiran Stage; Holocene; northwest Nelson; New Zealand

INTRODUCTION

The best known New Zealand fossil birds are the moas (Dinornithiformes), a group of large terrestrial birds which exhibited considerable species diversity. The New Zealand landbird fauna generally is characterised by low diversity, high degree of endemism, and a high proportion of species in which flight ability was reduced or absent. Since human occupation about 1000 years ago, much of this landbird assemblage has become extinct, and in fossil deposits a high proportion of the remains found are of extinct or very rare extant species.

Honeycomb Hill Cave (Fig. 1) is a system of c. 13.5 km of passages and tunnels, connecting some 70 entrances formed in Oligocene limestone adjacent to the Oparara River, northwest Nelson. It was discovered by cavers in 1976. It lies at about 250–300 m above sea level within a broad valley draining north–south. The strata dip c.10° to the east. The limestone overlies granite on which the present topography is formed west and north of the cave. To the south and east, the topography is developed on marine mudstones that overlie the limestone.

The prevailing vegetation is, or was before selective logging, a mixed beech/podocarp forest. Silver and red beech, rimu, miro, rata and in wetter zones, kahikatea, were the predominant species. The forest floor is primarily covered in mosses indicative of the very wet climate prevailing. The temperatures are generally cool with some frosts in winter.

A preliminary investigation (Millener & Bartle unpubl. 1982) indicated that the cave contained an abundance of fossil avian remains. A joint project between the New Zealand Forest Service and the National Museum of New Zealand, to determine the extent and nature of the fossil deposits in the cave, was completed in January 1984 (Millener unpubl. 1984), and the Graveyard, Eagles' Roost, Cemetery, and Moa Cave sites were identified as being of outstanding international importance.

This study presents results of an investigation of the Graveyard, a passage with very extensive fossil bone deposits within stratified stream sediments (Worthy unpubl. 1987a). Millener (1984) had shown that at least some of these deposits dated to the Otiran Glacial Stage (last glacial stage) which ended some 14 000 years ago. It was hoped that potential changes in the faunal composition from the glacial to the Holocene could be described. Stratified deposits containing extensive faunas from this time, when the climate and vegetation cover were very different from today (McGlone 1985), were previously unknown in New Zealand, although several more limited faunal assemblages are known (see odd specimens dating from this period listed by Millener (1981) and Worthy (1987b)).

Collections made by Millener (1984) were, predominantly, of lag deposit material from near Site 1, and from the Main Channel between Site 2 and Site 3 (Fig. 2)* Millener made small excavations on the surface and face of The Terrace and at the base of the slope leading towards the Main Channel in

Received 13 April 1988, accepted 1 August 1988

*In the interests of preserving the subfossil deposits, the complete map of the cave has not been made public by the Department of Conservation, so the relationship of the Graveyard to other passages in the system cannot be shown here. The cave is managed by the Department of Conservation, P.O. Box 357, Westport.

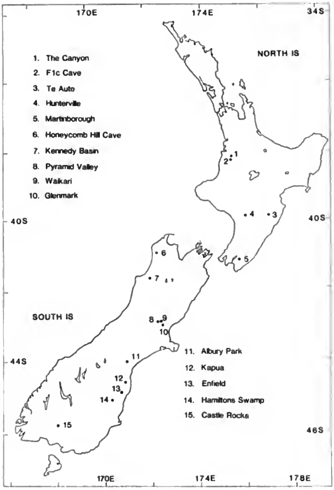

Fig. 1 Location of New Zealand fossil sites mentioned in the text.

what is now the middle of Site 3. Kea, *Nestor notabilis* (Gmelin), and the extinct Finsch's duck, *Euryanas finschi* Van Beneden, were abundant. Site stratigraphy was not reported.

During visits by Worthy in 1984 and 1986 it became apparent that deposits in the Graveyard were stratigraphically divided into at least two layers. A moa bone (*Dinornis torosus* Hutton), collected from the surface of an exposed moa bone breccia in the Main Channel (Fossil Record Number L27/f88)*, was dated at 16 200 ± 300 years B.P., and a tibiotarsus of *Pachyornis elephantopus* (Owen) (Fossil Record Number L27/f90), collected from the lag deposit beyond The Terrace, was dated at 14 500 ± 250 years B.P. (National Museum files). Because these dates indicate that some of the deposits were laid down before the end of the Otiran, a study of these layers could reveal the fauna of this largely unknown period in New Zealand's history and may also indicate changes following the warming at the commencement of the Holocene.

Material from lag deposits could not be used for proportional analyses of species because it contains a mixture of material from all pre-existing layers. The Terrace, however, was obviously extremely important, because the bone breccia in the Main Channel continued as the lowest part of The Terrace sequences beneath 0.5 m of other sediments. At the lowest part of the Walking Access Passage, just before the slope up to the Main Channel, a low-roofed chamber leads to the right (Fig. 2). Within it, small scale scour of sediments has revealed bones to a depth of 0.5 m.

Excavations were planned with two broad objectives: (1) determination of the age range, extent, and depositional environment of subfossil material; and (2) characterisation of the fauna for each layer, paleoenvironmental reconstruction, and the recording of any changes to the fauna such as species composition or changes in size or abundance of particular species.

METHODS

Fieldwork was undertaken periodically between 29 December 1986 and 19 May 1987.

Excavations at Site 1 revealed that faunal deposition had been limited because the site was on the outer curve of stream flow and thus subject to the greatest water velocity. This meant that correlation of bones in the observed stratigraphy with those in the Main Channel was virtually impossible, so Site 2, a 1 m^2 area adjacent to the bone breccia in the Main Channel, was excavated. This enabled correlation of material in Sites 1 and 2 with the unexcavated reference bank of bone breccia and with the trench from the Main Channel (1 m wide) through to the lowest point of the access passage (Site 3, Fig. 2). In this third trench it was planned to go as deep as necessary to determine the extent of the fauna-bearing deposits.

Excavations at Sites 1 and 2 required the complete removal and sieving of material. Following excavation, material was hauled by a rope and pulley system 10 m vertically to the rock shelter above where it was wet sieved. The volume of sediments processed was about 1.5 and 1 m^3 in Sites 1 and 2, respectively.

Before Site 3 was excavated, the entire Main Channel area was covered by a wooden stage to protect the bones. Deposits at Site 3 were mostly coarse sediments (sand and gravel) which did not need sieving. Bones were therefore sorted as they were excavated and the wastes dumped at the lower end of the Main Channel. The base of the exposed bone breccia in the Main Channel was followed downslope into the Walking Access Passage. Here the breccia deposit (layer 3, L3) fanned out over a clay deposit containing bones probably derived from up the Walking Access Passage. Excavations were made to 1 m depth, and the base of this bone layer (L4) was not reached.

Material was washed and dried upon arrival at the National Museum, then sorted by site, layer, and species, then registered. Measurements were made for complete limb bones of many moa and Finsch's duck.

Samples of moa bone from each layer were submitted for ^{14}C dating to the Institute of Nuclear Sciences, N.Z. Department of Scientific and Industrial Research. Pollen analysis of clay samples was undertaken by D. C. Mildenhall.

RESULTS

Stratigraphy and sediment description

Sites 1 and 2 (Fig. 3) Layer 1 (L1) is a thin (5–20 mm) deposit covering layer 2, consisting of limestone weathering

*New Zealand Fossil Record File number based on the metric (NZMS 260) topographic map series, sheet L27.

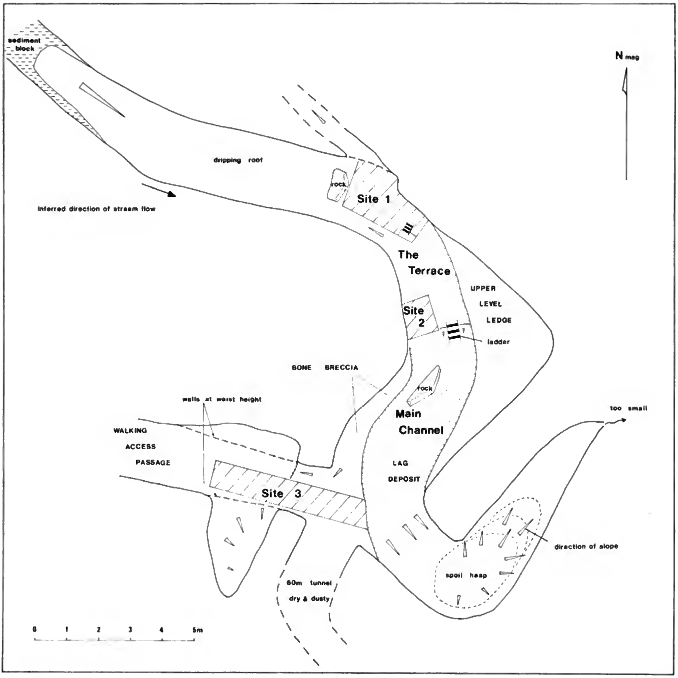

Fig. 2 Plan view of the Graveyard passage, Honeycomb Hill Cave, Oparara valley, showing location of excavation sites.

products from the cave walls and roof, and partially consolidated in places by calcite. It is therefore considerably younger than the underlying fluvial deposits. The only bones in L1 were remains of owlet-nightjars and some frogs (i.e., animals that had lived in or entered the cave relatively recently).

Layer 2 (L2) is the first layer of stream-laid sediments encountered. Its upper surface is of variable topography, apparently relating to roof drip erosion subsequent to its deposition. Its lower surface is even, although inclined downstream at c. 10–15°. L2 thus thickens downstream, reaching a maximum of 0.5 m.

The sediments in L2 are mainly fine silts and sands, with many quartz moa gastroliths. Small bird bones predominate in the faunal material, with relatively few moa bones and some moa eggshell fragments, probably derived from unlaid eggs from within trapped moas. The fauna of L1 and L2 is considered together since bones protruding from L2 were often incorporated in the calcite crust of L1.

Layer 3 (L3) is defined by the presence of bones within mainly coarse grit with some sand and gravel. In Site 1, which covered an area where the stream had been constrained between the wall and a large limestone rock, there are few bones. Below the L2–L3 interface a layer of sparse moa bones is found and very few are encountered till 0.4 m below. Here another sparsely fossiliferous layer defines the base of L3. Below the bones in L3 the sediments are uniform and only two small bone fragments were encountered in the next 0.3 m.

In Site 2 the interface of L2 with L3 is marked by a layer of angular limestone rocks. Both "upstream" and "downstream" of Sites 1 and 2 erosion has destroyed L2 (Fig. 3).

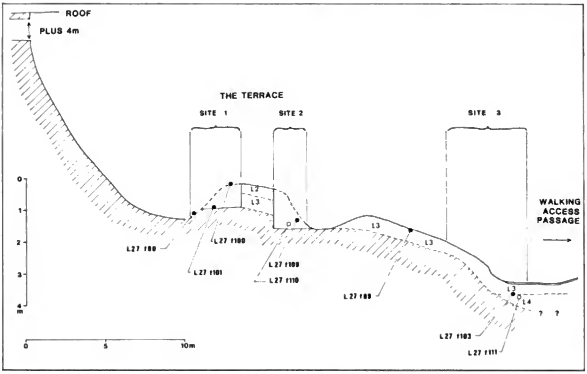

Fig. 3 Extended longitudinal section through the Graveyard deposits. N.Z. Fossil Record numbers (L27 series) show location of dated fossil bones (•) or pollen samples (○). Hatching delineates sediments in which there are no bones.

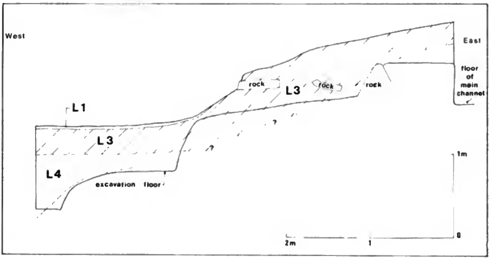

Fig. 4 Profile of the northern side of the Site 3 excavation. All L3 is hatched to differentiate it from L1 and L4.

Site 2 is slightly different in character because deposition was in the area of slow flow on the inside of the stream channel. The sediments in L2 are finer than those in Site 1 but are still predominantly coarse sands and grit. Below the layer of limestone rocks in the exposed section the bones occur only in the first 0.3 m of sediment but, elsewhere within the excavated area, they extend to 0.5 m depth. Interspersed with the bones are numerous stream cobbles up to 0.15 m diameter. Moa bones are very abundant as are smaller bones of, for example, kea and Finsch's duck. The base of L3 was taken to be at the depth at which bones and cobbles were no longer encountered (at this site, at a maximum of 0.5 m below the L2–L3 interface). Blue-grey silt continues to at least 0.7 m below the L2–L3 interface in the exposed section of Site 2. A feature of this zone is discontinuous bands of browner sediments. A 5 mm thick clay layer was found 0.6 m below the L2–L3 interface.

Site 3 (Fig. 4) To avoid confusion, layers encountered here are designated numbers that correspond to the equivalent layer in Site 2. The surface deposits at the eastern end of Site 3 were part of L3 which could be traced from Site 2 along the exposed bone breccia of the Main Channel as shown in the longitudinal section (Fig. 3). At the eastern end of Site 3 the base of L3 (i.e., where the bones ended) was only 0.2 m below the surface. Excavation was deep enough to identify the change from ossiferous sediments to those lacking bones and thus to reveal a sediment profile. In the first 3 m of the trench,

L3 slopes steeply (10–20°) down from the Main Channel, and levels out to form a 0.3 m thick layer extending from 20 to 320 mm depth below the surface. In the level area of the sediments (i.e., 3–5 m from the Main Channel), L3 was covered by a deposit similar in character to that of L1 in Sites 1 and 2. Thus, in Site 3, 0–20 mm depth over the level area is termed L1. It is nonsedimentary, derived from weathering breakdown of limestone and secondary calcite deposition, and is porous white and brown in appearance.

In the first metre from the Main Channel below L3 there are coarse silts and gravel without bones. A large limestone rock protrudes through these sediments between 0.75 and 1.5 m from the Main Channel. The base of L3 was not exposed between 1.5 and 3.0 m from the Main Channel so it is extrapolated as a dotted line in Fig. 4. Beneath the area where L3 is horizontal (i.e., 3–5 m from the Main Channel) is a layer of fine brown clay. At the excavation face, 5 m from the Main Channel, this layer (L4) extends from 0.3 m to the base of the excavation, at 1.0 m depth. However, it was deposited on a sloping layer of coarse blue-grey grit similar to that below L3 in the area 0–3 m from the Main Channel. L4 is thus inserted as a wedge between L3 and lower sediments.

Bones of moa predominate in L3 but there are also large numbers of medium sized birds, for example, kea and Finsch's duck, as in Site 2. Slabs of limestone probably derived from the roof are present in L3. In L4 there are bones of both moa and smaller birds.

Association of bones and their significance In L2, L3, and L4 there were numerous, partially articulated sets of bones, such as a pelvis and associated femora, or a row of vertebrae; one entire moa foot skeleton was articulated. This shows that the faunal material was deposited as recently dead carcasses that were probably rotting, since some dismemberment had occurred. These bones could not have been redeposited following erosion from an older deposit, and their age should reflect the age of the bones at similar stratigraphic levels within the deposit. Redeposition of some bones cannot be discounted but is considered very unlikely because all bones had similar preservation features.

L4 in Site 3, although not extensively excavated, contains a fauna with an even greater association of skeletal elements, suggesting that skeletons or animals reached this deposition zone largely intact. However, the very wet clays toward the base of L4 provided a poor medium for preservation and smaller, more porous bones are often irrecoverable.

Age of deposits

The results obtained by ^{14}C dating (Table 1) suggest that deposition of L3 began about 20 000 years ago. The upper limit for deposition of L3 may be about 14 000 years ago, since this is the age obtained for a bone of the heavy footed moa (L27/f90) assumed to have been eroded from this layer. It certainly continued until 16 000 years ago (L27/f88 collected in situ near the top of L3 in the Main Channel).

Dates obtained for L27/f100 (in situ at the top of L2) and L27/f102 (eroded out into the entrance of the passage revealed by excavations in Site 1) indicate that deposition continued until about 11 000 years ago.

Faunal composition

The abundance of the species present in the various layers of the Graveyard is detailed in Table 2.

The upland moa, *Megalapteryx didinus* (Owen), is the most common moa in all layers. A high proportion of its remains are of juvenile birds. Of 73 birds represented in L3, 56% are juvenile or subadult (determined from incomplete ossification). This is a very high proportion of young birds for any assemblage and greater than has been recorded for moas at any other locality. The bones of the crested moa, *Pachyornis australis* Oliver, are next most abundant but are present only in L3. These have been identified previously (Millener 1984) as the stout-legged moa, *Euryapteryx gravis*, but Worthy (1989, this issue) considers the crested moa to be a distinct species and that these bones are referable to it. 30% of the individuals of the crested moa represented by the bones are juvenile.

The moa species composition in the vicinity may have changed between the time of deposition of L3 and L1/L2. The little bush moa, *Anomalopteryx didiformis* (Owen), present in the small sample from L1/L2, is not within the much larger excavated areas of L3. This suggests bones of this species found in the lag deposits by Millener (1984) are likely to have been derived from L1/L2. Millener also recorded two bones of the little bush moa from Site 3. Examination of these bones indicates they were on the surface, and are therefore not necessarily contemporary with in situ material at this site. The heavy footed moa, *Pachyornis elephantopus*, is present in L3 and, like the crested moa, is absent from L1/L2.

Among bird species other than moa, Finsch's duck predominates in all layers. Worthy (1988) shows that birds of this population had significantly greater flight ability than later Holocene populations elsewhere in New Zealand. The kea is next most abundant in all layers except L4.

Harpagornis moorei Haast (Haast's eagle) is present in L3 but not L2.

The better representation of passerines in L2 than in L3 is explicable as a function of the energy of the stream that deposited each layer. There are almost no very small bones in L3; for example, no wrens are represented. However, in both layers a few kokako, *Callaeas cinerea* (Gmelin), bush robin, *Petroica australis* (Sparrman), and extinct crows, *Palaeocorax moriorum* (Forbes), are recorded. In L2, remains of five Stephen Island wrens, *Traversia lyalli* Rothschild, were recovered with individuals of a new species of wren (Millener 1988). Brown teal, *Anas aucklandica* (Gray), and piopio, *Turnagra capensis* (Sparrman), are absent from L3 and represented by only one individual each in L2.

Bones of five species of petrels occur in low numbers in L1, L2, and L3.

Differences in composition of the rail fauna are spectacular. In L3, *Aptornis otidiformis* (Owen) is very abundant and there are few weka, *Gallirallus australis* (Sparrman), but in L2 *Aptornis* becomes rarer than weka. Takahe, *Porphyrio mantelli*

Table 1 ^{14}C dates and stratigraphy of moa bones from the Graveyard. All dates based on bone collagen, Libby $T^{1}/_{2}$ 5568 years.

N.Z. Fossil Record no.	Species	Age	Location
L27/f100	*M. didinus*	11 200±150	–15 cm, L2, Site 1
L27/f88	*P. australis*	16 200±300	Top L3, Main Channel
L27/f101	*M. didinus*	19 300±400	–60 cm, base L3, Site 1
L27/f103	*P. australis*	20 600±450	Base L3 Site 3
L27/f109	*P. australis*	18 600±230	Base L3 Site 2
L27/f90	*P. elephantopus*	14 500±250	Lag deposit
L27/f102	*M. didinus*	10 980±140	Entrance to new passage

Table 2 Occurrence of birds in the Eagles' Roost and Graveyard (L1 & L2, L3, L4) deposits, Honeycomb Hill Cave. Minimum number of individuals of each species are shown (Worthy 1987a).

Order	Species	Common name	Eagles' Roost	Grave-yard L1 & L2	Grave-yard L3	Grave yard L4
Palaeognathiformes	*Anomalopteryx didiformis*	Little bush moa	0	2	0	0
	Megalapteryx didinus	Upland moa	3	4	73	6
	Pachyornis elephantopus	Heavy footed moa	0	0	4	0
	P. australis	Crested moa	0	0	30	4
	Dinornis torosus	Slender moa	1	0	0	0
	D. novaezealandiae	Large bush moa	0	0	1	0
	Apteryx australis/haasti	Brown or great spotted kiwi	3	0	1	0
	A. owenii	Little spotted kiwi	1	0	0	0
Procellariiformes	*Pterodroma inexpectata*	Mottled petrel	0	2	2	0
	P. cookii	Cook's petrel	2	0	2	0
	Puffinus gavia spp.	Fluttering shearwater	2	1	1	0
	Pachyptila turtur	Fairy prion	0	1	2	0
	Pelecanoides urinator	Diving petrel	1	1	1	0
Pelecaniformes	*Phalacrocorax carbo*	Black shag	1	0	0	0
Anseriformes	*Cnemiornis calcitrans*	S.I. extinct goose	1	0	0	1
	Euryanas finschi	Finsch's duck	3	45	36	4
	Hymenolaimus malacorhynchos	Blue duck	0	1	0	0
	Anas aucklandica	Brown teal	0	1	0	0
Falconiformes	*Harpagornis moorei*	Haast's eagle	2	0	5	0
	Circus eylesi	Extinct harrier	0	1	1	0
	Falco novaeseelandiae	N.Z. falcon	0	0	2	0
Galliformes	*Coturnix novaezelandiae*	N.Z. quail	2	1	1	0
Gruiformes	*Aptornis otidiformis*	Extinct giant 'rail'	0	2	19	1
	Gallirallus australis	Weka	14	5	9	0
	Gallinula hodgeni	Hodgen's Rail	1	2	1	0
	Fulica chathamensis	Extinct coot	0	0	0	0
	Porphyrio mantelli	Takahe	0	0	4	0
	Rallus philippensis	Banded rail	0	0	1	0
Charadriiformes	*Coenocorypha aucklandica*	N.Z. snipe	4	1	0	0
Psittaciformes	*Strigops habroptilus*	Kakapo	10	1	0	0
	Nestor notabilis	Kea	1	34	17	0
	Cyanorhamphus sp.	Parakeet	8	2	1	0
Strigiformes	*Sceloglaux albifacies*	Laughing owl	0	4	4	0
Caprimulgiformes	*Megaegotheles novaezealandiae*	Owlet night jar	4	4	1	0
Passeriformes	*Acanthisitta chloris*	Rifleman	21	0	0	0
	Xenicus longipes	Bush wren	12	0	0	0
	X. gilviventris	Rock wren	35	1	0	0
	Traversia lyalli	Stephen Island wren	14	5	0	0
	Pachyplichas yaldwyni	Extinct wren	36	1	0	0
	Wren n. gen.	Extinct wren	1	0	0	0
	Anthus novaeseelandiae	N.Z. pipit	1	0	0	0
	Mohoua novaeseelandiae	Brown creeper	5	0	0	0
	M. ochrocephala	Yellowhead	6	0	0	0
	Gerygone igata	Grey warbler	1	0	0	0
	Rhipidura fuliginosa	N.Z. fantail	2	0	0	0
	Petroica macrocephala	Pied tit	10	0	0	0
	P. australis	N.Z. robin	49	3	1	0
	Anthornis melanura	Belbird	2	0	0	0
	Prosthemadera novaeseelandiae	Tui	0	2	0	0
	Creadion carunculatus	Saddleback	9	1	0	0
	Callaeas cinerea	Kokako	55	6	5	0
	Turnagra capensis	Piopio	0	1	0	0
	Palaeocorax moriorum	Extinct crow	1	3	5	0
		Total number of birds	324	138	230	16

(Owen), are present only in L3 and are rare. One record of the banded rail, *Rallus philippensis* Linnaeus, was made from L3.

Only two bones of kiwi, *Apteryx* sp., were recovered from L3 sediments, despite the large volume examined. Individuals found in lag deposits are most likely to have been derived from L1 or L2, because kiwi found elsewhere in the cave system (Millener 1984; Worthy pers. obs.) are probably of more recent origin. The rarity of kiwi in this and other Honeycomb Hill deposits is hard to explain considering its abundance in other subfossil localities throughout New

Table 3 Taxa represented among spores and pollen in samples L27/f111 and L27/f110. For sample f111, 500 grains were counted. Spores are shown as a percentage of the total count, but pollen as a percentage of pollen only. Only 155 grains were counted for f110 and in this sample both spores and pollen grains are shown as a percentage of this total. Taxa forming < 1% of total count are indicated by an asterisk.

	L27/f111	L27/f110	
Spores			
Lycopodium australianum	*	–	
L. billardieri group	*	1	
L. fastigiatum	2	–	
L. scariosum	*	–	
L. volubile	*	–	
Cyathea	43	71	
C. smithii	*	–	
Dicksonia fibrosa	*	–	
D. squarrosa	*	–	
Grammitis	*	–	
Histiopteris incisa	*	–	
Hypolepis	*	–	
Ophioglossum	*	–	
Osmundaceae (Todea)	2	–	
Paesia scaberula	*	–	
Phymatodes (Phymatosorus) diversifolium	*	–	
Pteris	*	*	
Polypodiaceae	–	*	
unidentified monolete spores	16	13	
Pollen			
Dacrydium cupressinum	–	2.5	
Dacrydium bidwillii/biforme group	*	–	
Libocedrus	5	–	
Phyllocladus	*	*	
Podocarpus (?totara)	4	*	
?Araliaceae	2	–	
Astelia	2	–	
Balanophoraceae?	*	–	
Chenopodiaceae	1	–	
Compositae (Tubuliflorae)	31	–	
Coprosma	28	*	
Coriaria	1	–	
Dracophyllum	2	1	
Fuchsia	*	–	
Griselinia littoralis (?)	*	–	
Hebe	*	–	
Hydrocotyle	*	–	
Melicytus	2	–	
Myrsine	1	–	
Nothofagus fusca group	4	3	
Nothofagus menziesii	*	–	
Nothofagus brassi type	–	*	
Monosulcites	–	1	(?recycled)
Pittosporum	*	–	
Plagianthus	1	–	
Pseudowintera	*	–	
Umbelliferae	*	–	
Gramineae	3	–	
?Cyperaceae	–	*	
Phormium tenax	*	–	
Restionaceae (*Leptocarpus*)	*	–	
Unidentified tricolpate grains	2	1	)poorly
Unidentified tricolporate grains	9	–	)preserved

Zealand and the palynofloral evidence for forested conditions during deposition of at least part of L2/L3.

No bones of kakapo, *Strigops habroptilus* Gray, were found in L3 but a few occur in L2 and in the lag deposits. However, kakapo are abundant elsewhere in Honeycomb Hill Cave (e.g., Eagles' Roost; Millener 1984). Although none of these kakapo have been dated, it is likely that most are only a few thousand years old, since all are located below present entrance tomos (e.g., Eagles' Roost) or not far above present streams (e.g., Honeyflow Stream).

Palynological analyses

Pollen sample L27/f110 (Table 3) This sample, from a 5 mm layer of clay bounded by coarse grit 0.6 m below the L2–L3 interface in Site 2, gave inconclusive results. Two slides were prepared, and 155 spores and pollen grains (of which 110 are of *Cyathea*) were counted. Preservation is uneven with some grains deeply etched whereas others are perfectly preserved; some, for example, the late Tertiary species *Nothofagidites cranwellae* (Couper), are clearly recycled. This state of poor preservation is not unexpected because immediately before and after this clay was deposited the site carried a reasonably dynamic stream.

The palynoflora indicates forested conditions. The relatively high proportion of beech and rimu pollen suggests a lowland podocarp/beech forest, little different from that of the West Coast of South Island today. The abundance of fern spores indicates relatively high rainfall or a moist valley environment. The lack of pollen from herbaceous plants, excluding the possible Cyperaceae, suggests interglacial conditions, but the very poor palynomorph recovery and the evidence of some recycling of pollen make any conclusions as to climate and vegetational type speculative.

Pollen sample L27/f111 (Table 3) This sample was also from a stream environment but one where the flow rate was considerably less than that in L27/f110 because only clay was deposited. This sample was obtained from Site 3 immediately below L3 (Fig. 3), at the top of L4, which extends as a seemingly homogeneous layer (bones of individual skeletons were found over the entire excavated depth range) to over 1 m in depth at the western end of the site. It contains abundant spores and pollen grains, rare insect (?beetle) remains, and possible fish scales. The palynoflora is poorly preserved and has clearly been transported or reworked; some grains are well preserved and may have been transported only a short distance. These grains are easily identified and are therefore the most prominent ones in the count. The count is highly subjective because numerous "ghosts" of etched and biodegraded spores and pollen, especially saccate and tricolpate grains, could not be identified and counted.

The total assemblage is dominated by *Cyathea* spores (43%), primarily *C. smithii*, a frost tolerant, temperate–subalpine species. Robust spores such as those of *Cyathea* tend to be differentially preserved in such relatively high energy depositional environments. Unidentifiable, relatively small monolete spores form 16%, with various conifers 3% and angiosperms 31%. The other 7% consists of all other spores.

The pollen assemblage has a combination of taxa which suggests moist, disturbed conditions, cool temperatures, and a scrubland in the immediate vicinity of the cave, but with some forest nearby.

A number of taxa indicate cool temperatures. *C. smithii* has already been mentioned. *Lycopodium australianum* and *L. fastigiatum* are common. They are usually found in stony grasslands, low heath, and bog in montane to lower alpine areas, except when in exposed areas or subject to cold air

where they descend to lower levels (ecological data for this and succeeding taxa from Macphail & McQueen 1983). *Libocedrus* is frost tolerant to −13° and is common in upper montane and subalpine forests; in this sequence it forms 5% of total pollen, suggesting derivation from a disturbed environment at forest margins. Compositae (Tubuliflorae) (31% of total pollen) and *Coprosma* (28% of total pollen) are in percentages consistent with alpine or subalpine environments (or coastal scrub). *Nothofagus menziesii* is dominant in cool temperate forests and often forms the treeline in subalpine areas. *Pseudowintera* occurs on forest margins in temperate to lower montane areas of high rainfall, and, like *Libocedrus*, in scrub following forest destruction.

The only indication of emergent trees is the presence of relatively sparse *Nothofagus* (most poorly preserved), *Podocarpus* (poorly preserved, especially the sacci), and possible tricolpate grains of forest taxa. Otherwise, all taxa are common subalpine or cool climate taxa (many also common, however, in lowland areas).

Indications of wet conditions (high rainfall, persistent cloud cover, and/or poor drainage) include the abundance and variety of fern spores and the presence of some grains of *Fuchsia* (lower subalpine, common along streams), *Phormium tenax* (flax, common in swamps and lake and river margins), Restionaceae (probably *Leptocarpus*, family common in salt marshes and subalpine bogs), and lycopod spores.

Invertebrates

No invertebrate remains were found in L3, but a few snails and beetles, most of which occur in the forest today, were found in L1/L2 or lying on the surface. None were definitely from the fluvial sediments of L1/L2 and they are therefore most likely to have been recently deposited on the present surface after erosion revealed it.

DISCUSSION

Paleoenvironmental reconstruction

The palynological analyses are for deposits laid down immediately before 20 000 years B.P. At this time the cave was probably in a forested valley floor, along which a stream flowed, in a subalpine shrubland/wet montane forest interface zone.

The flightless bird fauna at this time was dominated by the upland moa and the crested moa. Among the smaller birds, Finsch's duck predominated. This duck nested in short, dry caves (McCulloch 1975) but this probably does not explain its abundance in the Graveyard. Several pitfall sites (e.g., Martinborough No. 1 Cave (Yaldwyn 1958) and Castle Rocks in Southland (Hamilton 1892)) have large numbers of bones of this species, so a pitfall origin for the large number of individuals in the Graveyard is likely. Finsch's duck probably had terrestrial habits, similar to those of the Australian wood duck, *Chenonetta jubata* (Latham), which grazes on ground plants and is less dependent on water than the grey duck, *Anas superciliosa* Gmelin. The giant gruiform, *Aptornis otidiformis*, was quite common, as were kea. Banded rail, New Zealand coot, *Fulica chathamensis* Hamilton, weka, takahe, and Hodgen's rail, *Gallinula hodgeni* (Scarlett), were all rare. Kakapo were apparently absent, and kiwi rare. Kokako, bush robin, and parakeets, *Cyanorhamphus* spp., were present in the trees, and extinct crows were probably using the tree/scrub boundary as their feeding zone (R.N. Holdaway, unpubl. data). So far as can be determined from historical sightings, South Island kokako preferred beech forest (Clout & Hay 1981), and so the presence of *Nothofagus* pollen in this site might be significant with respect to the presence of kokako bones. A range of predators and scavengers occurred, including the laughing owl, *Sceloglaux albifacies* (Gray), New Zealand falcon, *Falco novaeseelandiae* Gmelin, harrier (or goshawk), *C. eylesi* Scarlett, and Haast's eagle. Several species of petrels must have bred nearby, but it is likely that no major colony was adjacent to the cave because there are few bones. New Zealand quail, *Coturnix novaezelandiae* Quoy and Gaimard, was a shrubland/grassland inhabitant in Canterbury when Europeans arrived (Buller 1888), suggesting that shrubland or grassland was present in the cave's vicinity.

This fauna apparently changed little until about 14 000 years ago. At about that time the crested moa and the heavy footed moa disappeared to be replaced by the little bush moa. *A. otidiformis* became rarer, and Haast's eagle ceased to be represented. Although kea and Finsch's duck still predominated amongst the smaller birds, snipe, *Coenocorypha aucklandica* (Gray), kakapo, piopio, and brown teal made their first appearance. At this time three wrens, tui, *Prosthemadera novaeseelandiae* (Gmelin), and saddleback, *Creadion carunculatus* (Gmelin), were also present, but whether any or all of these were present in the Oparara valley before 14 000 years cannot be determined with certainty because the flow rate of water through the site was too great to allow small bones to be regularly deposited (see account of stratigraphy).

Comparison of the Graveyard fauna with that of the Eagles' Roost

The Eagles' Roost is only one of some 50 sites in the Honeycomb Hill Cave system that contains a subfossil fauna (Millener 1984; Worthy 1984a, 1987a) but research by Millener has revealed a rich fauna of mainly smaller species.

The fauna recovered from the Eagles Roost (Table 2) exhibits marked differences from that of the Graveyard. Millener (1984) envisaged that these bones were deposited by a stream. A re-examination of the site, with reference to the overall structure of the cave system (Worthy unpubl. 1984b), together with observations at other sites elsewhere in New Zealand, suggests an alternative. This shaft entrance (tomo) is of such dimensions that flying birds could easily have entered it deliberately. Filmy ferns on the tomo walls could have been an attractant, especially as they are a favoured food of kokako (Rod Morris pers. comm. 1987). Once in the tomo, most species would find the route out would be too steep (note the rarity in the deposits of the fantail *Rhipidura fuliginosa* (Sparrman) an acrobatic flier) and thus they would be trapped. It is doubtful that birds could escape when the only route to safety involved several steps. It is probable that, once in, a bird would attempt to fly straight out and so quickly exhaust itself and die. The ledge on which the majority of material was found is at the base of the tomo, and it is the only dry place, generally providing shelter from the incessant drips which are common to such sites. Bones at this site were embedded in sediments because percolation water has washed gently over them depositing fine silts that are mainly derived from limestone weathering.

Bones of larger birds (e.g., kakapo and weka) in the tomo, but not on this ledge, were not all collected and therefore may

be under-represented in the analysis. Allowing for this limitation, some useful comparisons between the Eagles' Roost fauna and that of the Graveyard can be drawn with reference to Table 1. Dates obtained from two moas at Eagles' Roost were 11 800 ± 200 years B.P. for (L27/f91) *D. torosus*, and 11 250 ± 150 years B.P.. (L27/f93) *M. didinus* (Worthy 1987a). This fauna has markedly fewer Finsch's duck, *Aptornis* is absent, the kea is represented by only one individual, and there are fewer *Palaeocorax*. There were more kakapo and abundant passerines, which, so far as their ecology is known, are all forest inhabitants except for the pipit. The crow, if of similar habit to extant crows, was probably an inhabitant of forest margins (Millener 1981). Riflemen, *Acanthisitta chloris* (Sparrman), were numerous, and rock wrens, *X. gilviventris* Petzeln, considerably outnumbered bush wrens, *Xenicus longipes* Gmelin. Rock wrens are generally considered to inhabit alpine rock scree, but Riney (1953) recorded them from scrub habitat with no scree in Fiordland. It is possible that in the past their ecological range was greater, as with takahe (Beauchamp & Worthy 1988), and that they are now restricted to areas that afford some protection from mammalian predators. Thus, the fauna of Eagles' Roost appears to be representative of that occurring during, or subsequent to, the deposition of L2 in the Graveyard (i.e., early Holocene). The subfossil birds of Eagles' Roost probably lived in similar conditions to those presently living in the vicinity.

Suggested habitat preferences of some species

These results enable suggestions to be made regarding the habitat preferences for some extinct birds. The upland moa and the crested moa dominated amongst flightless birds in a montane forest to subalpine shrubland habitat. With warmer conditions and the development of forest similar to that now found in the Oparara valley, the little bush moa made its appearance, together with a wider range of passerines (see later). Remains of the little bush moa are present at several sites in Honeycomb Hill Cave system close to entrances and in positions that suggest the remains are probably Holocene, for example, at the base of a mud bank sloping up to the forest at 'E' Entrance. Such an entrance certainly cannot have persisted for more than a very few thousand years. At the aven at 915E 1485N (cave map reference), beneath an entrance into which logs have recently fallen, are the remains of several of these moa. Often, in sites where deposition is considered to be of relatively recent origin, the large bush moa is also found (e.g., 'A' Entrance, Deer Drop, entrances in Enduro Passage, the aven at 915E 1485N, and an unnamed cave beside Honeycomb Arch). Other caves in northwest Nelson provide evidence for a similar succession of moa species with time. Haast examined caves in the Aorere valley and found bones of *A. didiformis* invariably occurred on the surface whereas those of *P. elephantopus* were much deeper (Buick 1931). Thus *A. didiformis* and *D. novaezealandiae* probably preferred wet dense lowland forests. Support for this contention is that these two moas dominated the moa fauna in the King Country (Millener 1981).

The heavy footed moa was rare in the alpine shrubland to montane forest habitat of the Otiran and absent later when lowland forest developed. However, east of the main ranges during the Holocene, this was one of the dominant species, in what were probably relatively xeric open forest scrubland areas, as the following data (proportion of moa fauna) from swamps in Otago and Canterbury (Fig. 1) show: Hamiltons 46%, Albury Park 36%, Enfield 17%, Glenmark 16%, Kapua 11%, Pyramid Valley 10% (data compiled by A. Anderson pers. comm. 1987). It is probable that this moa primarily preferred open, dry habitats thus explaining its rarity in western districts of the South Island.

The crested moa formed a very significant proportion of the Otiran fauna in the Oparara valley. A search of material in New Zealand collections has revealed further examples of this species. What had previously been identified as *Euryapteryx gravis* from a cave on Mt Owen (Bell & Bell 1971), and further material collected from Mt Owen in January 1987, are of this species. Two femora of this species, now in the Canterbury Museum, were found in Kennedy Basin near the confluence of the Inangahua River with the Buller River. In Southland Museum there are crania of this species collected from coastal dunes near Invercargill. This distribution, collated with the Honeycomb Hill Cave data, suggests that a cold or alpine climate combined with a habitat of relatively open areas was preferred by this species.

The greater proportion of juveniles among remains of the upland moa than in those of the crested moa can be explained by two factors. Juveniles of other moas are not uncommon in deposits elsewhere, but are more abundant in caves than in swamps. The proportion of juveniles of the crested moa is more similar to that usually observed in other moa species. Perhaps young upland moa spent a greater proportion of their time in the vicinity of the cave than did adults. If this was indeed an upland species, perhaps adults fed in the subalpine scrub and grasslands while juvenile and subadult birds were forced into the forest zone by snow earlier in the winter. This would increase the chance of juvenile birds being trapped.

Haast's eagle appears to have been common in the relatively open subalpine shrubland or marginal montane forest zone. Additional bones of this species from His and Hers Cave (Worthy 1987a) were associated with moa bones dated 15 900 ± 240 years B.P. and therefore were also deposited during glacial conditions. Eagles were rare in North Island (Millener 1981), occurring only in a swamp at Te Aute (possibly an Otiran site; Worthy 1987b) and again at Hunterville in Pleistocene deposits. Their remains are most abundant east of the main ranges in South Island in Holocene sites (R. Holdaway pers. comm. 1987). They probably preferred the open grassland or scrubland areas and not the dense lowland forests predominating in the North Island or western South Island during the Holocene.

Other extinct birds that may have preferred this relatively open forest/scrubland habitat are Finsch's duck and the giant gruiform *Aptornis*. Both are rare in Holocene King Country deposits which were laid down under dense lowland podocarp forests (Millener 1981). For example, in L2 of F1 Cave, dated 1680 ± 50 years B.P. (Worthy 1984a), *Aptornis* bones accounted for 1.2% and *Euryanas* bones 2.4% of the total minimum number of individuals represented. Both species were absent from the large fauna recovered from The Canyon, dated 2350 ± 90 years B.P. (Worthy 1987b). In the older but undated L8 in F1 Cave, both of these species were rather more abundant than in L2, but are still not as common as in sites at Martinborough (southeastern North Island) or Waikari in North Canterbury (Worthy 1988), both of which are regions of relatively low rainfall and hence unlikely to have supported dense podocarp-broadleaf forests such as were in the King Country.

Among extant birds, takahe were present only in deposits formed when montane forest to subalpine scrub predominated,

thus apparently supporting the argument of Mills et al. (1984) that takahe were Pleistocene relicts of alpine grasslands. However, the presence of only four individuals, representing < 2% of the fauna, suggests that takahe were rare in the area during the Otiran even though the cave was at the margin of the alpine zone. Such rarity leads to the contention of Millener (1981, p. 595) and Beauchamp & Worthy (1988) that takahe were, and are, primarily adapted to the lowland environment. Their relative rarity in the Graveyard deposits cannot be explained as a consequence of their bone size, because birds with both larger and smaller bones were considerably more numerous. Elsewhere in the cave, takahe bones are very rare, with the only records (all undated) being from the aven (located at the cave map grid reference 915E 1485N), on the rockfall inside 'T' Entrance and at Aven 12.

The record of banded rail, *Rallus philippensis*, is the first from cave deposits in New Zealand. The coincidence of this bird with restionad rushes may be significant because at present estuarine restionad beds form one of its main habitats. Wetland habitats are unlikely on the limestones in which the cave is formed but nearby granite and mudstone lithologies could have supported wetland habitats, as they still do.

The kea was an important component of the Otiran–early Holocene fauna in the Oparara valley. Although this bird is usually perceived as an alpine bird, its frequent use of lowland forests has been regularly reported (O'Donnell & Dilks 1986). This, and the extensive alpine areas in northwest Nelson, do not explain why, in historical times, kea was restricted to the mountainous areas in the south, and only extended its range north to include Nelson after 1870. The subfossil data show that the kea remained a major component of the fauna after the transition from subalpine/montane to lowland forest conditions. Its restriction in range thereafter is unexplained.

In contrast to the kea, the kakapo now has a very restricted distribution, surviving only in remote, inaccessible valleys in Fiordland, possibly northwest Nelson, and on Stewart Island. Subfossil evidence from throughout New Zealand shows that this bird was most abundant in lowland podocarp/broadleaf forests during the Holocene (Millener 1981; Worthy 1984a). Its absence in the Otiran deposits of the Graveyard, but presence in younger deposits, when forest in the vicinity became similar to that of the present day (mixed beech/podocarp), support the contention that lowland forest was its preferred habitat.

Although the Oparara forests now support populations of kaka, *Nestor meridionalis*, and pigeon, *Hemiphaga novaeseelandiae*, these species are very rare in the whole of Honeycomb Hill Cave and are absent from Eagles' Roost or the Graveyard. Presumably both species have only been able to use the area in the last few thousand years (extensive deposits of late Holocene age containing birds other than moa are unknown in the cave).

GLACIAL CHRONOLOGY OF NORTHWEST NELSON AND ITS VEGETATION HISTORY

Older Graveyard sediments were laid down over the last few thousand years of the Otiran glaciation and therefore span several minor glacial advances and retreats (see Mabin 1983a). The changes in composition of the bird fauna after 14 000 years B.P. coincide with the major climatic amelioration which occurred at this time. The palynological data suggest that, during the late Otiran, the treeline was about 250–300 m above present sea level (it is now about 1000 m a.s.l. here). This contrasts with the conclusions of all previous workers, who have suggested that a grassland/shrubland vegetation dominated the later stages of the Otiran in northern South Island (Suggate 1965; Suggate & Moar 1970; Nathan & Moar 1973; Moar & Suggate 1979; Mabin 1983a, b). However, none of these studies was for western areas of northwest Nelson, and, because they were mostly concerned with glacial chronology, were done near former glaciers where grassland/shrubland would have been much more likely to occur. As indicated by McGlone (1985), in these former studies, pollen samples were taken from sites of rapid sediment accumulation that were likely to have been sparsely vegetated.

Present evidence suggests that shrublands and grasslands were widespread during the Otiran on the West Coast of South Island, south of Westport (McGlone 1985). No information is available for northwest Nelson although Macphail (1983) has shown that the early Holocene vegetation was dominated by *Nothofagus menziesii* and *Cyathea smithii* later replaced by *N. fusca* group. McGlone (1985) suggested that podocarp forest must have been present but was very rare, with the major forest trees, the *Nothofagus fusca* group and *N. menziesii*, persisting as scattered forest remnants on hilly terrain. The persistence of forest remnants has been considered necessary to explain the rapidity with which all areas of New Zealand gained a podocarp forest at the end of the glacial period (McGlone 1985).

The discovery, in the Graveyard, of pollen indicating the presence of a forest at 250 m a.s.l. dominated by *Libocedrus*, *Podocarpus*, and *Nothofagus* supports the concept of remnant forests existing throughout glacial periods in northwest Nelson. Forest probably extended also to lower altitudes, indicating an altitudinal range of > 300 m, because sea level was lower at this time. Such forests could have spread over several, comparable high fertility sites to the west and north of the Oparara valley. Owing to frost and periodic drought, forests may not have been present on formerly extensive outwash plains in Golden Bay, and the forest remnants may have been isolated. This may be the factor that prevented faunal range expansion into what probably became acceptable habitats in North and South Islands for various species during that time. For example, the upland moa could have utilised suitable habitat in the North Island during the Otiran had it been able to get there.

ACKNOWLEDGMENTS

This study was made possible by generous support from the N.Z. Forest Service and the Department of Conservation. Practical field help by Mike Huaki, Mike Hurst, Mal Hanson, Norm Stopforth and Ian Gibson was most appreciated. The Institute of Nuclear Sciences, Department of Scientific and Industrial Research, made the ^{14}C determinations. The support of the National Museum director, J. C. Yaldwyn, and discussion with J. A. Bartle are gratefully acknowledged. I thank P. R. Millener, B. Marshall and J. G. Gregory for comments on earlier drafts of the text that resulted in its improvement.

REFERENCES

Beauchamp, A. J.; Worthy, T. H. 1988: The timing and reasons for the decline in distribution of the takahe *Porphyrio (Notornis) mantelli*: a re-examination. *Journal of the Royal Society of New Zealand 18 (1)*: 103–112.

Bell, C. J. E.; Bell, I. 1971: Subfossil moa and other remains near Mt Owen, Nelson. *New Zealand journal of science 14 (4)*: 749–758.

Buick, L. T. 1931: The mystery of the moa. New Zealand's avian giant. New Plymouth, Thomas Avery & Sons Ltd. 357 p.

Buller, W. L. 1888: A history of the birds of New Zealand. 2nd ed. London, privately published.

Clout, M. N.; Hay, J. R. 1981: South Island kokako (*Callaeas cinerea cinerea*) in *Nothofagus* forest. *Notornis 28*: 256–259.

Hamilton, A. 1892: On the fissures and caves at Castle Rocks, Southland; with a description of the remains of the existing and extinct birds found in them. *Transactions of the New Zealand Institute 25*: 88–106.

Mabin, M. C. G. 1983a: Late Otiran sedimentation and glacial chronology in the Warwick valley, southeast Nelson. *New Zealand journal of geology and geophysics 26*: 189–195.

———1983b: The late Pleistocene glacial sequence in the middle Maruia valley, southeast Nelson, New Zealand. *New Zealand journal of geology and geophysics 26*: 86–96.

McCulloch, B. D. 1975: Faunal remains from a cave at Waikari, North Canterbury. Unpublished B.Sc. (Hons) thesis, lodged in the Library, University of Canterbury.

McGlone, M. S. 1985: Plant biogeography and the late Cenozoic history of New Zealand. *New Zealand journal of botany 23*: 723–749.

Macphail, M. K. 1983: Holocene climatic change and successional dynamics in lowland rainforest stands in New Zealand. Pp. 107–108 *in*: A symposium of results and discussions concerned with late Quaternary climatic history of Australia, New Zealand and surrounding seas. *Proceedings of the 1st CLIMANZ Conference, Howman's Gap, Victoria, Australia, February 8–13, 1981.*

Macphail, M. K.; McQueen, D. R. 1983: The value of New Zealand pollen and spores as indicators of Cenozoic vegetation and climates. *Tuatara 26*: 37–59.

Millener, P. R. 1981: The Quaternary avifauna of the North Island of New Zealand. Unpublished Ph.D. thesis, lodged in the Library, University of Auckland. 2 Vols.

———1984: Honeycomb Hill Cave—a survey of scientific and scenic resources. Unpublished report of the National Museum of New Zealand. 100 pp.

———1988: Contributions to New Zealand's late Quaternary avifauna I—*Pachyplichas*, a new genus of wren (Aves: Acanthisittidae), with two new species. *Journal of the Royal Society of New Zealand 18 (4)*: 383–406.

Millener, P. R.; Bartle, J. A. 1982: Report on a visit to the Honeycomb Hill Cave, Oparara Valley, on 27 July, 1982. Unpublished report, New Zealand Forest Service. 12 p. and 9 photos.

Mills, J. A.; Lavers, R. B.; Lee, W. G. 1984: The takahe—a relic of the Pleistocene grassland avifauna in New Zealand. *New Zealand journal of ecology 7*: 55–70.

Moar, N. T.; Suggate, R. R. 1979: Contributions to the Quaternary history of the New Zealand flora. 8. Interglacial and glacial vegetation in the Westport District, South Island. *New Zealand journal of botany 17*: 361–387.

Nathan, S.; Moar, N.T. 1973: Age and correlation of late Quaternary terraces in the lower Inangahua Valley, West Coast, South Island, New Zealand. *Journal of the Royal Society of New Zealand 3*: 409–414.

O'Donnell, C. F. J.; Dilks, P.J. 1986: Forest birds in South Westland: status distribution and habitat use. *Occasional publication 10*. New Zealand Wildlife Service, Department of Internal Affairs, Wellington.

Riney, T. 1953: Notes on habitat and behaviour of the rock wren subspecies *Xenicus gilviventris rineyi* Falla. *Notornis 5*: 186–188.

Suggate, R. P. 1965: Late Pleistocene geology of the northern half of the South Island, New Zealand. *New Zealand Geological Survey bulletin 77.*

Suggate, R. P.; Moar, N. T. 1970: Revision of the chronology of the late Otira Glacial. *New Zealand journal of geology and geophysics 13*: 742–746.

Worthy, T. H. 1984a: Faunal and floral remains from F1, a cave near Waitomo. *Journal of the Royal Society of New Zealand 14*: 367–377.

———1984b: Honeycomb Hill Cave System—a description of the cave, its structure and development, with comments on its fauna, both recent and subfossil. Unpublished report, New Zealand Forest Service, 41 pp.

———1987a: The subfossil fauna of Honeycomb Hill Cave. I. A study of Otiran deposits in the Graveyard. II A reassessment of *Megalapteryx benhami*: Archey. Unpublished report, National Museum of New Zealand, 59 p.

———1987b: Sexual dimorphism and temporal variation in the North Island moa species *Euryapteryx curtus* (Owen) and *Pachyornis mappini* Archey. *National Museum of New Zealand records 36*: 59–70.

———1988: Loss of flight ability in the extinct New Zealand duck *Euryanas finschi*. *Journal of zoology 215:* 619–628.

———1989: Validation of *Pachyornis australis* Oliver (Aves; Dinornithiformes), a medium sized moa from the South Island, New Zealand. *New Zealand journal of geology and geophysics 32*: 255–266 (this issue).

Yaldwyn, J. C. 1958: Notes on the environment and age of subfossil deposits in the Martinborough Caves. *Records of the Dominion Museum 3*: 129–133.

New Zealand Journal of Geology and Geophysics, 1989, Vol. 32: 255–266
0028–8306/89/3202–0255 $2.50/0

Validation of *Pachyornis australis* Oliver (Aves; Dinornithiformes), a medium sized moa from the South Island, New Zealand

T. H. WORTHY
National Museum of New Zealand
P.O. Box 467
Wellington, New Zealand

Abstract On the basis of new material, the crested moa, *Pachyornis australis*, which was synonymised with the heavy footed moa, *P. elephantopus* (Owen), by Cracraft in 1976, is re-established as a valid species and redescribed. From its distribution data I conclude that this bird primarily occurred in subalpine habitats; its remains are rare because subfossil deposits in the subalpine zone are rare and restricted to karst regions. Extensive comparisons of bones of *P. australis* with those of *P. elephantopus* and *Euryapteryx geranoides* (Owen) are given to facilitate their correct identification. With the reinstatement of *P. australis* as a valid species, the number of moa taxa recognised in New Zealand is 11.

Keywords Dinornithiformes; Emeidae; *Pachyornis australis*; description; comparisons; ecology

INTRODUCTION

The giant, extinct moas (Order Dinornithiformes) of New Zealand, were divided into the families Dinornithidae and Anomalopterygidae by Archey (1941) and Oliver (1949). Although Cracraft (1976) only accepted one family (Dinornithidae), recent workers have favoured retention of two families: Dinornithidae for the Dinornis species and Anomalopterygidae for the rest, (e.g., Walker 1978). Cassels & Millener (1985) retained two families but transposed Emeidae for Anomalopterygidae, following Brodkorb (1963). I have previously used Anomalopterygidae (Worthy 1988b) but here follow Brodkorb (1963) in using Emeidae to describe this family. In the classification proposed by Cracraft (1976), 13 species were accepted, but more recent revisions (Millener 1982; Worthy 1988a) reduced this number to 11. Worthy (1988b) accepted only three Dinornis species, reducing *D. torosus* Hutton to synonymy with *D. struthoides* Owen and, in anticipation of this paper, listed *P. australis* as a distinct species, thereby again retaining 11 species. This paper presents the data supporting the resurrection of *Pachyornis australis* from synonymy with *P. elephantopus* as proposed by Cracraft (1976).

In Cracraft's classification the genus *Pachyornis* has one temporally variable species, *P. mappini* Archey, in the North Island (Worthy 1987a) and one, *P. elephantopus*, in the South Island. However, during the last century of moa research the possibility has been raised several times that a *Pachyornis* species smaller than *P. elephantopus* previously occurred in the South Island.

McKay (1879, p. 131) found many moa bones in a cave on the Salisbury Tableland, at the head of the Takaka River in Nelson. These included a skull and 20 vertebrae now preserved in the National Museum of New Zealand (NMNZ S26). Parker (1893, 1895) described the skull as *Mesopteryx* sp. B, and recognised it as similar to those of the genus *Pachyornis*. Yaldwyn (1979) reported that the vertebrae were lost, but an articulated set of 20 vertebrae, each bearing the number 26, was found recently during collection reorganisation and is almost certainly the missing set.

By 1891, similar sized bones to those expected for *Mesopteryx* had been discovered on Takaka Hill. For these, Hutton (1891) erected the species *Euryapteryx pygmaeus* but did not describe a specimen nor did he elect a holotype. Subsequently Hutton (1892) nominated a pair of tarsometatarsi from Takaka as "types", presumably syntypes. Five years later, he transferred the species to *Pachyornis* (Hutton 1897). This pair of tarsometatarsi remained in the Nelson Museum where Archey (1941) examined them and confirmed this generic placement, citing the raised intercondylar ridge as characteristic of *Pachyornis*. Archey also referred the skull NMNZ S26 to *P. pygmaeus* (Hutton) because it appeared to be from a small *Pachyornis*. Oliver (1949) rejected this suggestion because, in his opinion, the skull was too large to be associated with the tarsometatarsi on which Hutton founded *E. pygmaeus*. Moreover, Oliver considered the type tarsometatarsi to be more correctly referred to a species of *Euryapteryx*; indeed the types of *P. pygmaeus* (transferred from the Nelson Museum to the National Museum, now NMNZ S24322) have characters of the hypotarsal ridges and of the medial trochlea that clearly identify them as *Euryapteryx* (Worthy 1988b). Because the skull (NMNZ S26) was not referable to *E. pygmaeus* but rather had all the characteristic features of *Pachyornis*, Oliver described it as a new species, *P. australis*.

Oliver (1949, p.79) figured a small sternum in the Southland Museum which he referred to *P. australis*, and (on p. 75) figured a pelvis, then in the Nelson Museum, which he questioningly referred to *P. australis*. Two crania in the Southland Museum (A40.31, A42.6) were referred to *P. australis*. No other postcranial elements have been referred to this species.

Oliver (1949) also described as new *Pachyornis murihiku*, a complete skeleton from dune deposits in Southland; it is similar in size to *P. australis*. No other specimens have been referred to this species.

Received 21 June 1988, accepted 19 October 1988

There were small *Pachyornis* individuals present in the South Island, but they were very rare. Cracraft (1976), citing huge variability in crania of *P. elephantopus* (observed because he apparently accepted without question identifications given on specimen labels), synonymised *P. australis* with that species. He included *P. murihiku* in the synonymy of *P. elephantopus* because, although the specimen was small, the range of variability exhibited by the combined species was similar to that of several other moa species. In addition, Cracraft considered the specimen to be subadult. He, therefore, dismissed the former presence of a species of *Pachyornis* smaller than *P. elephantopus* in the South Island. Recently many bones of a small, stout legged moa were found in deposits in Honeycomb Hill Cave, Oparara, northwest Nelson, particularly those in the site called the "Graveyard"; the leg bones show some similarity to those of *Euryapteryx geranoides* (Owen) (sensu Cracraft 1976), but were referred to *Pachyornis australis* by Worthy (unpubl. 1987b).

In this paper I present the evidence on which *P. australis* is re-established, then redescribe the species. A cranium discovered with associated postcranial elements in the Graveyard deposits at Honeycomb Hill Cave is referred to *P. australis*, making possible, for the first time, a description of postcranial elements of that species. I make comparisons with *P. elephantopus* and *E. geranoides* to facilitate separation of bones of these species.

E. geranoides (Owen) was erected to accommodate bones larger than those of *E. curtus* (Owen). Later *E. gravis* (Owen) was founded for the *Euryapteryx* bones larger than *E. geranoides*, which were the most abundant in the South Island. Cracraft (1976) synonymised *E. gravis* with *E. geranoides*, so in the present study *E. geranoides* includes those individuals previously referred to as *E. gravis*. South Island specimens of *Euryapteryx* have great size variation, explained by Cracraft in terms of sexual dimorphism; however, because different size ranges have disjunct distributions, such an explanation is not entirely satisfactory. Cracraft's synonymy should be treated with caution until the genus is examined as a whole to determine the extent and causes of variability. In this study, bones of the large form of *Euryapteryx* (formerly *E. gravis*) and bones exclusively from Pyramid Valley (where only the larger form is found) have been used for comparative purposes.

MATERIAL

Specimens of *P. australis* used in this study include: National Museum of New Zealand (NMNZ) S (labelled DM) 26—holotype; 22672–3, 23028, 23031, 23056, 23087, 23484, 23486–7, 23726–32, 23735, 23741, 23800–1, 23810–18, 23844—Honeycomb Hill Cave; 23345, 23568—Mt Owen; 25512—Takaka Hill.

The following specimens of *P. elephantopus* were used in comparisons: Auckland Institute and Museum (AIM) MOA 10.12 (ex CM Av 8315), Canterbury Museum (CM) Av 8348, 8381–3, 8385–9, 8716, 15029, 19279, 20586—Pyramid Valley; NMNZ S22720, 23798–9, 23821—Honeycomb Hill Cave.

The following specimens of *E. geranoides* all from Pyramid Valley excavations were studied: CM Av 8373, 8375, 8378, 8472, 13773, 15034–5, 18931, 20115, 20586; NMNZ S471 (ex CM Av 8370) which is individual XXD (Allan et al. 1941).

RESULTS

Evidence from Honeycomb Hill Cave

Extensive investigations of deposits in the Graveyard, Honeycomb Hill Cave (Worthy 1987b), resulted in the following observations with regard to bones of a small, stout legged moa.

1. Articulated toes from this small, stout legged moa had the phalangeal formula 3:3:4:5, consistent with that of *Pachyornis* but not *E. geranoides* (3:3:4:4).
2. Associated bones of one individual of this small, stout legged moa were discovered. These included the cranium, pelvis, femora, tibiotarsi, and tarsometatarsi (all NMNZ S23800).
3. No premaxillae, mandibles, crania, sterna, or pelves found in the deposit were characteristic of *Euryapteryx*, but many had the features characteristic of a small *Pachyornis*.
4. Several bones in the same deposit were identical to those of *P. elephantopus* yet differed in several respects from those of the small, stout legged moa. The leg bones of the small, stout legged moa were examined in detail and characters which differentiate them from those of the similar sized *E. geranoides*, and the larger *P. elephantopus*, were identified. The cranium associated with bones of the individual (3 above) appeared similar to that of *P. australis*.

Comparison of the holotype crania of *P. australis* with the Honeycomb Hill Cave specimen

The holotype of *P. australis* NMNZ S26 was described in detail by Oliver (1949). The skull is vaulted; it has moderately wide temporal fossae, temporal and lambdoidal ridges separated by a wide, flat space, posttemporal fossae separated from temporal fossae by prominent inferior temporal ridges; zygomatic processes sharply ridged, pointed; premaxilla sharp pointed, length to jugal bar 75% of cranial length between the preorbital and opisthotic processes, culmen nearly straight; antrum inflated; quadratojugals curved markedly outward; mandible not much downcurved, stout, pointed; preorbital plate curved so that the anterior portion diverges little from the rostrum, lacrymal does not fuse with preorbital plate to enclose foramen. These characters of the holotype are consistent with the other species of the genus *Pachyornis*. The one difference cited by Oliver (1949) was that the basipterygoid processes in the holotype had a narrow base but were usually wide in other members of the genus. The holotype is specifically distinct in that the width between the zygomatic processes is markedly less than the postorbital width, the cranium is evenly rounded, and the temporal fossae meet abruptly with the dorsal surface of the cranium. It is also considerably smaller than is normal for *P. elephantopus*. An additional trait is the presence of many pits over the dorsal surface of the cranium, first noticed by Parker (1893), and evidence for the former presence of large feathers. Therefore I suggest the vernacular name "crested moa" for this species.

The crania NMNZ S23800 has all cranial characters listed above. Although the preorbital plate is missing, its alignment is discernible and apparently the same. The basipterygoid processes have a wide base. The widths between the orbits, across the postorbital processes, between the temporal fossae, and between the zygomatic processes are proportionally the same in both the holotype and NMNZ S23800 (Fig. 1 and 2). Therefore I do not hesitate to refer NMNZ S23800 to *P. australis*.

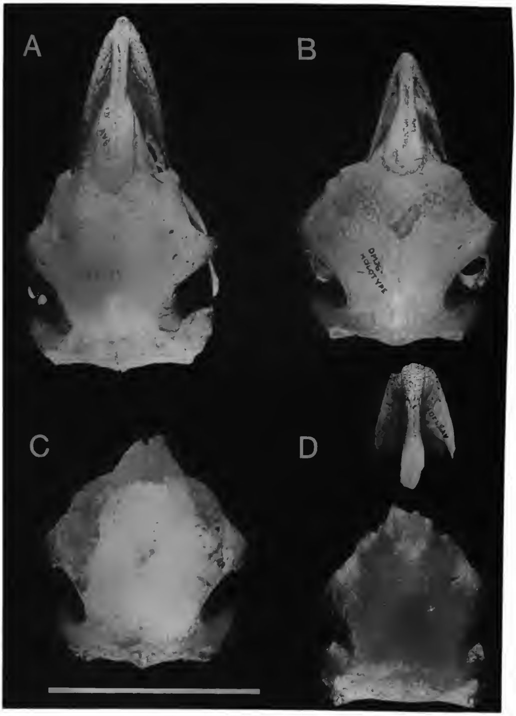

Fig. 1 Skulls in dorsal view. **A** *P. elephantopus* AIM MOA 10.12. **B** *P. australis* NMNZ S26, labelled DM 26. **C** *P. australis* NMNZ S23800 **D** *E. geranoides* NMNZ S471. Scale bar equals 100 mm.

Description of postcranial bones of *P. australis*

Because the cranium NMNZ S23800 was associated with other bones of apparently a single skeleton it is now possible to describe postcranial elements of *P. australis*. The pelvis is smaller than that of *P. elephantopus* and differs in dorsal view — the lateral parts of the escutcheon tend to have parallel sides and the escutcheon is widest midway along its length with each side having squared ends (Fig. 3A, B). The femur has a short, straight shaft with the popliteal fossa distal to the ectocondylar fossa, a lateral condyle which diverges from the shaft, and the unique feature of a large fossa (1 cm^2) enclosing a foramen on the pretrochanterian surface (Fig. 4A, D). The tibiotarsus has a medially flared distal end like other *Pachyornis* spp. but is distinctive in having a relatively long fibular crest (mean length equals 25% of total length, 20% in *P. elephantopus*) with the medulloarterial foramen adjacent to the distal end (Fig. 5A, D). The tarsometatarsus, as in all members of the genus, has an abrupt pronouncement of the middle trochlea but is smaller with the shaft and distal widths relatively narrower than in *P. elephantopus* (Table 1, Fig. 6).

Comparison of *P. australis, P. elephantopus,* and *E. geranoides*

Bones of *P. australis*, *P. elephantopus*, and *E. geranoides* are found in South Island subfossil deposits, and because the size range of bones for all three species overlaps and they are similarly robust, I list here distinguishing characters to aid in their identification.

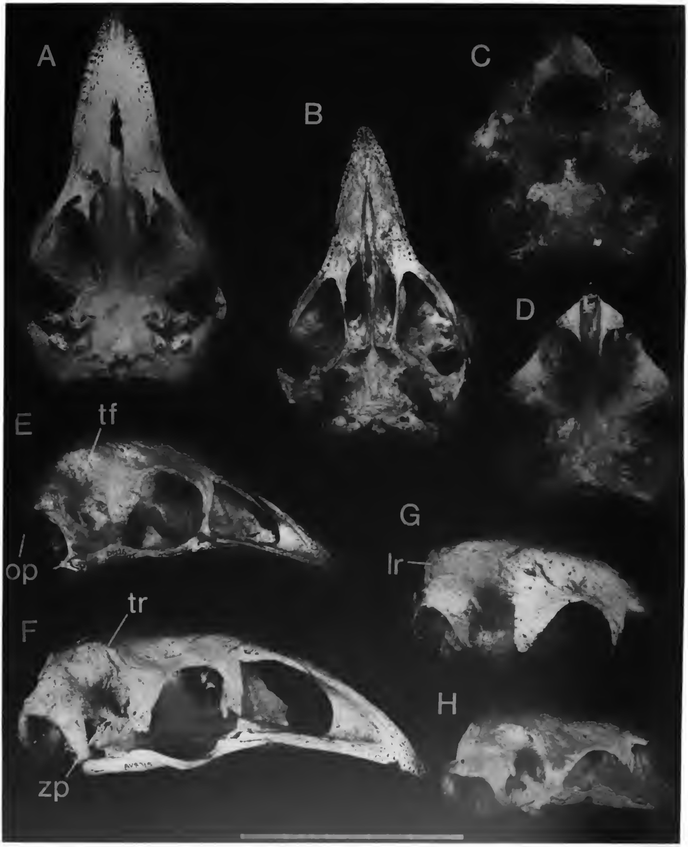

Fig. 2 Skulls in ventral (A–D) and right lateral (E–H) views. **A, F** *P. elephantopus* AIM MOA 10.12. **B, E** *P. australis* NMNZ S26. **C, G** NMNZ S23800. **D, H** *E. geranoides* NMNZ S471. lr, = lambdoidal ridge; op, opisthotic process; tf, temporal fossa; tr, temporal ridge; zp, zygomatic process. Scale bar equals 100 mm.

Fig. 3 *(opposite)* Pelves in right lateral (A, D, E) and dorsal (B, C, F) views. **A, B** *P. australis* NMNZ S23800; **C, D** *P. elephantopus* CM Av 20586; **E, F** *E. geranoides* NMNZ S471. Scale bar equals 200 mm.

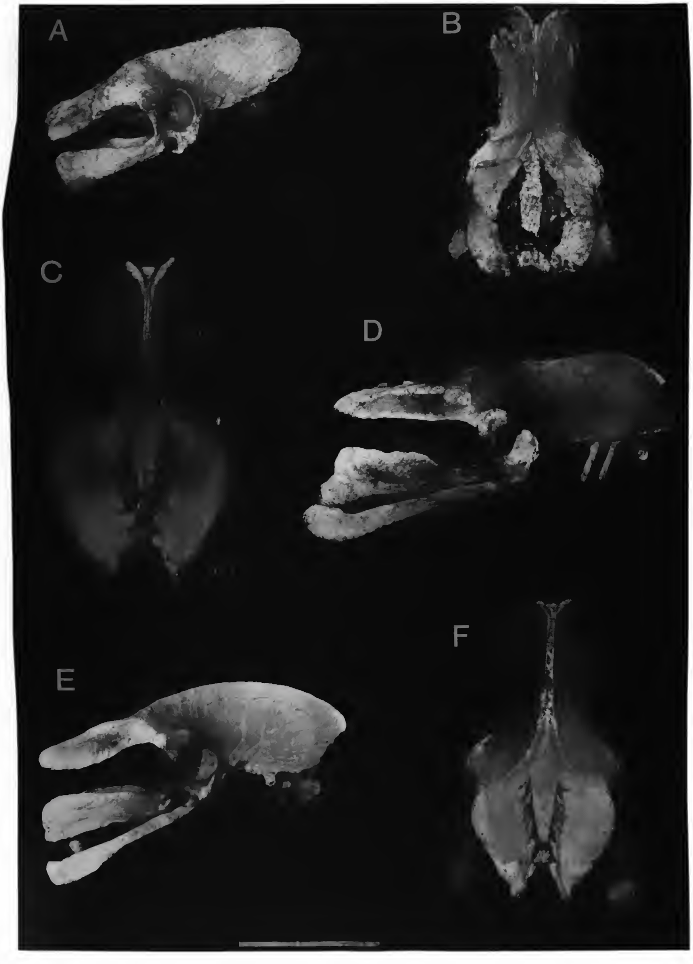
A
B
C
D
E
F

Skull In *P. australis* the postorbital width is much greater than that between the zygomatic processes, whereas in *P. elephantopus* it is only a little greater; in *P. australis* the skull anterior of the postorbitals narrows sharply and the premaxilla is shorter than the cranium, but in *P. elephantopus* the preorbital region is more elongate and the premaxilla length nearly equals that between the preorbital and opisthotic process, resulting in an overall more elongate skull; crania of *P. australis* are evenly rounded dorsally, but in *P. elephantopus* are flattened and irregular; in *P. australis* the temporal fossae meet steeply and abruptly, with the dorsal surface of the cranium resulting in a relatively wide space between the temporal ridges, and in *P. elephantopus* they extend further dorsally over the cranium; the space between the temporal and lambdoidal ridges is always wide (c. 10 mm) in *P. australis*, but varies from absent to about 10 mm, usually 2–5 mm, in *P. elephantopus*; the zygomatic process is stouter and the posttemporal fossae are relatively wider in *P. elephantopus*; the premaxillae and mandibles of *P. australis* are usually smaller than those of *P. elephantopus*.

Skulls of *Euryapteryx* differ obviously from those of *Pachyornis* (Fig. 1 and 2) in the great rounding of the premaxilla and mandible. Other notable differences are: (1) the temporal fossae are much narrower; (2) the temporal ridges are nearly parallel or only slightly convergent posteriorly (in *Pachyornis* they converge markedly); (3) the postorbital width equals the width between the zygomatic processes (in *P. australis* it greatly exceeds it); and (4) the olfactory chamber in *Euryapteryx* is considerably smaller than it is in *Pachyornis*.

Pelvis Although the pelvis is broad and massive in *P. australis*, *P. elephantopus*, and *E. geranoides*, there remain several differences between them (Fig. 3); in *Pachyornis* the ventral surface of the synsacrum is straight in lateral aspect, but arches dorsally posterior of the acetabular region in *E. geranoides*; in *Pachyornis* the anterior ventral synsacral surface is usually flat with two, low tubercles per fused vertebra, and in *E. geranoides* there are two, prominent tubercles per vertebra which generally fuse to form one large process on the most anterior sacral vertebra; in lateral view the zygomatic processes of the first sacral vertebra of *Pachyornis* are obscured by the ilia but in *E. geranoides* are visible beneath their lower margins; the dorsal profile of the escutcheon is flat and continues flat anterior of the acetabulum in *Pachyornis* but forms part of a continuous curve in *E. geranoides*; in dorsal view the lateral parts of the escutcheon of *P. australis* tend to have parallel sides and the escutcheon is widest midway along its length, with each side having squared ends, while in *P. elephantopus* the escutcheon tends to be rounded and is widest midway along its length, with each side terminating in a point. In contrast, in *E. geranoides* the escutcheon is widest anteriorly, with each side converging posteriorly to a point.

Table 1 Relative shaft and distal widths for tarsometatarsi of *P. australis*, *P. elephantopus*, and *E. geranoides*.

Species	Shaft width as % length			Distal width as % length		
	$\bar{x}$	n	SD	$\bar{x}$	n	SD
P. australis	22.89	11	0.018	52.25	11	0.021
P. elephantopus	26.04	12	0.018	59.40	12	0.018
E. geranoides	23.41	9	0.022	51.88	9	0.023

Sternum The sternum of *Pachyornis* is very distinctive, with widely diverging lateral processes, such that total width exceeds total length, whereas in *Euryapteryx* the lateral processes are long and diverge only slightly, so that total length markedly exceeds width; coracoidal articular grooves are deep in *Pachyornis*, very shallow or absent in *Euryapteryx*.

Femur Femora (Fig. 4) of the larger *Pachyornis* and of *E. geranoides* share several characteristics: both have short, straight, robust shafts; the popliteal fossa is more distal than the ectocondylar fossa, the lateral condyle diverges widely from the long axis of the shaft, and all species have a well-developed scar on the pretrochanterian surface for the insertion of the iliacus internus muscle. They differ as follows: the medial condyle of *P. australis* and *E. geranoides*, in dorsal view, is smaller than and parallel to the lateral condyle, but in *P. elephantopus*, the smaller medial condyle converges toward the anterior end of the lateral condyle; in *P. australis* and *E. geranoides* the proximal articular surface is markedly constricted between the femoral ball and the trochanter, but in *P. elephantopus* it is not; in *P. australis*, uniquely among emeid moas, there is on the pretrochanterian surface a wide (1 cm) fossa enclosing a foramen (possibly a pneumatic foramen) close to the proximal surface. *E. geranoides* and *P. elephantopus* only rarely have in this position a small (1–3 mm diam.) foramen. *E. geranoides* can also be separated from *P. elephantopus* on the form of the trochantal ridge on the ventral surface which in the latter is continuous to the ball but in the former ends abruptly so that the neck has an even curve to it.

Tibiotarsus All three species have robust tibiotarsi with large proximal and distal ends (Fig. 5). The posterior distal surface may be flat or deeply concave between the condyles.

The most distinctive feature differentiating these species is the relative length of the fibular crest: *P. elephantopus* mean ($\bar{x}$) = 20.75% total length (TL), sample size (n) = 11, standard deviation (SD) = 0.023; *P. australis* $\bar{x}$ = 25.29% TL, n = 14, SD = 0.012; *E. geranoides* $\bar{x}$ = 26.18% TL, n = 10, SD = 0.025. Related to the length of the fibular crest is the position of the nutrient foramen which in *P. elephantopus* is always markedly distal to the end of the fibular crest, in *P. australis* it is most often adjacent to the distal end of the fibular crest but occasionally is just distal to it, and in *E. geranoides* it is occasionally adjacent to, but usually is proximal to, the distal end of the fibular ridge. In *P. australis* and *P. elephantopus* the distal end of the tibiotarsus is widely flared medially (measured by expressing shaft width as a proportion of the height of the medial condyle). This value in *P. australis* is 91.58%, n = 14, SD = 0.066; *P. elephantopus* is 88.00%, n = 12, SD = 0.112; *E. geranoides* is 98.92%, n = 10, SD = 0.099; the height of the medial condyle in *E. geranoides* thus is equal to or often less than the shaft width.

Tarsometatarsi All three species are characterised by relatively short, very robust tarsometatarsi (Fig. 6). The height of the lateral hypotarsal ridge is greater than the medial in *P. australis* but is only variably so in *P. elephantopus* and *E. geranoides*. In *Pachyornis* the most medial point of the endotrochlea is level with the anterior extreme of the intertrochlear space, whereas in *Euryapteryx* this point of change in curvature is distal to the maximum depth of the intertrochlear space. The middle trochlea in *Pachyornis* rises abruptly from the long axis of the shaft, more gently in

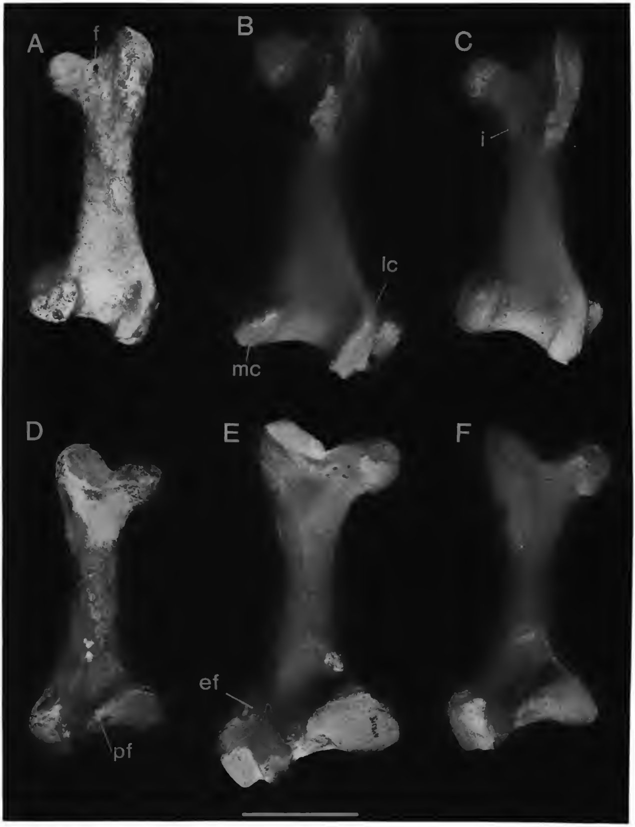

Fig. 4 Left femora viewed dorsally (upper) while at rest on femoral ball, trochanter and external condyle, and ventrally (lower). **A, D** *P. australis* NMNZ S23800. **B, E** *P. elephantopus* AIM MOA 10.12. **C, F** *E. geranoides* NMNZ S471. ef, ectocondylar fossa; f, fossa on pretrochanterian surface; i, scar for iliacas internus; lc, lateral condyle; mc, medial condyle; pf, popliteal fossa. Scale bar equals 100 mm.

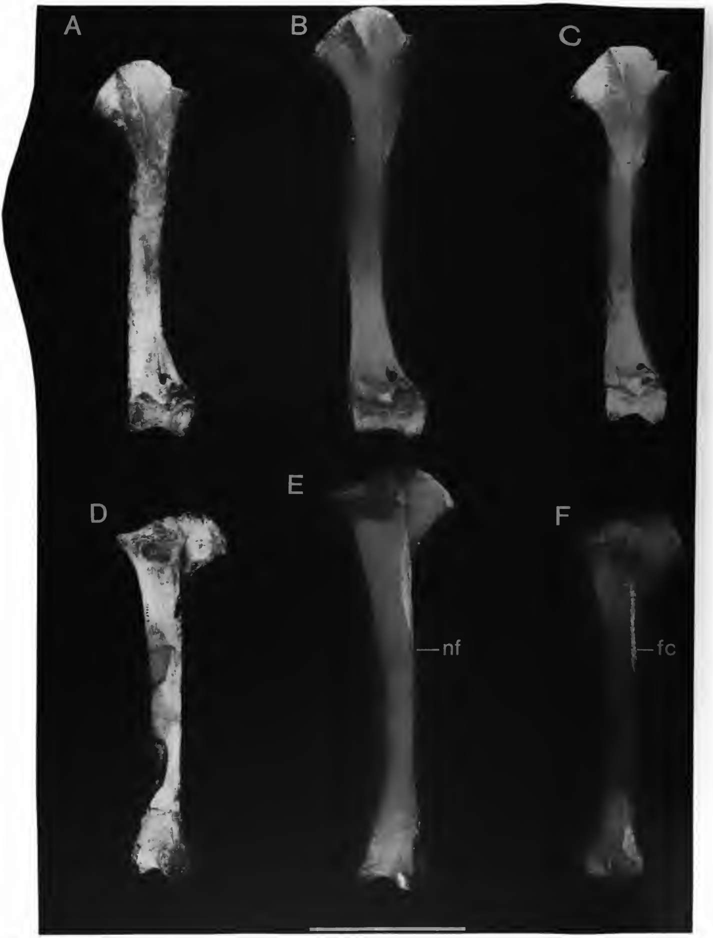

Fig. 5 Right tibiotarsi in anterior (upper), and posterior (lower) views. **A, D** *P. australis* NMNZ S23800. **B, E** *P. elephantopus* CM Av 8381. **C, F** *E. geranoides* NMNZ S471. fc, fibular crest; nf, nutrient foramen. Scale bar equals 200 mm.

Fig. 6 Right tarsometatarsi (at rest) in anterior view (upper) and posterior view (lower). **A, D** *P. australis* (NMNZ S23800. **B, E** *P. elephantopus* CM Av 8381. **C, F** *E. geranoides* NMNZ S471. e, endotrochlea; lhr, lateral hypotarsal ridge; mhr, medial hypotarsal ridge. Scale bar equals 100 mm.

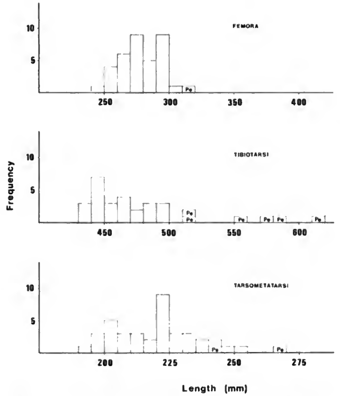

Fig. 7 Length/frequency histograms for femora, tibiotarsi, and tarsometatarsi of *Pachyornis australis* (unmarked) and *P. elephantopus* (marked Pe) from Graveyard deposits, Honeycomb Hill Cave, Oparara, northwest Nelson.

Euryapteryx. No consistent differences could be found between the three species in the shape of the proximal articular surface but on that of *P. elephantopus* the posterior lateral border was often evenly curved toward the medial hypotarsal ridge while being usually distinctly angled in *E. geranoides*. The ratio of shaft and distal widths to length varies (Table 1) being significantly greater in *P. elephantopus* ($P < 0.01$). The abruptness of the pronouncement of the middle trochlea from the line of the shaft and the point of change in curvature of the endotrochlea relative to the intertrochlear space distinguish tarsometatarsi of *Pachyornis* from *Euryapteryx*, and overall size plus the relative shaft width and/or distal width to length separate those of *P. australis* from *P. elephantopus*.

Phalanges *P. australis* is similar to *P. elephantopus* in its phalangeal formula of 3:3:4:5 and in having the length of the unguis in all digits more than twice the width (w = 48% length). By contrast *E. geranoides* has a phalangeal formula of 3:3:4:4 and the length of the unguis is less than twice the width (w = 57% length).

Size range of *P. australis*

Bones from the Graveyard deposits of Honeycomb Hill Cave, northwest Nelson, provide a large sample of *P. australis* for a length/frequency analysis, along with data for *P. elephantopus* from the same deposit (Fig. 7). In this sample, bones of *P. australis* are generally smaller than those of *P. elephantopus*. Although few, the data for *P. elephantopus* from the Graveyard are representative of other sites (e.g., Pyramid Valley, Table 2).

The length of specimens of *P. australis* from other sites are within the size range of this species in the Graveyard. The size distribution is not bimodal therefore there is no indication of sexual size dimorphism such as found in *Pachyornis mappini* Archey or *Euryapteryx curtus* (Owen) by Worthy (1987a).

Table 2 Length statistics for bones of *P. elephantopus* from Pyramid Valley, North Canterbury.

	Mean length (mm)	Range (mm)	n	SD
Femora	305.2	292–320	11	8.92
Tibiotarsi	551.9	506–612	12	27.63
Tarsometatarsi	224.5	206–259	12	13.39

Distribution of *P. australis*

Bones of *P. australis* are common in Otiran (late Pleistocene) deposits in Honeycomb Hill Cave, Oparara, northwest Nelson. The holotype is from Salisbury Tablelands, about 40 km to the east. I have collected additional specimens on Mt Owen in northwest Nelson, at about 1600 m above sea level (NMNZ S23568), and bones also from Mt Owen (NMNZ S23345) previously identified as *E. gravis* (Bell & Bell 1971) are here reidentified as *P. australis*. A left femur (NMNZ S25512) of approximate length 275 mm collected on Takaka Hill by F. W. Huffam and previously classified as *Dinornis torosus* is here reidentified as *P. australis*. In the Canterbury Museum, two femora (CM Av 28275) from Kennedys Basin near the junction of the Inangahua and Buller Rivers, are also of this species.

In Southland Museum several isolated crania, referred to *P. australis* by Oliver (1949), are from dunes at Greenhills and Wakapatu beaches, Southland. There are a number of other specimens from this region in the Southland Museum referable to a small *Pachyornis* species. A full list follows: E73.210 (type *P. murihiku* , skeleton), A40.44 (sterna from "The Narrows swamp"), 85.153 (a lot including a pelvis of a small *Pachyornis*), A40.30 (skull labelled *E. crassus* from Greenhills), A40.31 (skull labelled *P. australis* from ?Greenhills), and an unregistered skull from Colac Bay. Of these, the skeleton E.73.210, although much smaller than normal for *P. elephantopus*, exhibits most of the characteristics listed above for that species; relatively long premaxilla, pronounced preorbital region, temporal fossae spreading over cranium and stout zygomatic processes, femur with no fossa on the pretrochanterian surface, and tibiotarsus with a relatively short fibular crest, about 23% length. In addition it was a subadult individual at death (bones not entirely ossified). Thus I agree with Cracraft (1976) who synonymised this

Table 3 The species of moa and their presence (+) on either main island of New Zealand.

	North Island	South Island
Anomalopteryx didiformis	+	+
Megalapteryx didinus		+
Emeus crassus		+
Pachyornis mappini	+	
P. australis		+
P. elephantopus		+
Euryapteryx curtus	+	
E. geranoides	+	+
Dinornis struthoides	+	+
D. novaezealandiae	+	+
D. giganteus	+	+
Total	7	9

species with *P. elephantopus*. In E73.210 the area between the opisthotic and the zygomatic processes is abnormally close together on the right side. The cranium from Colac Bay is inflated between the orbits, has stout zygomatic processes, has a relatively long premaxilla, and the width between the postorbital and zygomatic processes is about equal. These are characteristics of *P. elephantopus*, and therefore I also refer this specimen to that species. It is slightly bigger than E73.210 (postorbital width 88 mm as opposed to 82 mm, and the width between temporal fossae 45 mm as opposed to 44 mm). However, in the two skulls A40.30 and A40.31, the postorbital width is markedly greater than the zygomatic width, each have a short premaxilla with a short preorbital region, and, in both, the cranium is evenly domed, characteristics of *P. australis*. In A40.31 the temporal fossae extend backward to reach the lambdoidal, a feature occasionally present in skulls of *P. elephantopus* but hitherto unknown in *P. australis*. Despite this, I agree with Oliver in referring these two crania to *P. australis*. Because both *P. elephantopus* and *P. australis* were present in Southland, the above mentioned sternum, unassociated as it is with any other bones, can only be referred to a small *Pachyornis* sp.; at the time of examination of the pelvis I was not able to distinguish pelves of these two species. Thus, no postcranial elements referable to *P. australis* are known from this region. In the National Museum a collection of bones from dunes at Greenhills, Southland, NMNZ S455, donated as a single skeleton of *E. crassus*, is comprised of the skull and sternum of a *Euryapteryx*, pelvis and vertebrae of *Emeus*, and the leg bones of an individual *P. elephantopus* of similar size to the type of *P. murihiku*.

The only other material ascribed to *P. australis* in the National Museum is the skull NMNZ S56A (marked DM 56A) of unknown locality but associated with other crania of *Euryapteryx* and *P. elephantopus* and therefore probably from eastern South Island.

Thus, the species is mainly known from northwest Nelson, but was also present in Southland.

Ecological preference of *P. australis*

A paleoenvironmental reconstruction made as a result of the study of the Graveyard deposits in Honeycomb Hill cave (Worthy 1987b; Worthy & Mildenhall 1989, this issue) suggests that during the Otira glaciation, when bones of *P. australis* were being deposited, the cave was situated in montane forests near the subalpine scrub zone, with considerable open areas nearby. Trees included species of *Libocedrus*, *Nothofagus*, and rare *Dacrydium*. Tree ferns were abundant and shrub species included *Pittosporum*, *Griselinia*, and *Melicytus*. The nearby subalpine scrubland contained abundant *Coprosma* species and members of the Compositae. Bones of *P. australis* found on Mt Owen must have been deposited during the Holocene and therefore in subalpine conditions because the collection sites are believed to have been ice covered during the last glacial. I suggest that the species was primarily an inhabitant of the subalpine environment; if correct, this explains its rarity in collections since there are few subfossil sites in subalpine locations.

CONCLUSION

The crested moa, *P. australis*, was apparently an upland or subalpine species which cohabited such areas with the upland moa, *Megalapteryx didinus* (Owen), which is more well known because of large bone deposits from Takahe valley, Fiordland, and several mummified specimens. It is the most common species in other subalpine cave sites (Worthy 1988a). The description of postcranial elements of *P. australis* will enable it to be recognised from further deposits.

The validity of *P. australis* means that 11 species of moa are now accepted (Table 3) based on the scheme of Cracraft (1976) with modifications (Millener 1982; Worthy 1988a,b). Of these species, seven occurred in the North Island and nine in the South Island. This disparity in distribution may be explicable in terms of the broad ecological requirements of each species and the type of available habitat. Species found on both islands are not discussed as each presumably occupied similar niches on each island. Among those restricted to only one island was *Euryapteryx curtus* which was most common in North Island coastal areas during the Holocene (Millener 1981), and common in a site of Otiran Glacial age in the Hawkes Bay (Worthy 1987a). From this distribution and the associated avifaunas (Millener 1981) I infer that it preferred more open, drier forest or scrub areas. In the South Island, *Emeus crassus* was restricted to the drier eastern areas during the Holocene, was dominant in the Southland dunes (unpubl. data), and was absent from areas of lowland broadleaf podocarp forest (unpubl. data) and therefore may have been the ecological equivalent of *E. curtus*. *P. mappini* and *P. elephantopus* differ principally in size, are probably North and South Island equivalents, and were apparently lowland species. In the South Island, bones of *P. elephantopus* and *E. geranoides* are usually found together. Bones of both these species have been found with those of *P. australis* in deposits of Otiran Glacial age in Honeycomb Hill Cave, but are comparatively rare; therefore it seems that *P. australis* replaced its larger congener in montane or subalpine habitats. This habitat was shared with *M. didinus*. Therefore the greater species diversity in the South Island reflects the greater ecological diversity (i.e., the additional presence of significant areas of montane and subalpine habitats).

The distinction of leg bones of *P. elephantopus* from those of *E. geranoides* in mixed collections, using characters identified in this study, will enable a reanalysis of material from swamp deposits. Previously, measurements were often the main criteria for separating these species and these are unreliable. Perusal of various collections has revealed many errors in identification since bones of both species share a similar size range. It is interesting that all the largest, more robust bones from Hamilton and Herbert, two swamp sites in Otago, are referable to *E. geranoides*, because *P. elephantopus* is usually considered to be the heavyweight among moas.

ACKNOWLEDGMENTS

I am pleased to acknowledge the support and sponsorship of the N.Z. Forest Service and the Department of Conservation, without which this project would not have been possible. Staff from the Karamea Office of the Department, especially Norm Stopforth, Mal Hanson, and Ian Gibson provided much in the way of practical assistance during excavations. Also Mike Huaki, Mike Hurst, and Chris Moore were of great assistance, not only in the field but also in washing and curation of specimens. The assistance of Beverly McCulloch and Brian Gill, respectively, at Canterbury Museum and Auckland Institute and Museum, for the loan of specimens, is gratefully appreciated. I thank J. A. Bartle and J. C. Yaldwyn for continued support and encouragement and C. D. Paulin and P. R. Millener for commenting on drafts of the manuscript. The photographs were taken by Mark Strange (NMNZ).

REFERENCES

Allan, R. S.; Percival, E.; Duff, R. S.; Falla, R. A. 1941: Preliminary report on excavations at Pyramid Valley swamp. *Records of the Canterbury Museum 4 (7)*: 325–353.

Archey, G. 1941: The moa a study of the Dinornithiformes. *Bulletin of the Auckland Institute and Museum 1*: 119 p.

Bell, C. J. E.; Bell, I. 1971: Subfossil moa and other remains near Mt Owen, Nelson. *New Zealand journal of science 14*: 749–758.

Brodkorb, P. 1963; Catalogue of fossil birds. Order Dinornithiformes. *Bulletin of the Florida State Museum biological sciences 7 (4)*: 202–218.

Cassels, R. J. S; Millener, P. R. 1985: Moa. Pp. 355–357 *in:* Campbell, B.; Lack, E. *ed.* Dictionary of birds. Calton & Vermillion.

Cracraft, J. 1976: The species of moa (Aves: Dinornithidae). *Smithsonian contributions to paleobiology 27*: 189–205.

Hutton, F. W. 1891: On the classification of the moas. *New Zealand journal of science 1:* 247–249.

————1892: The moas of New Zealand. *Transactions and proceedings of the New Zealand Institute 24*: 93–172.

————1897: The moas of the North Island of New Zealand. *Transactions and proceedings of the New Zealand Institute 29*: 541–557.

McKay, A. 1879: The Baton River and Wangapeka Districts, and Mt Arthur Range. Reports of geological explorations during 1878–79 with maps and sections. Wellington, Colonial Museum and Geological Survey of New Zealand.

Millener, P. R. 1981: The Quaternary avifauna of the North Island, New Zealand. Unpublished Ph.D. thesis, lodged in the Library, University of Auckland. 2 Vols, 897 p.

————1982: And then there were twelve: the taxonomic status of *Anomalopteryx oweni* (Aves: Dinornithidae). *Notornis 29*: 165–170.

Oliver, W. R. B. 1949: The moas of New Zealand and Australia. *Dominion Museum bulletin 15*: 205 p.

Parker, T. J. 1893: On the presence of a crest of feathers in certain species of moa. *Transactions and proceedings of the New Zealand Institute 25*: 3–6.

————1895: On the cranial osteology, classification and phylogeny of the Dinornithidae. *Transactions of the Zoological Society London 13 (11)*: 373–431.

Walker, C. A. 1978: Dinornithiformes. Pp. 24–25 *in:* Harrison, C. J. O. *ed.* Bird families of the world. New York, H. N. Abrams, Inc.

Worthy, T. H. 1987a: Sexual dimorphism and temporal variation in the North Island moa species *Euryapteryx curtus* (Owen) and *Pachyornis mappini* Archey. *National Museum of New Zealand records 3 (6)*: 59–70.

————1987b: The subfossil fauna of Honeycomb Hill Cave. I. A study of Otiran deposits in the Graveyard. II. A reassessment of *Megalapteryx benhami* Archey. Unpublished report of the National Museum of New Zealand. 59 p.

————1988a: A re-examination of the moa genus *Megalapteryx* in New Zealand. *Notornis 35*: 15–24.

————1988b: An illustrated key to the main leg bones of moas (Aves: Dinornithiformes). *National Museum of New Zealand miscellaneous series 17*: 37 p.

Worthy, T. H.: Mildenhall, D. 1989: A late Otiran – Holocene paleoenvironment reconstruction based on cave excavations in northwest Nelson, New Zealand. *New Zealand journal of geology and geophysics 32*: 243–253 (this issue).

Yaldwyn, J. C. 1979: The types of W.R.B. Oliver's moas and notes on Oliver's methods of measuring moa bones. Pp. 1–24 *in:* Anderson, A. *ed.* Birds of a feather. New Zealand Archaeological Association monograph II. (*British archaeological research series 12*).

New Zealand Journal of Geology and Geophysics, 1989, Vol. 32: 267–277
0028–8306/89/3202–0267 $2.50/0

Carbonate deposition and Ross Sea ice advance, Fryxell basin, Taylor Valley, Antarctica

M. J. F. LAWRENCE
Geology Department
University of Canterbury
Christchurch, New Zealand

C. H. HENDY
Chemistry Department
University of Waikato
Private Bag
Hamilton, New Zealand

Abstract Mechanisms of carbonate deposition in Lake Fryxell, Taylor Valley, Antarctica (75° 35′S, 163° 35′E) have been investigated. The lake lies within an area once covered by Ross Sea 1 ice (c. 20 000 years ago) and its proglacial lake. Lake sediments consist of five units, unit A being the lowermost deposit cored and unit E the uppermost. Three phases of carbonate deposition are evident in these sediments and result from climate changes associated with ice advances and retreat.

(1) About 20 000 years ago, a calcareous mud (unit B) was deposited in a deep proglacial Lake Washburn. The carbonate is of biogenic origin, and mixed calcite/aragonite mineralogy. Aragonite is the dominant phase.
(2) About 10 000 years ago the ice had retreated beyond the basin margins and the large volume of water then covered areas once under ice. This spreading of lake waters increased the ablation surface, resulting in evaporative concentration of lake waters, and a reduction in lake levels. Brine concentration caused the precipitation of the aragonite unit D. $\delta^{13}C$ values indicate that biogenic processes continued to operate but were overshadowed by inorganic carbonate deposition.
(3) Following the complete retreat of the Ross Sea ice, alpine glaciers then readvanced. Meltwaters therefrom flowed into the lake basin refilling the lake. Evaporated brines then rediffused up into the water column resulting in the present chemical stratification. Modification of the water column in the upper euphotic zone, mainly by photosynthetic algae, causes the precipitation of calcite which falls as a pelagic rain to the lake bed. Where the lake bed is within the euphotic zone, stromatolitic deposition occurs.

In addition to the three depositional mechanisms, there may be diagenetic alteration of the carbonates in units B and D.

Keywords Antarctica; Ross Sea; ice shelves; calcite; aragonite; evaporites; stromatolites; stratification; precipitation; evaporite deposits

Received 15 January 1987, accepted 12 July 1988

INTRODUCTION

The first major study of glacial deposits in the Dry Valleys was by Péwé (1960). Subsequent work, particularly by Denton et al. (1971), Hendy et al. (1979), and Stuiver et al. (1981) have further elucidated the glacial history of the area. More recently Denton and coworkers have been working on a complex glacial stratigraphy in the Marshall Valley. Both Marshall and Taylor Valley sequences consist of tills and associated glaciolacustrine deposits. Within the glaciolacustrine sediments, many carbonate, gypsum and even halite lake-bed deposits occur, in places associated with algal material. The lacustrine carbonates and algal material are particularly useful as datable deposits for obtaining absolute chronology of glacial sequences.

Until now, the mechanism of deposition of the carbonates has not been investigated. For this study, Lake Fryxell was chosen because: (1) it lies within the drainage basin of the Lower Taylor Valley (75° 35′S, 163° 35′E; Fig. 1), which was filled by the Ross Sea 1 ice advance of c. 20 000 years ago, and (2) preliminary investigation of Lake Fryxell indicated the presence of $CaCO_3$ covering the lake bottom, and deeper within lake sediments. This study determines how carbonate is presently deposited in Lake Fryxell and how it relates to past carbonate depositional phases.

ROSS SEA 1 ADVANCE IN THE LOWER TAYLOR VALLEY

The Ross Sea 1 drift covers most of the floor of the Lower Taylor Valley and extends upvalley as far as the present Canada Glacier (Stuvier et al. 1981). The ice advance dammed the lower end of the valley forming a large proglacial lake, "Glacial Lake Washburn" (Péwé 1960). Algal material deposited in the lake during the maximum stand of the advance ranges in age from 21 200 to 17 000 years B.P. (Stuvier et al. 1981). Following this resulting high lake-level, Stuvier et al. inferred a relatively rapid lake-level drop after 17 000 years B.P. (Fig. 2). Ice recession and minor advances caused fluctuating lake levels until c. 12 000–9200 years B.P. (Fig. 2) (Stuvier et al. 1981). The latter date probably marks the last occupation of the valley by the Ross Sea Ice Sheet (Lawrence 1982) which began a period of aridity. More recently, alpine glaciers have readvanced across Ross Sea 1 deposits to their present positions.

ANALYTICAL METHODS (from Lawrence 1982)

Sediments

Sediment samples consisted of a number of sediment cores covering most of the lake area. Carbonate samples were powdered in a ringmill for 3–4 s after air drying. Carbonate mineral proportions were determined by semiquantitative X-ray diffraction using a Phillips PW 1130/00 X-ray generator

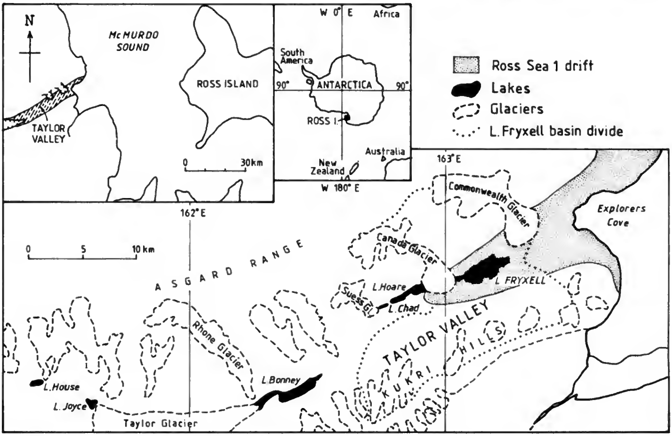

Fig. 1 Taylor Valley, showing Lake Fryxell in relation to the Ross Sea 1 drift.

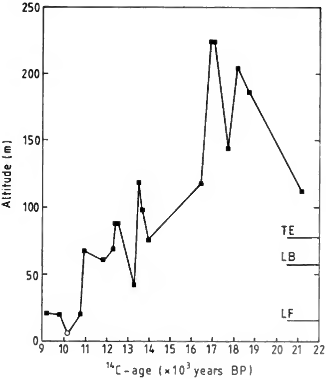

Fig. 2 Lake-level curve for the lower Taylor Valley. The open circle indicates the date for unit D, this study (from Stuiver et al. 1981; Lawrence & Hendy 1985) LF, Lake Fryxell; LB, Lake Bonney; TE, Basin divide near Explorers Cove.

with goniometer. Instrument settings were standardised usually at about 30–36 kV and 16 mA, using a standard powdered quartz (<4.5ø) ($d = 4.26$Å) to a standard peak height. Samples for scanning electron microscope (S.E.M.) study were initially coated in 500Å gold/platinum using a Polaron E5000 diode sputter coater and then examined under a JEOL-JSM 35 S.E.M. For trace and major element analyses, known weights of each sample were dissolved in c. 10% (V/V) analytical grade HCl. Once all visible reaction had ceased, the solutions were filtered through preweighed Type Ha 0.45 µm millipore filter papers and then made up to known volume ready for analysis. These solutions were analysed for Ca, Mg, Sr, Zn, and Mn; Ca, Mg, Zn, and Mn analyses were by atomic absorption spectroscopy using an Instrument Laboratory AA/AE spectrophotometer 357 air/acetylene flame. Sr was analysed by flame emission using a Varian Techtron model 1000 AAS nitrous oxide/acetylene flame. Stable carbon and oxygen analyses were performed using the technique of McCrea (1950). Isotope ratios were determined using a Micromass 602C double inlet mass spectrometer.

Water column

pO_2 was measured using a Delta Scientific 2010 automatic dissolved O_2 analyser with attached thermistor probe for temperature. A pHM64 research pH meter with standard glass and calomel electrodes was used for pH determinations. The inorganic ΣCO_2 was measured with a URAS 2T infrared gas analyser after first acidifying the sample with 0.1M HCl in a small CO_2 stripper, drying the CO_2 in a −20°C cold trap, and then admitting the gas to the infrared gas analyser for

measurement. Each CO_2 sample measurement was bracketed by two known standards. Turbidity was measured using a modified Turner III fluorometer. Water samples for inorganic analyses were collected for laboratory determinations. Aliquots of water were taken for $\delta^{13}C$ analysis; $Ba(OH)_2$ was added to precipitate $BaCO_3$ which was analysed as described above. Waters for elemental analyses were first filtered through Type Ha 0.45 µm millipore filters. These were X-rayed (with the above equipment) for the presence of carbonate. Analyses of waters were according to American Public Health Association [APHA] (1975) by atomic absorption/emission (Ca, Mg, Sr, Ba, Fe, Zn, Mn, K) using an IL 357 AA/AE spectrophotometer. Chloride was determined by argentometric titration, and Na by use of an Eel flame photometer.

TREATMENT OF WATER COLUMN CARBONATE DATA

Lake Fryxell's permanent ice cover and chemical stratification (Hoare et al. 1965; Torii et al. 1975; Lawrence & Hendy 1985) considerably reduce exchange between CO_2 in the lake and in the atmosphere. As such, the lake can be treated as a closed system, and hence H_2CO_3 can be treated as a nonvolatile acid (Stumm & Morgan 1981), that is,

$$[H_2CO_3^*] = [CO_2aq] + [H_2CO_3]$$

Numerical values for the equilibrium constants, K_1 and K_2, at various temperatures are listed in Stumm & Morgan (1981), from which K_1 and K_2 values for the water column are graphically interpolated. Pressure effects were then evaluated.

Pressure (P) at various depths was evaluated from:

$$P = \rho g h$$

where $\rho = 1 \times 10^{-3}$ g/kg; $g = 9.8$ m/s^2; and h = height (m) of water column to the top of the ice cover.

The effect of the pressure on the K-values was determined from

$$\ln \frac{K'_1}{K_1} = \frac{\Delta V°}{RT} \times (P_2 - P_1)$$

where K_1 = unadjusted K_1; K'_1 = adjusted K for pressure; $\Delta V°$ = −19 cm^3/mol for K_1, −10.7 cm^3/mol for K_2 (Li et al. 1969); $R = 8.314 \times 10^6$ cm Pa K^{-1} mol^{-1}; P_1 = atmospheric pressure (Pascals); P_2 = pressure at depth of interest (Pascals).

Finally salinity corrections were made using the equations of Larsen & Buswell (1942), namely

$$pK'_1 = pK_1 - \frac{0.5\sqrt{I}}{(1 + 1.4\sqrt{I})}$$

and

$$pK'_2 = pK_2 - \frac{2\sqrt{I}}{(1 + 1.4\sqrt{I})}$$

where $I = \frac{1}{2}\Sigma c_i z_i^2$
where c_i = measured concentration of species i
z_i = ionic charge of species i

Having corrected the $K_1 + K_2$ values, the various ionisation fractions were calculated using the equations of Stumm & Morgan (1981):

$$[H_2CO_3^*] = \Sigma CO_2\, \alpha_0$$
$$[HCO_3^-] = \Sigma CO_2\, \alpha_1$$
$$[CO_3^{2-}] = \Sigma CO_2\, \alpha_2$$

where

$$\alpha_0 = \left[1 + \frac{K_1}{[H^+]} + \frac{K_1 K_2}{[H^+]^2}\right]^{-1}$$

$$\alpha_1 = \left[\frac{[H^+]}{K_1} + \frac{K_2}{[H^+]}\right]^{-1}$$

$$\alpha_2 = \left[\frac{[H^+]^2}{K_1 K_2} + \frac{[H^+]}{K_2} + 1\right]^{-1}$$

The concentration condition for the validity of these calculations is

$$\Sigma CO_2 = [H_2CO_3^*] + [HCO_3^-] + [CO_3^{2-}]$$

$[H^+]$ was determined from

$$[H^+] = 10^{-pH}$$

For solubility profile interpretations, all concentrations of Ca^{2+} and CO_3^{2-} were converted to activities using the Güntelberg approximation:

$$\log \delta = \frac{-Az^2\sqrt{I}}{(1 + \sqrt{I})}$$

where A = 0.5; I = ionic strength; and z = charge of the ion. Maximum ionic strength in the Lake Fryxell water column was I = 0.2 (Lawrence 1982). These calculated ion activity coefficients for Lake Fryxell compared well with published values for similar ionic strengths calculated using different techniques in Whitfield (1975). These values were then compared to a similarly treated Ksp ($10^{-8.35}$; Krauskopf 1979) for various depths in the lake, which were then converted to equilibrium ion activity products (Berner 1980).

RESULTS

Water column

Analytical results are listed in Table 1. There is an overall increase in concentration with depth, reflecting the chemical stratification of the lake. This stratification is a result of chemical diffusion from an evaporative brine into overlying fresh waters which has formed a diffusion cell with a calculated age of c. 1000 years (Lawrence 1982; Lawrence & Hendy 1985). Ca deviates from the overall trend as do the transition elements. O_2 is at a maximum at 8–9 m and is negligible below 11 m depth. Importantly, $\delta^{13}C$ analyses are negative at 4–5 m depth, possibly due to moss and lichen respiration in the streams which supply Lake Fryxell with meltwater. The $\delta^{13}C$ values of c. 0‰ at 8–10 m depth reflect the withdrawal of isotopically light carbon from the dissolved inorganic carbon pool by algal photosynthesis.

Sediments

The sediment stratigraphy is outlined in detail in Lawrence (1982), and Lawrence & Hendy (1985). In this study, the three carbonate-bearing units are of primary interest (Fig. 3). Unit E contains flat, "flake-like" calcite at the sediment/water interface and occasionally interspersed further down the unit.

Unit D is a varve-like aragonite deposit with a composite ^{14}C date of 10 410 ± 120 years B.P. Unit B is a calcareous mud containing about 20% wt $CaCO_3$ of mixed calcite/aragonite (predominantly aragonite) mineralogy, with a composite date for the lower half of 21 000 ± 300 years B.P. Isopach maps constructed from the measured thicknesses of the units in 26 cores covering most of the lake (Lawrence 1982; Lawrence & Hendy 1985) show that unit D thickens towards the present shore and unit B thickens towards the centre of the present lake.

A summary of chemical and mineralogical analyses is given in Table 2. Ca and Mg vary antipathetically. The Ca versus Mg plot (Fig. 4) shows that unit E calcites generally plot as low-medium Mg-calcites. The aragonite plots in about the same field, probably because the aragonite lattice usually favours substitution by larger cations such as Ba and Sr. There appears to be a considerable spread of values for unit B. Accordingly a greater Sr content in unit D than in other units was expected, but this is not so. Mn analyses are similar for units D and E but much higher in unit B.

For individual cores, $\delta^{13}C$ of unit D decreases from the top to the bottom of the unit, whereas the reverse occurs in unit B. Unit E calcites have similar $\delta^{13}C$ values to those for the present water column at 8–10 m depth. There is an overall trend for $\delta^{13}C$ to increase with decreasing age (i.e., from unit B to E; Fig. 5). $\delta^{18}O$ values overlap for carbonate of units D and E but are more positive in unit B. From individual cores, unit D carbonates become isotopically heavier up the profile whereas unit B shows the reverse trend.

DISCUSSION

Carbonate deposition in Lake Fryxell can be subdivided into two systems:

(1) the system including the present Lake Fryxell water column and unit E calcites, which were deposited during a period of alpine glacial advance;

(2) the system prevailing during the deposition of units D and B, a period of Ross Sea ice advance and retreat.

Modern carbonate depositional regime

Lake Fryxell is a saline lake according to the criteria of Eugster & Hardie (1978). The compositional history of closed basin, saline lakes such as Lake Fryxell consists of two phases: (1) the acquisition of solutes, and (2) brine evolution and subsequent precipitation of salts (Hardie & Eugster 1970). The lake salts have a number of different sources and pathways which are important in different Dry Valley areas, though salts of marine origin are regionally and quantitatively predominant (Keys & Williams 1981). Marine salts may come directly from sea spray (House et al. 1966), sea spray deposited on ice which subsequently melts (Torii & Yamagata 1981), or possibly relict seawater. Chemical weathering, though slow, is a major source of Mg^{2+}, Ca^{2+}, CO_3^{2-} (Keys & Williams 1981), and Sr^{2+} (Jones & Faure 1978); in addition, salts dissolved from soils also contribute (Field 1975; Wilson 1981). Thompson et al. (pers. comm.) have shown that meltwaters from alpine glaciers are major suppliers of dissolved material to Lake Fryxell.

Lawrence (1982), and Lawrence & Hendy (1985) showed the chemical stratification of Lake Fryxell to be diffusion controlled, thus indicating that the lake has at least once been reduced to negligible depth. The resultant brine concentration and subsequent diffusion back up the water column following refilling make determination of a specific salt source difficult.

Biological activity also has an effect on the predominantly inorganic system described above. The pO_2 data indicate that Lake Fryxell has an upper euphotic (oxygenic) zone and a

Table 1 Summary of water column analyses for Lake Fryxell. Beg, beginning of summer season; Mid, middle of summer season; End, end of summer season. The pO_2 probe could not be properly calibrated, therefore values are relative. Analytical problems in the field meant no ΣCO_2 values for the end of season were obtained. For thermodynamic calculations (Fig. 6) mean values were used for the end of season profile.

Depth (m)	Ca^{2+} (ppm)	Mg^{2+} (ppm)	Sr^{2+} (ppm)	Ba^{2+} (ppm)	Fe^{2+} (ppm)	Mn^{2+} (ppm)	Zn^{2+} (ppm)	K^+ (ppm)	Na^+ (ppm)	Cl^- (ppm)	ΣCO_2 (mmol/l) Beg	Mid	$\delta^{13}C$ (‰PDB)
4.0	22.5	5.8								61			
4.5			2.5	9.8	0.7	0.08	2.1	33	263	204			
5.0	44.0	35.0	2.8	9.8	0.6	0.03	1.1	58	313	281	10.1	13.6	−18.25
6.0	51.5	25.0	3.6	8.8	0.9	0.05	0.3	45	426	440	7.5	12.0	−18.32
7.0	47.5	57.5	7.5	12.3	0.6	0.04	0.6	99	900	1103	9.9	17.6	−11.52
8.0	49.5	72.5	8.3	14.2	0.1	0.05	1.4	108	1119	1191	17.3	18.3	−1.41
9.0	87.0	92.5	10.8	17.0	0.2	0.26	0.6	127	1694	1694	24.9	28.2	−0.05
10.0	70.5	212.5	13.2	20.2	0.2	0.15	0.9	147	1813	2160	29.6	30.2	−9.40
11.0	49.5	237.5	15.1	21.6	1.6	0.14	0.7	158	1991	2470	49.0	34.1	−10.56
12.0	47.5	262.5	15.5	22.3	0.3	0.10	1.1	163	2126	2634	45.9	50.0	−9.45
13.0	57.5	280.0	16.5	23.7	0.5	0.06	2.1	191	2478	3099	89.2	57.4	−8.40
14.0	55.0	355.0	18.3	24.3	0.3	0.04	1.4	206	2579	3332	94.9	59.8	−5.47
15.0	56.0	350.0	18.5	23.9	0.4	0.05	2.4	214	2690	3520	95.0	58.3	−6.56
16.0	56.5	350.0	18.6	23.2	0.2	0.04	1.8	208	2800	3672	86.0	58.9	−6.85
17.0	51.5	320.0	18.9	22.0	0.2	0.04	0.8	200	2861	3768	107.0	99.5	−4.56
18.0	40.5	370.0								4007			−4.96

lower anaerobic zone (Lawrence & Hendy 1985). Organisms below about 10 m depth are generally CO_2 evolvers and those above are CO_2 fixers. The latter are predominantly algae and tend to be concentrated in the lower euphotic zone (Vincent 1981). The removal and/or fixation of CO_2 at various levels in the water column will govern the resultant pH. Removal of CO_2 from the inorganic carbon pool by algal photosynthesis will increase the pH and carbonate ion activity; CO_2 production through respiration and microbial oxidation will cause the reverse.

The products of photosynthesis are enriched in ^{12}C with respect to the original CO_2 starting material. This is shown in Lake Fryxell where $\delta^{13}C$ values of c. 0‰ occur at 10–9 m depth and coincide with maximum productivity. Photosynthesis, followed by the settling out of seston, will result in a greater loss of ^{12}C than ^{13}C from the euphotic zone. Any $CaCO_3$ precipitated under equilibrium conditions will contain relatively more ^{13}C than ^{12}C compared to the aqueous CO_2.

The mass budget for the simultaneous removal of seston and $CaCO_3$ is calculated as follows:
The $\delta^{13}C$ of the total carbon (aqueous inorganic carbon species and seston and calcium carbonate)

$$= \frac{\delta^{13}C_{\Sigma CO_2}\ \Sigma CO_2 + \delta^{13}C_p\, M_p + \delta^{13}C_c\, M_c}{\Sigma CO_2 + M_p + M_c} \qquad (1)$$

where $\Sigma CO_2 = [CO_2] + [HCO_3^-] + [CO_3^{2-}]$

M_p = moles/litre of photosynthates removed from the euphotic zone, and M_c = moles/litre of calcium carbonate precipitated from the euphotic zone. The subscripts ΣCO_2, p and c refer to total inorganic aqueous carbon, photosynthates and calcium carbonate, respectively.

Between pH values of 7.5 and 9.0, > 93% of the aqueous inorganic carbon will be in the form of bicarbonate ions, with the minor compound being aqueous carbon dioxide at the lower pH values and carbonate ions at the upper pH values. Thus, for the purposes of the mass budget calculations,

$\Sigma CO_2 \approx [HCO_3^-]$

$\delta^{13}C_{\Sigma CO_2}$, $\delta^{13}C_p$, and $\delta^{13}C_c$ are related through the respective isotopic fractionation with

$$\delta^{13}C_{\Sigma CO_2} \approx \delta^{13}C_{HCO_3^-}$$

$\delta^{13}C_c \approx \delta^{13}C_{HCO_3^-} + 2.2$ (‰) at 5°C (Friedman & O'Neil 1977).

For photosynthesis involving C3 enzyme limitation and not involving limitation through aqueous CO_2 diffusion,

$$\delta^{13}C_p \approx \delta^{13}C_{HCO_3^-} - 29.5 (‰)$$

Until carbonate saturation is achieved, $M_c = 0$, therefore,

$$\delta^{13}C_{(total\ carbon)} = \delta^{13}C_{HCO_3^-} - 29.5\,\frac{M_p}{\Sigma CO_2 + M_p}\ (‰) \qquad (2)$$

and where $M_p \ll \Sigma CO_2$

$$\Delta\delta^{13}C = 29.5\,\frac{M_p}{\Sigma CO_2 + M_p}\ (‰)$$

where $\Delta\delta^{13}C$ is the change in $\delta^{13}C$ of any species.

As the carbon being withdrawn from the aqueous system has no means of exchange with the remaining aqueous carbon, and is removed progressively, the process becomes one of Rayleigh distillation, with the carbon remaining in the aqueous inorganic carbon pool becoming progressively enriched in ^{13}C.

Once saturation with respect to calcite has been exceeded and calcite begins to precipitate, $M_p \approx M_c$ since for every mole of CO_2 removed from a $CaCO_3$ saturated solution, approximately 1 mole of $CaCO_3$ will be precipitated.

Under these conditions eq (1) reduces to:

$$\delta^{13}C_{(total\ carbon)} = \delta^{13}C_{HCO_3^-} - 27.3\,\frac{M_p}{\Sigma CO_2 + M_p}\ (‰) \qquad (3)$$

and where $M_p \ll \Sigma CO_2$

$$\Delta\delta^{13}C = 27.3\,\frac{M_p}{\Sigma CO_2 + 2M_p}\ (‰)$$

With continual removal of carbon from the aqueous pool by photosynthesis and precipitation of calcite, a process of Rayleigh distillation is established, and

$$\Delta\delta^{13}C = 27.3\ \ln\left(\frac{\Sigma CO_{2,t}}{\Sigma CO_{2,o}}\right)(‰)$$

where $\Sigma CO_{2,t}$ = the total concentration of aqueous inorganic carbon at time t and $\Sigma CO_{2,o}$ = the total concentration of aqueous inorganic carbon at the start. $\Delta\delta^{13}C$ = the change in the carbon isotopic ratio of any one species in parts per thousand.

Table 1 (*continued*)

pH			pO_2 (uncalibrated)			Calcite Present (P) Absent (A)
Beg	Mid	End	Beg	Mid	End	
8.0	7.9	7.8	9.5	10.4	6.8	A
8.1	7.9		7.7	11.5	8.5	A
8.2	7.9	7.8	7.3	11.6	9.6	A
8.1	7.9	7.8	6.1	11.8	8.6	A
8.1	8.2	8.1	6.8	14.5	10.0	A
8.0	7.9	7.8	7.7	11.0	9.5	P
7.7	7.4	7.6		0.2	3.2	P
	7.5	7.6	Below levels of detection			P
7.8						
	7.6	7.4				P
7.6						
	7.5	7.6				P
7.7						
	7.5	7.6				P
7.7						
	7.5	7.5				P
7.5						
	7.5	7.5				P
7.6						
	7.5	7.5				P
7.7						
	7.5	7.5				P

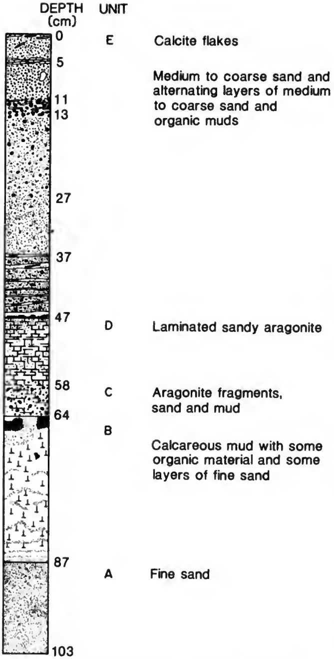

Fig. 3 Generalised stratigraphy of Lake Fryxell sediments (from Lawrence 1982).

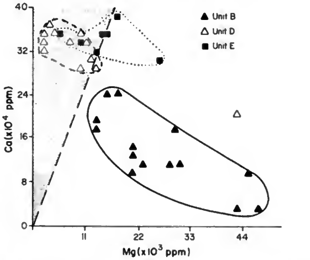

Fig. 4 Plot of Ca versus Mg. The shaded region denotes the low Mg-calcite field.

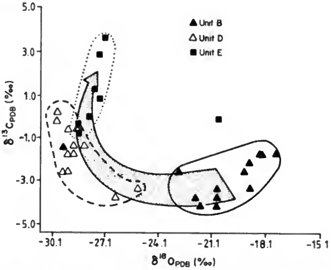

Fig. 5 Plot of $\delta^{13}C$ versus $\delta^{18}O$. The general trend is increasing $\delta^{13}C$ (arrow) with decreasing age. Unit B carbonates are more positive in $\delta^{18}O$ than units E and D.

This means that continued seston and carbonate removal will result in a steady increase in $\delta^{13}C$ for all species, assuming that there is no significant external replenishment. Thus the increasingly positive profile up the sedimentary column may be explained in terms of removal of CO_2 from the euphotic zone water, with the Rayleigh distillation model suggesting approximately half of the carbon removed from the euphotic zone.

The solubility product and activity product calculations show that the euphotic zone waters are supersaturated with respect to calcite, but not aragonite (Fig. 6). Calcite precipitation from these waters is thus feasible. X-ray diffractograms of the suspended sediments from 8 m depth and below show the presence of calcite, and $\delta^{13}C$ measurements of the ΣCO_2 in the water column (Table 1) show a marked enrichment in ^{13}C between 8 and 9 m depth with $\delta^{13}C$ values of between 0 and −1.4‰ with respect to PDB, contrasting strongly with $\delta^{13}C$ values of −18‰ above this horizon and −10‰ below it. With a pH of 7.9–8.0 between the depths of 8 and 9 m, 95% of the aqueous inorganic carbon will be in the form of bicarbonate ions, so that calcite produced in isotopic equilibrium with these waters will have $\delta^{13}C$ values between 0.8 and +2.2‰ with respect to PDB. The $\delta^{13}C$ values of calcite found in the surface sediments of Lake Fryxell (unit E) (Table 2) have a range of −1.59 to 3.35‰ and so bracket those that we would predict to be produced from depths of 8–9 m. They are well out of isotopic equilibrium from any other waters in Lake Fryxell.

Calcite appears to be precipitated from the lower euphotic zone (8–9 m depth) as a result of photosynthetic removal of

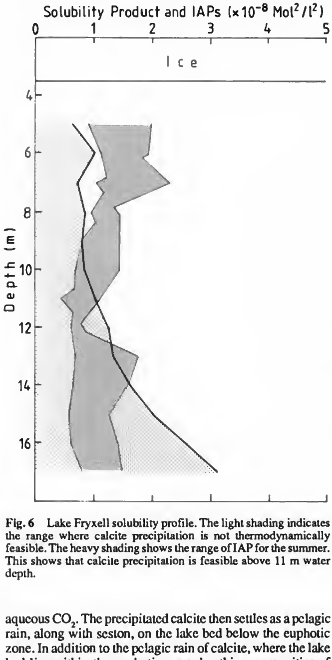

Fig. 6 Lake Fryxell solubility profile. The light shading indicates the range where calcite precipitation is not thermodynamically feasible. The heavy shading shows the range of IAP for the summer. This shows that calcite precipitation is feasible above 11 m water depth.

aqueous CO_2. The precipitated calcite then settles as a pelagic rain, along with seston, on the lake bed below the euphotic zone. In addition to the pelagic rain of calcite, where the lake bed lies within the euphotic zone, benthic communities of algae cause the precipitation of calcite resulting in a stromatolitic style of deposition in shallow waters (Parker & Simmons 1981; Parker et al. 1981; Wharton et al. 1982).

Addition of CO_2 through respiration brings about a lowering of pH. S.E.M. examination of calcite from the lake bed (top of unit E) showed broken and rounded crystals as opposed to the expected regular-shaped calcite rhombs. We suggest that this may result from dissolution in the lower water column or sediments. The occurrence of only sporadic calcite layers further down unit E may support this hypothesis.

Previous carbonate depositional regimes

The calcareous mud (unit B) has a low $CaCO_3$ content and consists primarily of aragonite with some calcite (Table 3). The fine grain size of the sediment and increasing thickness towards the deepest part of the basin suggest that this is a deep water deposit. Though slightly predating the maximum stand of the Ross Sea ice, the 21 000 year date on this deposit indicates it was deposited at or near the maximum level of Lake Washburn. At this time the greatly expanded ice volume provided an increased meltwater source thus filling the lake (Sturvier et al. 1981).

Present $\delta^{13}C$ values for the upper water column of the present lake Fryxell are surprisingly negative (Table 1). The increasingly negative $\delta^{13}C$ up through unit B is interpreted as a result of meltwater replenishing the carbon pool and swamping the effect of photosynthetic processes. The markedly more positive $\delta^{18}O$ values for unit B, as compared to unit D and E carbonates, cannot be explained in terms of temperature change. They suggest either drastic change in water composition or the presence of "imported" detrital carbonate of radically higher $\delta^{18}O$. $\delta^{18}O$ values for meltwaters feeding Lake Fryxell are about $-32‰_{SMOW}$, and thus carbonates precipitated from these waters at c. 3°C should have $\delta^{18}O$ values of about $-28‰_{PDB}$ (as in units D and E). The only plausible source of isotopically heavier water is seawater. Thus the unit B values are interpreted as being the result of a contribution of seawater and/or carbonate of seawater origin to water occupying the Fryxell basin. Such imported carbon may explain the slightly older than expected ^{14}C date of the sediment. An age of c. 19–20 000 years would be more likely. Within unit B itself, $\delta^{18}O$ values become lighter up the column, which may also suggest lake infilling.

The actual mechanism of carbonate deposition in unit B is inferred to be analogous to that of the present Lake Fryxell system. A major difference, however, is that XRD analyses suggest aragonite is the dominant phase. Lake infilling rules

Table 2 Chemical and mineralogical analyses for the three carbonate units. Most of the 10%wt aragonite in unit E is from samples below the sediment/water interface.

	Unit E		Unit D		Unit B	
	Mean	Range	Mean	Range	Mean	Range
Ca (ppm)	340 000	298 000 – 382 000	321 000	211 000 – 363 000	135 000	37 000 – 243 000
Mg (ppm)	13 900	5400 – 26 800	10 100	2050 – 42 800	26 400	12 700 – 47 100
Sr (ppm)	1540	954 – 3990	2010	831 – 4870	1890	1080 – 3490
Ba (ppm)	5490	683 – 7290	5870	2610 – 7500	4230	2410 – 6890
Fe (ppm)	551	158 – 1270	889	197 – 2330	2380	742 – 4630
Mn (ppm)	702	328 – 1500	644	212 – 2160	2130	1420 – 2540
Zn (ppm)	218	23 – 403	131	51 – 281	452	117 – 1320
$\delta^{13}C‰_{PDB}$	+0.54	−1.59 – +3.35	−1.58	+0.06 – −3.73	−2.90	−1.27 – −4.07
$\delta^{18}O‰_{PDB}$	−26.91	−20.74 – −28.67	−28.55	−26.59 – −29.84	−20.85	−17.63 – −29.56
calcite (wt%)	64	6 – 96	4	7 – 8	5	4 – 7
aragonite (wt%)	10	0 – 19	67	25 – 100	13	0 – 26

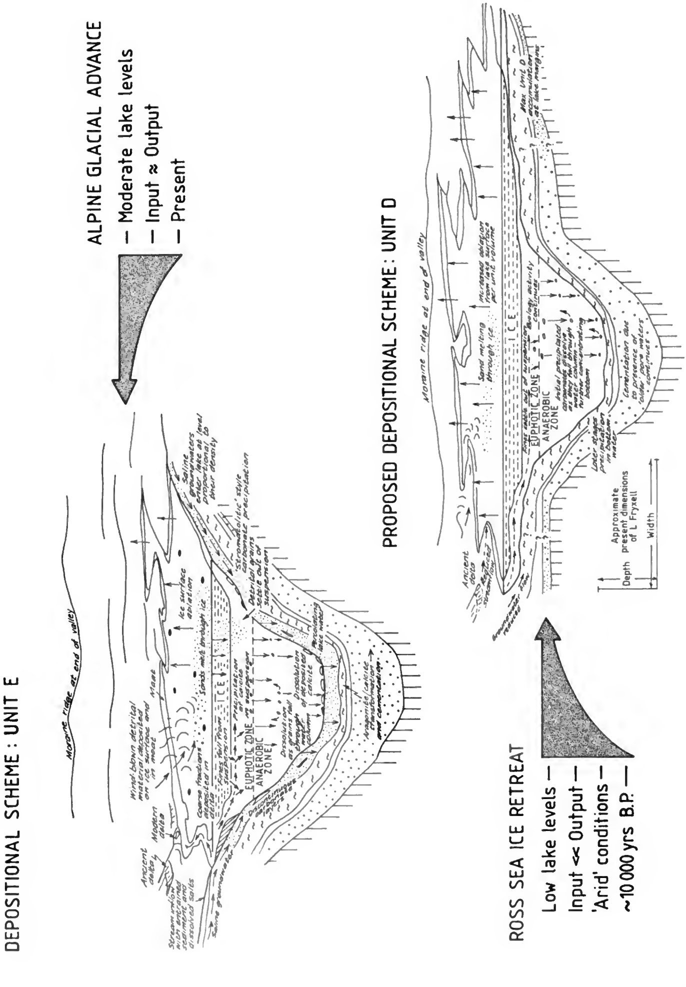
DEPOSITIONAL SCHEME : UNIT E
ALPINE GLACIAL ADVANCE
– Moderate lake levels
– Input ≈ Output
– Present
Moraine ridge at end of valley
Ancient delta
Modern delta
Stream inflow with entrained sediment and dissolved salts
Saline groundwater
Wind-blown detrital material deposited on ice surface and in moat
Moat
Ice surface ablation
Sands melt through ice
Coarse fractions deposited in delta
Fines fall from suspension
ICE
EUPHOTIC ZONE
ANAEROBIC ZONE
Precipitation of calcite
Dissolution as grains fall through water column
Dissolution of deposited calcite
Aragonite/calcite transformation and cementation
Saline groundwaters enter lake at level proportional to their density
Stromatolitic style carbonate precipitation
Detrital grains settle out of suspension
PROPOSED DEPOSITIONAL SCHEME : UNIT D
Moraine ridge at end of valley
Ancient delta
Reduced stream flow
Sand melting through ice
Increased ablation from lake surface per unit volume
Biology activity continues
EUPHOTIC ZONE
ANAEROBIC ZONE
Later stages precipitation in bottom water
Cementation due to presence of 'older' pore waters continues
Max Unit D accumulation at lake margins
Approximate present dimensions of L Fryxell
Depth
Width
ROSS SEA ICE RETREAT
Low lake levels –
Input << Output –
'Arid' conditions –
~10 000 yrs B.P. –

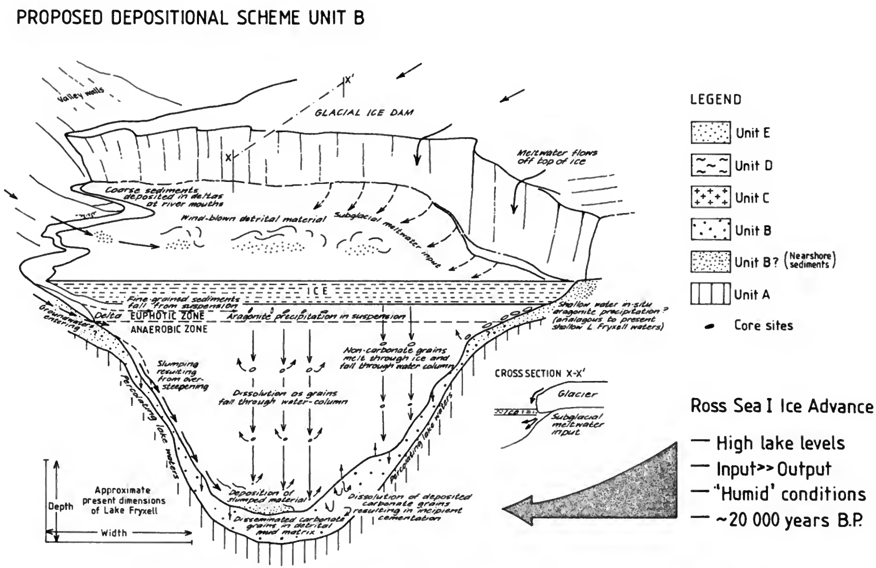

Fig. 7 (*above and facing page*) Conceptual models of glacial advance and carbonate deposition in the Lake Fryxell basin.

out evaporative concentration and also appears to mask the effect of biological activity.

Unit D samples become isotopically heavier up the column. Evaporation of an open body of water leads to $\delta^{18}O$ enrichment (Sofer & Gat 1974; Gat 1981) which continues until a steady state is attained. An ice-covered lake, however, would not show significant enrichment in ^{18}O with evaporative concentration. At c. 10 000 years ago (Fig. 2) there was a marked reduction in lake level, possibly as a result of the ice leaving the valley altogether. As the lake was no longer dammed at one end, it spread out, thus having a larger ablation surface area (Stuvier et al. 1981) resulting in evaporative concentration of lake waters, and producing a carbonate precipitate. Thickening of this deposit towards the present lake margin may reflect undersaturated deep waters. In the initial stages of evaporation, precipitated carbonate rain was dissolved as it fell through deep waters, as suggested for the present lake. $\delta^{13}C$ values indicate continued biological activity which enhanced the evaporative mechanism particularly in shallow waters. Here more efficient nutrient cycling would have been possible.

This increase in salinity can be inferred from Ca and Mg data. Calcite flakes in unit E are low–medium Mg-calcite whereas $CaCO_3$ in unit B lies in the high Mg-calcite field. Mg in the precipitating solution governs the carbonate polymorph (Müller et al. 1972; Folk 1974; Bathurst 1975). Bischoff & Fyfe (1968) and Folk (1974) demonstrated the inhibitory effect of Mg^{2+} in solution on the growth of calcite. Müller et al. (1972) have quantitatively estimated this effect on the carbonate mineralogy in terms of Mg/Ca ratio (Table 3).

Examination of the concentration gradients in Lake Fryxell (Table 1) shows that Ca and Mg have undergone different behaviour so that the Mg/Ca ratios rise from 0.3 below the ice cover, through 1.2 in the euphotic zone, to values of > 6 in the bottom waters. These differences are a consequence of the history of the lake and the process occurring within it.

Lake Fryxell is fed by at least eight meltwater streams. Their flow rates and compositions show considerable temporal variation in response to changes in the weather and solar insolation. To our knowledge, only one of these streams (flowing from the eastern side of the Canada Glacier, Fig. 1), has been monitored. The flow weighted mean for the 1981/82 season (K Thompson pers. comm.) shows the major cations in the following concentrations: Na 2.9 mg/l, K 0.8 mg/l, Ca 6.1 mg/l, and Mg 0.9 mg/l.

From the concentrations listed in Table 1 and the bathymetry of Lake Fryxell determined by Hendy (pers. comm. 1978) it can be shown that Lake Fryxell contains: Na 32 $\times 10^3$ t, K 2.9 $\times 10^3$ t, Ca 1.3 $\times 10^3$ t, and Mg 3.4 $\times 10^3$ t in solution. With a total surface area of 6.75 km^2, and an ablation rate of c. 30 cm/year, the concentrations observed in the Canada Glacier stream, if representative of all of the inflows into Lake Fryxell, would be sufficient to supply all of the sodium in 6800 years, all of the potassium in 2200 years, all of the magnesium in 2300 years, and all of the calcium in 136 years.

These calculations are consistent with the model for the evolution of Lake Fryxell presented above whereby the lake was evaporated to a low-volume sodium chloride brine during the Holocene and reflooded with glacial meltwaters initiating a diffusion cell c. 1000 years ago. The present inventory of magnesium and potassium would be accumulated in this time. If this model is correct, the calcium in solution accounts for only 6% of the calcium influx. We believe that the remaining calcium has been precipitated as calcite, frequently, if not continuously, during the refilling of the lake, thus accounting for the low and irregular calcium concentrations in the water column, and the 10–20 $\times 10^3$ t of calcium in the upper 10 cm of unit E. The low Mg/Ca ratio of the calcites found in unit E is also consistent with their origin being in the euphotic zone.

The aragonite and higher Mg/Ca ratios found in the carbonates in units B and D suggest much higher Mg/Ca ratios in the earlier phases. The dual carbonate mineralogy in unit D and in particular unit B poses a problem. Lake Fryxell carbonates are nonskeletal in origin, so biological differentation on such grounds is not possible. A possibility for unit B is imported carbonate. An alternative possibility is diagenetic change; this was noted in unit E calcites. Aragonite is the primary mineral in unit D and possibly also in unit B. For the aragonite/calcite transformation there is a Sr depletion, Zn remains constant, and Mn and Mg increase (Pingitore 1978). Plots of Mn versus wt% aragonite for units D and B show a crude inverse relationship, suggesting aragonite dissolution and calcite reprecipitation. From this, we suggest that reprecipitation of calcite may be occurring in Lake Fryxell sediments. Imported carbonate cannot be ruled out for unit B but is less likely in unit D as the meltwater supply had been drastically reduced.

Table 3 Relationship between Mg/Ca ratio and carbonate polymorph (after Müller et al. 1972).

Mg/Ca ratio in precipitating solution	Mineralogy
<2	low Mg-calcite
2–12	high Mg-calcite
>12	aragonite
very high values	hydrous Mg-carbonates

CONCLUSIONS

The conclusions are summarised in the conceptual model in Fig. 7. As the Ross Sea ice advanced, it dammed the lower end of the Taylor Valley. This enabled the buildup of a large lake, proglacial Lake Washburn, in the Fryxell basin. Meltwater was supplied by the greatly expanded ice volume. Unit B sediments were thus deposited on the outwash sands and gravels (unit A) laid down during early stages of the ice advance. Within the lake water column a carbonate system analogous to the present Lake Fryxell system operated. The influx of waters and detrital material, combined with possible dissolution effects in the lower water column, led to the low total weight percent of carbonate in the sediment. As the ice retreated beyond the basin margins, the lake waters spread over areas once covered by ice. The resultant increased ablation surface area caused evaporative concentration of lake waters. Aragonite precipitation was thus initiated and is probably responsible for the Ca depletion of the water column. This primarily inorganic mechanism was enhanced by continued biological CO_2 fixation. The lake was evaporated to a neglible depth. As alpine glaciers readvanced, the lake basin was refilled with glacial meltwaters. The concentrated brine rediffused back up the water column to create the observed chemical stratification in Lake Fryxell. Biological

influences now predominate with carbonate deposition being restricted to an algae-dominated euphotic zone. The carbonate is either precipitated from the water column and settles as a pelagic rain, or in shallow waters a benthic stromatolite-style deposition occurs and has resulted in most of the inflowing calcium being removed. Throughout these systems, carbonate dissolution and/or reprecipitation may play important roles in the sedimentary record.

Therefore, biogenic processes predominated in the deposition of unit E calcite and unit B mud, whereas unit D may have resulted from evaporative concentration. The changes in these depositional regimes are the result of evironmental changes caused by ice advances and/or retreats.

ACKNOWLEDGMENTS

We appreciate the logistic support of Antarctic Division, DSIR, the United States Navy, and the assistance in the field of W. Vincent (Ecology Division, DSIR), C. G. Harfoot, T. G. A. Green, C. Rickard, N. Rogers (University of Waikato), and D. Rees (Antarctic Division, DSIR). We thank the anonymous reviewers for their critical appraisal of this manuscript.

REFERENCES

American Public Health Association 1975: Standard methods for the examination of water and wastewater. 14th ed. New York.

Bathurst, R. G. C. 1975: Carbonate sediments and their diagenesis. 2nd ed. Developments in sedimentology 12. Amsterdam, Oxford, New York, Elsevier. 658 p.

Berner, R. A. 1980: Early diagenesis. A theoretical approach. Princeton, N. J., Princeton University Press. 241 p.

Bischoff, J. L.; Fyfe, W. S. 1968: Catalysis, inhibition, and the calcite-aragonite problem: I. The aragonite-calcite transformation. *American journal of science 266 (2)*: 65–79.

Denton, G. H.; Armstrong, R. L.; Stuiver, M. 1971: The late Cenozoic glacial history of Antarctica. Pp. 268–306 *in*: Turekian, K. K. *ed.* The late Cenzoic glacial ages. New Haven, Connecticut, Yale University Press.

Eugster, H. P.; Hardie, L. A. 1978: Saline lakes. Pp. 237–293 *in*: Lerman, A. *ed.* Lakes: chemistry, geology, physics. New York, Springer-Verlag.

Field, A. B. 1975: The geochemistry of soluble salts in the Wright and Taylor Valleys, South Victoria Land, Antarctica. Unpublished M.Sc. thesis, lodged in the Library, University of Waikato. 71 p.

Folk, R. L. 1974: The natural history of crystalline calcium carbonate: effect of magnesium content and salinity. *Journal of sedimentary petrology 44 (1)*: 40–53.

Friedman, I.; O'Neil, J. R. 1977: Compilation of stable isotope fractionation factors of geochemical interest. Data of geochemistry. 6th ed. *United States Geological Survey professional paper 440KK.*

Gat, J. R. 1981: Isotope hydrology of very saline lakes. Pp. 1–7 *in*: Nissenbaum, A. *ed.* Hypersaline brines and evaporitic environments. *Developments in sedimentology 28.* Amsterdam, Elsevier.

Hardie, L. A.; Eugster, H. P. 1970: The evolution of closed basin brines. *Mineralogical Society of America special paper 3*: 273–290.

Hendy, C. H.; Healy, T. R.; Rayner, E. M.; Shaw, J.; Wilson, A. T. 1979: Late Pleistocene glacial chronology of the Taylor Valley, Antarctica, and the global climate. *Quaternary research 11*: 172–184.

Hoare, R. A.; Popplewell, K. B.; House, D. A.; Henderson, R. A.; Prebble, W. M.; Wilson, A. T. 1965: Solar heating of Lake Fryxell, a permanently ice covered Antarctic lake. *Journal of geophysical research 70 (6)*: 1555–1558.

House, D. A.; Hoare, R. A.; Popplewell, K. B.; Henderson, R. A.; Prebble, W. M.; Wilson, A. T. 1966: Chemistry in the Antarctic. *Journal of chemical education 43 (9)*: 502–505.

Jones, L. M.; Faure, G. 1978: A study of strontium isotopes in lakes and surficial deposits of the ice-free valleys, Southern Victoria Land, Antarctica. *Chemical geology 22*: 107–120.

Keys, J. R.; Williams, K. 1981: Origin of crystalline, cold desert salts in the McMurdo region, Antarctica. *Geochimica et cosmochimica acta 45*: 2299–2309.

Krauskopf, K. B. 1979: Introduction to geochemistry. 2nd ed. New York, McCraw-Hill. 617 p.

Larsen, T. E.; Buswell, A. M. 1942: Calcium carbonate saturation index and alkalinity interpretations. *Journal of the American Water Works Association 34*: 1667–1684.

Lawrence, M. J. F. 1982: Origin and occurrence of Antarctic lacustrine carbonates, with special reference to Lake Fryxell, Taylor Valley. Unpublished M. Sc. thesis, lodged in the Library, University of Waikato.

Lawrence, M. J. F.; Hendy, C. H. 1985: Water column and sediment characteristics of Lake Fryxell, Taylor Valley, Antarctica. *New Zealand journal of geology and geophysics 28 (3)*: 543–552.

Li, Y-H.; Takahashi, T.; Broecker, W. S. 1969: Degree of saturation of $CaCO_3$ in the oceans. *Journal of geophysical research 74 (23)*: 5507–5525.

Mc Crea, J. M. 1950: On the isotopic chemistry of carbonates and a palaeotemperature scale. *Journal of chemical physics 18 (6)*: 849–857.

Müller, G.; Irion, G.; Förstner, U. 1972: Formation and diagenesis of inorganic Ca-Mg carbonates in the lacustrine environment. *Naturwissenschaften 59*: 158–164.

Parker, B. C.; Simmons, G. M. 1981: Blue-green algal mat—living stromatolites—from frigid light-limited Antarctic lakes. *Trends in biochemical sciences 6*: iii–iv.

Parker, B. C.; Simmons, G. M.; Love, F. G.; Wharton, R. A.; Seabury, K. G. 1981: Modern stromatolites in Antarctic Dry Valley lakes. *BioScience 31 (9)*: 656–661.

Péwé, T. L. 1960: Multiple glaciation in the McMurdo Sound region, Antarctica—a progress report. *Journal of geology 68 (5)*: 498–515.

Pingitore, N. E. 1978: The behaviour of Zn and Mn during carbonate diagenesis: theory and applications. *Journal of sedimentary petrology 48 (3)*: 799–814.

Sofer, Z.; Gat, J. R. 1975: The isotopic composition of evaporating brines: effect of the isotopic activity ratio in saline solutions. *Earth and planetry science letters 26 (2)*: 179–196.

Stuiver, M.; Denton, G. H.; Hughes, T. J.; Fastook, J. L. 1981: History of the marine ice sheet in West Antarctica during the last glaciation: A working hypothesis. Pp. 319–436 *in*: Denton, G. H.; Hughes, T. J. *ed.* The last great ice sheets. New York, Wiley and Sons.

Stumm, W.; Morgan, J. J. 1981: Aquatic chemistry. An introduction emphasising chemical equilibria in natural waters. 2nd ed. New York, Chichester, Brisbane, Toronto, Wiley-Interscience. 780 p.

Torii, T.; Yamagata, N. 1981: Limnological studies of saline lakes in the Dry Valley. *In*: McGinnis, L. D. *ed. Dry Valley Drilling Project Antarctic research series 33*: 141–159.

Torii, T.; Yamagata, N.; Nakaya, S.; Murata, S.; Hashomoto, T.; Matsubaya, O;.; Sakai, H. 1975: Geochemical aspects of the McMurdo saline lakes with special emphasis on the distribution of nutrient matyters. *In*: Torii, T. *ed. Memoirs of the National Instiurte of Polar Research special issue 4*: 5–29.

Vincent, W. F. 1981: Production strategies in Antarctic inland waters: phytoplankton eco-physiology in a permanently ice-covered lake. *Ecology 1 (5)*: 1215–1224.

Wharton, R. A.; Parker, B. C.; Simmons, G. M.; Seaburg, K. G.; Love, F. G. 1982: Biogenic calcite structures forming in Lake Fryxell Antarctica. *Nature 295 (5548)*: 403–405.

Whitfield, M. 1975: The extension of chemical models for seawater to include trace components at 25°C and 1 atm pressure. *Geochimica et cosmochimica acta 39 (11)*: 1545–1557.

Wilson, A. T. 1981: A review of the geochemistry and lake physics of the Antarctic dry area. *In*: McGinnis, L. D. *ed. Dry Valley Drilling Project Antarctic research series 33*: 185–192.

New Zealand Journal of Geology and Geophysics, 1989, Vol. 32: 279–291
0028–8306/89/3202–0279 $2.50/0

New Zealand hailstorms

J. T. STEINER
New Zealand Meteorological Service
P.O. Box 722
Wellington, New Zealand

Abstract From an analysis of reports of hail at climatological stations, return periods of various hail frequencies are derived. From this data set it is shown that in most parts of New Zealand there is a winter or spring maximum in the frequency of hail occurrences, and that there are generally more occurrences in the west than the east and in the south than in the north. An analysis of the occurrence of hail in hourly weather reports reveals little diurnal variability. There is a likelihood that these data sets include, at least at some sites, reports of ice particles that are strictly too small to be classified as hail.

A previous climatology based on reports of hail in the press is extended and reanalysed in terms of diurnal and seasonal frequencies in 11 regions. The eastern coastal regions have more than 60% of reported hail in spring and summer afternoons; regions exposed to the north have more than 50% of their hail events at these times.

An examination is made of the characteristics of 14 severe hailstorms identified from crop insurance claims. They occur in a variety of weather situations but have some common features. All occurred in the rear of the leading cold front of a cyclone system and in all cases there were indications of upward motion on a scale larger than that of an individual hailstorm. Most occurred with tropospheric temperatures below the seasonal average.

Keywords hail; hailstorms; climatology; New Zealand

INTRODUCTION

Horticulture is expanding rapidly in New Zealand; there was a 55% increase in the area used for fruit growing between 1981 and 1986. Consequently the economic effect of hail falls is becoming more significant. Some recent hail events have caused losses of over NZ$4 000 000 each. A knowledge of hail climatology is therefore needed. Climatology can be used in the planning of horticultural ventures, for establishment of insurance schemes, and in assessing the need for methods of hail damage abatement or hail suppression (Steiner 1988). In this paper a hail climatology is developed using a variety of data sources.

Kidson (1932) analysed climatological reports of hail in New Zealand. He noted that the frequency of hail was greatest in the west and south. In the North Island he found a maximum of hail in winter which he attributed to a temperature factor. In the South Island there was a minimum in February and a maximum in the spring which he related to the annual variability of the strength of the westerlies. Kidson noted that some east coast areas appeared to be especially liable to exceptionally severe storms with hailstones up to as much as 3 inches (76 mm) in diameter. He documented a storm at Oxford, Canterbury, when hailstones the size of tennis balls fell, some bouncing to a height of 16 feet (4.9 m). Neale (1977) produced a climatology of severe hailstorms in New Zealand based mainly on newspaper articles. Hailstorms were included if they were reported as having hailstones with long-axis diameters of at least 5 mm, or the storms caused property or crop damage. Neale partitioned his 444 hail events into regions west and east of the main axial ranges. In the east he found that severe hail events occurred mainly in the summer half-year and with a pronounced afternoon maximum. In the west the occurrence rate through the year was more uniform but with a maximum in winter and spring, and the diurnal variability was less pronounced, especially in the winter half-year.

The distribution of hail in space and time and the characteristics of hailstorms and of hailstones have been intensively studied in France and neighbouring countries and in parts of the North American plains. The motivation for such studies has been either to develop risk factors for hail insurance or to obtain background data for attempts at hail suppression.

In some areas, hail reports from observers are supplemented by data from hail pads and weather radar. Hail pads are indented by falling hail: the number and size of indentations in the pad indicate the hail kinetic energy. From weather radar, relationships between reflectivity and hail parameters can be established. For example, in Switzerland, Federer et al. (1978) found an empirical relationship between radar reflectivity and hail kinetic energy as measured by a hail-pad network.

In New Zealand, the sources of information on hail are limited. There is no weather radar in continuous operation and there are no hail pads. No central agency routinely collects all hail damage data from insurance claims or from any other sources. Data are available from climatological reports, hourly weather reports at a few locations, and the press. A set of insurance data was made available for this study and reference was made to descriptive comments by rainfall observers.

HAIL REPORTS AT CLIMATOLOGICAL STATIONS

There are almost 300 places in New Zealand where data are recorded once daily for climatological purposes. Observers are asked to record the occurrence of hail and some other

Received 28 January 1988, accepted 27 July 1988

weather phenomena in the course of the previous 24 hours. However not all stations record hail events and some have been recording for only a limited time. Data were analysed for all New Zealand sites, including those in outlying islands, that reported the incidence of hail during the 20 years 1966–85. The daily records were not examined directly: the study is based on totals for each month. There were 111 sites. These included 12 North Island sites staffed by New Zealand Meteorological Service (NZMetS) personnel, 47 other North Island sites, 6 South Island sites staffed by NZMetS personnel, 43 other South Island sites, and 3 outlying islands (Campbell Island, Chatham Island, Raoul Island) where there are NZMetS staff. From these data, statistics of hail frequency were derived for each month of the year, the four seasons, and annually.

The particular statistics derived included the mean, standard deviation, percentage of the annual frequency, and the observed frequency of particular numbers of events. In order to derive the expected frequency of various numbers of hail days the data were also fitted to a modified Poisson distribution (MPD). The MPD was selected rather than a Poisson distribution as it seemed likely that there was some persistence in the occurrence of hail from day to day. The formulation of the MPD is given by Brooks & Carruthers (1953) and Tomlinson (1976). Tomlinson has applied this distribution to New Zealand thunderstorm data. The goodness of fit of the MPD was tested by the use of the Kolmogorov-Smirnov test. The null hypothesis is that the observed data are a sample from the MPD. For all stations and periods except for some seasons and the year at Campbell Island the fit was satisfactory. The MPD routine used grouped all seasonal occurrences of more than 14 hail days and all yearly occurrences of more than 29 hail days in the highest class in fitting the data. This proved unsatisfactory for Campbell Island but the revision of the procedure for a single station was not warranted.

Examination of the data revealed very marked differences between sites in the same area. For example, two sites in the Palmerston North area (the airport and the DSIR observing site) 6.5 km apart, had mean annual hail frequencies of 0.7 and 4.6, respectively. Similarly, in Southland, Invercargill Airport had an annual frequency of 31.8 hail days whereas the other

Table 1 The seasonal and annual mean numbers of hail days, probability of zero hail days, and 1 in 50 year expected maximum number of hail days for selected climatological stations, based on data for 1966–85. Summer (Sum) is December, January, February.

	Mean					Probability of zero (%)					1 in 50 year expected maximum				
	Sum	Aut	Win	Spr	Ann	Sum	Aut	Win	Spr	Ann	Sum	Aut	Win	Spr	Ann
Kaitaia	0.2	0.4	1.3	0.7	2.5	85	75	35	46	18	1	3	5	3	9
Leigh	0.1	0.0	0.4	0.6	1.2	95	100	64	62	33	1	0	2	4	4
Whenuapai	0.2	0.6	1.4	1.6	3.8	79	59	32	34	11	1	3	5	7	12
Auckland	0.2	0.3	1.6	1.4	3.5	84	78	28	32	4	2	2	6	5	8
Auckland airport	0.3	0.6	1.3	0.9	3.1	74	46	24	51	7	1	2	3	5	8
Ruakura	0.2	0.3	0.6	0.4	1.6	79	70	59	64	25	1	2	3	2	5
Te Aroha	0.2	0.2	0.7	1.0	2.0	84	85	59	57	35	2	1	4	6	10
Tauranga	0.2	0.1	0.2	0.0	0.3	92	95	89	100	74	2	1	2	0	2
Rotorua	0.1	0.2	0.4	1.4	2.0	90	85	64	24	10	1	1	2	4	5
Kaingaroa Forest	0.5	0.3	0.8	2.2	3.9	66	66	45	20	3	3	1	3	8	9
Wairakei	0.2	0.1	0.2	0.9	1.3	85	90	89	59	43	1	1	2	6	6
Waiouru	1.3	1.3	3.2	5.1	10.9	33	31	9	7	0	5	4	9	16	24
New Plymouth	0.4	0.9	3.2	2.0	6.4	69	31	7	18	1	2	2	8	6	14
Stratford	0.2	0.9	1.7	1.9	4.7	84	38	33	24	5	1	3	7	7	13
Gisborne	0.9	0.5	0.5	1.5	3.3	59	73	60	21	12	6	4	2	4	11
Napier	0.2	0.0	0.1	0.4	0.7	84	100	95	67	60	2	0	1	3	4
Dannevirke	0.2	0.6	0.7	1.4	2.8	84	63	51	44	9	2	3	3	7	8
Wanganui	0.1	0.2	1.3	1.1	2.7	90	85	32	47	14	1	1	5	5	8
Ohakea	0.7	0.9	3.0	1.8	6.4	51	37	10	19	1	3	3	9	5	14
Palmerston North	0.5	0.6	2.0	1.4	4.6	61	57	20	44	3	3	3	6	7	11
Paraparaumu	0.2	0.3	1.1	1.1	2.8	85	76	22	29	4	1	3	3	3	6
Wellington	0.3	1.5	3.3	2.5	7.6	74	31	9	17	1	1	6	9	8	19
Westport	0.2	0.8	1.8	1.2	4.1	79	47	29	37	4	1	3	7	5	10
Hokitika	1.2	1.5	4.1	4.4	11.1	29	28	4	5	0	4	5	10	13	23
Milford Sound	1.3	1.2	1.8	2.0	6.2	55	41	31	16	4	9	5	7	6	18
Nelson	0.2	0.2	0.2	0.6	1.0	79	85	89	59	47	1	1	2	3	5
Blenheim	0.4	0.1	0.2	0.4	1.1	64	95	80	62	37	2	1	1	2	4
Kaikoura	0.9	0.6	2.0	2.3	5.8	43	65	14	22	2	3	4	5	8	14
Ashburton	0.9	1.0	1.6	2.0	5.4	48	36	32	23	1	4	3	6	7	13
Christchurch	1.1	1.3	1.9	2.2	6.5	41	33	12	20	1	5	4	5	8	15
Timaru	0.8	0.6	0.6	1.8	3.7	44	50	58	23	6	3	2	3	6	10
Dunedin Airport	2.1	1.5	3.2	5.3	12.1	15	35	9	1	0	6	6	9	11	24
Queenstown	0.5	1.3	1.2	2.7	5.7	58	41	51	13	3	2	6	7	8	15
Winton	0.5	1.2	1.9	1.8	5.3	68	67	40	32	15	3	11	10	8	22
Invercargill	4.5	6.4	8.7	12.2	31.8	4	3	1	0	0	12	17	20	20	†
Raoul Island	0.0	0.0	0.7	0.1	0.9	100	100	51	90	41	0	0	3	1	4
Campbell Island	8.4	16.9	20.1	22.8	68.8	0	*	*	*	*	18	*	*	*	*
Chatham Islands	1.2	4.6	7.4	4.1	17.4	38	4	2	2	0	5	12	20	9	33

*Unable to be resolved with the particular modified Poisson distribution program used.
†Unable to be determined accurately with the modified Poisson distribution used. 1 in 10 year expected maximum is 43.

3 Southland stations (Winton, Otautau and Hokonui Forest) all had annual frequencies of < 6 hail days. It is not possible to determine which of such differences are genuinely climatic and which result from difficulties in noting all hail events at sites where weather observation is not a principal task or the site is not staffed for the full 24 hours.

Sites staffed by the NZMetS might be expected to note a higher percentage of the local hail events than other sites. They might still miss some because not all NZMetS sites are staffed continuously throughout the day and night. For the 18 NZMetS staffed sites in New Zealand, the mean annual frequency of hail is 7.2 with a standard error of 7.0, whereas for the other 90 sites the mean is 2.2 with a standard error of 2.0. Similarly the mean probability of no hail days in a year is 6.5 for the 18 NZMetS staffed sites with a standard error of 11.3 but for the other sites the corresponding statistics are 32.4 and 23.7. For both parameters the variance ratio is highly significant.

If it is assumed that the propensity to notice hail at any site is the same in all seasons, then interseasonal variability of hail can be ascertained even if the reported seasonal occurrences are less than the actual number of occurrences. Some seasonal and annual statistics are shown in Table 1. The sites shown were selected to provide a distribution of data for most parts of the country including, where possible, NZMetS staffed sites. Other sites in Table 1 are considered to record a high proportion of the hail occurrences.*

Because there may be hail occurrences that are unrecorded at some sites, and also because there are likely to be important small scale variations in hail frequency, it is not possible to draw seasonal or annual hail frequency maps for New Zealand based on these data. However there is some spatial coherence in the proportion of hail in each season (Fig. 1 and 2).

Table 1 confirms the general increase of hail from north to south and from east to west noted by Kidson (1932). Sites sheltered from both onshore southerly and westerly winds have low hail frequencies (e.g., Leigh, Tauranga, Nelson, and Blenheim). The only North Island site in Table 1 with a mean occurrence >10 days per year is Waiouru which is 823 m above sea level. Stratford Mountain House (not shown), at a height of 846 m, has an average of over 14 days of hail per year. The only high level sites in the South Island for which data are available are Craigieburn Forest (height 914 m, annual mean 1.7 events) and The Hermitage, Mt Cook (height 765 m, annual mean 2.0 events). The relatively low occurrences at these sites may be related to sheltering from hail-producing airflows.

Hail frequency is highest in either winter or spring in most parts of New Zealand (Fig. 1): spring is the most frequent hail season in eastern areas. Only three stations have summer as the main hail season. These are all sites reporting very little hail and the seasonal partitioning may be unreliable. All three are in eastern areas with some sheltering from westerlies and southerlies. In the North Island the least hail season is either summer or autumn (Fig. 2). In the South Island the pattern is complex; there is a summer minimum in the south and in some western areas.

A harmonic analysis was made of the mean monthly hail data. As a check on the reality of the derived annual cycle, the 12 monthly means for each station were reordered randomly and the first harmonic of the series recomputed (Fig. 3). In the North Island there is a well-pronounced annual cycle almost everywhere. The greatest frequency of hail days in the west is in July or August. In eastern areas the annual cycle of hail has its maximum a month or two later. In the South Island there are many stations with no pronounced annual cycle, particularly about the east coast and in inland areas. A November maximum occurs in the Nelson area. The second harmonic was significant by the re-randomisation technique, only at Timaru Airport. There, and at a few other eastern and inland South Island places, maxima of hail days occur in April–May and October–November with the second harmonic explaining more than 30% of the annual variance.

In the west of both islands the month of maximum hail frequency as determined from climatological reports, is close to the month of maximum rainfall occurrences found by Thompson (1985). In the east of the North Island the month of maximum hail occurrences is about 2 months later than the month of maximum rain occurrences. In the east of the South Island the distributions of the maxima of these two parameters are complex and not closely related.

An interpretation of the variation in the number of hail days per year in the New Zealand area is shown in Fig. 4. For each of the seven locations for which mean freezing level data are available (i.e., for various periods of between 7 and 16 years up to 1973; Tomlinson 1975) the mean number of hail occurrences per year is plotted logarithmically against the mean freezing level. A regression fitted to the data for all seven stations between mean number of hail occurrences, n, and mean freezing level, F, yields: $n = 1326\exp(-197F)$. This equation explains 94% of the variance. The largest departures from the regression line in Fig. 4 are for Waiouru and Christchurch. The positive anomaly for the high level site, Waiouru, may be explained either by enhanced convection over the land or by less opportunity for melting. The negative anomaly at Christchurch may be the result of sheltering there from some cold air flows.

An examination of the monthly mean numbers of hail days and the mean monthly freezing-level heights at these stations shows that a mean freezing-level height of about 3400 m is a threshold for hail occurrence.

HAIL REPORTS IN HOURLY OBSERVATIONS

Coded hourly weather reports are made by NZMetS staff at 17 New Zealand sites, mainly at airports. The reports include a coding of the "present weather" which is defined as the weather over the 10 min interval ending on the hour (World Meteorological Organization 1984, code table 4677). The code selected is the highest representative two-digit number. If hail occurs during the observing time, then one of six codes (89, 90, 93, 94, 96, 99) is applicable. Weather other than hail could be included among occurrences of some of these code figures. This arises because the same codes relate to thunderstorms with snow as with hail and because in some circumstances ice pellets (crushable small hail), snow pellets, and hail are coded identically. The same period was used as for the climatological data analysis.

The number of reports of hail in hourly observations (Table 2) is small, less than one per year for some places. The spatial distribution of the reports is similar to that for hail days with generally more in the south and easily the greatest

*Tabulations for additional sites, for individual months and for additional frequencies are available from the New Zealand Meteorological Service.

Fig. 1 Season of most hail based on data from climatological stations for the years 1966–85. Shading indicates the proportion of annual hail in the season of most hail where this exceeds 40%

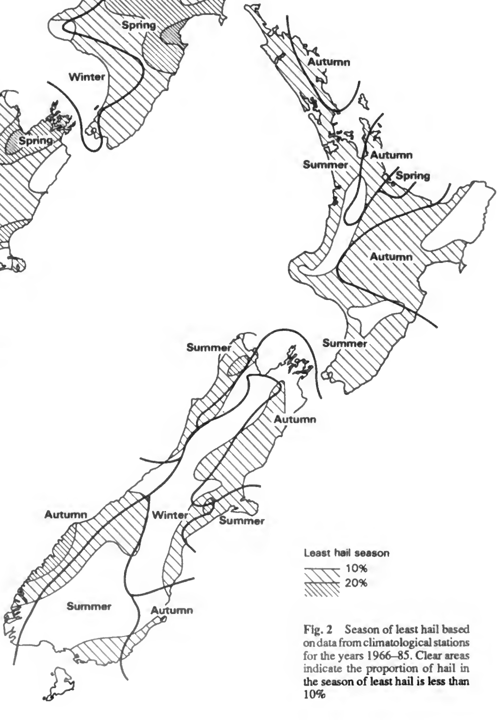

Fig. 2 Season of least hail based on data from climatological stations for the years 1966–85. Clear areas indicate the proportion of hail in the season of least hail is less than 10%

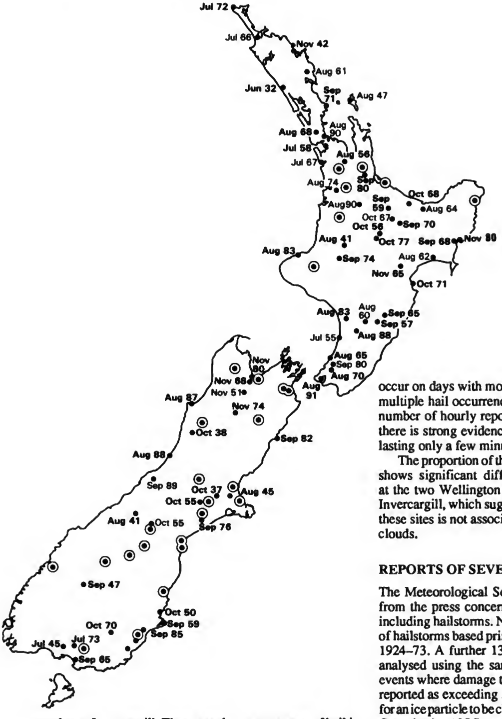

Fig. 3 Season of maximum hail based on a harmonic analysis of the mean annual hail data from climatological stations for the years 1966–85. Stations where the first harmonic explained less than 50% of the variance of the series are surrounded by open circles. At other sites the month corresponding to the maximum of the first harmonic is shown with the percentage of the annual variance explained by this harmonic. Where the cycle is significant by a re-randomisation test, the type is bolder.

number at Invercargill. There are also more reports of hail in hourly observations in the west than in the east.

An analysis of the diurnal frequency of hail in hourly reports was conducted for the 9 sites where observations are routinely made through the full 24 hours. Hail reports were partitioned into the four periods 0100–0600, 0700–1200, 1300–1800 and 1900–2400 h local time. At none of the stations was the diurnal distribution significantly different from a uniform distribution in time (using the χ^2 test).

The number of hail days, derived from the climatological data, greatly exceeds the number of occasions hail is reported as the present weather in hourly observations. This could have two causes; either hail events must be very brief or it must be rare for more than one event to occur per day. However, at some places, a large proportion of the hourly hail reports occur on days with more than one hail report per day. Since multiple hail occurrences per day must equal or exceed the number of hourly reports with hail as the present weather, there is strong evidence that hail events are brief, probably lasting only a few minutes each.

The proportion of the hail reports associated with thunder shows significant differences between sites. It is lowest at the two Wellington sites, followed by Christchurch and Invercargill, which suggests that much of the hail reported at these sites is not associated with particularly tall convective clouds.

REPORTS OF SEVERE HAILSTORMS

The Meteorological Service maintains an archive of items from the press concerning various types of weather event including hailstorms. Neale (1977) developed a climatology of hailstorms based primarily on this archive for the 50 years 1924–73. A further 13 years (1974–86) of data have been analysed using the same criteria: that is, by including all events where damage to crops occurred, the hailstones were reported as exceeding 5 mm in diameter (the minimum size for an ice particle to be classified as hail; World Meteorological Organisation 1956), or there was comment about the unusually large size of the hail. The method of entry of items into the archive has varied. During May 1976 to March 1982, fewer newspapers were searched on a regular basis. The only change to Neale's procedure has been the inclusion of some events where damage to property other than crops was reported though there was no reference to hailstone size. Data for the entire period of 63 years are treated as a single data set. Each report of hail in an area on a particular day is referred to as an event: some events may include more than one outbreak of hail.

Although the minimum size accepted for inclusion in the data set is 5 mm the vast majority of hail events reported in the press are significantly larger. Neale found that, where size information was available, 82% had sizes reported or inferred

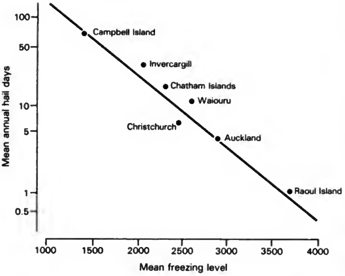

Fig. 4 The variation of mean annual number of hail days at sites which are both climatological and radiosonde sites, with the mean annual freezing level. The hail days data are for the years 1966–85. The freezing-level data (from Tomlinson 1975) is for 1966–73 for Waiouru, and 1958–73 for the other sites.

(from terms such as "walnut size", or "golf ball size") of at least 10 mm. The entire data set is therefore referred to as severe hail.

The 118 reports in the years 1974–86 were classified as to whether significant hailstone size was reported (80 events), there was damage reported to fruit crops or to orchards (40 events), there was damage to gardens or crops other than fruit (43 events), there was property damage (17 events), or injuries to animals or birds (2 events). Several events included more than one of these categories. The high incidence of events that would have been classified on the basis of reported hailstone size alone (76%), together with the reports of property damage, suggests that the seasonal variations in reports are probably real variations in severe hail occurrence and do not merely reflect a greater potential for plant damage in some seasons.

There are some additional deficiencies in the data. Neale showed that there was a tendency for large numbers of events to be reported in the more populous areas. Furthermore, hailstorms must compete with other news for space, and different editorial policies and deadlines may lead to a differing interest in reporting hail. There was sometimes a tendency for several subsequent reports of hail to follow a particularly severe event; this event had possibly made hail newsworthy. Although it has these limitations the data set provides some basis for analysing the occurrence of severe hail.

The data set was divided into 11 regional subsets. The regional codes and boundaries are shown in Fig. 5, together with the number of reports from each region. The left-side diagrams in Fig. 5 show the seasonal severe hail distribution for each region as a percentage of the annual total. The right-side diagrams show the seasonal distribution of hail at those climatological stations from which data is shown in Table 1. To produce the latter, where there was more than one climatological station available, the sum of the hail reports in each season from all stations was used.

The numbers of hail reports in proportion to the area are generally higher in the North Island regions than in the South Island though it is highest of all in the NE region. The lowest frequency per unit area is in WCSI. These distributions must partially reflect population differences and may not be reliable indicators of the regional distribution of severe hail.

The percentage of severe hail is least in 9 of the 11 regions in autumn. In the remaining two regions (CA and SD) there were no severe hail events in winter but there were also very few in autumn. The autumn percentage is everywhere only about one-half or less of what would be expected were severe hail events to be uniformly distributed throughout the year. The winter frequency is above 25% only in four regions, all adjacent to the western coast, and is low in all eastern areas. In the four South Island regions east of the ranges, more than one-half of the severe hail events occurred in summer.

A comparison of the seasonal distribution of hail in each district with a uniform seasonal distribution of the same number of total hail events was significant at the 5% level using the χ^2 test for all regions except WCSI and WMW. For NAW, CA, OT, and SD the differences were significant at the 0.1% level.

If severe hailstorms, as identified from newspaper reports at climatological stations, represented the same class of phenomena, then the seasonal distribution of the two would be similar. Figure 5 shows that, in all districts, a higher proportion of the severe hail events than of the climatological reports occurs in summer in all 11 areas. Correspondingly, in all districts except WCSI there is a smaller proportion of the hail events in winter in the severe event data. Except in 4 districts, BPT, TT, NE, and WCSI, the differences between the pairs of depicted seasonal distributions are significant at the 0.1% level.

A classification was also made for each region of the distribution of hail events by time of day. The events were partitioned into 4 periods, 0000–0600, 0600–1200, 1200–1800 and 1800–2400 h. In some newspaper reports the time was not given explicitly but could be inferred from more general

Table 2 Hourly reports on hail for New Zealand locations for the 20 years 1966–85. Column D is based on the climatological reports from the same sites. Asterisks indicate places where reports were not made regularly at some night hours. D/H is not calculated for these sites.

	No. of reports of hail in 20 years H	% of these reports with current or recent thunder	No. of reported hail days in 20 years D	D/H
Kaitaia*	16	75	48	
Whenuapai*	11	27	77	
Auckland	14	36	74	5.3
Auckland airport	15	47	62	4.1
Rotorua*	10	30	41	
Gisborne*	8	62	67	
New Plymouth*	25	64	139	
Ohakea	42	48	129	3.1
Paraparaumu*	14	57	56	
Wellington	27	4	144	5.3
Wellington airport	14	7	159	11.3
Nelson	9	56	27	3.0
Hokitika	54	53	223	4.1
Kaikoura*	24	38	115	
Christchurch	39	12	130	3.3
Dunedin	47	27	241	5.1
Invercargill	244	18	636	2.6

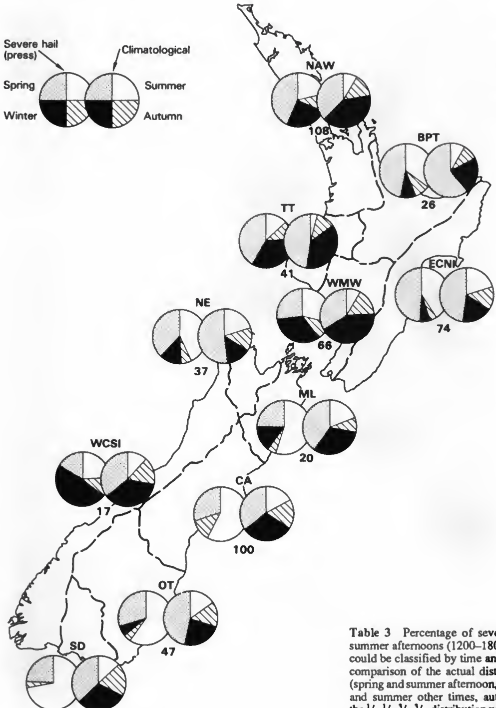

Fig. 5 The percentage of the number of severe hail reports in the press (left) and of the number of reports at selected climatological stations (right) in each season for various New Zealand districts. The symbols used in the text to denote the districts are above each pair of circles, and the actual number of hail reports in the press for the years 1924–86 is shown below.

Table 3 Percentage of severe hail occurrences on spring and summer afternoons (1200–1800 h), the total number of events that could be classified by time and season, and the value of χ^2 from a comparison of the actual distribution of events into four classes (spring and summer afternoon, autumn and winter afternoon, spring and summer other times, autumn and winter other times) with the $^1/_8$, $^1/_8$, $^3/_8$, $^3/_8$ distribution which approximates what would occur with a random distribution. The significance of the χ^2 value is in the right-hand column.

Region	Spring/summer afternoon (%)	Total	χ^2	Significance level (%)
ECNI	0.74	70	>200	0.1
OT	0.73	40	>100	0.1
SD	0.73	22	67	0.1
CA	0.63	87	>200	0.1
ML	0.56	18	26	0.1
NE	0.50	24	17	0.1
BPT	0.50	18	23	0.1
NAW	0.37	82	82	0.1
TT	0.32	34	11	2
WMW	0.31	45	17	1
WCSI	0.08	12	0	NOSIG

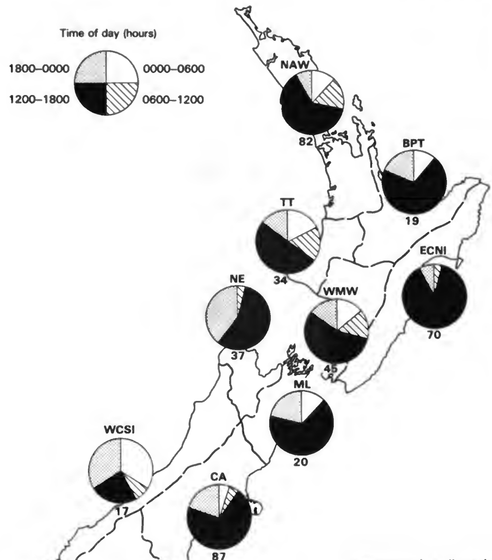
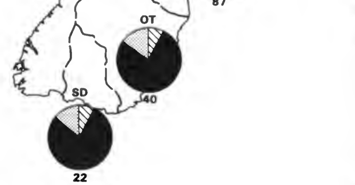

Fig. 6 The percentage of the number of severe hail reports in the press in the 4 quarters of the day for various New Zealand districts. Data are from the years 1925–86. The number of reports for which time data were available is shown beneath the circles.

statements (e.g., "morning" was taken to imply 0600–1200, "early hours of this morning", 0000–0600). There was no usable time information in some reports. The diurnal results (Fig. 6) reveal a maximum occurrence in the afternoon, including one-half or more of all events, that is found in all regions except WCSI. The patterns in Fig. 6 are mostly very significantly different from a uniform distribution. Using the χ^2 test, the difference is not significant for WCSI while for TT it is significant only at the 5% level. Elsewhere there is significance at the 1% level. The diurnal distribution is in marked contrast to that obtained from hourly weather reports.

The seasonal and diurnal patterns for severe hail in most regions, as revealed by Fig. 5 and 6, suggest a further classification. For each region the frequency of severe hail is partitioned into 4 time-season divisions: spring and summer afternoons (September–February, 1200–1800); autumn and winter afternoons; spring and summer, all other times (1800–0000–1200); autumn and winter, all other times.

If the events occurred uniformly both seasonally and diurnally, the percentage of events occurring on spring and summer afternoons would be approximately $^1/_8$th of the total. The actual percentages are in most cases far higher (Table 3). Only in WCSI is the partitioning into the four categories above not significantly different from the $^1/_8$th, $^1/_8$th, $^3/_8$th and $^3/_8$th distribution that would be approximated if events occurred uniformly in time and season.

The partitioning into time and season separates the regions into four groups. Four regions east of the main ranges, ECNI, CA, OT and SD, all have more than 60% of severe hail events in spring or summer afternoons. Three regions (BPT, NE, and ML) have between 50 and 60% of events at these times. In the remaining North Island regions (NAW, TT, WMW) 30–40% of events occur in spring and summer afternoons. Only in WCSI is the spring–summer afternoon percentage small.

The above results demonstrate that the spatial, seasonal, and diurnal distribution of the severe hail events reported in the press is different from the distributions derived from hail-day data at climatological stations or from hourly weather reports.

SOME DAMAGING HAIL EVENTS

Information on the number of hail claims in the period 1981–85 made to the insurers of wheat and of apples and pears is used to identify a sample of the most damaging hail events. Those selected are the 14 occasions in this period when at least 10 claims were received in a single area. Four of the events relate mainly to wheat crops and 10 to apples and pears. The wheat damage events all occurred in Canterbury. The apple and pear events occurred in Hawkes Bay (4), Nelson (3), Auckland (2), and Otago (1).

For each event an examination was made of the surface and upper level synoptic weather maps of the NZMetS, of satellite imagery, and of atmospheric sounding data from the radiosonde stations at Auckland, Christchurch, and Invercargill. Thickness, vorticity, vertical motion, and shear fields were calculated from the archived analyses using a technique developed by Sinclair (pers. comm.). Two of the events were the subject of earlier studies which were consulted —McGill (1987) on the 4 November 1984 west Auckland storm and I. M. Miller (unpubl. report) on the 19th January 1983 Canterbury storm.

There were some limitations in the data. Archived analyses were not available for the 1981 Canterbury event. In most cases, orbiting satellite imagery was available only for the early morning and evening. The geostationary satellite imagery is usually received at 3-hourly intervals but there were often gaps in the archive.

A summary of the characteristics of each event is contained in Table 4. Reference will be made to particular columns in the table.

Comments by rainfall and climatological observers were used to determine the time of occurrence of the events. The number of insurance claims and the number of hail reports by rainfall or climatological observers (column 1) are only moderately well correlated (correlation coefficient 0.49). Thus the dense observing network is unable to record all major storms. All but two of the storms were accompanied by reports of some manifestation of thunderstorms (column 2) in the affected area.

The synoptic pattern on the sea-level analysis (column 3) reveals that all of the thunderstorms occurred behind the main cold front of a trough system, the front having passed anything from a few hours to several days earlier. In general, the hail events occurred close to the low centre or in flows between south and west. The Auckland event of 4 November 1984 was exceptional—although the leading cold front had passed, the flow remained northerly.

In 10 events there was evidence of a mesoscale* feature related to the terrain associated with the hail event. In three events this was a "hanging back" trough. This feature, commonly identified on New Zealand weather maps, was discussed by Revell (1972). It is a boundary oriented from southwest to northeast between surface winds from a westerly quarter and from the easterly quarter imbedded within a generally southerly flow. Four of the events, all in eastern areas, were associated with a thermal trough. These features occur on warm afternoons as a result of intense solar heating of the surface and the transfer of heat to the lower atmosphere.

Satellite imagery indicated that for seven events there were prominent convective cloud masses over the sea which were advected to the area where hail fell without major changes in cloud organisation. In five events, including all but one of the Canterbury and Otago events, there was no evidence of such advection; the convective cloud cluster formed over the land though there was sometimes evidence of some convective activity over the sea. In two events there were insufficient satellite data to determine the source of the convection.

Columns 7–12 contain information of atmospheric stability, winds, and large scale dynamics. In assessing these the main object has been to select measures of the parameters for which some climatology is available so that the extent to which the hail events are associated with extreme values of any atmospheric condition can be assessed.

The only index of stability for which a climatology could readily be obtained was the Thickness Difference Index (TDI) defined by Hanssen (1965) as:

$$\mathrm{TDI} = (h_{700}-h_{1000})-(h_{500}-h_{700})$$

where h is the height of the subscripted pressure surface in units of hectopascals. Although TDI does not involve any consideration of humidity, it has been found useful in predicting thunderstorms in New Zealand (Steiner 1967). Column 7 shows the highest of the 50, 75, 90, and 97.5 seasonal percentiles of the TDI exceeded at a proximate radiosonde station (Auckland, Christchurch, or Invercargill). For the Hawke's Bay, Nelson, and Otago regions, which are located between radiosonde stations, the neighbouring station yielding the higher percentile was used. Whereas in all cases the TDI exceeds the 75 percentile there are only two events when the TDI exceeds the 97.5 percentile. TDI values are in column 8 and the TDI climatology is in Table 5.

The 300 hPa wind direction was in all events in the sector northwest to south (column 9). This is not surprising because the vast majority of winds at the 300 hPa level over New Zealand are within this sector. The range of upper winds associated with hail is rotated to be more equatorwards in New Zealand compared with that found in France by Molenat (1975).

The vertical shear of the wind in the middle troposphere, 500 hPa, exceeds 15 knots/100 hPa (approx. 0.005/s) in 6 events (column 10) but was < 5 knots/100 hPa in one event. It was not possible to construct accurate wind hodographs near the hailstorms. However the range of values of wind shear suggests that different storm cellular structures, each associated with a different vertical wind profile, may give rise to hailstorms in New Zealand.

*The term mesoscale relates to weather systems smaller than the major anticyclones and depressions. Mesoscale features have lengths between 100 and 1000 km.

Table 4 Data on hail events with at least 10 claims for damage to wheat, apples and pears in the four growing seasons 1981/82 to 1984/85.

Area	Date	Time (local)	Claims	1	2	3	4	5	6	7	8
AUCKLAND Kumeu Huapai Riverhead	30/11/82	Uncertain	23	0	N	Southerly flow	Y	Weak hanging back trough	Y	>90 AK	347
AUCKLAND Kumeu Huapai	4/11/84	0200–0300	17	1	Y	Post-frontal northerly flow	N	–	Y	>75 AK	339
HAWKE'S BAY Hastings Havelock North	7/1/82	1700–1800	61	2	Y	Low east of New Zealand	Y	Onset of southerly	Y	>75 CH/AK	339
HAWKE'S BAY Hastings	14/1/84	Uncertain	25	0	Y	South-westerly flow	Y	Thermal trough	?	>75 AK	330
HAWKE'S BAY Hastings	13/3/84	Uncertain	17	0	N	Complex	N	–	Y	>90	330
HAWKE'S BAY Hastings Pakowhai	22/10/84	1300	40	27	Y	South-westerly flow	N	–	Y	>97.5 CH	360
NELSON Mainly Upper Moutere and Hope	23/3/82	1700–2230	35	5	Y	Low east of South Island	Y	Hanging back trough	N	>75 AK	345
NELSON Mainly Upper Moutere, Motueka	29/11/82	1530–1730	44	5	Y	Southerly flow	Y	Hanging back trough	Y	>75 CH	345
NELSON Richmond Brightwater Upper Moutere	16/11/84	1645–1715	37	2	Y	Low moving east over South Island	N	–	?	>90 CH	330
CANTERBURY Rakaia Ashburton Geraldine	3/12/81	Afternoon	21	3	Y	South-westerly flow	Y	Thermal trough	N	>75 CH	338
CANTERBURY Mainly Christchurch Leeston	19/1/83	2030	65	11	Y	South-westerly flow	Y	Convergence line	N	>97.5 CH	392
CANTERBURY Ashburton to Amberley	13/1/84	1730–1800	67	15	Y	SSW flow	Y	Onset of southerly	N	>75 CH	354
CANTERBURY Darfield Rakaia Christchurch Ashburton	8/12/84	Afternoon	42	2	N	Col. Lows to NW and SE	Y	Thermal trough	Y	>75 CH	359
OTAGO Millers Flat Cromwell	20/1/84	1400	12	1	Y	Westerly flow	Y	Thermal trough	N	>75 NV	345

The information contained in the numbered columns is as follows:
1. Number of hail reports at climatological or rainfall stations in the area.
2. Association with thunderstorms, Y(es) or N(o)?
3. Synoptic situation.
4. Evidence for mesoscale features due to terrain or differential surface heating, Y(es) or N(o)?
5. Nature of mesoscale feature identified in 4.
6. Evidence for advection of convective cloud from sea to hail area, Y(es) or N(o)?
7. The Thickness Difference Index (TDI) percentile at a proximate radiosonde station (identified below—AK, Auckland; CH, Christchurch; NV, Invercargill).
8. The TDI over the hail area (from radio-sounding from Auckland and Christchurch for Auckland and Canterbury storms, from analyses for others) in gpm.

Hail damage can occur with a wide range of values of upper level (300 hPa) relative vorticity (column 11). Large values of cyclonic (negative) vorticity would be expected to be associated with deep, cold pools.

The large scale, vertical motion field derived from the archived analyses and computed at the 700 hPa level (column 12) shows that there was upward motion exceeding 2.5 hPa per hour for 7 of the 13 events for which data are available. These seven include the four events for which there was not a mesoscale surface feature related to the hail occurrence. A tentative conclusion is that either upward motion on the large scale, or some mesoscale feature providing low-level convergence, is a prerequisite for damaging hail.

In the remaining numbered columns, thermal parameters are compared with mean monthly statistics from Tomlinson (1975). The freezing level is generally low, on average 800 m

Table 4 (*Continued*)

9	10	11	12	13	14	15	16	17	18	Comments
SW	>15	–10	N	–1200	1800	<2.5 AK	<10 AK	–		26 hail reports, other North Island areas. Hail damage, western Bay of Plenty, evening thunderstorms elsewhere in North Island.
NW	10–15	–4	Y	+200	3200	c. 50 AK	c. 50 AK	–62 AK	c. 50	7 hail reports other North Island areas.
NW	>15	–4	Y	–1000	2400	<2.5 AK	<2.5 AK	–48 AK	>90	
NW	>15	–1	Y	–1200	2200	c. 2.5 AK	<2.5 AK	–48 CH	c. 90	
NW	10–15	–8	Y	–750	2800	c. 2.5 AK	c. 10 AK	–46 AK	>97.5	
WSW	10–15	0	Y	–550	1800	<2.5 CH	<10 CH	<45 CH	>90	34 hail reports other North Island areas. Sharp temperature drop with onset of southerly. Tornado reported in press. Snow inland.
S	>15	–5	Y	–600	2700	<2.5 AK	c. 25 CH	–49 AK	>90	Additional damage through jagged hail cutting fruit.
NW	10–15	–16	N	–1100	1500	<2.5 CH	c. 10 AK/CH	–		
WNW	>15	–10	Y	–300	2300	<2.5 CH	<2.5 CH	*		*Tropopause –44 at Christchurch. Auckland sounding did not reach tropopause.
W	–	–	–	–900	2200	<25 CH	c. 10 CH	–46 CH	c. 97.5	
WNW	>15	–17	N	–950	2250	c. 2.5 CH	<2.5 CH	–45 CH	c. 97.5	Hail associated with tornado in western suburbs of Christchurch. Hail stones up to 5 cm diameter.
WNW	<5	–7	Y	–950	2250	<10 CH	c. 2.5 CH	–55 CH	c. 75	
NW	>15	–5	N	–900	2000	<10 CH	<10 CH	–51 CH	c. 90	
WNW	5–10	–7	N	–800	1950	<25 NV	<25 NV	–47 NV	>90	Distance between locations suggests separate storms responsible.

9.Wind direction at 300 hPa (degrees).
10. Vertical shear of the wind at 500 hPa (knots/100 hPa).
11. Relative vorticity at 300 hPa (10^{-5}/s).
12 Upward motion at 400 hPa exceeding 2.5 hPa/h, Y(es) or N(o)?
13. Freezing-level departure from monthly mean as estimated from statistics for proximate radiosonde stations (gpm).
14. Actual freezing level (gpm).
15. 1000–500 hPa thickness percentile (gpm) at a proximate radiosonde station (identified below).
16. 300 hPa height percentile at a proximate radiosonde station (identified below).
17. Temperature (°C) at the lowest tropopause at a proximate radiosonde station (identified below).
18. The lowest tropopause percentile at a proximate station.

below the monthly mean. The 1000–500 hPa thickness is usually below the 25 percentile value and, in 9 cases, below the 2.5 percentile value at a proximate radiosonde station. The 300 hPa height is generally low, and the temperature at the lowest troposphere, where available, is usually high.

The hailstorm of 4 November 1984 in west Auckland is the exception for all the thermal parameters. The freezing level was higher than the average for the month and the other three parameters were all near normal.

The discussion above reveals that the occurrence of damaging hail storms is not uniquely related to any readily available meteorological parameter. Even within a single district there are marked differences in atmospheric flow patterns and other characteristics on days when hail occurs.

Table 5 Values of selected percentiles of the Thickness Difference stability parameter (TDI) for Auckland, Christchurch, and Invercargill. The analysis is based on all radiosonde data for the 4 years 1981–84. (At Christchurch radiosonde data are acquired only once daily.) Values are in geopotential metres.

	Midday				Midnight			
Percentile	Summer	Autumn	Winter	Spring	Summer	Autumn	Winter	Spring
Auckland								
2.5	272	281	282	272	268	280	286	275
10.0	289	294	303	292	286	293	303	292
25.0	300	304	317	305	302	306	315	304
50.0	314	318	328	318	313	318	327	316
75.0	328	333	340	333	328	330	341	332
90.0	336	343	350	344	335	343	350	341
97.5	346	355	360	355	348	354	359	354
Christchurch								
2.5	270	262	280	268				
10.0	288	291	298	296				
25.0	307	309	312	315				
50.0	330	329	331	334				
75.0	350	346	350	350				
90.0	366	359	362	368				
97.5	384	374	374	378				
Invercargill								
2.5	260	258	287	270	258	262	282	266
10.0	272	284	301	291	276	279	296	290
25.0	290	297	310	306	292	298	311	306
50.0	311	316	324	321	314	316	324	323
75.0	334	332	339	337	333	333	340	340
90.0	350	343	349	351	346	346	351	350
97.5	360	358	358	364	358	357	360	362

All of the hailstorms occurred in the rear of the main cold front of a cyclone system. On most occasions the troposphere was cold and unstable. From the small sample studied here a mesoscale or large scale weather pattern conducive to upward motion would seem to be necessary for damaging hail.

DISCUSSION

The previous sections reveal some apparent ambiguities in our knowledge of New Zealand hail. Whereas hail as reported at climatological stations is generally most common in winter and spring, and increases in frequency from north to south and from east to west, the hail climatology derived from the press data reveals a spring and summer maximum, there are high frequencies in eastern areas, and the marked increase in southern areas is absent. Furthermore the temporal distributions derived from hourly weather reports and from the press reports are different: there is no significant diurnal trend in the hourly data but a maximum afternoon occurrence in all but two regions in the data from the press.

These differences can partly be explained if the hourly and climatological data include a large number of events that are not strictly hail as officially defined. It is likely that much of the hail reported by climatological stations is indeed really ice pellets or small hail. The distributions of hail from climatological and hourly reports can then be explained if the principal source of the smaller frozen precipitations is cold showery outbreaks with the convection not necessarily deep. A low freezing level means there is only a shallow column in which partial melting can occur.

For true hail to occur more is required than just low temperatures and some instability. In some events, particularly in eastern areas, instability may well be increased by heating over the land between the time of the atmospheric sounding and the onset of hail. Other hailstorms develop through the release of potential instability (i.e., the atmospheric profile becomes unstable through upward motion arising from mesoscale circulations or from favourable flow patterns on the synoptic scale).

These considerations suggest the following explanation of the diurnal and seasonal hail distribution shown in Table 3. Hailstorms in eastern areas are primarily associated with intense radiational heating at the surface. In westerly flows, foehn conditions may also contribute to the heating. The warm, low layer may become deep, with increased instability above it through the air moving off the mountains being warmer than the air at the same levels elsewhere. The importance of this latter phenomenon in severe storm development is pointed out by Heimann & Kurz (1985). The storms commonly form where lifting is induced by such features as the sea-breeze boundary or locally generated southerly change lines. On the West Coast (South Island) most of the severe convective storms are probably already present over the sea. They may be enhanced by coastal or mountain effects. Hence there is little diurnal or seasonal variation. In the other areas, both locally generated storms and storms advected from the sea occur with a greater preponderance of the latter in areas exposed to the westerlies. The intermediate diurnal/seasonal distribution shown in Table 3 results. For the locally generated storms thermal troughs and hanging back troughs are an additional triggering mechanism.

Hail is one manifestation of strong atmospheric convection. Analyses of other manifestations of severe convective storms in New Zealand have been undertaken by Tomlinson (1976) and Revell (1984) on thunderstorms and by Seelye (1945) and Tomlinson & Nicol (1976) on tornadoes. The frequency

of thunderstorms decreases from west to east as it does for hail reports at climatological stations, but there is not the maximum in the south in the thunderstorms data that is found for the hail reports. The seasonal distribution of thunderstorms is rather like the seasonal distribution of severe hail as determined from the press reports, with a marked preference for summer afternoon occurrences in the east, but less variability in seasonal and diurnal occurrences in the west. The tornado distribution is quite different: there is a concentration of reports in western coastal areas and in the Bay of Plenty.

The differences in the spatial and temporal variability of all hail, severe hail, thunderstorms, and tornadoes is indicative of differing additional requirements for the development of these phenomena beyond those that lead simply to the formation of convective cloud. Large cloud depth is probably a requirement for all but some of the small ice particles included in the all hail data. For severe hail, the ambient flow must be such that the updraft is long lasting, or there are a succession of updrafts, so that the incipient hailstone is maintained for sufficient time in an environment conducive to its growth. Tornadoes require an initial source of vorticity.

Additional studies, including more detailed consideration of the ambient wind profile and of detailed mesoscale flow, are needed to verify the above hypotheses. They will provide further conceptual models to assist in hail prediction.

Objective methods, based on a combination of parameters, have been developed for hail prediction in some regions (Feteris 1965; Molenat 1975; Strong 1986). These regions in the Netherlands, France, and Canada are similar in size or larger than the individual hail areas considered here. Because of the complex topography of New Zealand, progress in developing hail forecasting techniques may need to focus on individual areas. More detailed mapping of hail falls is needed. There are additional requirements. It would be necessary to develop a climatology of additional parameters including 24 h changes in fields: such changes were found to be useful predictors in the Canadian studies. Another requirement is a monitoring system that ensures that the existence, size, and intensity of all hail events is recorded.

Forecasting based on numerical model output and objective methods, or better conceptual models, can be expected to indicate the general areas where hail is likely, but the methods will not pinpoint just which localities will be affected. Forecasts at this detail made an hour or two before the hail event might be possible with the use of continuous weather radar surveillance. The radar data would also provide additional information for developing the conceptual models and would be most desirable for any attempted hail suppression. The value of highly accurate, short term forecasts, without a suppression technique, must be limited. While some damage might be eliminated (e.g., by garaging cars or picking near-ripe fruit) much damage could not be prevented.

ACKNOWLEDGMENTS

Many colleagues in the Meteorological Service have assisted me in this work. Particular thanks are expressed to Allan Penney and John Waller for computing assistance, to Mark Sinclair and Michael Uddstrom who made particular analyses of archived data available, to Alex Neale for his summarised press reports of hail events, and to Chris Hayward for drafting the diagrams. I wish to thank the Farmers Mutual Insurance Company for providing summarised hail claim information.

REFERENCES

Brooks, C. E. P.; Carruthers, N. 1953: Handbook of statistical methods in meteorology. London, Her Majesty's Stationery Office.

Federer, B.; Schmid, W.; Waldvogel, W. 1978: The design of Grossversuch IV, a randomized hail suppression experiment in Switzerland. *Atmosphere-ocean 16*: 6–16.

Feteris, P. J. 1965: Statistical studies on thunderstorm situations in the Netherlands. *Journal of applied meteorology 4*: 178–185.

Hanssen, A. W. 1965: An objective technique for forecasting thunderstorms in the Netherlands. *Journal of applied meteorology 4*: 172–177.

Heiman, D.; Kurz, M. 1985: The Munich hailstorm of July 12, 1984: a discussion of the synoptic situation. *Beitrage zur physik der atmosphare 58*: 528–545.

Kidson, E. 1932: The frequency of frost, snow and hail in New Zealand. *New Zealand journal of science and technology 14*: 42–54.

McGill, M. 1984: Severe hail and wind damage West Auckland 1984. *New Zealand Meteorological Service scientific report 24*.

Molenat, J. 1975: Technique de la prévision des risques de grêle dans le sud-ouest de la France au bénéfice de l'Association Nationale de Lutte Contre les Fléaux Atmosphériques. *Annual report, Association Nationale de Lutte Contre les Fléaux Atmosphériques 23*: 19–20.

Neale, A. A. 1977: A climatology of severe hailstorms in New Zealand. *New Zealand Meteorological Service technical note 230*.

Revell, C. G. 1972: Interactions between different scales of motion in a North Island summer situation. *New Zealand Meteorological Service technical note 207*.

———1984: Annual and diurnal variation of thunderstorms in New Zealand and outlying islands. *New Zealand Meteorological Service scientific report 3*.

Seelye, C. J. 1945: Tornadoes in New Zealand. *New Zealand journal of science and technology 27*: 166–174.

Steiner, J. T. 1967: Objective techniques for forecasting thunderstorms over the North Island in summer. *New Zealand Meteorological Service technical note 172*.

———1988: Can we reduce the hail problem? *Weather and climate 8* : 23–32.

Strong, G. S. 1986: Operational procedures for using the synoptic index to predict organized convective weather. Paper presented at the Mesoscale Forecasting Workshop, Winnipeg, Manitoba, Canada, 4–6 February.

Thompson, C. S. 1985: Maps of rainfall parameters for New Zealand. *New Zealand Meteorological Service miscellaneous publication 187*.

Tomlinson, A. I. 1975: Upper air statistics for New Zealand stations. *New Zealand Meteorological Service miscellaneous publication 147*.

———1976: Frequency of thunderstorms in New Zealand. *New Zealand journal of science 19*: 319–325.

Tomlinson, A. I.; Nicol, B. 1976: Tornado reports in New Zealand 1961–1975. *New Zealand Meteorological Service technical note 229*.

World Meteorological Organization 1956: International cloud atlas, Vol I. Geneva, WMO.

———1984: Manual on codes. Geneva, WMO.

New Zealand Journal of Geology and Geophysics, 1989, Vol. 32: 293–298
0028–8306/89/3202–0293 $2.50/0

Note

A reversal of throw and change of trend on the Wellington Fault in Wellington Harbour

K. B. LEWIS
New Zealand Oceanographic Institute
Division of Marine and Freshwater Science
Department of Science and Industrial Research
Private Bag
Kilbirnie, Wellington

Abstract A high-resolution seismic survey of the northwestern side of Wellington Harbour shows that the most recent trace of the predominantly dextral strike-slip Wellington Fault crosses the coastline in the vicinity of the Thorndon interisland ferry wharf and lies 250–400 m from shore off Kaiwharawhara. Between Ngauranga and Petone, recent dislocation can not be detected with certainty beneath shallow, almost seismically "opaque", possibly methane-rich layers.

The recent trace in Wellington Harbour cuts sediments deposited after the postglacial rise of sea level. It has a trend that is similar to the recent trace at Petone and about 10° clockwise from the recent trace behind Wellington City. The change in trend occurs close to the Thorndon wharf.

An unusual, but not unique, feature is that the recent trace in the harbour is upthrown on the southeastern (harbour) side, whereas long-term movement has uplifted the northwestern (landward) side. Recent fault dislocation is defined by a scarp about 1.5 m high, at the ferry wharf. It is buried, progressively more deeply, towards the northeast. It is buried 3.5 m deep where it is lost beneath "opaque" layers.

Off Kaiwharawhara, seismic profiles show a scattering of stratified reflectors immediately landward of the fault. It is inferred that this scattering is caused by fresh water leaking along the fault from an aquifer.

Keywords Wellington Harbour; Wellington Fault; sediments; seismic profiles; tectonics; Holocene; aquifer

SETTING

The linear ramparts that form the northwestern boundary of Wellington Harbour are the eroded escarpment of a major active fracture, the Wellington Fault. This is one of several northeast-trending dextral shears at the edge of the Indo-Australian plate that take up the transcurrent motion of the obliquely subducting Pacific plate (Fig.1). Buckling of the generally downthrown southeastern side has produced major infilled basins, such as Wellington Harbour and Hutt Valley, separated by higher portions such as those at Hawkins Hill and Taita Gorge (Cotton 1951; Lauder 1962). A summary of the geology of this area is given by Stevens (1974).

During the 1–2 million years since movement began, a zone of sheared and shattered rock has formed adjacent to the main fracture. Within this zone are numerous splinter faults that are perpendicular, oblique, and parallel to the main trend. The main fault offset occurs within this zone and appears to have been located along the same line for long periods of time. The width of the shatter zone is partly a response to changes in composition of the rocks and trend of the fault trace. It is generally 200–400 m wide but seismic refraction data suggest that it may be much wider beneath the sediments of Wellington Harbour, perhaps as a response to a change in trend of about 10° that occurs somewhere between Thorndon and Petone (Davey 1971; Hochstein & Davey 1974).

Offsets formed by the most recent movement of the fault are evident at the foot of the 300 m high escarpment behind the national legislature and commercial centre of Wellington (Grant-Taylor 1967; Ota et al. 1981). Here they trend at N45°E. Recent fault displacement is also evident through Petone but trending N55°E. At both places, motion has included (besides any transcurrent motion) downthrow to the southeast. Interpolation between these two sites requires

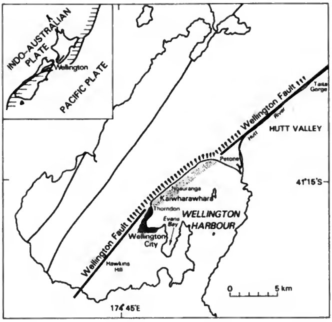

Fig. 1 Wellington Harbour showing (thick line) the position of the known onshore active traces of the Wellington Fault (from Ota et al. 1981), the fault escarpment along the northwestern side of the harbour (hatchured), and the inferred position of the shatter zone beneath the harbour (stippled) (from Hochstein & Davey 1974).

Received 8 March 1988, accepted 14 July 1988

either a bend or an offset in the fault somewhere along the northwestern side of the harbour. A bend in the cliff line at the Petone end has suggested an offset there (Grant-Taylor 1967) but this geomorphology can also be explained by wave erosion in the corner of the harbour that faces the full effect of southerly storms (Stevens 1974).

The active trace of the Wellington Fault must almost certainly lie somewhere seaward of the narrow, cliff toe, wave-cut platform that supports Wellington's main road and rail links. How far seaward has depended upon interpretations of data that were not specifically designed to show recent fault traces close to shore in the soft sediments. Cowan & Hatherton (1968) deduced from gravity data near the Petone foreshore that the Wellington Fault is approximately vertical and lies about 300 m east of the erosional escarpment (c. 200 m offshore), with basement downthrown about 300 m to the east. They further deduced a maximum of 1200 m downthrow off Ngauranga, but Hochstein & Davey (1974) modified this estimate to 400 m on the basis of seismic refraction data. Hochstein & Davey (1974) identified an intermediate velocity zone in the basement refractions along the northwestern side of the harbour as the shatter zone of the Wellington Fault. Its width of 500–1000 m is much greater than the width of the shatter zone elsewhere along the fault. The fault has not been identified at shallow depths beneath the seabed although some sparker records, collected for a study of the Hutt Valley aquifer, show reflections that might tentatively be attributed to fault dislocation 400–600 m from shore between Ngauranga and Petone (Reyners & Christoffel 1973).

Estimates of the most likely position of the Wellington Fault along the northwestern side of the harbour have been based on two suppositions. One is that the seaward edge of the wave-cut platform, which may be close to the reclaimed shoreline in the Kaiwharawhara area, best defines the line between rising greywacke and subsiding harbour basin. The other is that the centre of the crush zone in the deeply buried basement greywacke, projected vertically to the surface, is the most likely position of the fault trace because wave action has continuously cut back the shatter zone to relatively unshattered rock on the shore platform (Hochstein & Davey 1974). This latter supposition places the fault trace some 400–500 m offshore at Kaiwharawhara.

Because the precise position of the active fault trace has considerable significance in engineering planning and in the design of structures that may cross the trace, an uncertainty in position of 400 m required further work designed specifically to locate the fault in the vicinity of possible port development. Thus, the following survey was commissioned by Wellington Harbour Board and is published with their permission.

SURVEY METHODS

On 14 and 16 July 1986, the search for recent fault deformation was undertaken along the northwestern side of Wellington Harbour. An EG&G "Uniboom 230", high resolution seismic profiling system was operated from a 6 m aluminium launch. Navigation was controlled using the way-point and track guidance function of a Racal "MicroFix" microwave positioning system, which automatically recorded positions to within 1 m every 30 seconds. Seventeen tracks, 1 km long and 100 m apart were run in the area of primary interest between Thorndon and Ngauranga. Twelve lines 500 m apart were run between Ngauranga and Petone. Returning echos were filtered with a 400 Hz to 2 kHz bandpass filter and printed with 10 ms scale lines. All records are stored in either computer or hardcopy files under NZOI Survey Number 7109.

BASIS OF INTERPRETATION

Because the Uniboom sound source is relatively "clean" and free of resonance, most lines on the seismic profiles represent synchronous stratal surfaces where there is some vertical change in acoustic properties. These changes do not necessarily indicate a change in lithology that would be clearly recorded in a core. However, in a detailed survey such as this, adjacent profiles can be confidently correlated on the basis of seismic character and unconformities.

The velocity of sound in both water and soft sediment is taken to be 1500 m/s so that 10 ms scale lines represent 7.5 m depth. The horizontal scale on each profile varies with boat speed and paper feed rate. Most profiles have a vertical exaggeration of between 1:25 and 1:30.

SEISMIC STRATIGRAPHY

Most of the profiles show the protective batter of the coastal reclamation as a steep, seismically opaque reflector that has prograded over seaward-thickening harbour sediments. Nearshore, north of Kaiwharawhara, profiles show the harbour sediments, up to 9 m thick, onlapping a steeply dipping, strong reflector, that is inferred to be the interface with greywacke basement (Fig. 2A, B).

At many places there is a seismically transparent surface layer, up to 3.5 m thick, overlying either an intrasedimentary "opaque" reflector (Fig. 2A, B) or a seaward thickening, well stratified, near-parallel bedded sequence that onlaps a conspicuous unconformity (Fig. 2B, C, D, E). Hummocky reflectors beneath the unconformity indicate harbour sediments that are of a quite different character to the evenly stratified sequence above. The unconformity is about 10 m below the seabed (30 m below sea level) 1 km offshore from Kaiwharawhara but it shoals landward and southward to crop out at the seabed close to the Thorndon wharfs (Fig. 2E).

The seismic stratigraphy in this area shows some similarities to a borehole-correlated seismic stratigraphy 6 km away in Evans Bay (Lewis & Mildenhall 1985). There, the onlapping, parallel-bedded sequence was deposited since the sea flooded that part of the harbour about 10 000 years ago. The underlying sequence that is transgressively onlapped includes peaty sediments deposited in a swampy valley during glacially lowered sea level. At Kaiwharawhara, the hummocky reflectors and an infilled channel perpendicular to the shore are consistent with incisement by a low sea level extension of Kaiwharawhara Stream.

OPAQUE REFLECTORS

Reflectors that almost obliterate seismic penetration to underlying layers (Fig 2A, B) occur beneath much of the central harbour (Reyners & Christoffel 1973) but not close to the shore. These "opaque" reflectors scatter seismic energy and are at several stratigraphic levels. Only faint indications of bedding are visible beneath them. They were considered by Reyners & Christoffel (1973) to be layers of either flat-lying shells or gas-rich sediment. A similar reflector that was cored

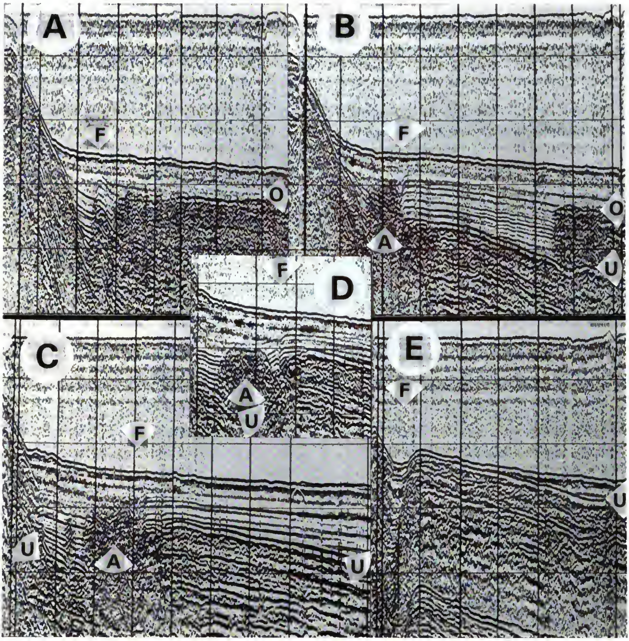

Fig. 2 High-resolution seismic profiles from between Thorndon and Ngauranga showing the active fault trace (F), intrasedimentary "opaque" layers (O), an unconformity of inferred early Holocene age (U), and diffuse reflectors thought to indicate fresh water escaping from an aquifer (A). Profiles are in order from north to south and their positions are shown in Fig. 3. Vertical scale lines are at 10 ms (7.5 m) intervals. Vertical exaggeration is about 1:25.

in Evans Bay appeared to correlate with an unconformity and a layer of 10 000 year old wood and plant roots whose decay could have produced small amounts of methane in the sediment (Lewis & Mildenhall 1985). The opaque reflectors along the northwestern side of the harbour overlie the unconformity, and also the change to parallel-bedded sediments, so they are inferred to have been deposited well after the postglacial rise of sea level. Nevertheless, generation of small amounts of biogenic methane, possibly in plant-rich flood deposits, seems a more probable explanation than mass mortality and current sorting of bivalves. Opaque reflectors are absent from the seabed off stream mouths in Evans Bay, Thorndon, and Kaiwharawhara. It is inferred that, in times of flood, these small streams may have both supplied sandy sediments that do not trap gas and limited influx of plant-debris charged, muddy, Hutt River water.

THE FAULT TRACE

A strong vertical displacement of reflectors is seen in all harbour profiles from off Thorndon and Kaiwharawhara (Fig. 2). The displacements plot as a linear feature subparallel to the shore (Fig. 3). Thus, they are interpreted as the active trace of the Wellington Fault.

The trace is slightly curved, extending from close to the Thorndon interisland ferry wharf to about 400 m from shore at Kaiwharawhara and curving back to about 250 m from shore between Kaiwharawhara and Ngauranga (Fig. 3, 4).

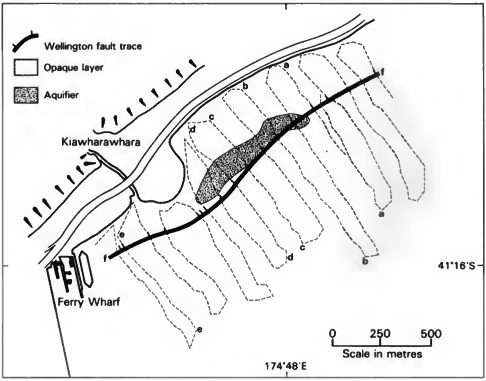

Fig. 3 Chart of the seabed off Kaiwharawhara showing the trace of the Wellington Fault f–f, the position of the opaque layer (stippled), and the position of the aquifer plume (patterned). Dashed lines show the position of the profiles; a–a, b–b, c–c, d–d and e–e are illustrated in Fig. 2.

Strike-slip motion can not be measured in seismic data, but the recent fault trace between Thorndon and Ngauranga includes a vertical displacement of 2–3 m for the top of the parallel-bedded sequence and about 7 m for the underlying unconformity (Fig. 2C, D). Displacement is **upthrown on the southeastern (harbour) side**. This is surprising in view of the long-term uplift of the northwestern (landward) side indicated by the high, erosional escarpment onshore. Basement greywacke rises over 200 m above sea level at the top of the escarpment and is estimated to descend to over 400 m below sea level beneath the harbour. However, similar recent changes of throw do occur elsewhere along the Wellington Fault, notably north of Upper Hutt (Lensen 1958; Brown & Wood 1983).

Close to Thorndon wharf, the fault is exposed on the seabed as a smoothed "scarp" in apparently pre-unconformity (glacial age) sediments (Fig. 2E). Off Kaiwharawhara, the well-stratified (postglacial) cover beds are included in the deformation, and the surface expression is less clearly defined; ··pthrown side crops out at the seabed, but a trough een fault scarp and shore has been at least partly led with the transparent (youngest) sediments. Towards uranga, the crest of the upthrown scarp is buried by m of transparent sediment (Fig. 2A, B, C). Although this r shows no evidence of deformation, it may be too fluid support such evidence. Still further to the northeast, the ult is beneath one of several, 2.0–3.5 m deep, seismically opaque layers. The increasing thickness of cover reflects an increasing sediment supply towards the mouth of the Hutt River. Between Ngauranga and Petone, there are only tentative indications, about 400 m from shore, of the Wellington Fault in the faint bedding beneath the opaque layer. However, because the fault may change its throw from up to the southeast to up to the northwest in this area, there may be little for seismic data to detect.

The slight curvature of the fault, and the reversal of throw, may be an expression in soft, surface sediments of an offset and a 10° change of trend in the fault in basement rock. Alternatively they might be a secondary effect associated with a tentatively identified rotational slump in the basement fault scarp behind Thorndon (G. J. Lensen pers. comm, reporting observations of the late T. G. Grant-Taylor). However, this feature was not noted in a recent survey of active landslides in the Wellington area (Dellow 1988).

The last movement of the fault clearly postdates the unconformity of the postglacial rise of sea level and much of the sediment that overlies it. Northeast of Kaiwharawhara, the fault is apparently buried. In the light of some uncertainties in the age of the deformed sediments, and ability of the overlying sediments to record deformation, Stevens's (1974) estimate that the last movement was about 1000 years ago is not unreasonable.

THE AQUIFER

For a distance of about 700 m northeast of the mouth of the Kaiwharawhara Stream, there is a zone of diffuse reflections along, or immediately landward of, the fault trace (Fig. 2B, C, D, Fig. 3). The marked change in acoustic properties could indicate escaping biogenic gas, but a more likely explanation, in view of notations of "fresh water springs" in old charts of this area (Wellington Harbour Board 1978), is that the diffusion effect is caused by escape of fresh water from either the Hutt Valley aquifer or a small local aquifer assocated with the Kaiwharawhara Stream.

At various places around the harbour, steep-sided "holes" in the seabed are inferred to have been formed by leakage from aquifers, and in general the leakage appears to be associated with greywacke-aquifer contact at depth, being probably initiated during earthquake stress (Reyners & Christoffel 1973). Except for the exposed "scarp" at Thorndon, no obvious holes were crossed in the survey, but leakage in

Fig. 4 Photograph of Wellington showing position of the active trace of the Wellington Fault behind Wellington City (from Ota et al. 1981) and offshore at Thorndon/Kaiwharawhara.
(Photo: D. L. Homer, NZGS).

the past may have locally modified the expression of the fault in soft harbour muds producing the smoothed, symmetrical depression seen in some profiles.

CONCLUSIONS

1. The recent trace of the Wellington Fault ranges up to 400 m offshore along the northwestern side of Wellington Harbour between Thorndon and Ngauranga. It can not be identified with certainty between Nguaranga and Petone.
2. A degraded fault scarp, upthrown on the southeast (harbour) side is exposed at the seabed at Thorndon but buried by up to 3.5 m of sediment to the northeast.
3. The recent trace of the Wellington Fault curves offshore at Thorndon. There is a change in trend of about 10° between the trace through Wellington and the trace through the harbour and Petone.
4. Diffuse reflectors along the fault trace may indicate escape of fresh water from an aquifer along the fault trace.

ACKNOWLEDGMENTS

I am indebted to Wellington Harbour Board for permission to publish these results, to John Mitchell, Ed Arron, and Ruth Baldwin for assistance with data collection, and to L. Carter (NZOI), K. Berryman (NZGS), and G. J. Lensen for discussion, ideas, and constructive critisism of the manuscript.

REFERENCES

Brown, I. R.; Wood, P. R. 1983: Strain movements across Wellington Fault at Te Marua. *In*: Procedings of the 3rd South Pacific Regional Conference on Earthquake Engineering, Wellington, New Zealand. *New Zealand National Society for Earthquake Engineering 3*: 509–519.

Cotton, C. A. 1951: Fault valleys and shutter ridges in Wellington. *New Zealand geographer 7:* 62–68.

Cowan, M.; Hatherton, T. 1968: Gravity surveys in Wellington and Hutt Valley. *New Zealand journal of geology and geophysics 11*: 1–15.

Davey, F. J. 1971: Seismic surveys in Wellington Harbour. Wellington, New Zealand. Department of Scientific and Industrial Research. *Geophysics Division report 70:* 20 p.

Dellow, G. D. 1988: Earthquake generated landslides in the Wellington – Lower Hutt area. Unpublished M.Sc. thesis, lodged in the Library, University of Canterbury. 224 p.

Grant-Taylor, T. L. 1967: Fault movement and deformation on the Wellington Fault in the Wellington region. *New Zealand Geological Survey report 27*: 14 p.

Hochstein, M. P.; Davey, F. J. 1974: Seismic measurements in Wellington Harbour. *Journal of the Royal Society of New Zealand 4*: 125–140.

Lauder, W. R. 1962: Port Nicholson and the "plough" mechanism in transcurrent faulting. *New Zealand journal of geology and geophysics 5*: 189–191.

Lensen, G. J. 1958: The Wellington Fault from Cook Strait to Manawatu Gorge. *New Zealand journal of geology and geophysics 1*: 178–196.

Lewis, K. B.; Mildenhall, D. C. 1985: The late Quaternary seismic, sedimentary and palynological stratigraphy beneath Evans Bay, Wellington Harbour. *New Zealand journal of geology and geophysics 28*: 129–152.

Ota, Y.; Williams, D. N.; Berryman, K. R. 1981: Parts sheets Q27, R27 and17 R28—Wellington. Late Quaternary tectonic map of New Zealand 1:50 000. With notes. Wellington, New Zealand. Department of Scientific and Industrial Research.

Reyners, M.; Christoffel, D. A. 1973: A continuous seismic reflection survey of part 17 of Wellington Harbour. *Victoria University of Wellington Physics Department report 17173*: 60 p.

Stevens, G. R. 1974: Rugged landscape. The geology of central New Zealand. Wellington, Reed. 286 p.

Wellington Harbour Board 1978: Thorndon Container Wharf to Kaiwharawhara—Sounding plan. Wellington Harbour Board.

New Zealand Journal of Geology and Geophysics, 1989, Vol. 32: 299–302
0028–8306/89/3202–0299 $2.50/0

Note

Sediments of the Paekakariki–Otaki River sand-dune sequence, New Zealand

L. W. WRIGHT
Department of Geography
Queen Mary College
University of London
Mile End Road
London E1 4NS, England

Abstract Thirty-eight samples collected from the southern North Island west coast, between Paekakariki and Otaki (i.e. Kapiti coast) were analysed by mechanical sieving to determine if chronologically distinct dunes exhibited characteristic sedimentary parameters. Slight differences do appear to occur but the contrasts are of insufficient magnitude to be used alone as a diagnostic feature. The study indicates a strong environmental uniformity has been in existence for over 6000 years notwithstanding large changes in the quantity of sediments available for dune building and the input of volcanic material.

Keywords Quaternary; sand dunes; sediments; Kapiti coast

OBJECTIVES

The depositional chronology of the sand-dune sequence of the Kapiti coast has been discussed by several authors (Adkin 1910, 1919, 1951; Cotton 1918; Te Punga 1962; Fleming 1953, 1972; and Gibb 1978), and much emphasis has been placed upon morphological criteria. The sedimentary characteristics of the dunes have been investigated by Oliver (1948) who commented only that the material exhibited good sorting and small grain size, a point also noted by Smith (1982). Gibb (1977) has shown that the present-day beach sands are likewise well sorted and fine grained although he noted variations along the beach. The present study seeks to provide more sedimentological data on the dune system and in particular to determine whether a particular phase of dune building can be identified from the physical characteristics of its sediments.

TECHNIQUES

This note is based upon the analysis of 38 samples collected in three bands normal to the shore in the south, centre, and north of the area. All samples were taken from deep within the dune, usually more than 2 m below the surface. Each sample was then analysed using standard sieving procedures, with nested sieves of $^1/_4$ ϕ intervals for 9 min, and the data plotted using Folk & Ward (1957) parameters. These are detailed in Tables 1 and 2.

Table 1 Grain-size analyses of sand-dune samples from the Kapiti (west) coast, southern North Island, using Folk & Ward (1957) parameters.

Grid reference*	Mean size	Sorting	Skewness	Kurtosis
Southern area				
N156 509619	2.72	0.35	−0.34	1.46
N156 511622	2.00	1.02	−0.63	0.81
N156 509619 (Fig. 1A)	1.73	0.67	0.04	0.85
N156 509619	2.30	0.62	−0.40	0.86
N156 510618 (Fig. 1D)	2.71	0.29	−0.23	1.24
N156 512625	2.12	0.87	−0.53	0.67
N156 512625	2.57	0.44	−0.40	1.24
N156 513629	2.70	0.24	0.26	1.86
N156 511615	2.90	0.21	0.03	1.09
N156 512615	2.91	0.20	0.02	1.11
N156 517648	2.69	0.38	−0.04	1.50
N156 520642	2.73	0.25	0.32	1.20
N156 520642 (Fig. 1E)	2.75	0.31	−0.21	1.51
N156 522 642	2.64	0.35	0.050	1.95
N156 525643 (Fig. 1G)	2.84	0.21	−0.05	1.10
N156 530640	2.84	0.20	−0.03	1.11
N156 530640	2.72	0.24	0.34	1.55
Central area				
N156 519692	2.74	0.27	0.27	1.11
N156 519693 (Fig. 1B)	2.77	0.24	−0.16	1.12
N156 529715	2.72	0.23	−0.09	1.03
N156 542700	2.71	0.24	−0.05	1.05
N156 551690	2.74	0.21	−0.02	1.02
N156 563698 (Fig. 1H)	2.98	0.21	0.03	0.99
Northern area				
N156 589772	2.76	0.24	−0.13	1.08
N156 589772	1.85	0.43	0.26	1.23
N156 589770	2.77	0.25	−0.19	1.14
N156 613818	2.70	0.30	−0.22	1.22
N156 624841	1.95	0.41	0.16	1.00
N156 625841 (Fig. 1C)	1.97	0.46	0.08	1.05
N156 624831	2.59	0.38	−0.05	1.23
N156 631838 (Fig. 1F)	2.77	0.27	−0.11	1.05
N156 631838	2.66	0.36	0.02	1.31
N156 631838	2.84	0.26	0.16	0.68
N156 632838	2.82	0.28	0.25	0.74
N156 632837	2.65	0.35	0.02	1.30
N156 632837 (Fig. 1I)	2.78	0.25	−0.15	1.10
N156 642835	2.70	0.35	0.27	0.19
N156 643834	2.00	0.52	0.27	0.94

*Grid references taken from N. Z. topographical map series NZMS 1, sheet N156 & pt N157—Kapiti.

Received 30 October 1986, accepted 19 July 1988

SOUTHERN AREA

Three phases of dune building are clearly represented in the area between Paekakariki and Raumati South. Contemporary embryo/foredunes occur south of the Whareroa Stream in the Queen Elizabeth Park. Behind these are bold rugged dunes of the Taupo Pumice Dunesand phase, and further inland are the more subdued dunes of the Foxton Dunesand phase. The sedimentary characteristics of these dunes are shown graphically in Fig. 1. The embryo dunes (Fig. 1A) show a lack of peakedness and a relatively wide size-range expressed in a sorting coefficient of 0.66. The mean grain size of 2.29 ϕ indicates a relatively coarse, though still fine, sand. This sample clearly differs from all the others, suggesting the dominance of some local source material derived via the Whareroa Stream and the beach.

Morphological and mineralogical contrasts are usually sufficient to distinguish between the Taupo and Foxton dunes. There is some suggestion from the grain-size parameters that the Foxton dunes have a more peaked pattern (Fig. 1D, G) but variation within both groups makes identification difficult and highlights the problem of sampling sand dunes effectively. Although both the Taupo and Foxton dunes consist of several dune ridges, the density of sampling used failed to reveal any intradune ridge contrasts.

CENTRAL AREA

The sand dune area from Paraparaumu Beach inland to Paraparaumu shows a remarkably uniform sedimentary environment. Apart from embryo dunes at the coast, at least three other dune-building phases have been identified—the Waitarere, Taupo, and Foxton phases. The grain size of these dunes is similar (Fig. 1B, E, H). They are very well sorted (sorting coefficient between 0.20 and 0.31), fine-grained sediments. This uniformity is further emphasised by the similarity between the parameters of skewness and kurtosis.

Table 2 Grain-size analysis of sand-dune samples from the Kapiti coast, showing percent weight in each ϕ class limit.

Class limits (ϕ):	−0.50	−0.25	0.00	0.25	0.50	0.75	1.00	1.25	1.50	1.75	2.00	2.25	2.50	2.75	3.00	3.25	3.50	3.75	4.00	Rest
Southern area																				
N156 509619	0.34	0.09	0.17	0.13	0.31	0.65	0.48	0.80	0.57	0.91	2.36	4.15	8.41	26.06	39.03	14.00	0.30	0.16	0.03	0.04
N156 511622	3.49	1.07	1.26	1.53	3.14	6.52	4.40	5.80	3.52	3.79	4.42	4.59	8.11	23.05	20.67	4.18	0.19	0.13	0.02	0.03
N156 509619 (Fig. 1A)	0.00	0.89	0.20	0.46	1.52	4.90	6.28	13.53	12.32	14.35	12.99	9.34	9.57	10.38	3.46	0.43	0.05	0.03	0.00	0.00
N156 509619	0.00	0.00	0.03	0.06	0.21	1.29	2.16	4.76	5.50	7.44	9.95	9.31	11.41	22.29	20.86	4.24	0.10	0.26	0.06	0.01
N156 510618 (Fig. 1D)	0.00	0.00	0.00	0.02	0.03	0.10	0.09	0.17	0.32	0.85	2.48	4.42	10.01	31.81	39.60	9.68	0.21	0.09	0.02	0.02
N156 512625	0.09	0.09	0.31	0.78	2.58	6.70	5.95	7.66	5.40	5.83	5.59	4.32	5.25	14.50	27.43	7.10	0.16	0.07	0.02	0.06
N156 512625	0.00	0.02	0.07	0.09	0.14	0.28	0.39	1.49	1.85	3.18	5.35	7.06	11.13	26.65	34.05	7.75	0.21	0.13	0.04	0.02
N156 513629	0.00	0.00	0.00	0.00	0.01	0.02	0.04	0.04	0.14	0.49	1.64	2.15	8.35	62.53	10.72	12.88	0.65	0.23	0.03	0.02
N156 511615	0.00	0.00	0.00	0.00	0.00	0.00	0.03	0.02	0.04	0.03	0.18	0.50	2.22	17.62	50.67	25.49	1.19	0.76	0.33	0.84
N156 512615	0.00	0.00	0.00	0.00	0.00	0.00	0.00	0.00	0.00	0.02	0.08	0.28	1.67	15.94	53.83	26.30	0.80	0.54	0.15	0.33
N156 517648	0.00	0.01	0.00	0.01	0.04	0.08	0.08	0.12	0.44	2.49	5.66	2.57	10.09	44.65	14.74	16.82	1.36	0.63	0.12	0.01
N156 520642	0.00	0.00	0.00	0.00	0.00	0.00	0.00	0.00	0.02	0.06	0.35	0.98	10.44	57.63	13.34	14.82	1.54	0.68	0.06	0.00
N156 520642 (Fig. 1E)	0.00	0.00	0.00	0.00	0.00	0.01	0.01	0.04	0.09	0.43	2.32	5.11	10.51	25.81	37.31	16.35	0.61	0.48	0.19	0.61
N156 522642	0.00	0.02	0.00	0.00	0.00	0.01	0.04	0.00	0.13	0.47	4.29	6.25	14.69	48.87	10.76	9.11	1.91	2.21	1.14	0.00
N156 525643 (Fig. 1G)	0.00	0.00	0.00	0.00	0.00	0.00	0.00	0.00	0.00	0.47	0.30	0.96	3.60	23.35	51.84	18.47	0.69	0.43	0.12	0.14
N156 530640	0.00	0.00	0.00	0.00	0.00	0.00	0.00	0.00	0.00	0.01	0.09	0.30	1.85	25.64	53.65	16.89	0.67	0.43	0.13	0.25
N156 530640	0.00	0.04	0.00	0.04	0.00	0.01	0.01	0.02	0.04	0.07	0.47	1.05	8.64	62.77	11.36	11.92	1.73	1.33	0.42	0.00
Central area																				
N156 519692	0.00	0.00	0.00	0.00	0.00	0.00	0.02	0.04	0.10	0.39	1.46	2.37	8.85	54.03	12.75	18.58	1.05	0.25	0.02	0.00
N156 519693 (Fig. 1B)	0.00	0.00	0.00	0.00	0.00	0.02	0.04	0.05	0.08	0.17	0.85	2.62	7.39	29.65	45.95	12.50	0.38	0.19	0.02	0.01
N156 529715	0.00	0.00	0.00	0.00	0.00	0.01	0.02	0.02	0.06	0.19	1.18	3.71	10.78	39.06	38.97	5.68	0.13	0.07	0.01	0.03
N156 542700	0.02	0.00	0.00	0.01	0.01	0.02	0.01	0.03	0.04	0.11	0.82	3.54	12.20	37.81	37.25	6.69	0.31	0.35	0.18	0.51
N156 551690	0.00	0.00	0.00	0.00	0.00	0.00	0.00	0.00	0.02	0.02	0.22	1.29	7.85	40.48	41.56	7.08	0.30	0.36	0.21	0.54
N156 563698 (Fig. 1H)	0.00	0.00	0.00	0.00	0.00	0.00	0.00	0.00	0.00	0.00	0.00	0.06	0.70	9.53	43.69	38.43	6.98	0.23	0.20	0.13
Northern area																				
N156 589772	0.00	0.00	0.00	0.00	0.01	0.00	0.02	0.03	0.05	0.10	0.68	2.52	9.19	31.62	43.07	11.67	0.50	0.33	0.01	0.11
N156 589772	0.00	0.03	0.00	0.18	0.18	0.51	0.29	3.57	12.51	28.96	25.32	11.66	6.55	4.71	3.64	1.39	0.18	0.03	0.03	0.18
N156 589770	0.00	0.00	0.00	0.00	0.01	0.01	0.03	0.05	0.07	0.24	1.39	2.96	7.69	27.19	46.08	13.40	0.38	0.16	0.11	0.14
N156 613818	0.00	0.00	0.00	0.00	0.02	0.04	0.03	0.05	0.13	0.63	2.78	5.34	10.95	30.85	38.45	9.32	0.56	0.42	0.14	0.20
N156 624841	0.00	0.00	0.00	0.01	0.06	0.16	0.87	2.08	6.66	21.43	30.85	14.19	13.87	7.36	1.18	0.94	0.11	0.11	0.03	0.00
N156 625841 (Fig. 1C)	0.00	0.00	0.00	0.00	0.06	0.46	0.98	4.39	7.30	17.83	24.86	17.96	12.46	8.39	3.98	0.70	0.10	0.10	0.10	0.26
N156 624831	0.00	0.00	0.00	0.00	0.01	0.01	0.02	0.04	0.12	0.89	7.12	9.04	18.56	37.43	12.45	12.61	0.95	0.59	0.08	0.00
N156 631838 (Fig. 1F)	0.01	0.01	0.01	0.00	0.00	0.00	0.00	0.02	0.02	0.08	0.78	3.43	11.15	28.41	38.82	14.59	0.86	0.83	0.29	0.57
N156 631838	0.00	0.02	0.01	0.01	0.01	0.01	0.01	0.02	0.11	1.02	4.40	5.66	15.72	42.87	11.98	15.72	1.29	0.87	0.18	0.00
N156 631838	0.00	0.00	0.00	0.00	0.01	0.02	0.02	0.01	0.01	0.03	0.25	0.70	4.09	39.78	20.99	29.59	2.57	1.66	0.16	0.00
N156 632838	0.00	2.07	0.00	0.00	0.00	0.00	0.00	0.00	0.04	0.02	0.20	0.52	3.78	43.26	15.51	29.84	2.88	1.62	0.18	0.00
N156 632837	0.00	0.00	0.00	0.00	0.00	0.00	0.02	0.05	0.26	0.88	8.59	6.03	17.53	42.33	13.71	13.66	1.08	0.70	0.08	0.00
N156 632837 (Fig. 1I)	0.00	0.00	0.00	0.00	0.00	0.00	0.00	0.00	0.04	0.20	1.06	2.55	8.27	28.54	43.25	14.70	0.60	0.48	0.09	0.17
N156 642835	0.00	0.00	0.00	0.01	0.07	0.19	1.11	2.68	9.61	21.56	24.00	9.11	12.07	11.64	2.86	3.10	0.67	0.83	0.41	0.00
N156 643834	0.00	0.00	0.00	0.00	0.00	0.01	0.05	0.12	0.24	1.05	3.83	6.67	11.06	24.41	35.47	14.17	1.15	1.06	0.26	0.40

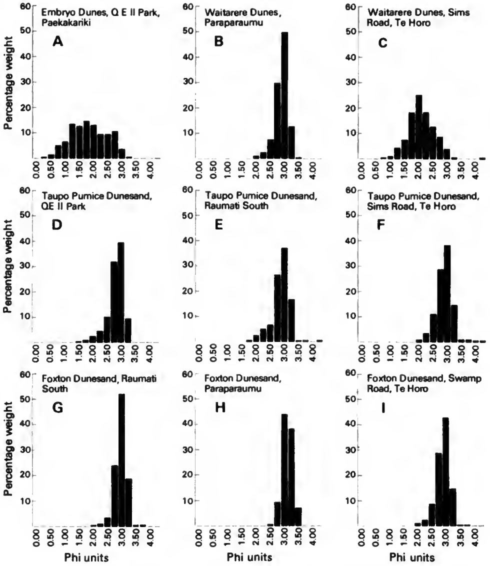

Fig. 1 Histograms of selected samples based on the proportion of sand retained on sieves stacked at $^1/_4$ ϕ intervals.

NORTHERN AREA

Although not forming the largest dunes, this area has a sequence of dune deposition that is most complete and morphologically most distinct expecially between the coast and Te Horo. Again the dominant feature of the sediments across the whole sequence is their degree of sorting and their fine grain size. The Taupo dunes and Foxton dunes have remarkably similar physical characteristics, a condition which applies also to the younger Motuiti dunes which are well developed here.

All three members show a peakedness in the 2.75–3.25 range and a sorting coefficient of between 0.25 and 0.35, while skewness ranges only from –0.11 to –0.26 and kurtosis from 1.05 to 1.19 (Fig. 1F, I). The pattern is slightly different in the sample taken from the Waitarere dunes (Fig. 1C), which is less peaked, slightly coarser, and less well sorted, perhaps indicating the input of a larger proportion of locally derived sediments. Other samples taken from these youngest dunes show that the variation within this phase is more marked than in the older dunes.

CONCLUSIONS

Sample analysis confirms the findings of Oliver (1948) that the sediments throughout the area are dominated by fine grained, well sorted sands. Variations within this grouping do occur (1) locally within a particular dune, (2) normal to the shore, and (3) parallel to the shore. The present study was designed to ascertain if variations normal to the shore were sufficiently distinctive to allow dune sequences to be distinguished where the more easily obtained evidence from morphology, pedology, and mineralogy has, for some reason, become obscured. I conclude that, although this is a useful means of distinguishing recent dunes from older phases of depostion in some locations, this particular analysis is not especially helpful in distinguishing between the older dune-building phases or between dune-building periods within a particular phase. Minor differences between samples do occur but they tend to be of a scale insufficient to build a chronology in the absence of supporting material.

ACKNOWLEDGMENT

The author wishes to thank the Central Research Fund of London University for financial support towards this project.

REFERENCES

Adkin, G. L. 1910: The post Tertiary geological history of the Ohau River and the adjacent coastal plain, Horowhenua county, North Island. *Transactions of the New Zealand Institute 43*: 496–520.

———1919: Further notes on the Horowhenua coastal plain and the associated physiographic features. *Transactions of the New Zealand Institute 51*:108–118.

———1951: Geology of the Paekakariki area of the coastal lowland of western Wellington. *Transactions of the New Zealand Institute 79*: 157–76.

Cotton, C. A. 1918: The geomorphology of the coastal district of south western Wellington. *Transactions of the New Zealand Institute 50*: 212–222.

Fleming, C. A. 1953: The geology of the Wanganui Subdivision. *New Zealand Geological Survey bulletin 52*.

———1972: The contribution of C14 dates to the Quaternary geology of the 'Golden Coast' Wellington. *Tuatara 19*: 61–69.

Folk, R. L.; Ward, W. C. 1957: Brazos river bar; a study in the significance of grain size parameters. *Journal of sedimentary petrology 27*: 3–26.

Gibb, J. G. 1977: Sediment data for beaches and rivers North Island, New Zealand. *Geology Department publication 7*. Wellington, Victoria University of Wellington.

———1978: The problem of coastal erosion along the 'Golden Coast', western Wellington. *Water and soil technical publication 10*:1–19.

Oliver, R. L. 1948: The Otaki Sandstone and its geological history. *New Zealand Department of Scientific and Industrial Research geological memoir 7*: 1–49.

Smith, S. P. 1982: Progradation of the Kapiti Coast: Paraparaumu Beach to Raumati Beach. Unpublished B.A. (Hons) dissertation, Department of Geography, Massey University.

Te Punga, M. T. 1962: Some geological features of the Otaki–Waikanae district. *New Zealand journal of geology and geophysics 5*: 517–530.

New Zealand Journal of Geology and Geophysics, 1989, Vol. 32: 303–304
0028–8306/89/3202–0303 $2.50/0

Letter to the Editor

The age of the Waiho Loop terminal moraine, Franz Josef Glacier, Westland

Comment

The late J. H. Mercer has brought out an extremely good point in showing that different radiocarbon ages can be obtained from the same wood sample, suspected to be contaminated, possibly with modern soil organics and soil carbonate, after being given different pretreatments before counting (Mercer 1988). It is not known how much extraneous organic material can be picked up by a piece of wood, after some historic geological event has left it buried over a long period of time in a sedimentary layer. Also, it is not known whether all naturally acquired contaminating material can be removed by acid-alkali treatment because I have shown that wood, artificially contaminated in the laboratory with soil organic compounds, will lose only part of this contamination during an acid-alkali pretreatment.

In a laboratory experiment performed in 1980 (Currie 1980), limit-age wood, containing no radiocarbon, was contaminated with modern organic compounds obtained from a local stream which drained swampy ground, and which was laden with organic compounds formed from the decomposition of plant material, in a colloidal solution. After the acidified stream water was percolated through groundup limit-age wood for several days, the sample was homogenised, then one-half was subjected to acid-alkali treatment and the other half was merely washed with water to remove traces of acid. Each half sample was then analysed for radiocarbon, when it was observed that the untreated wood had acquired a radiocarbon level of some 7.4% modern with respect to 0.95 NBS Oxalic Acid Standard, but after treatment the other half of the wood sample still measured 2.8% modern with respect to 0.95 NBS Oxalic Acid Standard, despite the fact that 50% of the mass of the wood had been lost during the acid-alkali treatment. The results of this experiment suggest that it may not be possible to remove all the organic contamination with an acid-alkali treatment. It seems worthwhile to consider the Waiho Loop radiocarbon measurements and attempt to calculate a contamination-free age, assuming that the fraction of contamination retained after acid-alkali treatment was similar to that retained in my laboratory experiment. If the wood was contaminated with soil organic compounds, then the samples measured in New Zealand would still contain all the original contamination, if these samples behaved similarly to the untreated samples measured by me in 1980, which were also given only an aqueous wash. Carbonate would not have been removed because there had been no acid wash. The mean ^{14}C age of the New Zealand samples was, in round figures, 11 600 years B.P. On the other hand, the samples measured in the United States would have had all contaminating carbonate removed by the acid treatment but soil organic compounds present could have been retained perhaps in similar proportion to those retained in the contaminated wood pretreated by me. The mean ^{14}C age of the American samples, according to Mercer, and confirmed by me, was some 12 440 years B.P. A simple calculation using the above mean ages, and assuming acid-alkali treatment will remove 62% of the contamination which is assumed to be all organic, enables determination of a Libby age for the sample, unaffected by contamination, of some 13 000 years B.P. If only carbonate had been present as a contaminant then the age calculated in the United States would be a good estimate of the age of the Waiho Loop terminal moraine. If the above postulated soil organic contamination had a radiocarbon level of 0.95 NBS Oxalic Acid Standard, then c. 5% contamination would reduce the true Libby age of 13 000 years B.P to 11 600 years B.P. If various mixtures of both carbonate and organic contamination had been present, each with ^{14}C level equal to 0.95 NBS Oxalic Acid Standard, the true Libby age would lie between 12 440 and 13 000 years B.P. One needs to know how effectively an acid-alkali treatment removes soil organic compounds if confidence is to be had in any estimated radiocarbon ages. Also, it is desirable to identify species of contaminants present and separate them from components of the wood.

During the 13th International Conference on Radiocarbon Dating, M. J. Head of The Australian National University, described solvent extraction of soil organic compounds and methods of separating these compounds into various classes, by a range of techniques. This technology may be capable of completely separating the contamination components from those of the wood, but this remains to be seen. If the process were feasible, care would need to be taken to prevent the solvent from becoming another contaminant, as demonstrated by Jansen (1972) of the Institute of Nuclear Sciences.

Finally, soil organic contamination need not necessarily be composed of only contemporary material, for if fossil wood were buried in a paleosol containing ancient organic compounds, there arises the possibility that contamination older than the sample could occur as well as younger contamination. For the Waiho Loop sample, this sort of occurrence does not seem likely. If it did occur, and if the older contamination were harder to remove than the younger, then the situation could arise where a sample initially having too young a radiocarbon age through contamination could, after treatment, have an age greater than the true age. Although Grant-Taylor & Rafter (1971) came to the conclusion that acid treatment of contaminated wood was more effective than alkali treatment, this result is not believed to be generally true. I have demonstrated in laboratory experiments, using artificial contamination, that acid treatment alone will not remove organic contaminants from wood at all, but younger soil organic compounds can be preferentially dissolved by acid from a mixture of young and old soil organic compounds (Currie 1980).

In conclusion, it is important to know whether or not a radiocarbon sample is contaminated, and it is equally important to be able to identify any contaminants because one can then judge the effectiveness of any decontaminating procedures.

16 November 1988

D. R. CURRIE
Institute of Nuclear Sciences
Department of Scientific and Industrial Research
P.O. Box 31312
Lower Hutt, New Zealand

REFERENCES

Currie, D. R. 1980: Experiments to determine the efficiency of two standard decontamination procedures for radiocarbon samples. *Institute of Nuclear Sciences INS-R—272*.

Grant-Taylor, T. L.; Rafter, T. A. 1971: New Zealand radio-carbon age measurements—6. *New Zealand journal of geology and geophysics 14:* 364–402.

Jansen, H. S. 1972: Transfer of carbon from solvents to samples. Proceedings of the 8th International Conference on Radiocarbon Dating. Pp 171–176.

Mercer, J. H. 1988: The age of the Waiho Loop terminal moraine, Franz Josef Glacier, Westland. *New Zealand journal of geology and geophysics 31:* 95–99.

New Zealand Journal of Geology and Geophysics, 1989, Vol. 32: 305–306
0028–8306/89/3202–0305 $2.50/0

Book review

Directions in paleoseismolgy edited by A. J. Crone and E. M. Omdahl. *Proceedings of Conference XXXIX. United States Geological Survey open-file report 87-673*. Denver, Colorado, 1988, 456 p.

Since the first "Redbook Conference" on unusual animal behaviour in 1976, the U.S. Geological Survey has continued to sponsor a wide range of state-of-art conferences related to earthquake hazards. The proceedings of the 39th conference continue the high standards set by previous conferences by publishing a wide range of up-to-date research on the geological aspects of earthquakes and Quaternary dating. Paleoseismology, as defined by Bob Wallace (U.S. Geological Survey), is "the identification and study of prehistoric earthquakes", and the 45 papers in this publication attempt to summarise the techniques, results, and future directions for studies in paleoseismology. Speed of publication in this rapidly evolving field (11 months from the conference to publication!) necessitates a further addition to the rapidly growing mountain of "grey literature" that is not generally available to a New Zealand audience. However, this volume can be obtained free on request from the editors, and will be of interest to Quaternary geologists, seismologists interested in the geology of earthquakes, and engineers who are concerned with methods used by geologists to arrive at their estimates of seismic hazard. The volume follows the same order of presentation as the meeting from which it was produced, with division into six major sections in addition to introductory and concluding remarks: Quaternary Dating Techniques; Recognition of Paleoseismic Events in the Geological Record; Quaternary Slip Rates and Coseismic Deformation; Modelling Fault-Scarp Degradation; The Behaviour of Seismogenic Faults; Aspects of Seismic Hazard Analysis. Each section contains up to 11 short papers written by predominantly U.S. experts in appropriate fields and concludes with a summary of the discussion session that took place among the 71 participants at the conclusion of paper presentations.

Quaternary dating correctly gains first place in this volume because it is the basis from which all estimates of the timing of past fault movements, slip rates, and recurrence intervals are made. The 11 papers focus mostly on recent developments in the newer techniques of thermoluminescence (TL), electron spin resonance (ESR), ^{10}Be, rock varnish thickness, as well as good background reviews of amino acid, fission track, paleomagnetic, and dendrochronological techniques. Recent breakthroughs by researchers at California Institute of Technology and University of Texas indicate that one standard deviation errors from < 1–4% can be achieved for ^{230}Th coral dates. Historic earthquakes from Vanuatu are dated at A.D. 1785 ± 5 years and interglacial marine terraces at 123 000 ± 1100 years ago! High-precision dating provides a strong challenge to Quaternary stratigraphers to have well-determined paleoenvironments and offers hope that very high quality late Quaternary eustatic sea level record can be established. A timely review of radiocarbon tandem accelerator dating and its limitations is provided by Paul Damon (Arizona State University). As dates from this method become more commonplace in New Zealand, N.Z. Quaternary geologists and archeologists should be aware of the differences between this method and conventional radiocarbon dating. The comparisons between radiocarbon dating methods outlined in Damon's paper are also applicable to N.Z. situations.

Recognition of past earthquake magnitude and location from the stratigraphic record is the major emphasis of paleoseismology. Trenching of active fault scarps has been the most popular method for recognising past earthquake events, and papers are presented that summarise the major diagnostic tectonic features from extensional, contractional, and strike-slip regimes. Interpretation of flights of marine terraces, which is gaining increasing prominence in New Zealand, is summarised by George Plafker (U.S. Geological Survey), and folds, liquefaction features, landslides, and seismic profiling techniques are all examined to determine their potential for recognising the magnitude of past earthquakes.

Sometimes slower rates of tectonic movement or erosion preclude the recognition of individual earthquakes but a variety of techniques can be used to quantify rates of deformation. Bill Bull (Arizona State University) and Chris Menges (University of New Mexico) show how mountain front geomorphology can be assessed to determine relative rates of fault movement, while Stan Schumm (Colorado State University) shows how slow rates of tectonic movement can be detected from fluvial drainage patterns. Peter Knuepfer (State University of New York) interprets his data from the Awatere and Hope Faults to claim that large fluctuations in fault slip rate can occur in periods of just a few thousand years. Other papers emphasise the need for detailed studies of historic earthquakes to adequately interpret those seen from the geologic record.

Five papers discuss the knowns, unknowns, and perspectives on the problems of fault-scarp dating by diffusion equation modelling. The potential for dating fault scarps from their morphology was recognised by Bob Wallace (U.S. Geological Survey) and quantitive modelling by Tom Hanks (U.S. Geological Survey) and others raised hopes that in arid and semi-arid regions, where little organic material is available for radiocarbon methods, fault movements could be accurately dated from the morphology of fault scarps. Initial hopes have dimmed as multiple movements complicate scarp morphology, and calibration of the diffusion model has not proven easy. Few studies of this type have been carried out in New Zealand, but this section provides an excellent overview of the necessary considerations and potential problems for anyone contemplating scarp degradation studies in New Zealand.

The behaviour of seismogenic faults, both at the surface and within the brittle crust, is reviewed in five papers. Rick Sibson (University of California, Santa Barbara) proposes that fault heterogeneities play an important role in the initiation and termination of fault rupture, while Bill Ellsworth (U.S. Geological Survey) discusses implications of fault segmentation for frequency-magnitude relations and

earthquake stress drops. The scientific body of the volume concludes with three papers reviewing existing methods for seismic hazard analysis and how they serve the public.

The editors are to be congratulated for the speedy publication of current thinking in a field that is of equal importance to the scientific communities in the U.S. and New Zealand. All papers have been reviewed by the editors who have managed a uniformity in presentation while still retaining a wide variety in authorship style. Diagrams and the limited number of photographs are particularly well reproduced for a publication of this sort, although the variation in font styles can detract from the content. Papers usually do not concern themselves with local studies but emphasise the principles involved with studying paleoseismology by reference to the large body of published literature. The session summaries are particularly valuable in that they indicate the trends of on-going and future research that may take several years to appear in major journals. This volume is good reading for both Quaternary geologists and paleoseismolgy specialists and, if more readily available, could form the core for a series of graduate seminars in Quaternary geology and its applications.

ALAN G. HULL
University of California, Santa Barbara
California 93106, U.S.A.

DSIR Publications in Earth Sciences

DSIR Bulletins

No.			$
BL092	1945	Soil erosion in the High Country of the South Island. *H. S. Gibbs, J. D. Raeside* and others	6.00
BL117	1955	Geothermal steam for power in New Zealand. *L. I. Grange* (compiler)	6.00
BL122	1957	General account of the Chatham Islands 1954 expedition. *G. A. Knox*	6.00
BL123	1957	Physics of the New Zealand thermal area. *C. J. Banwell* and others	6.00
BL134	1959	New Zealand coals, their geological setting and its influence on their properties. *R. P. Suggate*	6.00
BL136	1960	The hot springs and geothermal resources of Fiji. *J. Healy*	11.00
BL140	1961	New Zealand IGY Antarctic expeditions, Scott Base and Hallett Station. *T. Hatherton*	11.00
BL155	1963	Waiotapu geothermal field and maps.	11.00
BL166	1964	Earthquake-generated forces and movements in tall buildings. *R. I. Skinner*	11.00
BL168	1966	A geophysical study of the Southland Syncline. *T. Hatherton*	11.00
BL169	1966	Heat and mass transfer in the earth: hydrothermal systems. *J. W. Elder*	11.00
BL189	1968	Peat classification by pedological methods applied to peats of western Wellington, New Zealand. *W. F. Harris*	11.00
BL191	1968	Engineering study of Caracas earthquake, Venezuela, 29 July 1967. *R. I. Skinner*	6.00
BL194	1969	Gisborne earthquake, New Zealand, March 1966. *R. M. Hamilton* and others	11.00
BL199	1970	Seddon earthquake, New Zealand, April 1966. *R. D. Adams* and others	11.00
BL203	1970	Topographic-isostatic gravity corrections for New Zealand. *W. I. Reilly*	11.00
BL211	1973	The geomagnetic field in New Zealand at epoch 1970.5. *W. I. Reilly and A. L. Burrows*	11.00
BL212	1974	Cenozoic geology of the Lower Nevis Basin with special reference to oil shale deposits. *G. J. Williams*	11.00
BL213	1974	Microzoning for earthquake effects in Wellington, New Zealand. *T. L. Grant-Taylor* and others	16.00
BL215	1974	The Parahaki Volcanics and their associated clays. *F. E. Bowen*	6.00
BL218	1977	Geochemistry. *A. J. Ellis* (editor)	24.00
BL220	1978	Stable isotopes in the earth sciences. *B. W. Robinson* (editor)	24.75
BL221	1978	Landsat II over New Zealand. *P. J. Ellis, I. L. Thomas and M. J. McDonnell*	25.70
BL224	1978	The eruption of Ruapehu, New Zealand on 22 June 1969. *J. Healy* and others	11.00
BL225	1980	The Marlborough earthquakes of 1848. *G. A. Eiby*	11.00
BL229	1981	Geothermal energy for New Zealand's future. *J. W. Lawless* and others	11.00
BL237	1986	Antarctic Cenozoic history from the MSSTS-1 drillhole, McMurdo Sound. *P. J. Barrett* (editor)	60.50

DSIR Information Series

No.			
IS047	1965	The Ross Dependency in pictures. *L. B. Quartermain*	6.00
IS103	1974	A tramper's geology of the Tararuas. *G. R. Stevens*	8.50
IS111	1975	Geology of the Whakarewarewa hot springs. *E. F. Lloyd*	8.50
IS115	1976	DSIR's first fifty years. *J. D. Atkinson*	8.00
IS118	1977	Materials for the New Zealand potter. *J. C. Schofield*	8.50
IS122	1977	Slope stability in urban development. *D. K. Taylor, J. G. Hawley and B. W. Riddolls*	8.50
IS124	1977	Groundwaters of the Hutt Valley–Port Nicholson alluvial basin. *I. G. Donaldson and D. G. Campbell*	8.50
IS133	1978	Electromagnetic forming. *R. K. King and J. M. Thorp*	8.50
IS150	1981	Illustrations of New Zealand fossils. *I. G. Speden and I. W. Keyes*	13.75
IS161	1985	Lands in collision: discovering New Zealand's past geography. *G. R. Stevens*	23.40
IS164	1988	Walking on Jelly. The Bay of Plenty Earthquake 1987. *Q. W. Ruscoe et al.*	21.70

Miscellaneous

No.			
MP007	1986	Key to Prosperity—Science and Technology. Report of the Ministerial Working Party, November 1986	19.95
MP008	1987	New Zealand Geology 1:2 000 000. *Patricia M. Riddolls*	49.00
MP030	1988	DSIR Annual Report 1988	7.60
CP001	1986	New Zealand Geological Survey Basin Studies No.1. Cretaceous and Cenozoic sedimentary basins of the West Coast region, South Island, New Zealand	98.35

ALPHA Extension information leaflets

No.	
AL001	The earthquake problem in New Zealand
AL006	Volcanoes in New Zealand
AL012	Petroleum exploration in New Zealand
AL013	Fossils
AL016	Geological time
AL017	New Zealand's changing geography
AL018	Life in antarctic lakes and rivers
AL019	Active earth deformation
AL032	Coal geology in New Zealand
AL044	Discovering New Zealand's ancient shorelines
AL060	Edgecumbe earthquake 1988

Single copies of "Alphas" are free but please send a 60 cent stamp with your order.

10 or more copies are 50 cents each.

Walking on Jelly: the Bay of Plenty (Edgecumbe) Earthquake 1987
by Quentin Ruscoe and others

On 2 March 1987, shortly after 1.42 p.m., a major earthquake sent shock waves across the eastern Bay of Plenty. For those living in the area, it was a time of terror and devastation. The earth rolled like the sea. More shocks followed. By evening, the Bay of Plenty earthquake had caused more damage than any other in New Zealand since 1968.

Walking on Jelly is about the people of the Bay of Plenty and their response to the events of that extra-ordinary day. It is a story of fear and panic but also of a community working together to restore order. Superb black and white photos illustrate vivid eye-witness accounts which appear alongside contributions from experts in disaster relief. A summary of activity below the Earth's surface is illustrated with simple line drawings.

"This book has come at an opportune time, while the disaster which struck the Bay of Plenty is still fresh in people's minds and lessons are still being evaluated .... I congratulate the authors and hope the book will be widely read in the interests of public safety."

Edward Latter
Director of Civil Defence

Contents— **The Earthquake Strikes * This Solid Earth ? * People Power * Damage To Homes * More Damage * The Civil Defence Response * Informing The World * Coping With The Earthquake * Some Lessons Learnt * Do It Now, And In The Event !**

Price:

New Zealand/Australia	Mail order	NZ$22.70	— Retail NZ$19.95
Outside NZ/Australia	Mail order	US $22.70	

1988, ISBN 0-477-02526-9, 96 pages, softcover. DSIR Information Series No. 164

Contains advice on how to prepare for the next major earthquake

Orders

Publications listed may be obtained by completing the order form below.
All prices include postage and packaging (and GST within New Zealand).
Please send payments with order.
Make cheques or money orders payable to the "Department of Scientific and Industrial Research".
Purchasers outside New Zealand and Australia should remit payment in US$.

Return to:

The Publications Officer
DSIR Publishing
P.O. Box 9741
Wellington
New Zealand
Tel: (04) 858-939
Fax: (04) 850 631

Name ______

Address ______

______

Please send me ______

☐ I enclose payment of $______

☐ Charge my credit card account $______

My credit card number is: Visa/Amex/Bankcard

Expiry date ______

☐ Please tick if tax invoice required

Signature ______